

**SYNTHESIS OF CYANURYL, 8-SUBSTITUTED ADENINYL
PNA ANALOGUES AND BIOPHYSICAL STUDIES OF
THEIR DNA/RNA HYBRIDISATION PROPERTIES**

THESIS SUBMITTED TO
THE UNIVERSITY OF PUNE
FOR THE DEGREE OF
DOCTOR OF PHILOSOPHY

IN
CHEMISTRY

BY
RAMAN VYSABHATTAR

Research Guide
Dr. K. N. Ganesh

**DIVISION OF ORGANIC CHEMISTRY
NATIONAL CHEMICAL LABORATORY
PUNE 411008**

March, 2008

CERTIFICATE

This is to certify that the work presented in the thesis entitled “**Synthesis of Cyanuryl, 8-substituted Adeninyl PNA Analogues And Biophysical Studies of Their DNA/RNA Properties**” submitted by the candidate **Raman Vysabhatar**, National Chemical Laboratory, Pune, under my supervision. Such materials as obtained from other sources have been duly acknowledged in the thesis.

Dr. K. N. GANESH

(Research Guide)

J. C. Bose Fellow,
National Chemical Laboratory,
Pune-411 008,
INDIA.

March, 2008

CANDIDATE'S DECLARATION

I here by declare that the thesis entitled “**Synthesis of Cyanuryl, 8-substituted Adeninyl PNA Analogues And Biophysical Studies of Their DNA/RNA Properties**” submitted for the degree of *Doctor of Philosophy* in *Chemistry* to the University of Pune has not been submitted by me to any other university or institution. This work was carried out at the National Chemical Laboratory, Pune, India.

(Raman Vysabhatar)

National Chemical Laboratory
Pune 411 008.

March, 2008

ACKNOWLEDGEMENT

MathrudevoBhava, PithrudevoBhava, Acharyadevobhava

First of all I want to express my sincere and profound thanks to my parents Sri S. V. Narasimha Bhattar and Smt. Udaya Sree, in bringing me up to become “The complete man”.

It gives me an immense pleasure to express my deep sense of gratitude towards my *Guruji* (research guide) Prof. K. N. Ganesh for all the advice, guidance, support and encouragement during every stage of this work. He made me realize the importance of doing quality research, in a better way at crucial stage of my career.

My special thanks to Dr. V. A. Kumar and Mrs. Anita Gunjal for their help and encouragement during the course of this work. I am also thankful to Mrs. M. V. Mane and Mrs. S. S. Kunte for HPLC analysis, Mrs. Shantakumari and Dr. Mahesh kulkarni for mass analysis. The kind support from NMR group is greatly acknowledged and thanks to Dr. Rajmohanan, Dr. usha palgune and Mrs. Kavitha.

I thank Dr. Pradeep Pallan, Dr. Ramesh Babu, Dr. Meena Sharma, Dr. Moneesha, Dr. Nagamani, Dr. Pallavi, Dr. Nagendra, Dr. Dinesh, Dr. Govind, Dr. Praveen, Dr. Umashankara, Dr. Gourishankar, Madhuri, Smita, Dr. Sunil, Khirud, Patwa, Ashwini, Sreedhar, Geetali, Nasreen, Satish, Roopa, Manaswini, Pradnya, Sachin, Mahesh, Seema, Parameshwar, Namratha and Harshal. I also thank Pawar and Bhumkar for their assistance. I thank to the research group of Dr. A. R. A. S. Deshmukh and Dr. Gumaste.

My sincere thank goes to my guru *Sri Nagavalli Vasudeva Reddy*, who taught me organic chemistry.

My sincere thank to the members of the families of Venkata Bhattar, Narasimha Bhattar, Vagvijiya Bhattar, A.V. Acharya, A. Narasimhacharya and Chandamarutha Bhattar. I would like to take the opportunity to thank Vedagopuram Ramachary, Madusoodana Bhattar and M. N. Acharya. I would like to acknowledge my *ardhangi* Sripriya for her support at the final stage of this work.

I express special gratitude to Razmannar, for his support during my Ph. D and I extend it to Venu *bava*, Prasad *babai* and Raju *annayya* and Bhoj *anna*.

My special thanks to D. Srinivas *anna* and Pallavi *vodina*, *Megastar* Suresha Sunil *anna* and Veena *vodina*, Swaroop, Rajender Reddy and Yogitha, Dr. Uma *akka* for their constant support for during the course of this work.

I am very much thankful to my great friends, *Megastar* Suresha, Prakasha Reddy, Swarnendo, Swaroop, Kosgi, Rajender, Srikanth, Satyanarayana Reddy, Raju, Murali, Abhijeet, Nageswar Reddy, Raghupathi, Shiva, Srinivasa Rao Naidu, Nookaraju, Bhargava, Chandra Kiran, Srinivas, Indu, Bala, Atul, Kishore, Srikanth (Bio), Venkateshan, Rambabu, Ramesh, Vilas, Sreenu, Santosh, Giri, Ravi, who made cheerful and pleasant atmosphere in and around NCL.

I thank to my elder friends at NCL, Dr. Gnaneshwar, Vasudeva Naidu, Dr. Praveen, Ch., Dr. Maheshwar, Mallikarjun and others for their scientific and emotional support.

I am very glad to express my thanks to Kannada Group, Umashankara, Bennur *anna*, Govind, Prasanna *Ravare*, Manje gowda, Satish, Shashidhar (bio), Nagaraju, Sumanth and others.

It is great pleasure for me to thank families of my childhood friends, Rambabu, Muthoju Kiran, Partha Saradhi, Naveen, Shyam, Anil, Vinay, Rajaneekar, Bommakanti, Surender, Gopi and lots of others, whose wishes and blessings which were always with me.

I am very much thankful to my source of inspiration, Neela and Kishore.

I thank K. Kiran Kumar, Srimannarayana, Swapna, Janardhana Chary, Ahmed. M.D., Srinivasa Reddy, Yella Reddy, Rakesh, Radha Krishna and others for their constant support, during my Ph. D.

I thank director NCL, for allowing me to work in this premier institute, providing the infrastructure. It is my sincere thanks to CSIR, New Delhi, for the financial support

Raman Vysabhatar.

ABBREVIATIONS

β -ala	β -alanine
A	Adenine
aeg	Aminothylglycine
aep	Aminoethylprolyl
ala	Alanine
amp	Aminomethyl prolyl
ap	Antiparallel
Boc Tert.	butyloxycarbonyl
C	Cytosine
Cbz	benzyloxy carbonyl
CD	Circular Dichroism
dA	Deoxy adenine
DCC	Dicyclohexylcarbodiimide
DCM	Dichloromethane
dG	2'-deoxyguanine
DIPEA	Diisopropylethylamine
DMF	N,N-Dimethylformamide
DNA	2'-deoxyribonucleic acid
ds	Double stranded
FPLC	Fast Protein Liquid Chromatography
g	Gram
G	Guanine
gly	Glycine
h	Hours
HBTU	<i>O</i> -(1H-Benzotriazol-1-yl) <i>N,N,N</i> l, <i>N</i> l-tetramethyluronium hexafluorophosphate
HOBt	1-Hydroxybenztriazole
HPLC	High Performance Liquid Chromatography
Hz	Hertz
IR	Infra red
ITC	Isothermal Titration Calorimetry
Lys	L-Lysine
MALDI-TOF	Matrix Assisted Laser Desorption Ionisation-Time Of Flight
MF	Merrifield Resin
MBHA	4-Methyl benzhydryl amine
mg	Milligram
MHz	Megahertz
M	Molar
μ M	Micromolar
ml	Milliliter
mmol	Millimoles

N	Normal
nm	Nanometer
NMP	N-methyl pyrrolidine
NMR	Nuclear Magnetic Resonance
ONs	Oligonucleotides
p	Parallel
PCR	Polymerase Chain Reaction
PPh ₃	Triphenyl phosphine
PNA	Peptide Nucleic Acid
Pro	Proline
Pyr	pyrrolidinone
RNA	Ribonucleic acid
r.t.	Room temperature
ss	Single strand/ Single stranded
s	Seconds
T	Thymine
TBTU	<i>O</i> -(1H-Benzotriazol-1-yl) <i>N,N,N</i> ₁ <i>N</i> ₁ -tetramethyl uronium tetrafluoroborate
TEA	Triethylamine
TFA	Trifluoroacetic acid
TFMSA	Trifluoromethanesulphonic acid
THF	Tetrahydrofuran
UV-Vis	Ultraviolet- Visible

CONTENTS

	Title	Page No.
PUBLICATIONS		i
ABSTRACT		ii
CHAPTER 1	INTRODUCTION	
1.1	Nucleic Acids: Chemical Structure	1
1.2	Oligonucleotide as therapeutic agents	2
1.3	Chemical Modifications of DNA	4
1.3.1	Nucleobase modifications and duplex/triplex stability	5
1.3.1a	Stacking and Hydrophobicity Contributions	5
1.3.1b	Hoogsteen base pairing	5
1.3.1c	Modified nucleobases stabilize duplex/triplex	7
1.3.1d	Modifications that increase hydrogen bonding and staking interactions	8
1.3.1e	Functionalities enhancing hydrogen bonding potentials	9
1.3.1f	Stabilization of triplex through electrostatic forces	9
1.3.1g	Modifications that form Hoogsteen hydrogen bonding:	10
1.3.2	Phosphate modified linkages	11
1.3.3	Sugar modifications	12
1.3.3a	Sugar skeleton modifications	12
1.3.3b	Carbocyclic nucleic acids	13
1.3.3c	Locked nucleic acids (LNA)	14
1.3.3d	Morpholino nucleosides	15
1.4	Peptide Nucleic Acid	16
1.4.1	Introduction	16
1.4.2	Triplex formation with complementary DNA and RNA	17
1.4.3	Duplex formation with complementary DNA and RNA	18
1.4.4	Structure of PNA complexes	19
1.4.4a	Structure of PNA-DNA/PNA-RNA duplexes	19
1.4.4b	Structure of PNA ₂ -DNA triplexes	20
1.4.5	Disadvantages of PNA	21
1.4.6	Chemical Modifications of PNA	21
1.4.6a	Introduction of cationic functional groups into the PNA	22
1.4.6b	Construction of bridged structures	23

1.4.6c	Morpholino PNA	25
1.4.7	PNA analogues with modified nucleobases	26
1.4.7a	Modified Nucleobases with larger surface area	26
1.4.7b	G-clamp as modified nucleobase	27
1.4.7c	Modified nucleobase with additional hydrogen bonding sites	28
1.4.7d	Fluorescent moieties used as modified nucleobases	30
1.4.7e	Universal bases	31
1.4.7f	Non-heterocyclic aromatic bases	32
1.4.7g	Nucleobase replacement with non-aromatics	33
1.5	Present work	33
1.6	Reference	35

CHAPTER 2 Synthesis and Characterization of Cyanuryl PNA and 8-Substituted Adeninyl PNA

2.1	Introduction	43
2.2	Rationale design behind the work	
2.2.1	Importance of cyanuric acid as a modified nucleobase	46
2.2.2	Biological relevance of cyanuryl nucleoside	48
2.2.3	Importance of 8-aminoadenine as a modified nucleobase	49
2.2.4	Biological relevance of 8-aminoadenosine	51
2.3	Objectives	51
2.3.1	Synthesis of cyanuryl PNA monomer	52
2.3.1a	Cyanuryl ring construction followed by monomer synthesis	53
2.3.1b	Alkylation of cyanuric acid with ethylbromoacetate/bromoacetic acid	54
2.3.1c	Alkylation of cyanuric acid with PNA backbone	56
2.3.2	Synthesis of 8-bromoadeninyl PNA monomer	58
2.3.3	Synthesis of <i>aeg</i> PNA monomers ($A^Z/G/C^Z/T$)	60
2.3.4	Site specific incorporation of base modified PNA monomers into PNA oligomers	64
2.3.4a	Solid Phase Peptide Synthesis	64
2.3.4b	Protocols	65
2.3.4c	Synthesis of cyanuryl/8-bromoadeninyl PNA oligomers	69
2.3.5	Conversion of 8-bromoadeninyl PNA oligomers to 8-aminoadeninyl PNA oligomers	70
2.3.6	Purine-Pyrimidine Mix Sequences	75
2.3.7	Cleavage of the PNA oligomers from solid support, purification and characterization	75

2.4	Synthesis of Complementary Oligonucleotides	78
2.5	Conclusions	79
2.6	Experimental details	80
2.6.1	General	80
2.6.2	Functionalization of MBHA resin	90
2.6.3	Picric acid assay for the estimation of the amino acid loading	90
2.6.4	Cleavage of the PNA oligomers from the solid support	91
2.6.5	Purification of the PNA oligomers	91
2.7	Reference	93
2.8	Appendix	99

CHAPTER 3 Biophysical Studies of Cyanuryl PNA and 8-Substituted Adeniny PNA

3.1	Introduction to Biophysical techniques	119
3.1.1	Circular Dichroism Spectroscopy	119
3.1.2	CD spectroscopy of PNA:DNA triplexes	120
3.1.3	Binding Stoichiometry of PNA:DNA complexes	122
3.1.4	Binding stoichiometry through UV-mixing curves (Job's plot)	123
3.1.5	UV-Spectroscopic study of PNA:DNA complexes	124
	RESULTS AND DISCUSSION	125
3.2	Biophysical studies of cyanuryl PNA	125
3.2.1	Establishment of binding stoichiometry of cyanuryl PNA with <i>c</i> DNA	125
3.2.2	UV-Melting studies of cyanuryl PNA ₂ :DNA complexes	126
3.2.3	UV-Melting studies of cyanuryl PNA complexes with complementary DNA	126
3.2.4	UV-Melting studies of cyanuryl PNA complexes with mismatch DNA	128
3.3	Biophysical studies of adenine containing-PNAT ₈ (H-T _n AT _m -LysNH ₂)	130
3.3.1	UV-Melting studies of adenine containing PNA ₂ :DNA complexes	130
3.4	Biophysical studies of 8-bromo/aminoadeniny PNA	132
3.4.1	Establishment of binding stoichiometry of 8-bromo/aminoadeniny PNA with <i>c</i> DNA	132
3.4.2	UV-Melting studies of 8-bromo/aminoadeniny PNA ₂ :DNA complexes	133
3.5	UV-Melting studies of adeniny/8-bromo	138

	adeninyl/8-aminoadeninyl PNA complexes with mismatch DNA	
3.6	UV- T_m studies of cyanuril/8-bromoadeninyl/8- aminoadeninyl PNA:DNA Duplexes (parallel/antiparallel)	140
3.7	Discussion	142
3.8	3.8 Binding stoichiometry of 8-bromoadeninyl PNA and 3',5'-O-disilyl thymidine/ thymidinyl PNA monomers through NMR titrimetry	143
	3.8.2 Rationale design behind the work	144
	3.8.3 Complexation titrimetry for evaluation of binding constants through NMR studies:	145
	3.8.4 Experimental method of NMR titrimetry	145
	3.8.5 Calculation of Binding Constant Through NMR Titration Method	154
3.9	General Experimental Procedure of Biophysical studies	155
	3.9.1 UV studies	155
	3.9.2 UV- T_m studies	155
	3.9.3 Circular Dichroism	156
	3.9.4 Job's plot through Circular Dichroism	156
	3.9.5 Job's plot through UV-mixing curves	157
	3.9.6 NMR titration experiment	157
3.10	Conclusions	158
3.11	References	160

LIST OF PUBLICATIONS

1. Cyanuryl Peptide Nucleic Acid: Synthesis and DNA Complexation Properties
Vysabhatter, R.; Ganesh, K. N., *Tetrahedron Lett.* **2008**, *49*, 1314–1318.
2. Property Ending of Peptide Nucleic Acids (PNA): gem-dimethyl, Cyanuryl and 8-Amino adenine PNAs
Ganesh, K. N.; Goruishankar, A.; **Vysabhatter, R.**; Bokil, P. *Nucleic Acids Symp Ser* **2007**, *51*, 17-18.
3. A novel *In-situ* conversion of 8-bromoadeninylyl PNA oligomers into 8-sustituted adeninylyl PNA oligomers
Raman Vysabhatter and Krishna N. Ganesh (Manuscript under preparation for *Tetrahedron Letters*)
4. 8-Substituted adeninylyl Peptide Nucleic Acids: Synthesis and DNA complexation properties
Raman Vysabhatter and Krishna N. Ganesh (Manuscript under preparation for *Tetrahedron*)

ABSTRACT

The thesis entitled “**Synthesis of Cyanuryl, 8-substituted AdeninyI PNA Analogues and Biophysical Studies of Their DNA/RNA Hybridisation Properties**” is divided into three following chapters, as follows.

Chapter-1: This introduces the background literature for undertaking the present research work.

Chapter-2: This chapter describes synthesis of cyanuryl, 8-bromoadeninyI PNA monomers and the synthesis of cyanuryl, 8-bromodeninyI, and 8-aminoadeninyI PNA oligomers for hybridisational studies with complementary DNA. These PNA oligomers were characterized by HPLC and MALDI-TOF mass spectroscopy.

Chapter-3: This chapter reports about the biophysical studies of cyanuryl PNA, 8-bromoadeninyI PNA, 8-aminoadeninyI PNA with complementary DNA. The binding stoichiometry between modified 8-bromoadeninyI PNA monomer and 3',5'-di-O-silyldeoxyribothymidine/thymidinyI PNA were studied through NMR titration experiment.

Chapter 1: Introduction

Employing the potential of DNA as antigene and antisense agent has led to the evolution and synthesis of a number of its analogues. Unmodified oligonucleotides suffer from poor resistance to cellular enzymes and the negative charge of the phosphodiester linkage affects its cell permeability as well the binding efficacy to the complementary sequences. Hence chemical modifications are needed to make oligonucleotides as effective therapeutic agents in biological systems and to understand the structural changes in the oligonucleotides incorporating them. Nucleobase, sugar ring and the phosphate backbone are the three possible chemical sites to induce modifications.

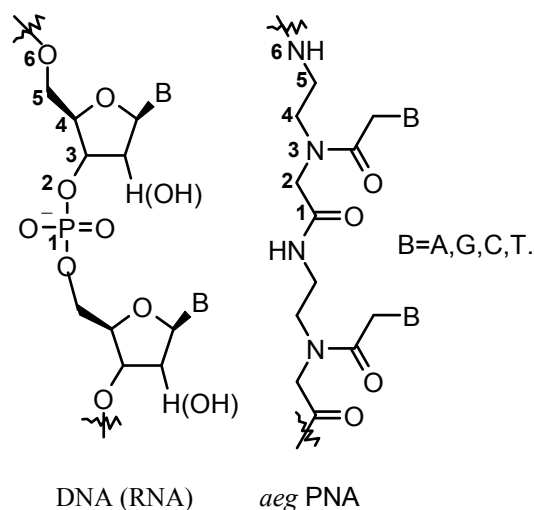


Figure1: DNA(RNA) and PNA structures

Among the innumerable DNA mimics, PNA (peptide nucleic acid) (Figure 1) was found to mimic many of the oligonucleotide properties. The repeating unit of PNA consists of N-(1- aminoethyl)-glycine unit linked by amide bonds. The nucleobases are attached to the backbone through methylene carbonyl linkages. These make PNA neutral, achiral and homomorphous to DNA. PNA is also resistant to cellular enzymes (proteases, nucleases) and possesses strong affinity towards complementary DNA/RNA. PNA oligomers bind strongly to complementary DNA by Watson-Crick and Hoogsteen bonding to form duplexes and triple helices that are much more stable than the corresponding DNA-DNA hybrids. The unique character of PNA is to bind duplex DNA by strand invasion and form both parallel and antiparallel (N-terminus of PNA to 5' end of the DNA; C-terminus to 3' end respectively) complexes. In contrast to homopyrimidine sequences, mixed sequences of PNA bind to complementary DNA/RNA with 1:1 stoichiometry to form duplexes.

However, major limitations for the therapeutic application of PNAs are their poor aqueous solubility due to self aggregation, insufficient cellular uptake and ambiguity in orientation selectivity of binding. The possibility of rotamers due to tertiary amide linkage of nucleobase attachment to PNA backbone (Figure 2) leads to *n*-number of different conformations and among these, only a few are potent for hybridization with corresponding complementary oligonucleotide.

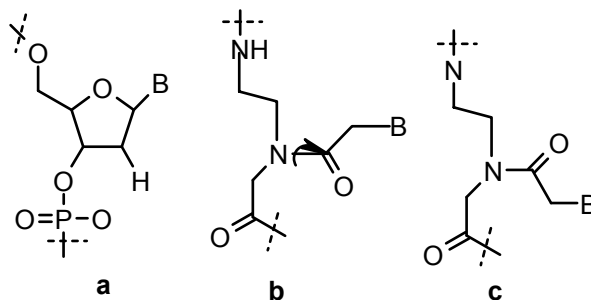


Figure 2. Structures (a) DNA, (b) PNA, and (b, c) rotamers of *aeg* PNA along *tert.* amide bond

To overcome these drawbacks, several modifications have been attempted e.g. introduction of chirality in the PNA backbone to impart orientational preferences, attachment of polycationic ligands such as polylysine, spermine to the *C*-terminus of the PNA to improve solubility. Search for the functional synthetic PNA analogs remain a continuing area of research. This introduction section briefly reviews the recent advancements in the area of chemistry of peptide nucleic acids.

Chapter 2: Synthesis and Characterization of Cyanuryl PNA, 8-Substituted Adeniny PNA

To overcome the problems associated with PNA, there is considerable interest in chemical modifications of PNA. Much of the modifications of PNA are centered on changing the structure of backbone and new opportunities remain to be explored through modification of the heterocyclic base.

A basic requirement for triplex formation is that the central base of the triad must be able to form hydrogen bonds from either the sides.⁵ Research has been carried out in this direction towards modified base to increase the hydrogen bonding sites on nucleobases.

Cyanuric acid and 8-aminoadenine are well suited for such purposes as pyrimidine and purine mimics since, these have potential to form hydrogen bonding from both sides (Figure 3). Cyanuric acid, a six-membered cyclic imide with alternate arrangement of hydrogen bond donors and acceptors is potentially well suited for such a purpose (Figure 3). This feature may lead them to form stable triplexes and duplexes.

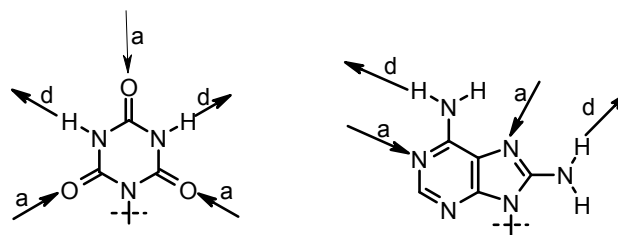


Figure 3: The hydrogen bonding sites on *N*-alkyl cyanuric acid and *N*⁹-alkyl 8-aminoadenine (a=hydrogen bond acceptor, d=hydrogen bond donor)

Introducing amino group at C-8 position of adenine increases the stability of triple helix due to combined effect of the gain of one Hoogsteen purine-pyrimidine hydrogen bond (Figure 4) and the propensity of the amino group to be integrated into the ‘spine of hydration’ located in the minor-major groove of the triplex structure.

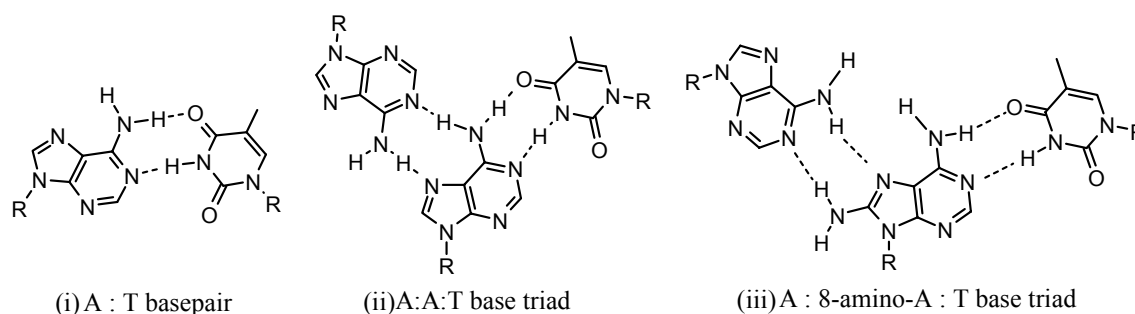


Figure 4: Hydrogen bonding in (i) adenine-thymine base pair and (ii) adenine-adenine-thymine base triad (iii) adenine: 8-amino adenine: thymine base triad

2.1 Synthesis of cyanuryl PNA and 8-bromoadeninyl PNA monomers

The above resume on cyanuric acid and 8-aminoadenine prompted the synthesis of cyanuryl PNA (Figure 5a) and 8-aminoadeninyl PNA. 8-Bromoadeninyl PNA (Figure 5b) used as synthetic precursor for the synthesis of 8-aminoadeninyl PNA.

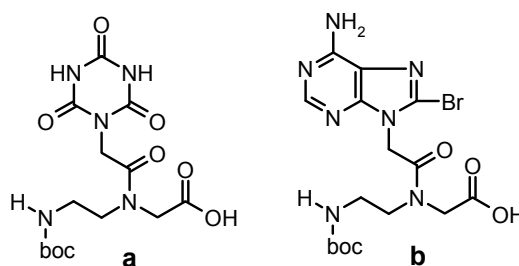
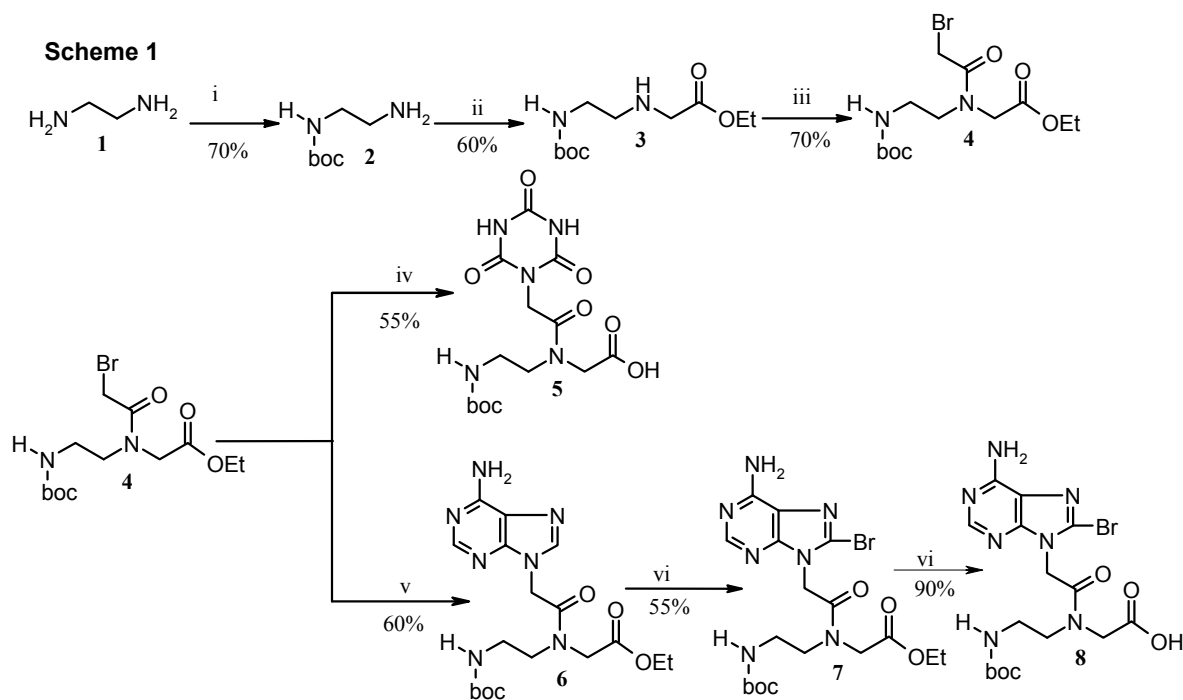


Figure 5: Structures of (a) cyanuryl PNA monomer (b) 8-bromoadeninyl PNA monomer

Ethylenediamine was reacted with Boc_2O with high dilution in THF at ice temperature yielded *N*-Boc-ethylenediamine **2**, which upon alkylation with ethylbromoacetate in acetonitrile and triethylamine afforded ester **3**. Compound **3** upon treatment with bromoacetyl chloride in DCM, triethylamine yielded bromo derivative **4**.

Cyanuric acid reacted with compound **4** in presence of K_2CO_3 in DMSO, followed by ester hydrolysis with aq. LiOH afforded respective cyanuryl PNA monomer **5** (Scheme 1). Adenine reacted with compound **4** in presence of K_2CO_3 in DMSO, to give appropriated protected adeninyl *aeg* PNA monomer **6**, which upon bromination with molecular bromine in dioxane and 10% Na_2HPO_4 yielded the required compound **7** with good yield (55%). The hydrolysis of ester followed by neutralization yielded 8-bromoadeninyl PNA monomer (**8**) (Scheme 1), which can be used for coupling in solid phase peptide synthesis.



Reagents: (i) Boc_2O , THF; (ii) Ethylbromoacetate, Et_3N , acetonitrile; (iii) Bromoacetyl chloride, Et_3N , DCM; (iv) (a) Cyanuric acid, K_2CO_3 , DMSO; (b) aq. LiOH, methanol (iv) adenine, K_2CO_3 , DMF; (v)(a) Br_2 , dioxane; 10% Na_2HPO_4 ; (b) aq. LiOH, methanol

2.2 Site specific incorporation of cyanuryl PNA monomer and 8-bromoadeninyl PNA monomer into PNA oligomers

The protected PNA monomers of cyanuric acid (**5**) and 8-bromoadenine (**8**) were synthesized and incorporated at specific sites in *aeg* PNA- T_8 using solid phase peptide synthesis protocols, on L-lysine derived (4-methyl benzhydryl) amine (MBHA) resin with *boc* chemistry strategy (Figure 6).¹⁵ Amination of 8-bromoadeninyl PNA (**4**) on solid support yielded 8-aminoadeninyl (**a**) PNA oligomers. The oligomers were cleaved from the solid support using trifluoromethanesulphonic acid (TFMSA) in the presence of trifluoroacetic acid (TFA) (“Low, High TFMSA-TFA method”), which yielded the oligomers with amides at their C-termini. All the cleaved oligomers were subjected to initial gel filtration, subsequently purified by HPLC and characterized by MALDI-TOF mass spectroscopy.

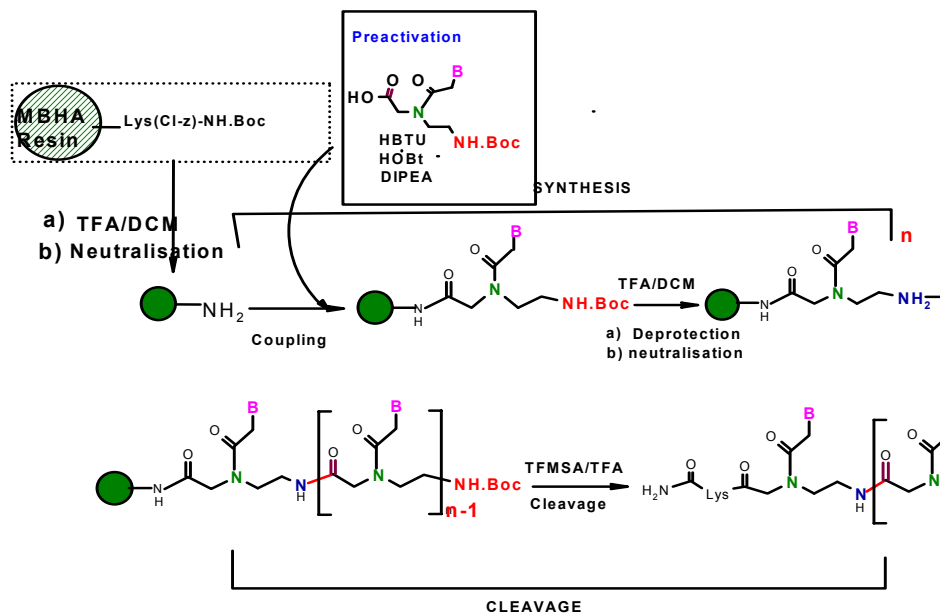


Figure 6: Schematic representation of solid phase peptide synthesis and cleavage

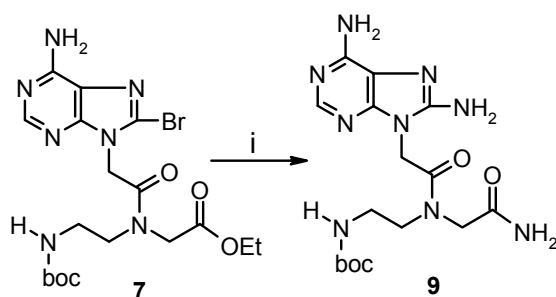
2.3 Synthesis of 8-aminoadeninyl PNA oligomers

2.3.1 Attempts towards the synthesis of 8-aminoadeninyl PNA monomers

The main objective of the work is synthesis of cyanuryl PNA and 8-aminoadeninyl PNA. 8-bromoadeninyl PNA monomer (**7**) may be used as a synthetic precursor for the synthesis of 8-aminoadeninyl PNA monomer (Figure 7a), to avoid use of interfering protecting groups for amino group at C-8 position of 8-aminoadenine.

8-Bromoadeninyl PNA monomer **7**, when treated with *aq.* ammonia, yielded 8-aminoadeninyl PNA monomer with carboxy amide functionality **9**, (instead of ester functionality) which is undesirable for present application (Scheme 2).

Scheme 2



Reagents: (i) *aq.* ammonia, methanol

As mentioned, the protecting group selection for the amino at C-8 position of adenine is fairly difficult, because of its guanidinium character (Figure 7a). According to earlier reports¹⁶ amino at C-8 position can be protected as Schiff's base with dimethylaminoformamide dimethylacetal ($\text{Me}_2\text{N-CH(OMe)}_2$) (Figure 7b) but this group is not compatible with solid phase peptide synthesis protocols, where 50% TFA in DCM is used for the deprotection of 'boc' group.

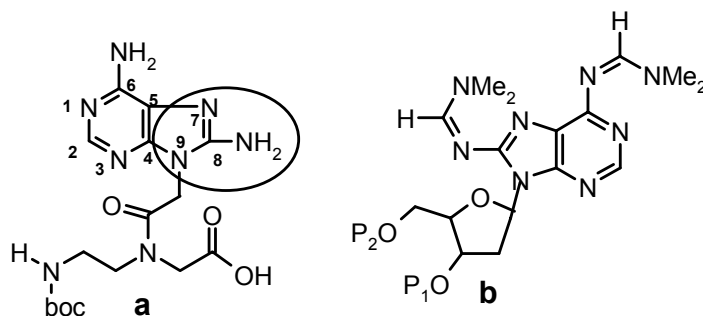
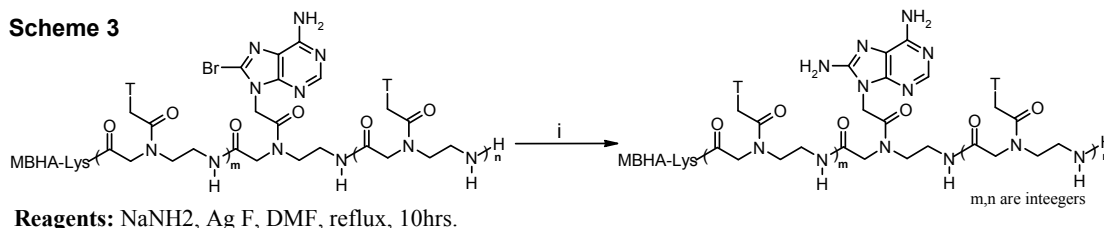


Figure 7: structure of (a) 8-aminoadeninyl PNA monomer (b) protected 8-aminoadenosine

2.3.2 Conversion of 8-bromoadeninyl PNA oligomers to 8-substituted adeninyl PNA oligomers

Since problems occurred in finding a suitable protecting group for 8-amino function in 8-aminoadenine at monomeric level, the direct conversion of 8-bromoadenine PNA oligomers to 8-aminoadenine oligomers was attempted on solid support.



8-Bromoadeninyl PNA oligomer was reacted with sodamide/THF under reflux conditions to yield the corresponding 8-aminoadeninyl PNA oligomers. However, this reaction did not work satisfactorily with all PNA oligomers the containing 8-bromo adenine. The reaction conditions were modified by addition of silver fluoride to facilitate the removal of bromine by silver and make it more labile for amination (Scheme 3). These reactions were carried out on the 8-bromoadeninyl PNA oligomers bound to the resin (Table 1) and the reaction completion was monitored by HPLC, after the PNA cleavage from the resin and confirmed by MALDI-TOF spectroscopy

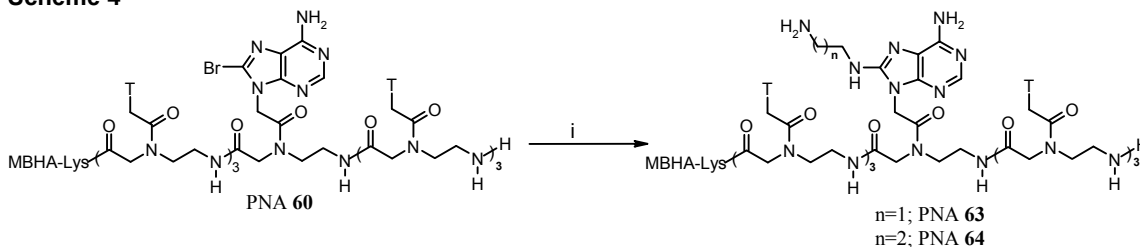
Table 1: Conversion of 8-bromoadeninyl PNA to 8-aminoadeninyl PNA

Sl. No.	8-bromoadeninyl PNA oligomer (Reactant)	8-aminoadeninyl PNA oligomer (Product)
1	HATTTTTTTT-Lys-NH ₂	H-aTTTTTTTT -Lys-NH ₂
2	H-TTTTTTTT A-Lys-NH ₂	H-TTTTTTTT a-Lys-NH ₂
3	H-TTTTATTT-Lys-NH ₂	H-TTTT aTTT-Lys-NH ₂
4	H-ATTT ATTT-Lys-NH ₂	H-aTTT aTTT-Lys-NH ₂
5	H-GTAGATCACT-Lys-NH ₂	H-GT aGaTCaCT-Lys-NH ₂

A= 8-bromoadeninyl PNA; a= 8-aminoadeninyl PNA

The diversity in the reaction of 8-bromoadeninyl PNA into different 8-aminosubstituted adeninyl PNA on solid supported oligomers was explored. The MBHA resin supported 8-bromoadeninyl PNA oligomer PNA 60, was individually treated with 1,2-diaminoethane and 1,3-diamino propane under reflux conditions (Scheme 4).

Scheme 4



Reagents: Ethylenediamine or 1,3 diamino propane, reflux, 16 hr.

These reactions were carried out on the 8-bromoadeninyl PNA oligomers bound to the resin and the reaction completion was monitored by HPLC, after the PNA cleavage from the resin and confirmed by MALDI-TOF mass spectroscopy

All the purified PNA oligomers are characterized by MALDI-TOF mass spectroscopy.

Table 2: HPLC and MALDI-TOF mass spectral analysis of synthesized PNAs

Entry no.	Sequence	Calculated mass (HRMS)	Observed mass
PNA 69	H-TTTTTTTT-Lys-NH ₂	2273.93	2275.24
PNA 70	H-CyTTTTTTT-Lys-NH ₂	2276.91	2300.64(M ⁺ +Na)
PNA 71	H-TTTTTTTTCy-Lys-NH ₂	2276.91	2276.62
PNA 72	H-TTTTCyTTT-Lys-NH ₂	2276.91	2280.34
PNA 73	H-CyTTTCyTTT-Lys-NH ₂	2279.88	2301.56(M ⁺ +Na)
PNA 74	H <u>A</u> TTTTTTT Lys-NH ₂	2282.95	2281.32
PNA 75	H-TTTTTTT <u>A</u> Lys-NH ₂	2282.95	2284.84
PNA 76	H-TTTT <u>A</u> TTT-Lys-NH ₂	2282.95	2305.27(M ⁺ +Na)
PNA 77	H- <u>A</u> TTT <u>A</u> TTT-Lys-NH ₂	2291.96	2293.13
PNA 78	H <u>A</u> TTTTTTT Lys-NH ₂	2360.85	2364.68
PNA 79	H-TTTTTTT <u>A</u> Lys-NH ₂	2360.85	2364.68
PNA 80	H-TTTT <u>A</u> TTT-Lys-NH ₂	2360.85	2363.88
PNA 81	H- <u>A</u> TTT <u>A</u> TTT-Lys-NH ₂	2447.78	2452.79
PNA 82	H- <u>a</u> TTTTTTT -Lys-NH ₂	2297.96	2300.84
PNA 83	H-TTTTTTT <u>a</u> -Lys-NH ₂	2297.96	2297.68
PNA 84	H-TTTT <u>a</u> TTT-Lys-NH ₂	2297.96	2300.11
PNA 85	H- <u>a</u> TTT <u>a</u> TTT-Lys-NH ₂	2321.98	2320.91
PNA 86	H-GT <u>A</u> G <u>A</u> TC <u>A</u> CT-Lys-NH ₂	2852.52	2856.08
PNA 87	H-GCy <u>A</u> G <u>A</u> CyC <u>A</u> CCy-Lys-NH ₂	2861.45	2863.28
PNA 88	H-GT <u>A</u> G <u>A</u> TC <u>A</u> CT-Lys-NH ₂	3089.85	3093.7
PNA 89	H-GT <u>a</u> G <u>a</u> TC <u>a</u> CT-Lys-NH ₂	2897.6	2899.64
PNA 90	H-TTTT <u>A'</u> TTT-Lys-NH ₂	2339.96	2338.39
PNA 91	H-TTTT <u>A''</u> TTT-Lys-NH ₂	2354.96	2360.09

A/G/C/T = PNA monomers of adenine/guanine/cytosine/thymine; *Cya*= cyanuryl PNA monomer; *A* = 8-bromoadeninylyl PNA monomer, *a* = 8-aminoadeninylyl PNA monomer, *A'*= 8-(aminoethyl)aminoadeninylyl PNA and *A''* = 8-(3-amino ethyl) aminoadeninylyl PNA

Chapter 3: Biophysical Studies of Cyanuryl PNA and 8-Substituted Adeninylyl PNA

Biophysics is an interdisciplinary field in which the techniques from the physical sciences are applied to understand the biological structure and function. The biophysical techniques are useful in studying structure and properties of nucleic acids, proteins, peptides and their analogues.

In this chapter, the binding selectivity and specificity of modified nucleobase containing PNAs towards complementary DNA has been investigated using the biophysical techniques Circular Dichroism Spectroscopy (CD spectroscopy) and temperature dependent UV-spectroscopy (UV- T_m studies). The stoichiometry of the PNA:DNA complexes was determined using Job's method. The UV-melting studies were carried out with all modified PNA:DNA complexes and analyzed with respect to that of control PNA:DNA complexes. These give information on the stability of the complexes of modified PNAs with DNA.

3.1 Determining the stoichiometry between 8-bromo/aminoadeninylyl PNA and thymidine/thyminylyl PNA

The binding stoichiometry of PNA:DNA was determined by the continuous stoichiometry variation method. Keeping the total concentration constant, a series of mixtures having different relative molar equivalent amounts of PNA and DNA were generated and the CD spectra at different molar ratios showed an isodichroic point at around 265 nm (Figure 8A&B). This systematic changes in the CD spectral features upon variable stoichiometric mixing of PNA and DNA components was used to generate Job's plot which indicated a binding ratio of 2:1 for the PNA:DNA complexes, confirming the formation of triplexes.

The UV absorbance of each sample was recorded at 260nm. The stoichiometry of complexation is derived from absorbance with respect to mole fraction, from the obtained

minimum (Figure 8C). It was found that the stoichiometry of PNA: DNA complexation is 2:1.

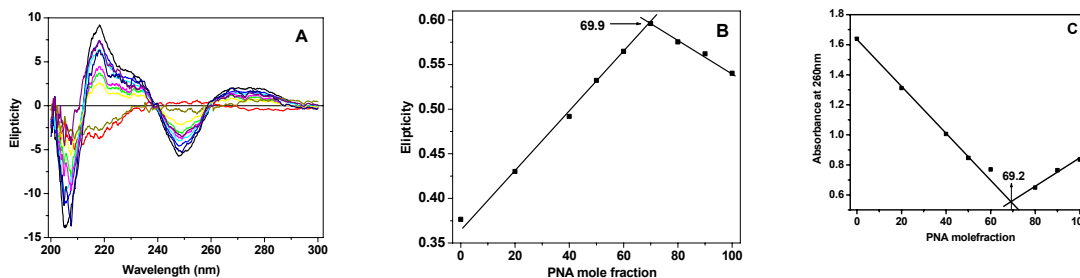


Figure 8: A) CD-curves for PNA **79**, H-TTTTTT4-Lys-NH₂ and the complementary DNA **93** d(GCTA₇CG) mixtures in the molar ratios of 0:100, 20:80, 40:60, 50:50, 60:40, 70:30, 80:20, 90:10, 100:0 (Buffer, 10 mM Sodium phosphate pH 7.0, 100 mM NaCl, 0.1 mM EDTA), B) CD-Job plot corresponding to 255 nm, C) UV-job plot corresponding to above mixtures of different molar ratios, absorbance recorded at 260 nm.

3.2 UV- T_m studies of PNA: DNA complexes

The stoichiometry of the PNA: DNA complex was first determined using Job's method, prior to investigate the binding selectivity towards complementary DNA. The UV- melting studies were carried out with all the synthesized oligomers and the melting temperature (T_m) data was compared with the control PNA:DNA complexes.

- (i) UV- T_m studies of *cyanuryl* PNA-DNA complexes
- (ii) UV- T_m studies of *8-bromoadeniny*l PNA-DNA complexes
- (iii) UV- T_m studies of *8-aminoadeniny*l PNA-DNA complexes

Various synthesized cyanuryl, 8-bromoadeniny and 8-aminoadeniny PNA oligomers (PNA **69-89**) were used to investigate the binding efficiency towards complementary DNA. The UV-melting studies were carried out and the T_m data was compared with that of control *aeg* PNA-T₈. The CD spectra of all PNA single strands and the corresponding complexes with complementary DNA were recorded.

3.2.1 UV- T_m studies of *cyanuryl* PNA-DNA complexes

The complexes of *aeg* PNA-T₈ (PNA **69**) with complementary DNA gave melting temperature of 44.6 °C. Among the modified oligomers of cyanuryl PNA, PNA **71** (*C-terminus modification*) stabilized the PNA₂:DNA triplex by 23.2 °C. (Entry **3**), PNA **72** (*middle modification*) stabilized the corresponding triplex by 19.5 °C, while PNA **70** (*N-*

terminus modification) destabilized the triplex by 10.4 °C. Since PNA **72** having modification in middle stabilized the corresponding PNA₂:DNA hybrid, PNA **73** having two modifications (*with N-terminus and middle modification*) still forms triplex with stability as good as the control PNA **69**.

Table 1: UV-Melting temperatures (T_m values in °C)^a of cyPNA₂:DNA triplexes

Entry No	Triplex (PNA ₂ :DNA)	T_m (°C) PNA ₂ :c DNA triplex	ΔT_m (°C)	ΔT_m (°C)/ modification
1	PNA 69 , H ₂ N-Lys-TTTTTTTT- H DNA 92 5'CG-AAAAAAAAA-GC3' PNA 69 H-TTTTTTTT-Lys-NH ₂	44.6	--	--
2	PNA 70 , H ₂ N-Lys-TTTTTTTT Cya - H DNA 92 5'CG-AAAAAAAAA-GC3' PNA 70 , H- Cya TTTTTTTT-Lys-NH ₂	34.2	-10.4	-5.2
3	PNA 71 , H ₂ N-Lys- Cya TTTTTTTT- H DNA 92 5'CG-AAAAAAAAA-GC3' PNA 71 , H-TTTTTTTT Cya -Lys-NH ₂	67.8	+23.2	+11.6
4	PNA 72 , H ₂ N-Lys-TTTC Cya TTTT- H DNA 92 5'CG-AAAAAAAAA-GC3' PNA 72 , H-TTTC Cya TTTT-Lys-NH ₂	56.7	+12.1	+6.0
5	PNA 73 , H ₂ N-Lys-TTTC Cya TTTC Cya - H DNA 92 5'CG-AAAAAAAAA-GC3' PNA 73 , H- Cya TTTC Cya TTT-Lys-NH ₂	44.2	-0.4	-0.2

T_m = melting temperature (measured in the buffer 10 mM sodium phosphate, 100 mM NaCl, pH = 7.3), PNA₂-DNA complexes. Values in the ΔT_m indicate the difference in T_m with the control experiment PNA **66**. The values reported here are the average of 3 independent experiments and are accurate to $\pm 0.5^\circ\text{C}$

3.2.1a UV-Melting studies of cyanuryl PNA complexes with mismatch DNA

The sequence specificity of PNA hybridization was examined through studying hybridization properties of PNA with DNA having single mismatch at middle, DNA **89** (Figure 7). The PNA₂:DNA complexes comprising control sequence (PNA **69**: DNA **96**) and the C- terminus modified cyanuryl PNA (PNA **71**: DNA **96**) were individually subjected for UV-melting (Figure 8). The control sequence PNA **69** formed triplex with single mismatch sequence (DNA **96**) with T_m lower by 9.6°C (entry 2, Table 2), while C-terminus modified cyanuryl PNA **71** exhibited destabilization by 13.2 °C. Cyanuryl PNA

thus showed a better sequence discrimination (entry 4, Table 2). The melting profiles were exhibited in figure 8.

Table 2: UV-Melting temperatures (T_m values in °C)^a of *cy*PNA₂:DNA triplexes

Entry No.	Triplex (PNA ₂ :DNA)	T_m (°C) PNA ₂ :c DNA triplex	ΔT_m (°C)	ΔT_m (°C)/ modification
1	PNA 69 , H ₂ N-Lys-TTTTTTTT- H DNA 92 5'CG-AAAAAAAAA-GC3' PNA 69 H-TTTTTTTT-Lys-NH ₂	44.6		
2	PNA 69 , H ₂ N-Lys-TTTT T TTT- H DNA 96 5'CG-AAAACAAA-GC3' PNA 69 H-TTTTTTTT-Lys-NH ₂	34.4	-10.2	-5.1
3	PNA 71 , H ₂ N-Lys- Cya TTTTTTT- H DNA 92 5'CG-AAAAAAAAA-GC3' PNA 71 , H-TTTTTTTT Cya -Lys-NH ₂	67.8		
4	PNA 71 , H ₂ N-Lys- Cya TTTTTTT- H DNA 96 5'CG-AAAACAAA-GC3' PNA 71 , H-TTTTTTTT Cya -Lys-NH ₂	54.5	-13.3	-6.6

^a T_m = melting temperature PNA₂:DNA complexes (measured in the buffer 10 mM sodium phosphate, 100 mM NaCl, pH = 7.3). Values in the parenthesis (ΔT_m) indicate the difference in T_m with the control experiment PNA **69**.

3.2.2 UV- T_m studies of 8-bromo/aminoadeninyl PNA-DNA complexes

Among the modified oligomers of 8-bromoadeninyl PNA (PNA **78-81**), PNA **78** (*N-terminus modification*) stabilized the corresponding triplex with 8.2 °C. PNA **79** (*C-terminus modification*) and PNA **81** (*N-terminus and middle modification*) stabilized the PNA₂: DNA triplexes by 4.8 °C and 7.7 °C respectively. However, PNA **80** with middle modification destabilized the hybrid by 10.0 °C.

Among the modified oligomers of 8-aminoadeninyl PNA (PNA **82-85**), PNA **83** (*C-terminus modification*) and PNA **84** (*middle modification*) stabilize the derived triplex by +9.3 °C and +30.8 °C, respectively PNA **82** (*N-terminus modification*) Bis modified PNA **85** (*N-terminus and middle modification*) destabilized the triplex by 25.0 °C and 6.5 °C respectively.

Table 3 UV- T_m s of adeninyl, 8-bromoadeninyl, 8-aminoadeninyl PNA oligomers with complementary DNA (according to modification position)

Entry No.	Triplex (PNA ₂ :DNA)	T_m (°C) PNA ₂ :c DNA triplex	ΔT_m (°C)	ΔT_m (°C)/ modification
<i>N</i> -Terminus modifications				
1	PNA 74 H ₂ N-Lys-TTTTTTT A -H	60.0	--	
	DNA 93 5'GCAAAAAAATCG3'			
	PNA 74 H A TTTTTTTTLys-NH ₂			
2	PNA 78 H ₂ N-Lys-TTTTTTT A -H	68.2	+8.2	+4.1
	DNA 93 5'GCAAAAAAATCG3'			
	PNA 74 H A TTTTTTTTLys-NH ₂			
3	PNA 82 H ₂ N-Lys-TTTTTTT a -H	35.0	-25.0	-12.5
	DNA 93 5'GCAAAAAAATCG3'			
	PNA 82 H a TTTTTTTTLys-NH ₂			
<i>C</i> -Terminus modifications				
4	PNA 75 H ₂ N-Lys- A TTTTTTTT-H	65.5	--	
	DNA 93 5'GCAAAAAAATCG3'			
	PNA 75 H-TTTTTTT A Lys- NH ₂			
5	PNA 79 H ₂ N-Lys- A TTTTTTTT-H	70.2	+4.7	+2.4
	DNA 93 5'GCAAAAAAATCG3'			
	PNA 79 H-TTTTTTT A Lys- NH ₂			
6	PNA 83 H ₂ N-Lys- a TTTTTTTT-H	74.8	+9.3	+4.7
	DNA 93 5'GCAAAAAAATCG3'			
	PNA 83 H-TTTTTTT a Lys- NH ₂			
Middle modifications				
7	PNA 76 H ₂ N-Lys-TTT A TTTT-H	44.4	--	
	DNA 94 5'GCAAATAAAACG3'			
	PNA 76 H-TTTT A TTT-Lys-NH ₂			
8	PNA 80 H ₂ N-Lys-TTT A TTTT-H	34.4	-10.0	-5.0
	DNA 94 5'GCAAATAAAACG3'			
	PNA 80 H-TTTT A TTT-Lys-NH ₂			
9	PNA 84 H ₂ N-Lys-TTT a TTTT-H	75.2	+30.8	+15.4
	DNA 94 5'GCAAATAAAACG3'			
	PNA 84 H-TTTT a TTT-Lys-NH ₂			
Bi modifications				
10	PNA 77 H ₂ N-Lys-TTT A TTT A -Lys-H	56.0	--	
	DNA 95 5'GCAAATAAAATCG3'			
	PNA 77 H- A TTT A TTT-Lys-NH ₂			
11	PNA 81 H ₂ N-Lys-TTT A TTT A -Lys-H	63.7	+7.7	+1.9
	DNA 95 5'GCAAATAAAATCG3'			
	PNA 81 H- A TTT A TTT-Lys-NH ₂			
12	PNA 85 H ₂ N-Lys-TTT a TTT a -Lys-H	49.5	-6.5	-1.6
	DNA 95 5'GCAAATAAAATCG3'			
	PNA 85 H- a TTT a TTT-Lys-NH ₂			

A= adenine, **A**=8-bromoadenine and **a**=8-aminoadenine; All values are an average of at least 3 experiments and accurate within $\pm 0.5^\circ\text{C}$, Buffer: Sodium phosphate (10 mM), and 100 mM NaCl, pH 7.2.

3.2.2a UV-Melting studies of adeninyl/8-bromoadeninyl/8-aminoadeninyl PNA complexes with mismatch DNA

The sequence specificity of PNA hybridization was examined through studying hybridization properties of PNA with single mismatch containing DNA to examine the sequence specificity properties.

The complex of control sequence PNA **75** formed triplex with single mismatch sequence (DNA **97**) with T_m lower by 8.1 °C (entry 1&2, Table 5), while C-terminus modified 8-bromoadeninyl PNA **79** (entry 3&4, Table 5) exhibited destabilization by 8.5 °C and C-terminus modified 8-aminoadeninyl PNA **83** (entry 5&6, Table 5) showed 8.4 °C respectively. Thus 8-bromo/aminoadeninyl PNA showed sequence discrimination as good as the control sequence PNA **75**. The functionality bromo or amino at C-8 position of adenine were showed lower influence on sequence specificity over adeninyl PNA.

Table 4 UV-Melting temperatures (T_m values in °C)^a of adeninyl/8-bromoadeninyl/8-amino adeninyl PNA₂:DNA triplexes

Entry No.	Triplex (PNA ₂ :DNA)	T_m (°C) PNA ₂ :c DNA triplex	ΔT_m (°C) (match-mismatch)
1	PNA 75 H-TTTTTTTT <u>A</u> Lys- NH ₂ DNA 93 5'GCAAAAAAATCG3' PNA 75 H ₂ N-Lys- <u>A</u> TTTTTTTT-H	65.5	8.1
2	PNA 75 H-TTTTTTTT <u>A</u> Lys- NH ₂ DNA 97 5'GCAAACAAATCG3' PNA 75 H ₂ N-Lys- <u>A</u> TTTTTTTT-H	57.4	
3	PNA 79 H-TTTTTTTT <u>A</u> Lys- NH ₂ DNA 93 5'GCAAAAAAATCG3' PNA 79 H ₂ N-Lys- <u>A</u> TTTTTTTT-H	70.2	8.5
4	PNA 79 H-TTTTTTTT <u>A</u> Lys- NH ₂ DNA 97 5'GCAAACAAATCG3' PNA 79 H ₂ N-Lys- <u>A</u> TTTTTTTT-H	61.7	
5	PNA 83 H-TTTTTTTT <u>a</u> Lys- NH ₂ DNA 93 5'GCAAAAAAATCG3' PNA 83 H ₂ N-Lys- <u>a</u> TTTTTTTT-H	74.8	8.4
6	PNA 83 H-TTTTTTTT <u>a</u> Lys- NH ₂ DNA 97 5'GCAAACAAATCG3' PNA 83 H ₂ N-Lys- <u>a</u> TTTTTTTT-H	66.4	

^a T_m = melting temperature (measured in the buffer 10 mM sodium phosphate, 100 mM NaCl, pH = 7.3), PNA₂-DNA complexes. Values in the parenthesis (ΔT_m) indicate the difference in T_m of PNA with complementary sequence (DNA **93**) and single mismatch sequence (DNA **97**).

3.3 UV- T_m studies of cyanuryl/8-bromoadeniny/8-aminoadeniny PNA:DNA Duplexes (*parallel/antiparallel*)

The mixed purine -pyrimidine sequence, PNA **86** was synthesized to examine the duplex stability. The *cyanuryl* PNA **87**, was synthesized by replacing the thyminy PNA units of PNA **86** with cyanuryl PNA unit, whereas *8-bromoadeniny* PNA **88** was synthesized by replacing the adeniny PNA with 8-bromoadeniny PNA and 8-aminoadeiny PNA **89** was synthesized by direct amination of solid supported 8-bromoadeniny PNA oligomer as mentioned in Chapter 2 (2.35.2).

The control sequence PNA **86**, showed 2.7 °C of sequence discrimination between parallel and antiparallel complementary DNA sequences, whereas corresponding *cyanuryl* PNA **87** showed 2.5 °C of discrimination in sequence orientation (*antiparallel or parallel*). The 8-bromoadeniny PNA (PNA 88) and 8-aminoadeniny PNA (PNA 89) showed better discrimination of 3.6 °C and 6.7 °C in sequence orientation respectively. Eventhough the modifications 8-bromo/aminoadeniny PNAs may not enhance the binding strength with complementary DNA in duplexes, they discriminate the *parallel* and *antiparallel* sequences better than the control sequence PNA **86**.

Table 5 UV-Melting temperatures (T_m values in °C)^a of PNA:DNA duplexes

Entry No	Duplex (PNA:DNA)	T_m (°C)	
		PNA:DNA duplex	ΔT_m (°C) (<i>ap-p</i>)
1	PNA 86 H-GT <u>A</u> G <u>A</u> T <u>C</u> ACT-Lys-NH ₂ DNA 98 5' AGTGATCTAC 3'	51.3	2.7
2	PNA 86 H-GT <u>A</u> G <u>A</u> T <u>C</u> ACT-Lys-NH ₂ DNA 99 5' CATCTAGTGA 3'	48.6	
3	PNA 87 H-G <u>Cy</u> <u>A</u> G <u>A</u> <u>Cy</u> C <u>ACC</u> <u>Cy</u> -Lys-NH ₂ DNA 98 5' AGTGATCTAC 3'	48.2	2.5
4	PNA 87 H-G <u>Cy</u> <u>A</u> G <u>A</u> <u>Cy</u> C <u>ACC</u> <u>Cy</u> -Lys-NH ₂ DNA 99 5'CATCTAGTGA3'	45.7	
5	PNA 88 H-GT <u>A</u> G <u>A</u> T <u>C</u> ACT-Lys-NH ₂ DNA 98 5' AGTGATCTAC 3'	53.3	3.6
6	PNA 88 H-GT <u>A</u> G <u>A</u> T <u>C</u> ACT-Lys-NH ₂ DNA 99 5'CATCTAGTGA3'	49.7	
7	PNA 89 H-GT <u>a</u> G <u>a</u> T <u>Ca</u> CT-Lys-NH ₂ DNA 99 5'CATCTAGTGA3'	52.8	6.7
8	PNA 89 H-GT <u>a</u> G <u>a</u> T <u>Ca</u> CT-Lys-NH ₂ DNA 98 5' AGTGATCTAC 3'	46.1	

Cy= cyanuryl, **A**= adenine, **A**=8-bromoadenine and **a**=8-aminoadenine a T_m is measured in the buffer 10 mM sodium phosphate, 100 mM NaCl, pH = 7.3. Values in the ΔT_m indicate the difference in the melting temperatures of the PNA:DNA **98** and DNA **99** The values reported here are the average of 3 independent experiments and are accurate to $\pm 0.5^\circ\text{C}$

3.4 Binding stoichiometry of 8-bromoadeninyl PNA and 3',5'-O-disilyl thymidine/thymidinyl PNA monomers through NMR titrimetry

In view of the variable results on PNA:DNA triplex/duplex stabilization in oligomers, it was thought worthwhile to understand difference in their base pairing properties at the monomer level.

The specific association of purine and pyrimidine bases is fundamental to the function of nucleic acids. Forces that contribute to the stability of double stranded nucleic acids can be conceptually expressed as sum of base-base hydrogen bonding and stacking interactions. The hydrogen bonding between the base pairs adenine:thymine and guanine:cytosine was proposed by Watson-Crick in 1953. However complete understanding of physical basis for this observed complementarity has proved difficult.

The binding stoichiometry was established through NMR titration between 3',5' di-O-silyl thymidine (**10**) with 8-bromoadeninyl PNA (**7**) monomer. For this, control titration experiment was carried out with adeninyl PNA monomer (**6**). Similar experiment repeated for thymidinyl PNA monomer (**11**): adeninyl PNA monomer (**6**), and thymidinyl PNA monomer (**11**):8-bromoadeninyl PNA monomer (**7**) complexation. All experiments indicated a 1:1 binding stoichiometry.

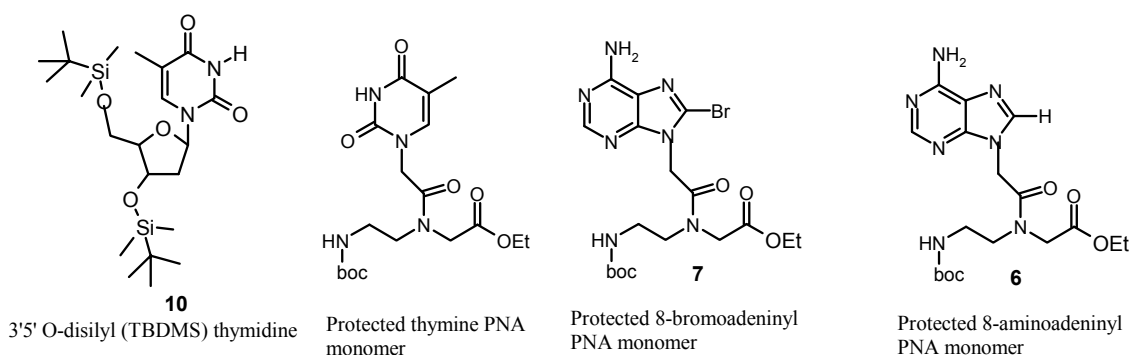


Figure 9: The monomers used for NMR titration experiment for the calculation of binding stoichiometry

CHAPTER 1

Introduction

1.1 Nucleic Acids: Chemical Structure

Nucleic acids are large biopolymers, dominating the modern molecular science after the Watson-Crick discovery of the double helical structure of DNA (Figure 1).¹ Their vital roles are fundamental for the storage and transmission of genetic information within the cells and contain all the information required for transmission and implementation of steps necessary to make proteins which are another important class of biopolymers, necessary for cellular function.

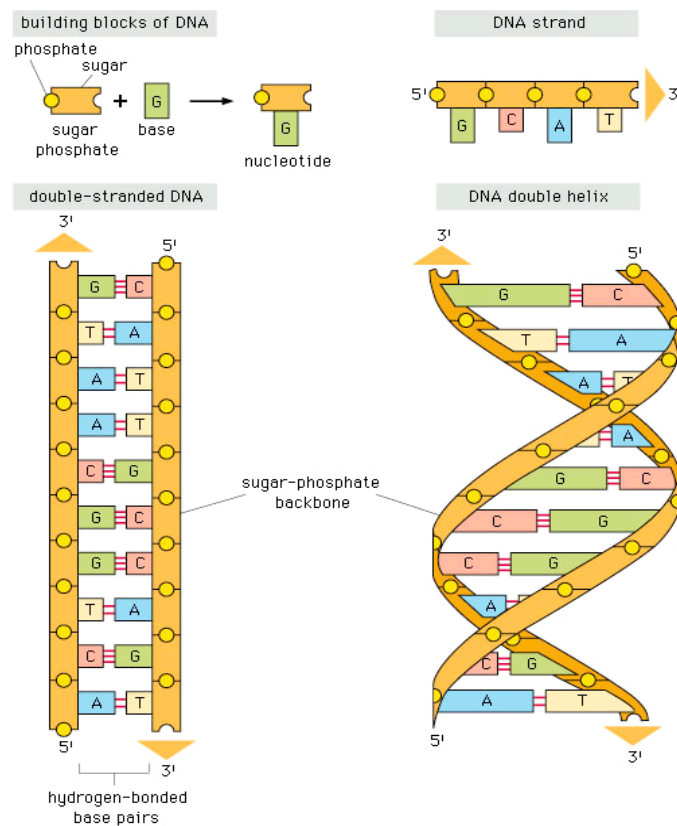


Figure 1: Model of DNA

DNA is the basic genetic material, consisting of two complementary strands held together by Watson-Crick hydrogen bonds through the donor-acceptor sites of the four

nucleobases A, T, G and C (Figure 2).² All biological functions of DNA take place via specific molecular recognition of nucleobases.

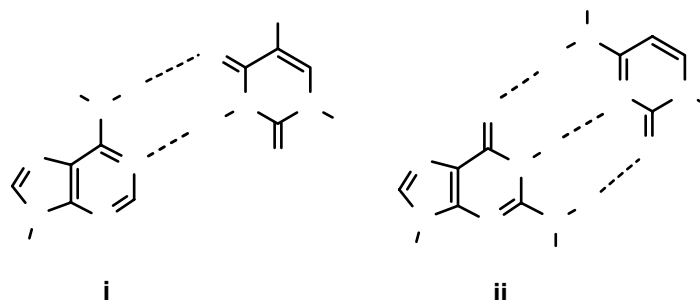


Figure 2: Base pair recognition by Watson-Crick Hydrogen bonding i) A:T base pair, ii) G:C base pair (a= hydrogen bond acceptor, d= hydrogen bond donar)

The structure of the double-stranded DNA allows it to have a number of molecular interactions with other molecules such as proteins, drugs, metal ions etc. through electrostatic, intercalation^{3,4} and groove binding mechanisms⁵⁻⁷ (Figure 3) Such molecular recognition mediated by weak non-covalent interactions are important in regulating the biological functions.

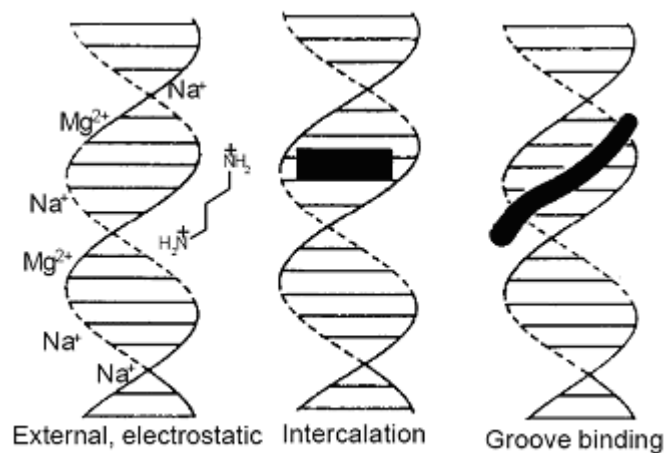


Figure 3 The three primary binding modes seen in DNA

1.2 Oligonucleotide as therapeutic agents

The concept of 'antisense oligonucleotides' as potential therapeutic agents⁸ introduced by Zamecnik and Stephenson⁹ has arouse much interest in search of potent

DNA mimics. Antisense oligonucleotides (Figure 4) recognize a complementary sequence on target m-RNA through Watson-Crick base pairing and form a duplex (RNA-DNA hybrid) that is not processed by the protein synthesis machinery and hence would retard the expression of the corresponding protein. When target proteins are disease related, this will have a therapeutic value.

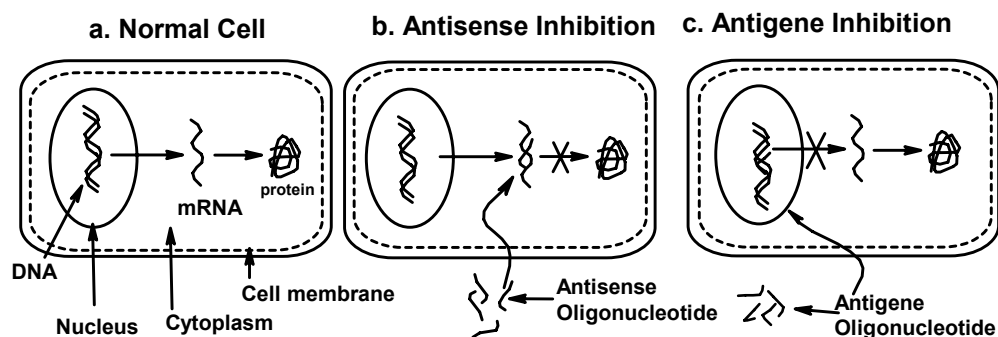


Figure 4: Mechanism of action of antisense and antigene oligonucleotides

In another approach, the ‘antigene strategy’, (Figure 4) obstruction of gene expression can be achieved by binding of oligonucleotides to duplex DNA through Hoogsteen hydrogen bonds (Figure 5) leading to the formation of a triple helix.¹⁰ Thus the double stranded DNA itself can act as a target for the third strand oligonucleotides or their analogue, and the limitation for triplex formation is that it is possible only at homopurine stretches of DNA, since it requires purine to be the central base.^{10, 11}

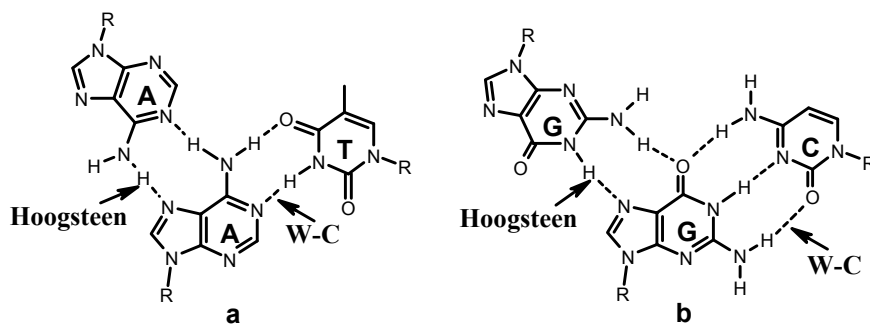


Figure 5: Watson-Crick (W-C) and Hoogsteen hydrogen bonds of A:A:T and G:G:C triads

The prime requisites for oligonucleotides to be effective as antisense/antigene oligonucleotides are (a) they should have high specificity to the RNA/DNA template, which is the target strand, (b) improved cellular uptake and (c) resistance to cellular enzymes such as nucleases and proteases.

Natural oligonucleotides have exhibited both antisense and antigene properties *in vitro*.¹² However, a serious drawback that limits the use of oligonucleotides as therapeutic agents is that they are rapidly degraded by nucleases *in vivo*.¹³ To overcome these drawbacks chemical (structural) modifications of oligonucleotides are needed.

1.3 Chemical Modifications of DNA

The different chemical modifications for applications as ‘antisense oligonucleotides’ corresponds to that of nucleobases, phosphate function, sugar and sugar-phosphate backbone (Figure 6).

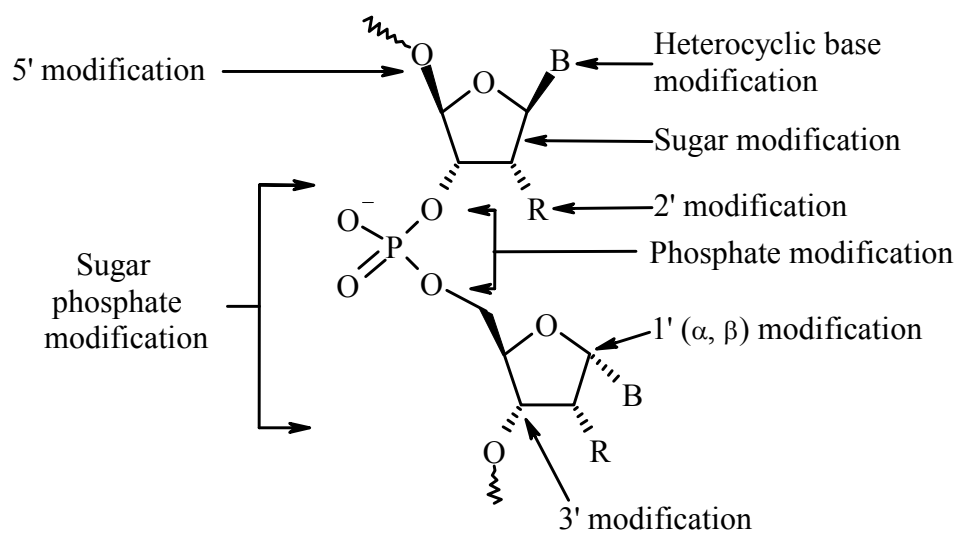


Figure 6: Structurally possible various DNA modifications

1.3.1 Nucleobase modifications and duplex/triplex stability^{16, 17}

Modification of the heterocyclic bases may enhance the binding affinity with the complementary DNA/RNA through the increased/enhanced hydrogen bonding via combined contribution of both Watson – Crick and Hoogsteen hydrogen bonding.

The stability of duplex or triplex also depends on both *syn-anti* conformations of nucleobase (Figure 7a&b) as well as *endo-exo* conformations of 5-membered sugar (ribose or deoxy ribose), which is signified as ‘ring puckering’ (Figure 7c&d)

The stability of duplex/triplex also increases as the modified base interacts with natural bases present on the strands through π - π overlapping interactions.

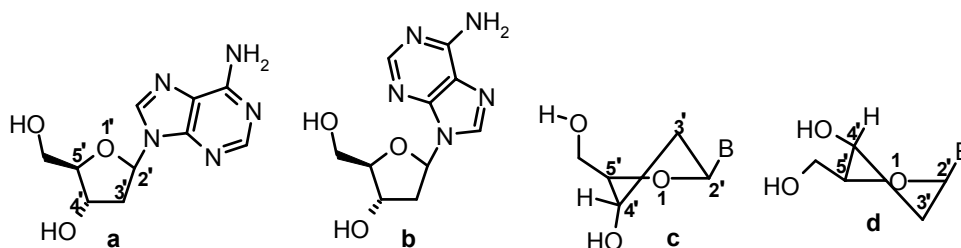


Figure 7: Structures of different conformations of adenosine a) *anti* conformation b) *syn* conformation c) 2' endo 3' exo conformation and d) 3' endo conformation

1.3.1a Stacking and Hydrophobicity Contributions

The bases in the triplex orient in such a way that the π bonds of nucleobase of TFO (triplex forming oligonucleotide) overlaps with the adjacent base pair of duplex due to stacking and thus stabilize the triplex.

1.3.1b Hoogsteen base pairing

A Hoogsteen base pair is a type of base-pairing in nucleic acids, involving the 5-membered ring of purines A and G, recognizing the third strand T and C respectively . In

this manner, two nucleobases on each strand can be held together by hydrogen bonds in the major groove through Watson-Crick pattern.

Hoogsteen base pair formation involves the *N*-7 position (five membered ring of purine) and the functionality present at *C*-6 of purine (six membered ring), binding the the pyrimidine base or another purine base (Figure 8). The triplex forming oligonucleotide (TFO) recognizes the duplex (consisting Watson-Crick basepairs) through Hoogsteen hydrogen bonds and by winding around the duplex to form triple-stranded helices eg. (poly(dA)•2poly(dT)). The stability of triplex enhances, as the number of Hoogsteen hydrogen bonds increase.

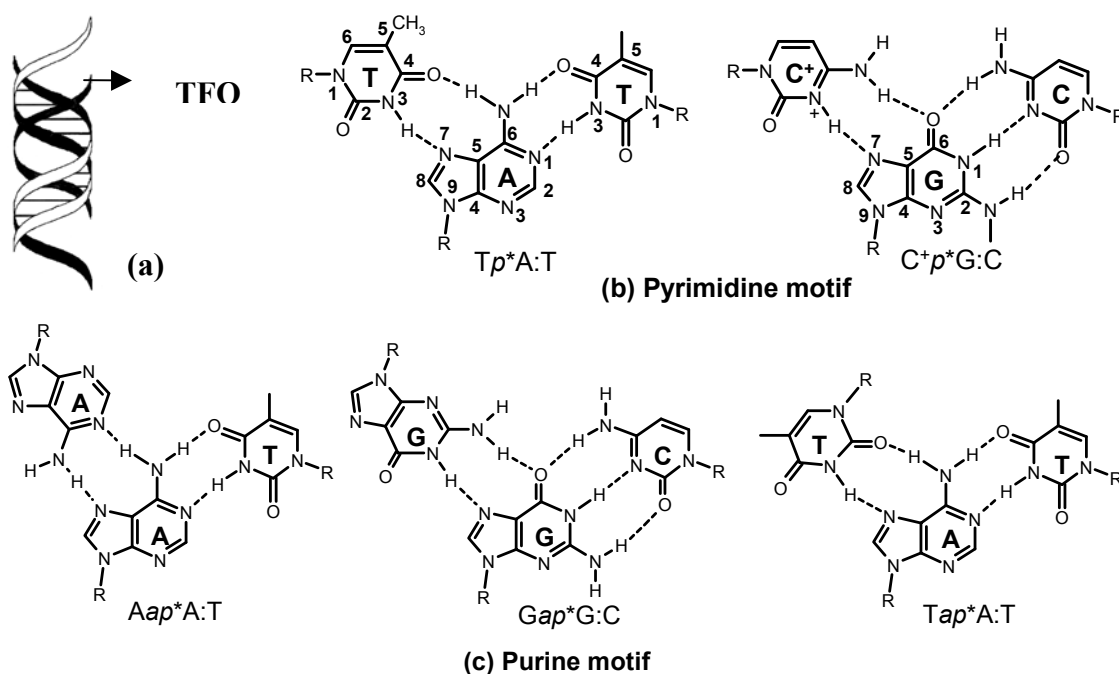


Figure 8: (a) The ribbon model demonstrating the relative position of a triplex forming oligonucleotide (TFO) in the major groove of DNA. (b) The pyrimidine binding motif- the binding of a TFO in a parallel orientation (*p*) to the polypurine strand of DNA. The two canonical base triplets of this motif (a) involving protonated cytosine in the $C^+G:C$ triplet and $T^*A:T$. (c) The purine motif- the binding of TFO in antiparallel orientation (*ap*). The three canonical base triplets in this motif: $Ap^*A:T$, $G^*G:C$ and $Tp^*A:T$. ‘ * ’ represents Hoogsteen hydrogen-bonds and ‘ : ’ denotes Watson-Crick (WC) hydrogen bonds.

Triple helical stability is due to a combination of electrostatic and stacking interactions, Hoogsteen/reverse Hoogsteen hydrogen-bond formation, hydration forces and hydrophobic interactions. The relative contributions are difficult to evaluate in such a system.

1.3.1c Modified nucleobases stabilize duplex/triplex:

The modified nucleobase consisting of phenyl or biphenyl aromatic groups (Figure 9a& b),¹⁸ or the intercalators (Figure 9c)¹⁹ stabilize the duplex through π -stacking interactions. The modifications of pyrimidines at an unpaired site (C^6 -position is not involved in Watson-Crick hydrogen bonding) stabilize the *syn*- conformation and leads to duplex destabilization. The oligonucleotides containing modified nucleobases, which has fused aromatic system at C^4 and C^5 , stabilize the derived duplex (Figure 9d).¹⁷

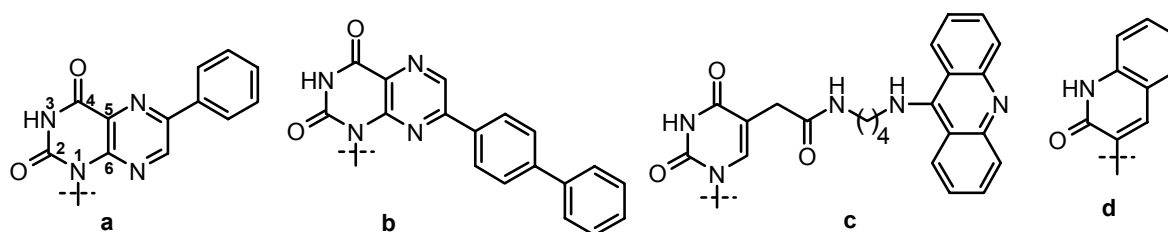


Figure 9: The Duplex-stabilizing modifications a) 6-phenyllumazine, b) 7-(4-biphenyl)lumazine, c) pyrimidine- C^5 -intercalator, d) 2-hydroxy quinoline

The pyrimidine nucleosides consisting of unsaturated substituents at C -5 position in pyrimidine (Figure 10a, b)²⁰ and 7-alkynyl-7-deaza-substituent in purines (Figure 10c-f)²¹ have a pronounced influence on duplex stabilization. The triple bond stacks with the adjacent base pair and stabilizes the duplex.

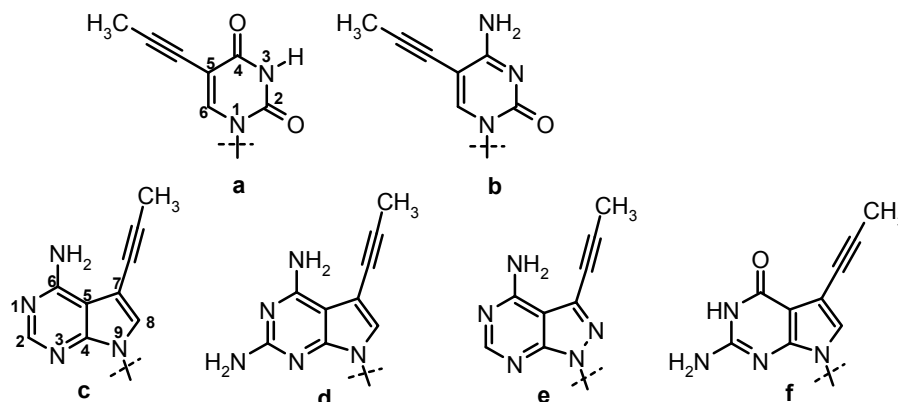


Figure 10: The structures of a) 5-propynyl uracil, b) 5-propynyl cytosine c) 7-propynyl-7-deaza-adenine, d) 7-propynyl-7-deaza-2,6-diamino purine, e) 7-propynyl-7-deaza-8-aza-adenine, f) 7-propynyl-7-deazaguanine

The modifications of pyrimidine ring consisting of planar aromatic groups such as thiazolyl or 5-methylthiazolyl at *C*-5 stabilize the oligonucleotide complexes through enhancing the base stacking interaction with adjacent base pairs of duplex (Figure 11).^{22,23}

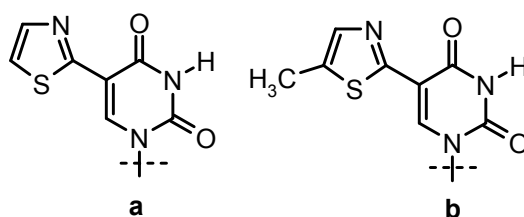


Figure 11: The structures of modified pyrimidine bases having coplanar aromatic groups a) 5-thiazolyl uracil, b) 5-methylthiazolyl uracil.

1.3.1d Modifications that increase hydrogen bonding and staking interactions:

Another kind of nucleobase modification involves making the pyrimidine or purine base into bicyclic or tricyclic heterocycles. These stabilize the duplexes through stacking interactions as well as increase the number of available hydrogen bonding sites. Most of the reported derivatives are cytosine analogues with fused aromatic ring at *N*⁴-*C*⁵ (Figure 12a-c).²⁴ These analogues bind guanine better than the natural unmodified cytosine. The oligonucleotides containing two adjacent modified tricyclic nucleobases,

form stable duplexes because of better π - π overlap between the two tricyclic nucleobases with adjacent base pairs in the duplex. The tetracyclic adenine derivative (Figure 12d) pairs with thymine.²⁵

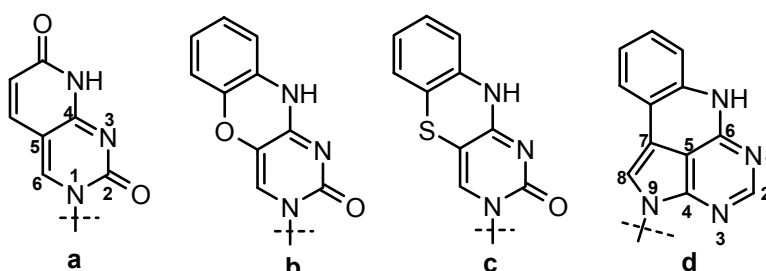


Figure 12: Duplex stabilizing bicyclic and tricyclic heterocyclics a) pyridopyrimidine, b) phenoxazine, c) phenothiazine, d) tetracyclic adenine

1.3.1e Functionalities enhancing hydrogen bonding potentials:

C^5 -Methyl group of pyrimidine stabilizes the duplex as in 5-methyl cytosine (Figure 13a). The alkyl groups have positive inductive effect, increasing the pKa through increased electron density on ring, thus enhancing the hydrogen bonding efficiency of the carbonyl at $C-4$.²⁶ The 5-bromo group in bromo uracil (Figure 13b) with electron withdrawing effect, enhances the acidity of N^3 -H to participate in hydrogen bonding, thereby increasing the stability of the duplex.²⁷

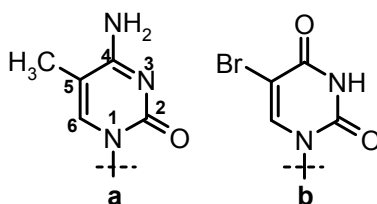


Figure 13 : The structures of a) 5-methyl cytosine and b) 5-bromo uracil

1.3.1f Stabilization of triplex through electrostatic forces:

Another kind of modified nucleobases stabilize duplexes through introducing positively charged functionalities as substituents in the major or minor groove and

interacting with negatively charged phosphate groups and by decreasing the anionic repulsions of both strands (Figure 14).^{17,28-30}

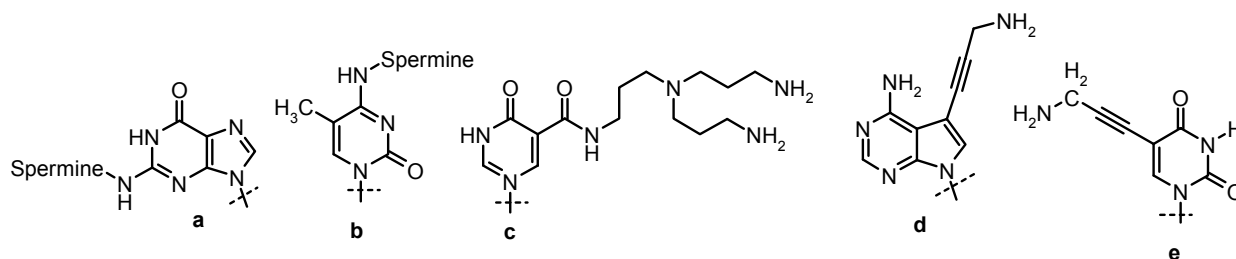


Figure 14: The modified nucleobases containing positively charged functional groups a) spermine-conjugated guanine, b) 5-methyl- N^4 -spermine-cytosine, c) triaminoalkylamido uracil, d) 7-(3-amino propynyl)-7-deaza adenine, e) 3-aminopropynyl uracil

1.3.1g Modifications that form Hoogsteen hydrogen bonding:

The incorporation of pseudouracil (Figure 15a) and alkylated pseudouracil (Figure 15b) containing (deoxy) nucleotides are isosteric to thymine analogues. Incorporation of these into oligomers enhances the stability of duplex, whereas 1,3-dialkylpseudouracil (Figure 15c) containing oligonucleotides destabilize the duplex. The tautomerization in pseudoisocytidine (Figure 15d) has a negative impact on Watson-Crick base pairing and decreases duplex stability.^{16,31-34} 5-Aminouracil (Figure 15e) stabilizes triplex when present on central strand.³⁵

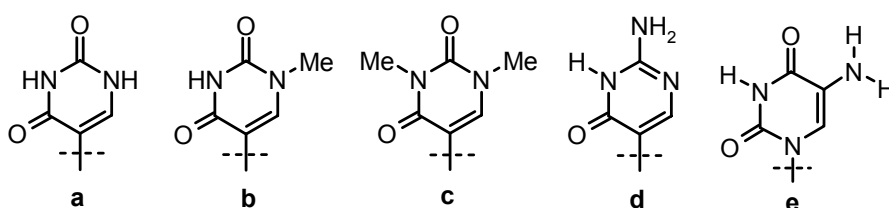


Figure 15 : Structures of a) pseudouracil, b) 1-methyl pseudouracil, c) 1,3-dimethyl pseudouracil, d) pseudoisocytosine, e) 5-aminouracil.

In case of purine, the electron donating substituents such as amino, methylamino, N,N -dimethylamino, hydroxy at $C-8$, increase the electron density on $N-7$ of purine³⁶

thereby enhancing its ability to participate as hydrogen bond acceptor in Hoogsteen base pairing (Figure 16).³⁷⁻⁴⁰

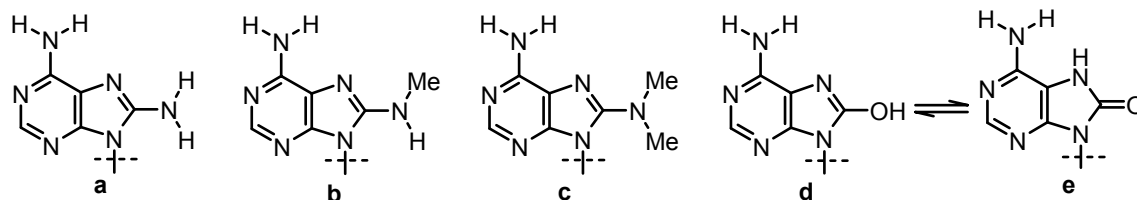


Figure 16: structures of a) 8-amino adenine, b) 8-(*N*-methyl amino) adenine, c) 8-(*N,N*-dimethyl amino) adenine, d) 8-hydroxy adenine, e) 8-oxo-adenine (keto form of 8-hydroxy adenine).

1.3.2 Phosphate modified linkages

In the first generation ‘antisense oligonucleotides’ (Figure 17) the phosphodiester backbone has been replaced by phosphorothioates (Figure 17a), phosphorodithioates (Figure 17b), methyl phosphonates (Figure 17c), hydroxymethyl phosphonates (Figure 17d&e) and phosphoramidates (Figure 17 f&g). The backbone modifications displayed a greatly improved resistance towards nucleases⁴¹ and a therapeutic agent Vitravene, based on phosphorothioates has already been approved as a drug by US FDA to treat cytomegalovirus (CMV), affected eye patients.⁴² The chemical modifications also modulate the binding ability of analogs to complementary sequences.

The boranophosphate diester (Figure 17h) is isoelectronic with phosphodiesters, isosteric with the methylphosphonate group and is chiral.⁴³ These oligos are highly water soluble, but are more lipophilic than DNA.

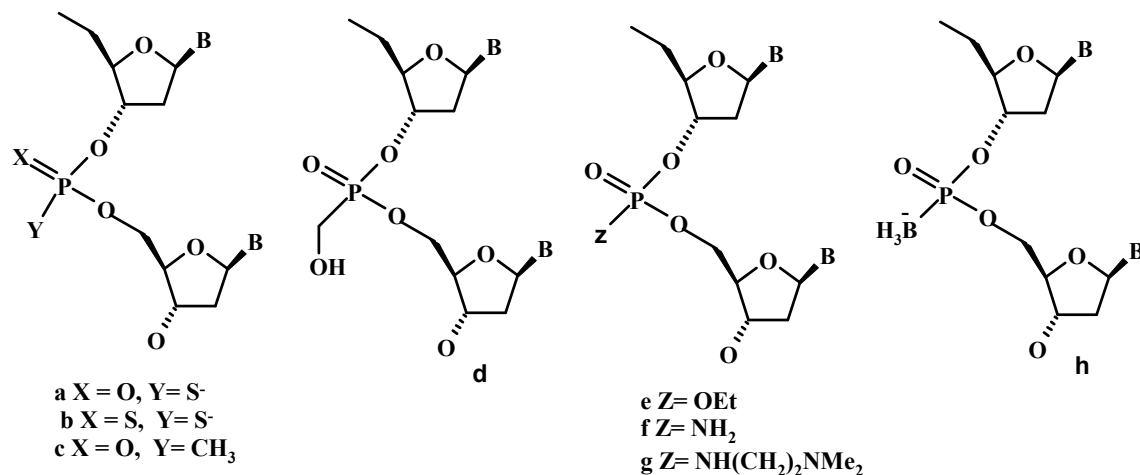


Figure 17: Phosphate modifications

1.3.3 Sugar modifications

Sugar modifications have also been used to enhance the stability and affinity for complementary strands. The (α -anomer of a 2'-deoxyribose sugar has the base inverted in configuration at C-1 with respect to the natural anomer. ODNs containing β -anomer sugars (Figure 18) are resistant to nuclease degradation and bind in a parallel mode to the RNA target.⁴⁴

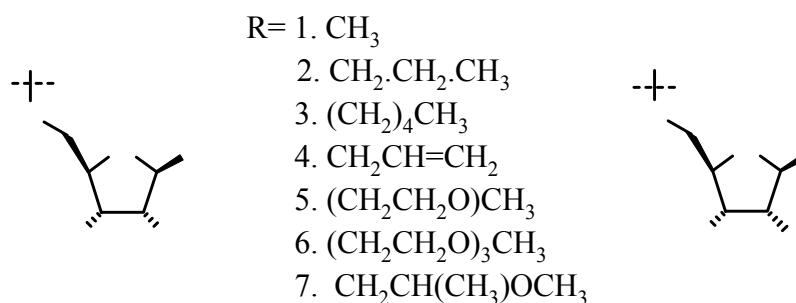


Figure 18: 2' modified oligonucleotides

1.3.3a Sugar skeleton modifications

Apart from the 2' modifications of sugar moiety, other modifications related to sugar skeleton are hexitol nucleic acids (HNA), D-altrioI nucleic acids (ANA),

pentapyranosyl and threofuranosyl (TNA).^{45a} The (l)-(L-lyxopyranosyl-(4'→3')-oligonucleotide system is a member of a pentopyranosyl oligonucleotide family containing a shortened backbone and is capable of cooperative base-pairing with DNA and RNA. In contrast, the corresponding (d)-D-ribopyranosyl-(4'→3')-oligonucleotides do not show base-pairing under similar conditions (Figure 19).^{45b}

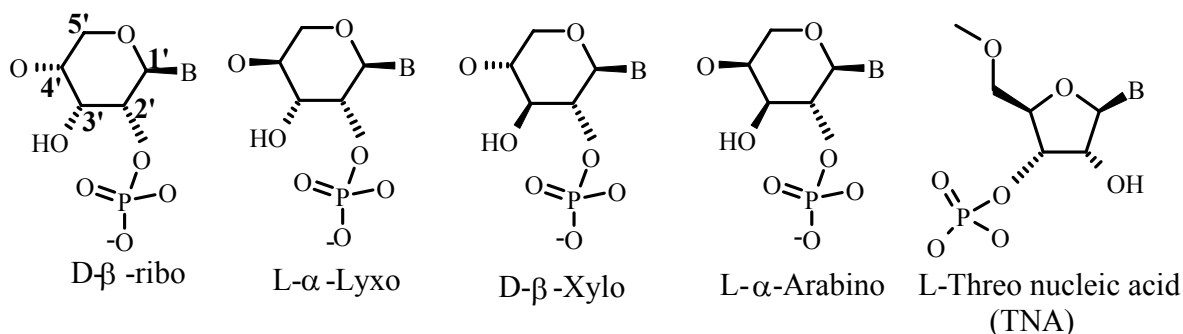


Figure 19: The family of four (4'→3') penta pyranosyl and threo fuanoysl oligonucleotides

1.3.3b Carbocyclic nucleic acids

In carbocyclic nucleic acids, the furanose ring is completely replaced by saturated cycloalkane or cycloalkene rings (Figure 20). The replacement of the furanose moiety of DNA by a cyclohexene ring gives cyclohexene nucleic acids (CeNA).⁴⁶

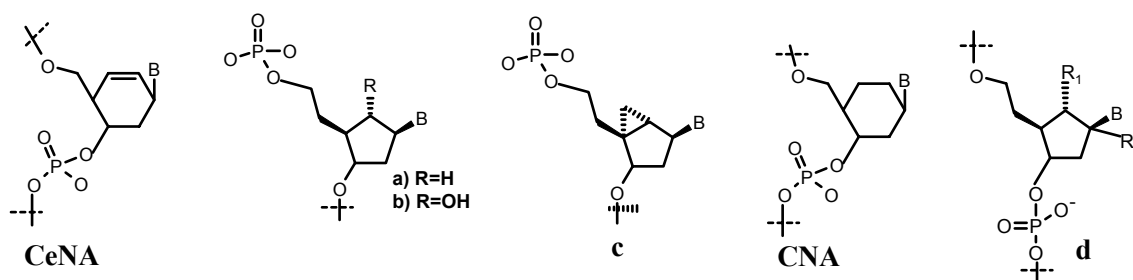


Figure 20: Carbocyclic analogues

Incorporation of cyclohexenyl nucleosides in a DNA chain increases the stability of a DNA/RNA hybrid. CeNA is stable against degradation by proteases in serum and a

CeNA/RNA hybrid is able to activate RNase H of *E. Coli*, resulting in cleavage of the RNA strand.⁴⁴

1.3.3c Locked nucleic acids (LNA)

Locked Nucleic Acid (LNA) was first described by Wengel⁴⁷ and Imanish^{48a} et al as a novel class of conformationally restricted oligonucleotide analogues. LNA is a bicyclic nucleic acid where a ribonucleoside is linked between the 2'-oxygen and the 4'-carbon atom with a methylene unit (Figure 21).

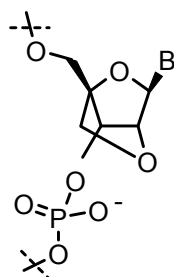


Figure 21: Locked Nucleic Acid (LNA)

The design and ability of LNA oligos to bind to supercoiled, double-stranded plasmid DNA in a sequence-specific manner has been described by Catchpole et al^{48b} for the first time. LNA oligos are more stably bound to plasmid DNA than the similar peptide nucleic acid (PNA) 'clamps' for procedures such as particle mediated DNA delivery.

1.3.3d Morpholino nucleosides

So far, only a few attempts to replace the entire (deoxy) ribose phosphate backbone have been successful. One of this is the morpholino oligomer (Figure 22) wherein the monomers are linked through a carbamate linkage.^{49a} The second generation of morpholino DNA with a phosphoramidate (Figure 22)^{49b} linkage exhibited better

stability in *in-vitro* assay. To avoid the loss of bioactivity through major structural modifications and impart only the nuclease resistance, oligonucleotides having only 5' or 3' terminal modifications have been studied.

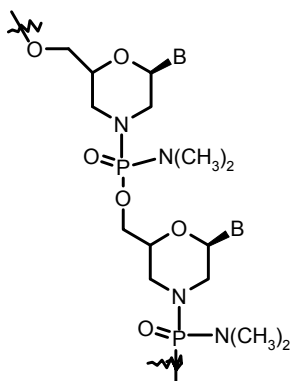


Figure 22: Morpholino nucleoside

1.4 Peptide Nucleic Acid:

1.4.1 Introduction

PNA refers to peptide nucleic acid (Figure 23) invented by Nielsen et. al 1991⁵⁰ with physical properties similar to DNA or RNA but differing in the composition of its "backbone." PNA is unnatural and is chemically synthesized for use in biological research and diagnostics.⁵¹

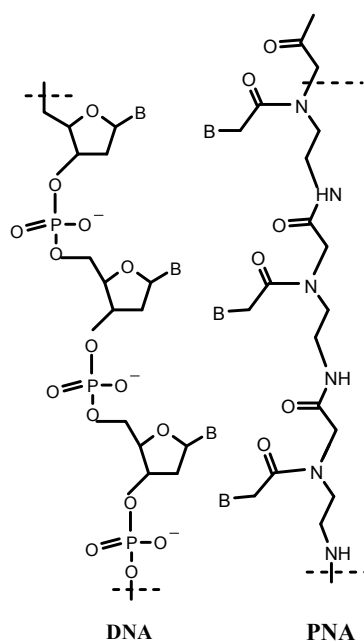


Figure 23: Chemical structure of DNA and PNA

DNA and RNA have backbone containing deoxyribose and ribose sugars respectively, whereas the backbone of PNAs is composed of repeating N-(2-aminoethyl)-glycine units linked by peptide bonds. The various purine and pyrimidine bases are linked to the backbone by methylene carbonyl bonds. PNAs are depicted like peptides, with representation of sequence from N-terminus (left) to C-terminus (right) (Figure 24).

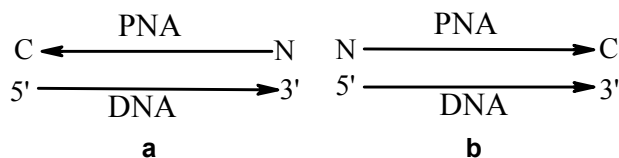


Figure 24: a) anti parallel and b) parallel orientation of PNA in PNA:DNA duplex

Since the backbone of PNA is uncharged, the binding between PNA/DNA strands are stronger than DNA/DNA strands, due to the lack of electrostatic repulsion during hybridization. Early experiments with homopyrimidine strands (strands with repeated pyrimidine bases) have shown that the T_m ("melting" temperature) of a 6-base thymine PNA/adenine DNA double helix was 31°C in comparison to an equivalent 6-base DNA/DNA duplex that denatures at a temperature less than 10 °C.^{52,56}

Synthetic peptide nucleic acid oligomers have been used in recent years in various molecular biology protocols, diagnostic assays and for potential antisense therapeutics.⁵¹ Due to their higher binding strength, even shown PNA oligomers are opt for use in these roles, which otherwise need longer oligonucleotides (20-25 bases). PNA oligomers also show greater specificity in binding to complementary DNAs, with single PNA/DNA base mismatch being more destabilizing than a similar mismatch in a DNA/DNA duplex. This binding strength and specificity also applies to PNA/RNA duplexes. PNAs are resistant to enzyme degradation,^{53,54} and stable over a wide pH range. Finally, their uncharged nature should make them cross through cell membranes easier, improving their therapeutic value.

1.4.2 Triplex formation with complementary DNA and RNA

Homopyrimidine peptide nucleic acids are known to form highly stable and sequence specific triplexes upon binding to complementary homopurine sites of ssDNA and dsDNA.⁴² Displacement of the second, homopyrimidine strand takes place upon

binding of PNA to dsDNA, forming a so-called P-loop.⁵⁵ The extremely high thermal stability of PNA₂/DNA triplexes,⁵⁶ is at least partly due to the charge neutrality of the PNA backbone, that excludes electrostatic repulsion from the DNA molecule, and the presence of additional hydrogen bonds between the Hoogsteen strand of the PNA and the oxygen atoms of the DNA backbone.⁵⁷ A unique property of PNAs is their ability to displace one strand of a DNA double helix to form strand invasion complexes, which is absent in DNA or any other DNA analogues studied so far.

1.4.3 Duplex formation with complementary DNA and RNA

PNAs obey Watson- Crick rules of hybridization with complementary DNA (Figure 25) and RNA. Antiparallel PNA-DNA hybrids are considerably more stable than the corresponding DNA-DNA complexes.⁵⁰ Antiparallel PNA-RNA duplexes are even more stable than both DNA-RNA hybrids and PNA-DNA duplexes. Base pair mismatches result in reduction of the T_m value by 8-20 °C.⁵²

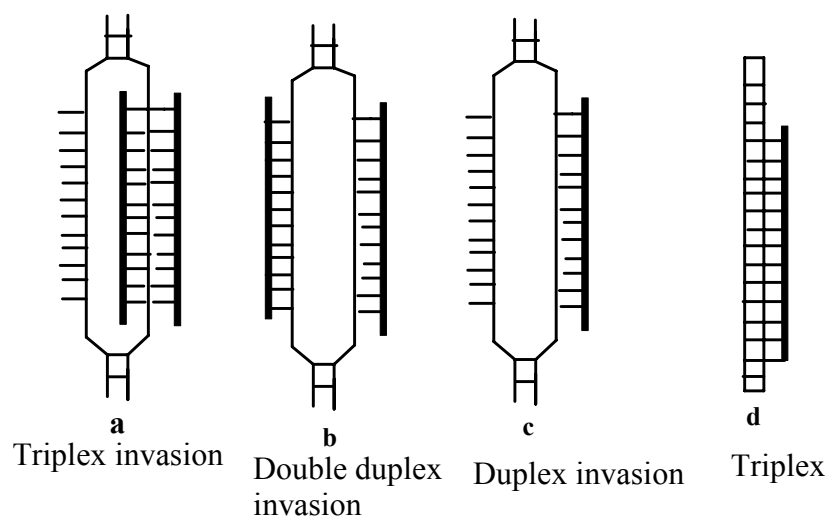


Figure 25: Schematic representation of PNA binding for targeting *ds* DNA, PNA (Thick line)

1.4.4 Structure of PNA complexes

Till date, the three-dimensional structures of four PNA complexes have been established. The PNA-RNA⁵⁷ and PNA-DNA⁵⁸ duplex structures were determined by NMR methods, while the structures of a PNA₂:DNA triplex⁵⁹, PNA-PNA duplex⁶⁰ and PNA-RNA duplexes were solved by X-ray crystallography (Figure 26).

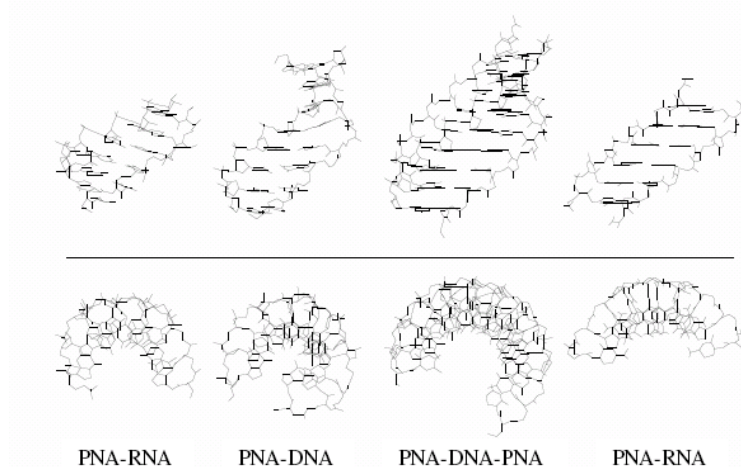


Figure 26: Structures of various PNA complexes shown in side view (upper panel) or top view (lower panel)

1.4.4a Structure of PNA-DNA/PNA-RNA duplexes

Almost complete structural information has been deduced from the NMR spectroscopic study of two antiparallel PNA-DNA duplexes.⁵⁹ The DNA strand is in a conformation similar to the B-form, with a glycosidic *anti*-conformation, and the deoxyribose in *C2'-endo* form.

A more recent NMR study^{58,61} showed that an octameric antiparallel PNA-DNA duplex contained elements of both A-form and B-form. The primary amide bonds of the backbone are in *trans* conformation and the carbonyl oxygen atoms of the backbone-nucleobase linker point towards the carboxy-terminus of the PNA strand. In case of RNA, the study revealed that the glycosidic torsion angle in the RNA strand indicates an

anti-conformation, and the ribose sugars are in the 3'-*endo* form. The RNA strand thus resembles an A-form structure.

The CD spectra of antiparallel PNA-DNA complexes are similar to DNA-DNA spectra and indicate the formation of right handed helix.⁶² The CD spectra of antiparallel PNA-RNA duplexes also indicate the formation of a right-handed helix with geometry similar to the A- or B-form.

1.4.4b Structure of PNA₂-DNA triplexes

The structure of PNA₂-DNA triple-helix was resolved by the X-ray crystal structure analysis of the complex formed by bis-(PNA) and its complementary antiparallel DNA.⁵⁹ The nucleobases of the PNA strand bind to the DNA through Watson-Crick pairing and Hoogsteen hydrogen bonding. The structure exhibited, both A-form and B-form DNA, and forms a “P-helix” with 16 bases per turn. The DNA phosphate groups are hydrogen bonded to the PNA backbone amide protons of the Hoogsteen strand. These hydrogen bonds, together with additional Van der Waal contact and the lack of electrostatic repulsion are the main factors responsible for the enormous stability of the triplex. The deoxyribose sugar adopted C3'-*endo* conformation like A-form and bases lie almost perpendicular to the helix axis, which is characteristic of B-form DNA. The crystal structure is in agreement with the CD spectra of PNA₂-DNA triple-helices measured in solution.⁶² The X-ray structure of self-complementary PNA-PNA duplex bears a strong similarity to the P-form of PNA₂-DNA triplex.⁵⁹

Several general conclusions can be drawn from these structural studies. Since PNA has flexible backbone, it exhibits the ability to adapt its partner's conformation (DNA/RNA) in the complexes.

1.4.5 Disadvantages of PNA

PNA has great ability to bind to complementary DNA/RNA forming stable duplexes or triplexes. It has an ability to discriminate complementary sequences with even single base mismatches. Besides these advantages, PNA suffers from few drawbacks such as low aqueous solubility, ambiguity in DNA binding orientation (parallel/antiparallel) and poor membrane permeability.

1.4.6 Chemical Modifications of PNA

The limitations of PNA restrict its ability to be used as a therapeutic agent. Chemical modifications of PNA are needed to overcome these drawbacks. Structurally, the analogues can be derived from modifications of ethylenediamine or glycine sections of the monomer, linker to the nucleobase, the nucleobase itself or a combination of the above. The strategic rationale behind the modifications⁶³ (Dueholm et al., 1997) are (i) introduction of chirality into the achiral PNA backbone to influence the orientation selectivity in complementary DNA binding, (ii) rigidification of PNA backbone via conformational constraint to preorganize the PNA structure and to entropically drive the duplex formation (α - α' , β - β' , β - α'' and α'' - β'' of Figure 27), (iii) introduction of cationic functional groups directly into the PNA backbone, in a side chain substitution or at the N or C terminus of PNA, (iv) modulation of nucleobase pairing either by modification of the linker or the nucleobase itself and (v) conjugation with 'transfer' molecules for effective penetration into cells. In addition to improving the PNA structure for therapeutics, several modifications are directed towards their applications in diagnostics.

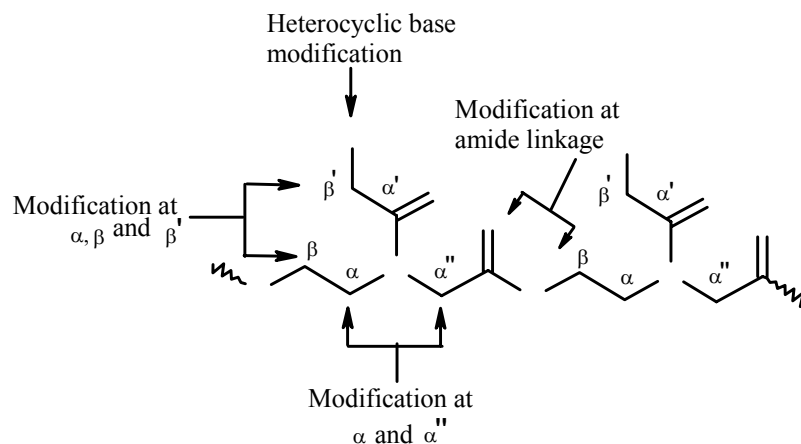


Figure 27: Structurally possible various PNA modifications

1.4.6a Introduction of cationic functional groups into the PNA

Solubility in aqueous media was improved by introducing positive charges in the PNA monomers or by introducing ether linkages in the backbone. Charges were integrated into the PNA by replacing the acetamide linker with a flexible ethylene linker⁶⁴ (Figure 28a) or by the attachment of terminal lysine residues⁶⁵ (Figure 28c). Recently, a novel class of cationic PNA (Figure 28b) (DNG/PNA) analogs has been reported.⁶⁶ In these, alternating PNA /DNG chimeras, the O-(PO₂)-O- linkage of nucleotide was replaced by strongly cationic guanidino [N-C(=N⁺H)-N] function. These analogs with neutral and positive linker showed high binding affinity with DNA/RNA targets.

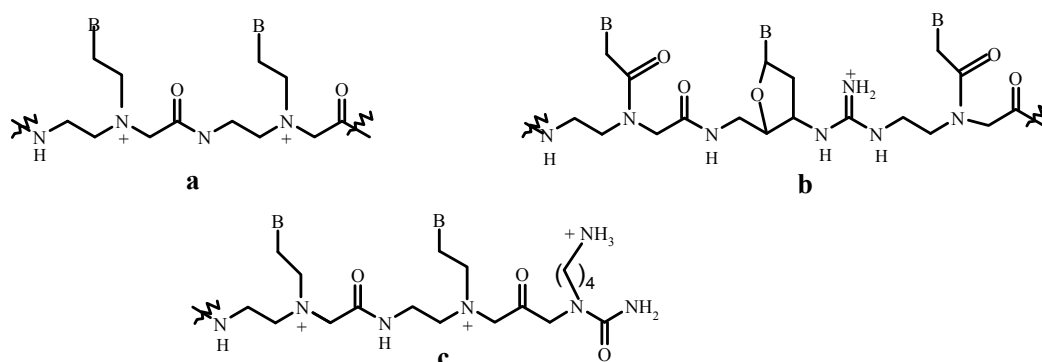


Figure 28: Positively charged PNAs a) Flexible ethylene linker, b) Guanidinium linkages, c) Lysine residues

Introduction of negative charges in the PNA backbone (Figure 29 a-g) improved aqueous solubility and showed good binding with both DNA and RNA. These modifications have been well studied and reviewed.^{67,68} However, many of these modified complexes were found to have less thermal stability compared to the unmodified PNA sequences. Ether linked PNAs (Figure 29 h&i) showed co-operative binding with complementary antiparallel RNA in a sequence specific manner.^{69,70}

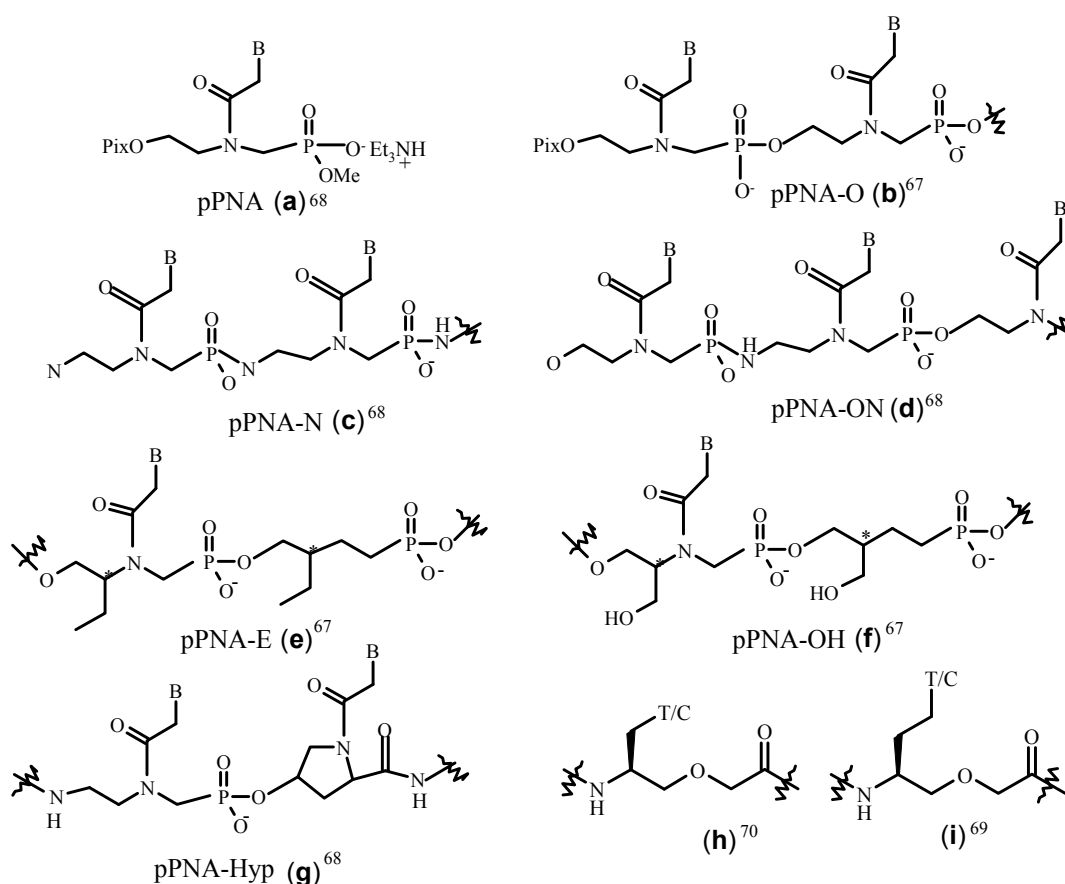
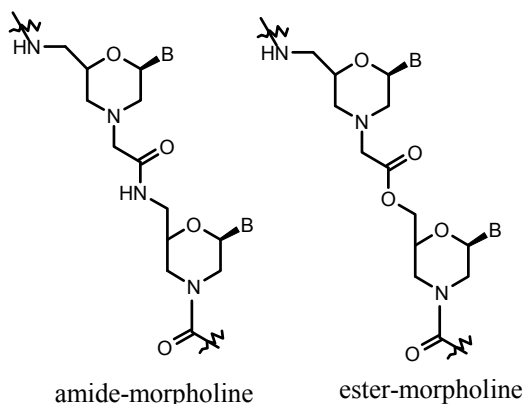


Figure 29: Anionic PNAs (a-g) and oxy PNAs (h-i)

1.4.6b Construction of bridged structures

The *cis* and *trans* rotamers arising from the tertiary amide linkage in each PNA unit lead to a variety of rotameric conformations that cause different PNA:DNA/RNA

hybridization kinetics in parallel and antiparallel hybrids. The high rotational energy barrier between *cis* and *trans* rotameric populations makes these rotamers non-interconvertible. Any favorable structural preorganization of PNA may activate a shift in equilibrium towards the preferred complex formation because of the reduced entropy loss upon complex formation, provided that the enthalpic contributions suitably compensate. This may be achieved if the conformational freedom in *aeg*-PNA is reduced by bridging the aminoethyl/glycyl acetyl linker arms to give rise to cyclic analogs with preorganized structure. Such modifications also restrain the flexible domains of the *aeg*-PNA (glycyl and ethylene diamine) in addition to introducing the chirality into PNA monomeric units. It also offers with the possibility of further fine-tuning the structural features of PNA to mimic DNA (Figure 30). The development in this area of research are described in recent reviews.⁷¹



amide-morpholine

ester-morpholine

Figure 31: Structures of Morpholino PNA

1.4.7 PNA analogues with modified nucleobases⁷³

1.4.7a Modified Nucleobases with larger surface area

In order to increase the stability of complexes formed by PNA with target nucleic acids, bases that possess a larger surface area (for greater hydrophobic/stacking interactions), make additional H-bonds or that are positively charged have been prepared. A wide variety of 5-substituted uracils were synthesized and their ability for triplex formation have been studied (Figure 32).⁷³⁻⁷⁶

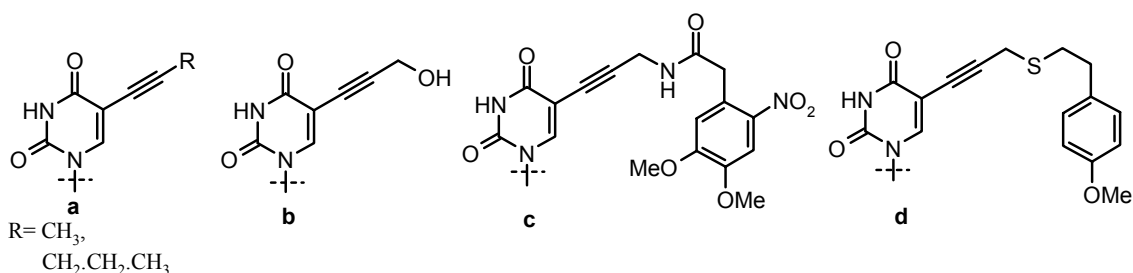


Figure 32: Structures of the a) 5-alkynyluracils, b) 5-(propargyl alcohol)uracil, c) 5-(*N*-(4,5-dimethoxy-2-Nitrobenzyl)propargylcarbamate)uracil; d) 5-(*p*-methoxy-benzylthiopropargyl ether)uracil

Among the bicyclic derivatives of 1,8-Naphthyridin-2(1*H*)-derivative (Figure 33), 7-chloro-1,8-naphthyridin-2(1*H*)-one (7-Cl-bT) stabilize the duplex and triplex.⁷⁷⁻⁷⁸ Thermodynamic analysis showed that the stabilization was due to enthalpic in origin due to increased stacking interactions.

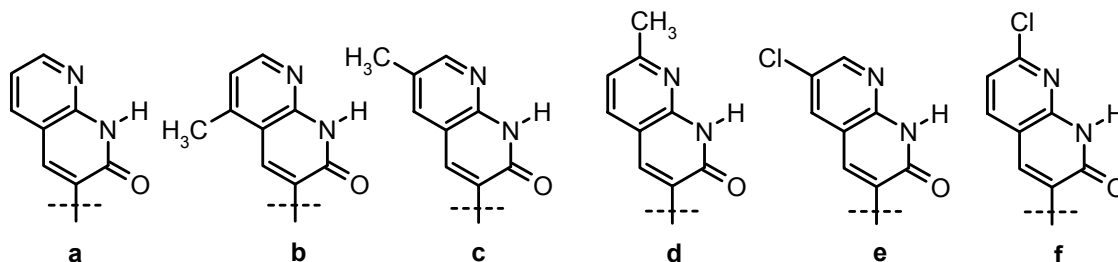


Figure 33: Structures of 1,8-Naphthyridin-2(1H)-derivatives substituted with a) un substituted b) 5-methyl, c) 6-methyl, d) 7-methyl, e) 6-chloro and f) 7-chloro 1,8-Naphthyridin

Bicyclic analogs of thymine or cytosine stabilize the duplex/ triplex. The concept was extended to tricyclic analog (Figure 34), since the three rings with greater surface may give more extensive stacking interaction. The tricyclic analog of cytosine (Figure 34b&c) gave better results over the tricyclic analogue of thymine (Figure 34a).⁷⁹⁻⁸¹

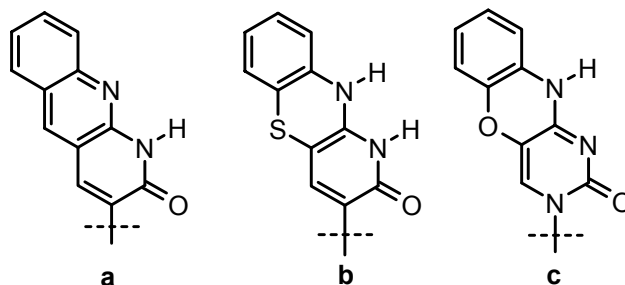


Figure 34: Structures of a) phenazine, b) phenothiazine, c) phenoxazine.

1.4.7b G-clamp as modified nucleobase

In order to build in specific, additional bonding interactions with guanine, the G-clamp base (Figure 35a) was developed. The phenoxazine (cytosine analog) derivative containing extended amine provides an additional H-bond to its complement, guanine on oligonucleotide chain (Figure 35b&c).⁸²⁻⁸⁴ The additional interaction is demonstrated in Figure 35 d.

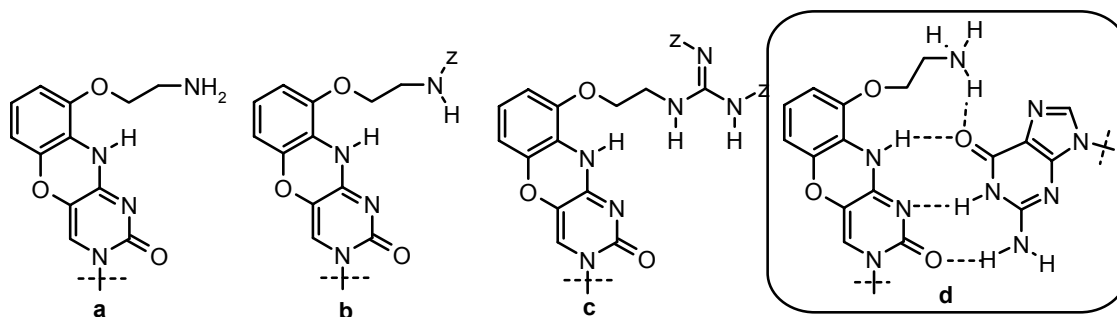


Figure 35: Structures of a) G-clamp, b) *cbz*-G clamp, c) guanidinium G clamp d) the interaction between G-clamp and guanine.

1.4.7c Modified nucleobase with additional hydrogen bonding sites

Modifications of the hydrogen bonding properties of nucleobases change their interactions and specificity for a complementary nucleobase. This concept has been used to increase the complex stability and sequence selectivity. In case of PNA the first example is the use of 2,6-diaminopurine (DAP), in place of adenine (Figure 36 a). The DAP having additional H-bonding sites for binding to thymine, increases the thermal stability of complexes by 4-6 °C per substitution as well as showed better discrimination towards mismatch sequences.

In triplexes the central nucleobase needs to form hydrogen bonding from both the sides to form stable triplexes and cytosine can form triplexes under acidic conditions only. The modified bases that can form hydrogen bonds from both the sides may form stable triplexes. Pseudoisocytosine, was the first mimic of this kind in PNA, which is termed the “J base” (Figure 36 b).⁸⁵ The “J” base containing bisPNA, eliminated the pH-dependence C-for formation of triplexes.^{86,87}

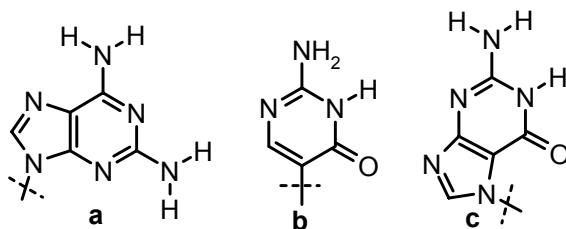


Figure 36: Structures of a) 2,6-diamino purine, b) pseudoisocytosine (J-base), c) *N*⁷-guanine

*N*⁷-guanine (Figure 36 c) incorporated in bisPNA was found to form triplex with G:C base pair through parallel or reversed-Hoogsteen bonding in preference, because *N*⁷G can mimic protonated cytosine in the pyrimidine motif forming stable triplexes at neutral pH with the recognition of G:C base pair.⁸⁸⁻⁹⁰

The design of modified pyrimidine nucleobase, which can be the center base of a triplex triad, has been a challenging task. Thymine is the most difficult nucleobase to achieve such possibility, because the methyl group (C-5 position) does not allow Hoogsteen type of hydrogen bond formation.

One of the pyrimidine modifications is E-base (3-oxo-2,3-dihydropyridazine) (Figure 37 a), which can form a triad with A:T base pair (Figure 37 c). The E-base binds to thymine more strongly than guanine. It even binds to uracil, more favorably than thymine. Its derivative, the conformationally locked analog, the E_{ag} base (Figure 37 b), binds to thymine less preferentially than the E base. It showed least preference for uracil.

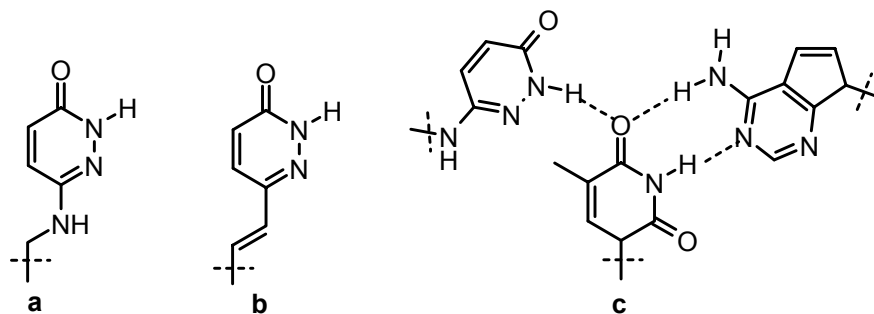


Figure 37: The structures of a) 3-oxo-2,3-dihydropyridazine (E-base), b) E_{ag} base, c) The proposed structure of the 3-oxo-2,3-dihydropyridazine E:T:A triplet.

1.4.7d Fluorescent moieties used as modified nucleobases:

It would be useful to have intrinsically fluorescent nucleobases that are complementary to the remaining natural nucleobases.

2-aminopurine is a modified nucleobase (Figure 38 a), which has fluorescence property. Whenever this was used as a complementary base to thymine, successful hybridization can be detected through a decrease in the fluorescent intensity of 2-aminopurine.⁹¹ 5-Phenyl ethynyluracil (5-yne-U) (Figure 38b) and 6-phenylpyrrolocytosine (pC) (Figure 38c), retain their selectivity for A and G, respectively. The oligomers respond to the state of hybridization, even though 5-phenyl ethynyluracil shows it weak fluorescence.⁹²

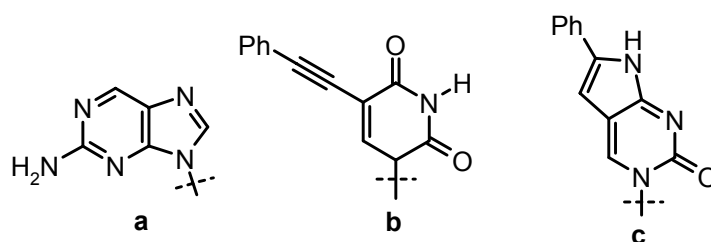


Figure 38: Structures of a) 2-aminopurine, b) 5-phenylethynyluracil, c) 6-phenylpyrrolocytosine

The phosphorescent PNA is useful for diagnostic applications. The chromophores having phosphorescence property were introduced into PNA through substitution of nucleobase. 2-Amido anthraquinone (AQ2) (Figure 39 a) is a phosphorescent moiety (an analogue of anthraquinone). The phosphorescence of 2-amido anthraquinone containing PNA was quenched, upon its hybridization with complementary nucleic acids.

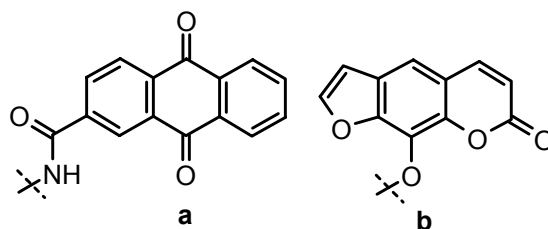


Figure 39: Structures of a) 2-amido anthraquinone (AQ2) and b) 8-oxapsoralen

With the 8-oxapsoralen (Figure 39 b) as a modified nucleobase attached to PNA, it was observed that it stabilized the duplex at either the *C*- or *N*-terminal end, but the duplex is destabilized when the modification is incorporated in the middle. Hybridization between the modified PNA oligomer and the complementary DNA can be detected through quenching of fluorescence by 43%.⁹⁴

Further development of this concept has led to application of intercalating nucleobase as a fluorescent probe. The positively charged thiazole orange (TO) was used as a modified base, since the positive charge would benefit the hybridization (Figure 40 a).⁹⁵ It undergoes a large fluorescence enhancement upon intercalation. The placement of the modified residue at a central position enforces intercalation regardless of the opposing base. Evaluation of the best linkage of the fluorophore to the PNA backbone and attachment of the TO via the quinoline ring, has produced the most responsive probes (Figure 40 b).⁹⁶

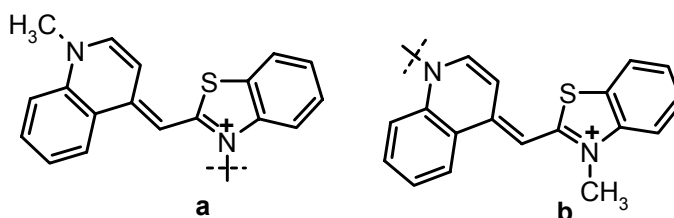


Figure 40: Structures of positively charged thiazole orange (TO) with attachment to PNA backbone through a) thiazole ring, b) quinoline ring

1.4.7e Universal bases:

The design of unnatural nucleobases that do not contain hydrogen bonding acceptors or donors, but are capable of efficient base stacking, are highly pursued for use as “universal bases” (Figure 41). These universal bases show less discrimination among the natural nucleobases (A, G, C, T).⁹⁷ The introduction of a universal base into PNA would expand the repertoire of its use as an antisense/antigene agent or diagnostic tool.

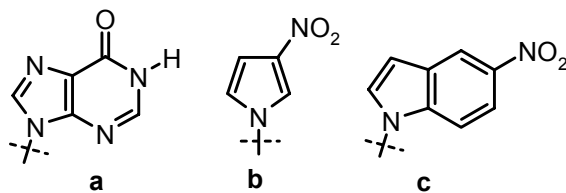


Figure 41: The structures of universal bases a) hypoxanthine, b) 3-nitropyrrole, c) 5-nitroindole

Natural nucleobase mimic hypoxanthine (Figure 41 a) and unnatural heterocycles 3-nitropyrrole (Figure 41 b) and 5-nitroindole (Figure 41 c) have been used as potential universal bases in PNA.⁹⁸ While these universal bases do show little base discrimination, they also destabilize the duplex nearly as much as a mismatch in oligonucleotides.

1.4.7f Non-heterocyclic aromatic bases:

Benzene and pyrene (Py) rings have been incorporated into PNA-like oligomers (Figure 42), designed as bis-intercalators. Unlike the heterocyclic aromatic modified base containing oligonucleotides, phenyl ring containing PNAs showed destabilization.

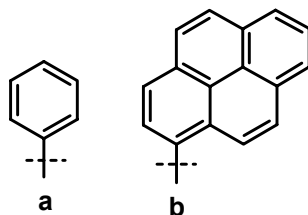


Figure 42: Aromatic groups, a) phenyl and b) pyrene replaced nucleobase in PNA

PNAs containing 2,4-difluorophenyl, pentafluorophenyl and 2,4-difluoro-5-methylphenyl 4-fluorophenyl (4-FPh), pentafluorophenyl (PFP), and β -heptafluoro-naphthalene (HFN) monomers were synthesized and incorporated into a PNA oligomers for studying the derived duplexes stability (Figure 43).⁹⁹

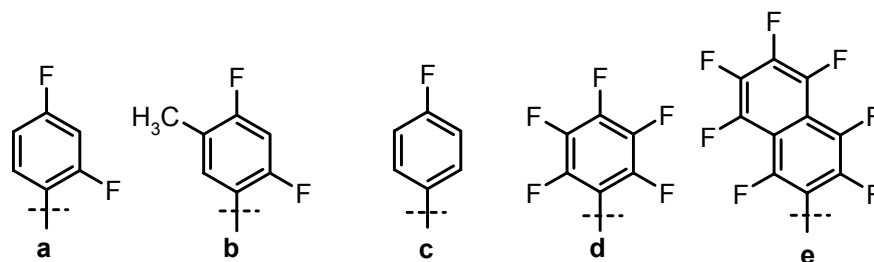


Figure 43: Fluro aromatics, a) 2,4-difluorophenyl, b) 2,4-difluoro-5-methyl phenyl, c) 4-fluorophenyl (4-FPh), d) pentafluorophenyl (PFP), e) β -heptafluoro-naphthalene (HFN) replaced nucleobase in PNA

1.4.7g Nucleobase replacement with non-aromatics

The complete replacement of the nucleobase by a nonaromatic group has been reported, but this area of research hasn't been explored enough. The α -acetyl-2- amino ethylglycine unit has been used as an abasic site in PNA (Figure 44a). Researchers incorporated either neutral (Figure 44 a) or positively charged (Figure 44 b) hydrophilic moieties into the termini of PNA as solubility enhancers.^{100a}

A combinatorial approach has been attempted towards the discovery of a synthetic protease for myoglobin with aptamer-like PNAs containing cyclen PNA monomer (Figure 44 c), which acts as a metal chelating ligand.^{100b}

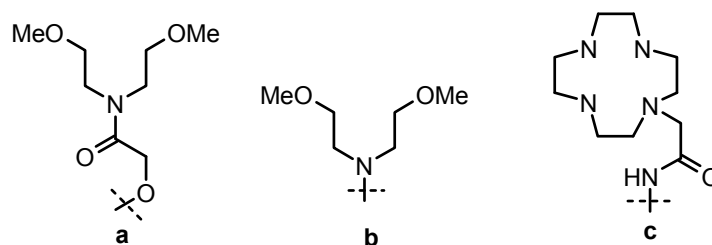


Figure 44: Structures of a) α -acetyl-2- amino ethylglycyl PNA, b) *N,N*-dimethoxyethyl amino PNA , c) cyclen PNA

1.5 Present work

The above sections describe the current literature on Peptide Nucleic Acids with reference to structural variations and duplex/triplex stabilization applications. The strand

invasion property along with its high affinity and specificity to complementary DNA/RNA has prompted it as a useful tool in therapeutics and biology. However, due to limitations like poor aqueous solubility, self-aggregation, poor cellular uptake, ambiguity in binding orientation and possibility of various conformations has limited further exploitation of PNA in practical applications. In order to circumvent these problems further modifications and the synthesis of newer PNAs to improve their properties, continue to elicit interest. To overcome the problems associated with PNA, there is considerable interest in chemical modifications of PNA.

In this connection Chapter 2 deals with the synthesis and characterization of cyanuryl and 8-bromoadeninylyl PNA monomers and their site specific incorporation into PNA oligomers. 8-Bromoadeninylyl PNA monomers were converted into 8-aminoadeninylyl PNA oligomers on resin bounded oligomer. The rationale behind the synthesis of cyanuryl and 8-aminoadeninylyl PNA was to induce Hoogsteen hydrogen bonding to stabilize the triplex structures.

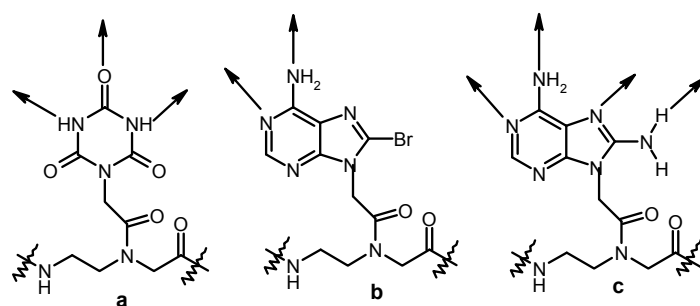


Figure 45: Structures of a) cyanuryl PNA, b) 8-bromoadeninylyl PNA and c) 8-aminoadeninylyl PNA (The sites of the molecule involve in hydrogen bonding are showed with arrows)

Chapter 3 describes the biophysical studies of various cyanuryl, 8-bromo adeninylyl and 8-aminoadeninylyl PNA oligomers (octamers). The triplex formation of the modified PNA oligomers (cyanuryl/8-bromoadeninylyl/8-aminoadeninylyl) with complementary DNA was studied through circular dichroism spectroscopy (CD)

spectroscopy) and UV-mixing curves. The stability of triplex was studied through UV-melting experiments. Studying on base pair complexation in PNA monomers have been attempted used NMR spectroscopy.

1.6 Reference:

1. Watson, J. D.; Crick, F. H. C. *Nature* **1953**, *171*, 737.
2. Sanger, W. *Principles of Nucleic Acid Structure* Springer Verlag, New York **1984**.
3. Assa-Munt, N.; Denny, W. A.; Leupin, W.; Kearns, D. R. *Biochemistry* **1985**, *24*, 1441.
4. Hogan, M.; Dattagupta, N.; Crothers, D. M. *Biochemistry* **1979**, *18*, 280.
5. Kopka, M. L.; Yoon, C.; Goodsell, D.; Pjura, P.; Dickerson, R. E. *J. Mol. Biol.* **1985**, *183*, 553.
6. a) Kopka, M. L.; Yoon, C.; Pjura, P.; Goodsell, D.; Dickerson, R. E. *Proc. Natl. Acad. Sci.* **1985**, *82*, 1376. b) Reddy, B. S. P.; Sondhi, M.; Lown, J. W. *Pharmacology & Therapeutics* **1999**, *84*, 1.
7. Sanghvi, Y. S. *Antisense Research and application*. Eds. Crooke, S. T.; Lebleu, B. **1993**, CRC Boca Raton. (b) Phillips. I. M.; Zhang, Y. C. (Ed.) *Methods in Enzymology* **2000**, *313*, 46.
8. Zamechnik, P.C.; Stephenson, M. L. *Proc. Natl. Acad. Sci.* **1978**, *75*, 280.
9. (a) Felsenfeld, G.; Davies, D. R.; Rich, A. *J. Am. Chem. Soc.* **1957**, *79*, 2023. (b) Moser, H. E.; Dervan, P. B. *Science* **1987**, *288*, 645. (c) Beal, P.A.; Dervan, P. B. *Science* **1991**, *251*, 1360.
10. Soyfer, V. N.; Potamann, V. N. *Triple Helical Nucleic Acids* **1996**, Springer-Verlag, NY.

11. Chan, P. P.; Glazer, P. M. *J. Mol. Med.* **1997**, *75*, 267.
12. Strivchak, E. P.; Summerton, J. E.; Weller, D. D. *Nucleic Acids Res.* **1989**, *17*, 6129.
13. Nielsen, P. E. *Annu. Rev. Biophys. Biomol. Struct.* **1995**, *24*, 167.
14. Varma, R. S. *Syn Lett.* 1993, *9*, 621.
15. Moriguchi, T.; Shinozuka, K. *Frontiers in Organic Chemistry, Vol. 1* (Atta-ur-Rahman (Ed.)), 163-194
16. Luyten, I.; Herdewijn, P. *Eur. J. Med. Chem.* **1998**, *33*, 515.
17. Herdewijn, P. *Antisense Nucleic Acid Drug Dev.* **2000**, *10*, 297
18. Rosler, A.; Peleiderer, W. *Helv. Chim. Acta.* **1997**, *80*, 1869.
19. Ozaki, H.; Ogawa, Y., Mine, M., Sawai, H. *Nucleosides Nucleotides*, **1998**, *17*, 911.
20. (a) Wanger, R. W.; Matteucci, M. D.; Lewis, J. G.; Gutierrez, A. J.; Moulds, C.; Froehler, B.C. *Science*, **1993**, *260*, 1510. (b) Froehler, B. C.; Wadwani, S.; Terhorst, T. J.; Gerrard, S.R. *Tetrahedron Lett.* **1992**, *33*, 5307.
21. Buhr, C. A.; Wanger, R. W.; Grant, D.; Froehler, B. C. *Nucleic Acids Res.* **1996**, *24*, 2974.
22. Gutierrez, A. J.; Froehler, B. C. *Tetrahedron Lett.* **1996**, *37*, 3959.
23. Gutierrez, A. J.; Terjprst, T. J.; Matteuci, M. D.; Froehler, B.C. *J. Am. Chem. Soc.* **1994**, *116*, 5540.
24. (a) Inoue, H.; Imura, A.; Ohtsuka, E. *Nucleic Acids Res.* **1985**, *13*, 7119. (b) Lin, K. Y.; Jones, R. J.; Matteucci, M. *J. Am. Chem. Soc.* **1995**, *117*, 3873.
25. Buhr, C. A.; Matteucci, M. D.; Froehler, B. C. *Tet. Lett.* **1999**, *40*, 8969.

26. Lee, J. S.; Woodsworth, M. L.; Latimer, L. J. P. Morgan, A. R. *Nucleic Acids Res.* **1984**, *12*, 6603.
27. Povsic, T. J.; Dervan, P. B. *J. Am. Chem. Soc.* **1989**, *111*, 3059.
28. Schmid, N.; Behr, J. P. *Tetrahedron Lett.* **1995**, *36*, 1447.
29. Haginoya, N.; Ono, A.; Nomura, Y.; Ueno, Y.; Matsuda, A. *Bioconj. Chem.* **1995**, *8*, 271.
30. (a). Barawkar, D. A.; Rajeev, K. G.; Kumar, V. A.; Ganesh, K. N. *Nucleic Acids Res.* **1996**, *24*, 1229. (b) Seela, F.; Zulauf, M. *Helv. Chim. Acta.* **1999**, *82*, 1878.
31. Adam V.; Sproat B.S. *J. Chem. Soc. Perkin Trans.* **1994**, *1*, 3423.
32. Rosenberg. I.; Tocik. Z.; Watanabe. K. A. *Nucleic Acids Res.* **1991**, *24*, 43.
33. Rosenberg. I.; Farras J. S.; Tocik Z.; Ren W. Y.; Ciszewski. L. A.; Kois. P.; Pankiewicz. K. W.; Spassova. M.; Watanabe. K. A. *Nucleosides Nucleotides* **1993**, *12*, 381.
34. Ono. A.; Tso. P.O.P.; Kan L. S. *J. Org. Chem.* **1992**, *57*, 3225.
35. Rana. V. S.; Ganesh. K. N. *Nucleic Acids Res.* **2000**, *28*, 1162.
36. Chattopadhyaya, J. *Tetrahedron*, **1991**, *47*, 4693.
37. Kumar R. K.; Gunjal A. D.; Ganesh K. N. *Biochem. Biophys. Res. Comm.* **1994**, *204* (2) 788.
38. Kawai, K.; Saito, I.; Sugiyama, H. *Tetrahedron Lett.* **1998**, *39*, 5221.
39. Soliva, R.; Garcia, G. R.; Blas, J. R.; Eritja, R.; Asensio, J. L.; Gonza' lez, C.; Luque, F. J.; Orozco, M. *Nucleic Acids Res.* **2000**, *28*, 4531.
40. Cubero, E.; Avino, A.; de la Torre, B. G.; Frieden, M.; Eritja, R.; Luque, F. J.; Gonzalez, C.; Orozco, M. *J. Am. Chem. Soc.* **2002**, *124*, 3133.

41. Toulme, J. J. *Nature Biotech.* **2001**, *19*, 17.
42. (a) Chin, D. J.; Green, G. A.; Zon, G.; Szoka, Jr. F. C. *New Biologist*, **1990**, *2*, 1091.
(b) Leonetti, J. P.; Mechti, N.; Degols, G.; Gagnor, C.; Lebleu, B. *Proc. Natl. acad. Sci. USA.* **1991**, *88*, 2702.
43. (a) Sood, A.; Shaw, B. R.; Spielvogel, B. F. *J. Am. Chem. Soc.* **1990**, *112*, 9000.
(b) Shimizu, M.; Wada, T.; Oka, N.; Saigo, K. *J. Org. Chem.* **2004**, *69*, 5261.
44. Freier, M. S.; Altmann, K. H. *Nucleic Acids Res.* **1997**, *25*, 4429.
45. (a) Allart, B.; Khan, K.; Rosemeyer, A. H.; Schepers, G.; Hendrix, C.; Rothenbacher, K.; Seela, F.; Aerschot, V.; Herdewijn, P. *Tetrahedron* **1999**, *55*, 6527. (b) Harald, W.; Folkert, R. Rene.; Mahesh, R.; Griet, A.; Martin, B.; Ramanarayanan K.; Albert E. *Bioorg. Med. Chem.* **2001**, *9*, 2411.
46. Jing, W.; Birgit, V.; Ingrid, L.; Eveline, L.; Matthias, F.; Chris, H.; Helmut, R.; Frank, S.; Arthur, V.; Herdewijn, P. *J. Am. Chem. Soc.* **2000**, *122*, 8595.
47. (a) Petersen, M.; Wengel, J. *Trends Biotechnol.* **2003**, *21*, 74. (b) Koshkin, A.; Singh, S. K.; Nielsen, P.; Rajwanshi, V. K.; Kumar, R.; Meldgaard, M.; Olsen, C. E.; Wengel, J. *Tetrahedron* **1998**, *54*, 3607. (c) Singh, S. K.; Nielsen, P.; Koshkin, A. A.; Wengel, J. *Chem. Commun.* **1998**, 455.
48. (a) Obika, S.; Nanbu, D.; Hari, Y.; Andoh, J. I.; Mori, K. I.; Doi, T.; Imanshi, T. *Tetrahedron Lett.* **1998**, *39*, 5401. (b) Hertoghs, K. M.; Ellis, J. H.; Catchpole, I. R. *Nucleic Acid Res.* **2003**, *20*, 5817.
49. (a) Stirchak, E. P.; Summerton, J. E.; Weller, D. D. *Nucleic Acids Res.* **1989**, *17*, 6129. (b) Summerton, J.; Weller D. *Antisense Nucleic Acid Drug Dev.* **1997**, *7*, 187
50. Nielsen, P. E.; Egholm, M.; Berg, R. H.; Buchardt, O. *Science*, **1991**, *254*, 1497.

51. (a) Ray, A.; Norden, B. *FASEB J*, **2000**, *14*(9), 1041. (b)Corradini, R.; forza, S. S.; Tedeschi, T.; Totsingan, F.; Marchelli, R. *Curr. Top. Med. Chem.* **2007**, *7*, 681-694.
52. Egholm, M.; Buchardt, O.; Christensen, L.; Behrens, C.; Freier, S. M.; Driver, D. A.; Berg, R.H.; Kim, S. K.; Nordon, B.; Nielsen, P. E. *Nature*, **1993**, *365*, 566.
53. Jensen, K. K.; Qrum, H.; Nielsen, P. E.; Norden, B. *Biochemistry* **1997**, *36*, 5072.
54. Protozanova, E.; Demidov, V. V.; Nielsen, P. E.;Kamenetskii, M. D. F. *Nucleic Acids Res.* **2003**, *31*, 3929.
55. Møllegaard, N. E.; Buchardt, O.; Egholm, M.; Nielsen, P. E. *Proc. Natl. Acad. Sci.* **1994**, USA *91*, 3892.
56. (a) Jensen, K. K.; Qrum, H.; Nielsen, P. E.; Norden, B. *Biochemistry*, **1997**, *36*, 5072.
(b) Kuhn, H.; Demidov, V. V; Nielsen, P. E.; Frank-Kamenetskii, M. D. *J. Mol. Biol.***1999**, *286*, 1337.
57. Brown, S. C.; Thomson, S. A.; Veal, J. M.; Davis, D. G. *Science* **1994**, *265*, 777.
58. Eriksson, M.; Nielsen, P. E. *Nature Struct. Biol.* **1996**, *3*, 410.
59. Betts, L.; Josey, J. A.; Veal, J. M.; Jordan, S. R. *Science* **1995**, *270*, 1838.
60. Rasmussen, H.; Kastrop, J. S.; Nielsen, J. N.; Nielsen, J. M.; Nielsen, P.E. *Nature Struct. Biol.* **1997**, *4*, 98.
61. Leijon, M.; Gräslund, A.; Nielsen, P. E.; Buchardt, O.; Nordén, B.; Kristensen, S. M.; Eriksson, M. *Biochemistry* **1994**, *33*, 9820-9825.
62. Kim, S. K.; Nielsen, P. E.; Egholm, M.; Buchardt, O.; Berg, R. H.; Nordén, B. *J. Am. Chem. Soc.* **1993**, *115*, 6477-6481.
63. Dueholm, K. L.; Nielsen, P. E. *New J. Chem.* **1997**, *21*, 19-31.

64. Hyrup, B.; Egholm, M.; Rolland, M.; Nielsen, P. E.; Berg, R. H.; Buchardt, O. J. *Chem. Soc., Chem. Commun.* **1993**, 518-519.
65. (a) Haiima, G.; Lohse, A.; Buchardt, O.; Nielsen, P. E. *Angew. Chem. Int. Ed. Engl.* **1996**, *35*, 1939. (b) Sforza, S.; Haiima, G.; Marchelli, R.; Nielsen, P. E. *Eur. J. Org. Chem.* **1999**, 197. (c) Zhang, L.; Min, J.; Zhang, L. *Bioorg. Med. Chem. Lett.* **1999**, *9*, 2903.
66. Barawkar, D. A.; Bruice, T. C. *J. Am. Chem. Soc.* **1999**, *121*, 10418.
67. Efimov, V. A.; Choob, M. V.; Buryakova, A. A.; Chakhmakhcheva, O. G. *Nucleos. Nucleot. Nucl.* **1998**, *17*, 1671.
68. Efimov, V. A.; Buryakova, A. A.; Choob, M. V.; Chakhmakhcheva, O. G. *Nucleos. Nucleot. Nucl.* **1999**, *18*, 1393.
69. Kuwahara, M.; Arimitsu, M.; Shisido, M. *Tetrahedron* **1999**, *55*, 10067-10078.
70. Altmann, K. H.; Chiese, C. S.; Garcia-Echeverria, C. **1997**, *7*, 1119-1112.
71. (a) Kumar, V. A.; Ganesh, K. N. *Acc. Chem. Res.* **2005**, *38*, 404. (b) Kumar, V. A. *Eur. J. Org. Chem.* **2002**, 2021.
72. Maison, W.; Schlemminger, O.; Westerhoff, O.; Martens, J. *Biorg. Med. Chem.* **2000**, *8*, 1343.
73. Wojciechowski, F.; Hudson, R. H. E. *Cur. Top. Med. Chem.* **2007**, *7*, 667.
74. Bajor, Z.; Sagi, G.; Tegye, Z.; Otvos, L. *Nucleos. Nucleot. Nucl.* **2003**, *22*, 1215.
75. Bajor, Z.; Sagi, G.; Tegye, Z.; Kraicsovits, F. *Nucleos. Nucleot. Nucl.* **2003**, *22*, 1963.
76. Hudson, R. H. E.; Li, G.; Tse, J. *Tetrahedron Lett.* **2002**, *43*, 1381.

77. Eldrup, A. B.; Nielsen, B. B.; Haaima, G.; Rasmussen, H.; Kastrup, J. S.; Christensen, C.; Nielsen, P.E. *Eur. J. Org. Chem.* **2001**, *9*, 1781.
78. Eldrup, A. B.; Christensen, C.; Haaima, G.; Nielsen, P. E. *J. Am. Chem. Soc.* **2002**, *124*, 3254.
79. Lin, K. Y.; Jones, R. L.; Matteucci, M. *J. Am. Chem. Soc.* **1995**, *117*, 3873.
80. Lin, K. Y.; Matteucci, M. D. *J. Am. Chem. Soc.* **1998**, *120*, 8531.
81. Wilds, C. J.; Maier, M. A.; Tereshko, V.; Manoharan, M.; Egli, M. *Angew. Chem. Int. Ed.* **2002**, *41*, 115.
82. Rajeev, K. G.; Maier, M. A.; Lesnik, E. A.; Manoharan, M. *Org. Lett.* **2002**, *4*, 4395.
83. Ausin, C.; Ortega, J. A.; Robles, J.; Grandas, A.; Pedroso, E. *Org. Lett.* **2002**, *4*, 4073.
84. Christensen, L.; Hansen, H. F.; Koch, T.; Nielsen, P. E. *Nucleic Acids Res.* **1998**, *26*, 2735.
85. Egholm, M.; Christensen, L.; Dueholm, K. L.; Buchardt, O.; Coull, J.; Nielsen, P. E. *Nucleic Acids Res.* **1995**, *23*, 217.
86. Griffith, M. C.; Risen, L. M.; Greig, M. J.; Lesnik, E. A.; Sprankle, K. G.; Griffey, R. H.; Kiely, J. S.; Freier, S. M. *J. Am. Chem. Soc.* **1995**, *117*, 831.
87. Kuhn, H.; Demidov, V. V.; Frank-Kamenetskii, M. D.; Nielsen, P. E. *Nucleic Acids Res.* **1998**, *26*, 582.
88. Kumar, V. A.; D'Costa, M.; Ganesh, K. N. *Nucleos. Nucleot. Nucl.* **2001**, *20*, 1187.
89. D'Costa, M.; Kumar, V. A.; Ganesh, K. N. *J. Org. Chem.* **2003**, *68*, 4439.
90. Shirude, P. S.; Kumar, V. A.; Ganesh, K. N. *Eur. J. Org. Chem.* **2005**, *24*, 5207.
91. Gangamani, B. P.; Kumar, V. A.; Ganesh, K. N. *Biochem. Biophys. Res. Comm.* **1997**, *240*, 778.

92. Hudson, R. H. E.; Dambeniaks, A. K.; Moszynski, J. M. *Proc. SPIE-The International Society for Optical Engineering*, **2005**, 5969, 59690J/1.
93. Armitage, B.; Koch, T.; Frydenlund, H.; Orum, H.; Schuster, G. B. *Nucleic Acids Res.* **1998**, 26, 715.
94. Okamoto, A.; Tanabe, K.; Saito, I. *Org. Lett.* **2001**, 3, 925.
95. Seitz, O.; Bergmann, F.; Heindl, D. *Angew. Chem., Int. Ed.* **1999**, 38, 2203.
96. Koehler, O.; Jarikote, D. V.; Seitz, O. *ChemBioChem* **2005**, 6, 69.
97. (a) Loakes, D. *Nucleic Acids Res.* **2001**, 29, 2437. (b) Kool, E. T. *Acc. Chem. Res.* **2002**, 35, 936.
98. Challa, H.; Styers, M. L.; Woski, S. A. *Org. Lett.* **1999**, 1, 1639.
99. (a) Shibata, N.; Das, B. K.; Honjo, H.; Takeuchi, Y. *J. Chem. Soc., Perkin Trans.1* **2001**, 14, 1605. (b) Frey, K. A.; Woski, S. A. *Chem. Commun.* **2002**, 19, 2206.
100. (a) Gildea, B. D.; Casey, S.; MacNeil, J.; Perry-O'Keefe, H.; Sørensen, D.; Coull, J.M. *Tetrahedron Lett.* **1998**, 39, 7255. (b) Jeon, J.W.; Son, S.J.; Yoo, C.E.; Hong, I.S.; Suh, J. *Bioorg. Med. Chem.* **2003**, 11, 2901.

CHAPTER 2

Synthesis and Characterization of Cyanuryl PNA
and 8-Substituted Adeninyl PNA

2.1 Introduction

As described in Chapter 1, the search for effective antigene/antisense agents has led to the development of new classes of DNA/RNA analogues in the past few years,¹⁻⁸ and the most prominent outcome of this search is the invention of peptide nucleic acids (PNA).⁹⁻¹⁴

In this class of compounds, the negatively charged sugar-phosphate backbone of DNA is replaced by a neutral and achiral polyamide backbone consisting of N-(2-aminoethyl) glycine units. The nucleobase is attached to the backbone through a conformationally rigid tertiary amide linker (Figure 1). The inter-nucleobase distance in PNA is conserved, allowing its binding to the target DNA/RNA sequences with high sequence specificity and affinity. Moreover PNA is stable to cellular enzymes like nucleases and proteases.¹⁵

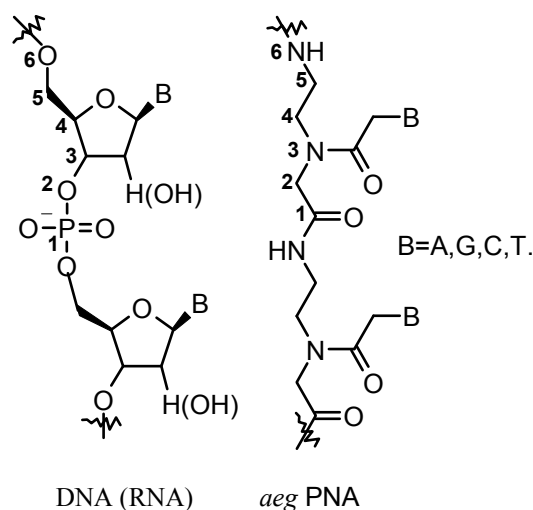


Figure1: DNA(RNA) and PNA structures

However, major limitations for the therapeutic applications of PNAs are their poor aqueous solubility due to self-aggregation, insufficient cellular uptake, and

ambiguity in orientation selectivity^{16, 17} of binding (parallel/ antiparallel) with DNA/RNA. The tertiary amide linkage of nucleobase attachment to PNA backbone (*syn-anti*) (Figure 2) leads to different rotameric conformations. Although X-ray structure in solid state indicates major portion of these are PNA (in oligomer) exhibits *syn* conformation,^{18a} it is not certain that it is competent for hybridization with the corresponding complementary oligonucleotide in solution state.^{18b}

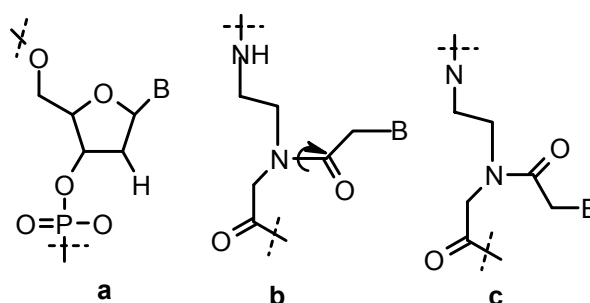


Figure 2. Structures (a) DNA, (b) PNA, and (b, c) rotamers of *aeg* PNA along *tert.* amide bond

In the past few years, significant attempts have been made to address these problems in an effective and rational manner. Introduction of chirality into PNA by linking chiral amino acids, peptides as well as other ligands as conjugates into PNA backbone were aimed at improving the orientation selectivity of binding, solubility and cell penetration.¹⁹⁻²²

In view of these, there is considerable interest in chemical modifications of PNA. Although most of the modifications of PNA are centered on changing the structure of backbone, many new opportunities remain to be explored through modification of the heterocyclic base to influence the base pairing properties.

To address the rotamer problem, introduction of a modified base, which can form hydrogen bonding from either side, could be a worthwhile concept.²³ In case of

oligonucleotides some effort has been carried out in the direction of modified bases to increase the hydrogen bonding sites on purine bases eg. 2,6 diaminopurine etc.^{24,25} For pyrimidines Cyanuric acid (Figure 4) may well suit this purpose, since being symmetrical the potential of H-bonding via increased number of sites is enhanced.

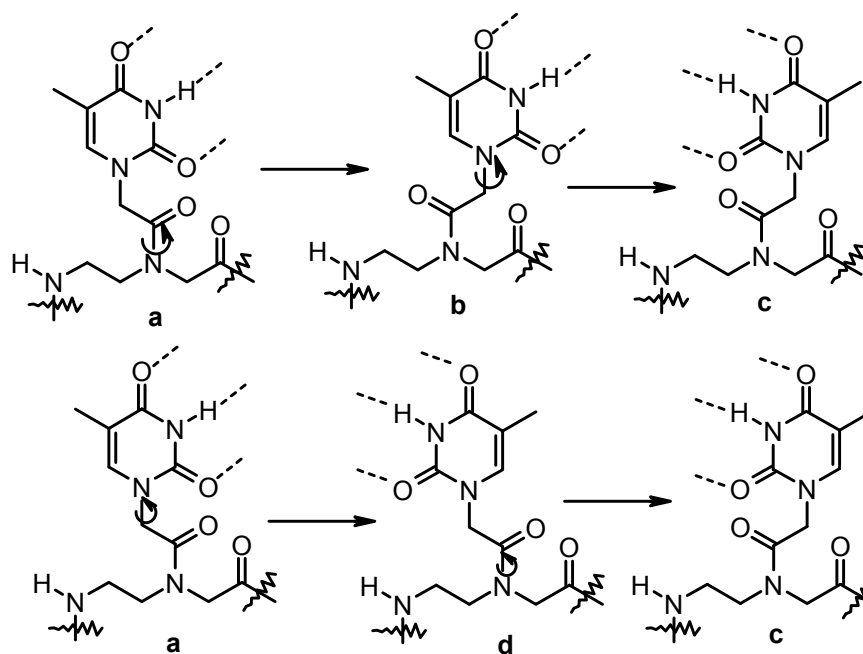


Figure 3: The structures of the rotamers along tertiary amide bond and along the C-N bond (along nucleobase attached to PNA backbone) The sites of the molecule involve in hydrogen bonding are showed with dashes.

Nucleobase attached to PNA backbone through C-N single bond, has the ability to rotate along 360° and hence can assume various conformations and the tertiary amide bond through which base is attached to backbone can from both *syn* and *anti* conformations (Figure 3a&b). Hydrogen bonding in nucleic acid complexes is nucleobase orientation specific. The different rotameric and conformational structures of *aeg* PNA thymine monomer are shown in Figure 3. Among these only some may be productive for hydrogen bonding with the complementary nucleobase adenine depending on its rotameric orientation. This concept is similar to all PNA monomers

consisting of natural nucleobases that can recognize the complementary nucleobases in one specific direction only. The modified nucleobase, which can form hydrogen bonding from either sides, may therefore enhances the hydrogen bonding possibility by two folds. In such a case the conformation of rotamer may not matter, since the base can recognize the complementary nucleobase from either face through hydrogen bonding.

Cyanuric acid and 8-aminoadenine are well suited for such purposes as pyrimidine and purine mimics since, these have potential to form hydrogen bonding from both sides (Figure 4). This feature may lead them to form stable triplexes and duplexes.

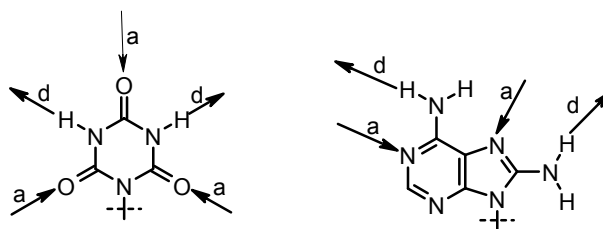


Figure 4: The hydrogen bonding sites on *N*-alkyl cyanuric acid and *N*⁹-alkyl 8-aminoadenine (a=hydrogen bond acceptor, d=hydrogen bond donor)

2.2 Rationale design behind the work

2.2.1 Importance of cyanuric acid as a modified nucleobase

A basic requirement for triplex formation is that the central base of the triad must be able to form hydrogen bonds from either side. A vast literature exists in use of modified bases to increase the hydrogen bonding sites on nucleobases both pyrimidines and purines in oligonucleotides for this purpose.²³ However in PNA field such literature is lacking.

Cyanuric acid is a six-membered cyclic imide with alternate arrangement of hydrogen bond donors and acceptors and it is potentially well suited for hydrogen

bonding from either side. In its free form, it is known to form a network of well-defined robust hydrogen-bonded system through self assembly leading to a molecular tape.^{26,27} Each tape is formed by continuous formation of double hydrogen bonds in one direction, while the tapes are held together in the other direction by single hydrogen bonds as shown in Figure 5a. Mono N-substitution of cyanuric acid perturbs this hydrogen-bonding network, as shown for *N*-methylcyanuric acid, which forms a hexagonal network^{28a} (Figure 5b), with the interaction of C-H---O bonds. Thus Cyanuric acid and *N*-methylcyanuric acid show different supramolecular structures (Figure 5 a&b) with complete saturation of all H-bonding donor and acceptor sites.

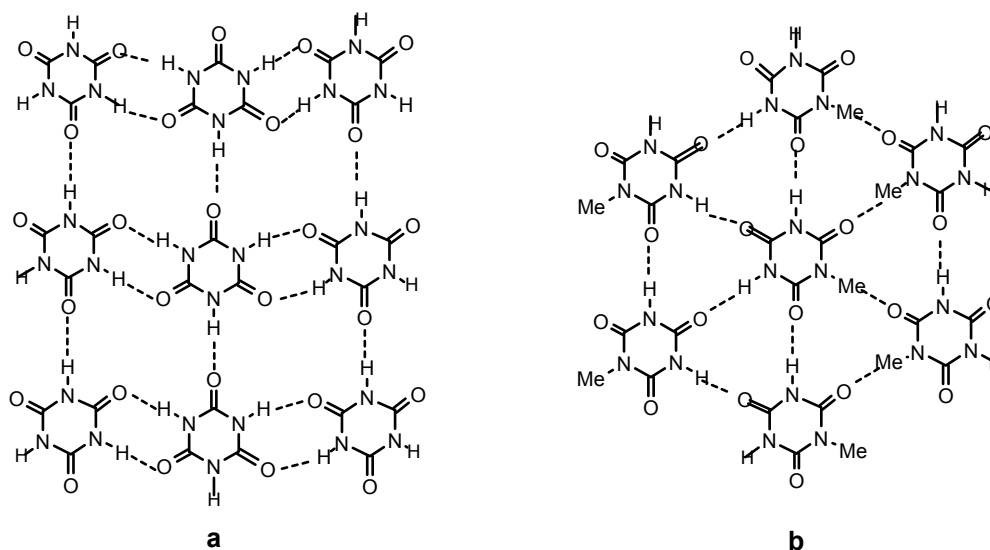


Figure 5: Hydrogen bond arrangements in (a) cyanuric acid (b) *N*-methyl cyanuric acid

Cyanuric acid (CA) and *N*-methylcyanuric acid (MCA) have close structural resemblance to uracil and form a variety of hydrogen-bonded base pairs.^{28b} Adenine is the complementary nucleobase for uracil. The hydrogen bonding interaction between *N*⁹-ethyladenine (EA) and *N*-methylcyanuric acid and with cyanuric acid studied independently.^{28c} The arrangement of the molecular strips in two-dimensional sheets is

however unique with each strip containing molecules of both EA and MCA existing as pairs (Figure 6). There are two distinct types of hydrogen-bonded interactions in the complex of EA and MCA homomeric (MCA \cdots MCA, EA \cdots EA) and heteromeric (MCA \cdots EA). Each strip consists of a polymeric chain made up of continuous hydrogen bonded networks of alternating homo and hetero dimers of methyl cyanuric acid and ethyladenine as, MCA \cdots MCA \cdots EA \cdots EA \cdots MCA \cdots MCA \cdots . In both cases, the N-H \cdots O and N-H \cdots N hydrogen bonds form distinct cyclic rings.

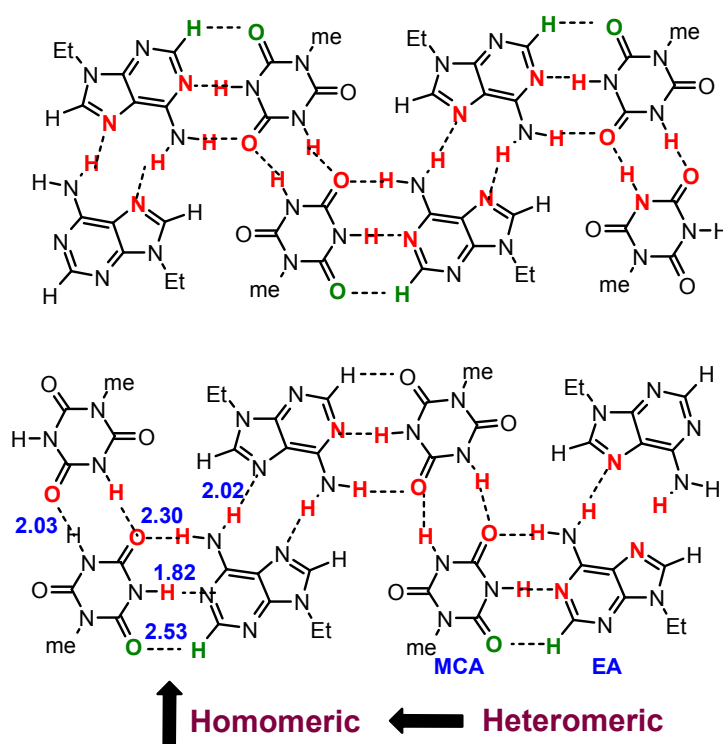


Figure 6 Molecular strips showing homomeric and heteromeric arrangement of the molecules of MCA and EA in the complex MCA:EA.

2.2.2 Biological relevance of cyanuric nucleoside

Cyanuric acid nucleosides have been shown to originate in radiation-exposed deoxyguanosine samples²⁹ and DNA oligomers containing this base have been

synthesized.³⁰ It has been observed that the cyanuric acid nucleoside-containing DNA oligomers are stable to base excision repair enzymes, formamidopyrimidine DNA *N*-glycosylase (Fpg) and endonuclease III (endo III). The presence of cyanuric acid nucleoside in DNA also induces a total resistance to digestion by enzymes SVPDE (3'-exo) and CSPDE (5'-exo).³⁰ On the basis of these established facts, the objective was to prepare cyanuric acid containing PNA oligomers to check their ability to form complexes with complementary DNA and RNA.

2.2.3 Importance of 8-aminoadenine as a modified nucleobase

A simple purine analogue, which is capable of forming hydrogen bonds from either sides, can be designed by introducing suitable substitution at C-8 of purine. Introduction of amino group (-NH₂) at C-8 position of adenine increases the stability of triple helix due to gain of one Hoogsteen purine-pyrimidine hydrogen bond³¹⁻³³ (Figure 7).

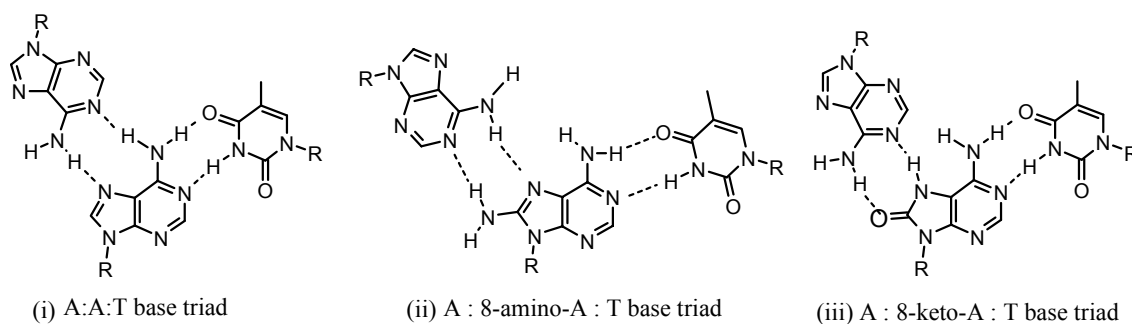


Figure 7 Hydrogen bonding in (i) adenine-adenine-thymine base triad (ii) adenine: 8-aminoadenine: thymine base triad and (iii) adenine-8-ketoadenine:thymine base triad

The propensity of the C-8 amino group located in major groove compared to normal motif in influencing the ‘spine of hydration’ affects the stability of the triplex structure.^{31,33} 8-Amino derivatives of purine class of modified bases are able to increase the stability of DNA hairpins.³⁴ Theoretical studies have also supported the increased

triplex stability through introduction of the electron donating groups like bromo, hydroxyl or amino group at *C*-8 position of adenine.^{35a} These enhance the H-bond accepting potential of *N*-7, through delocalization of lone pair electrons on 8-NH₂ group (Figure 8). 8-Keto group similarly enhances the H-bonding donor potential of 7-NH. ¹⁵N NMR experimental studies have shown increased electronic density on *N*-7 indicates that the structure-based predictions were correct and that 8-aminopurines can be used to obtain stable purine: purine: pyrimidine triplexes.^{35b}

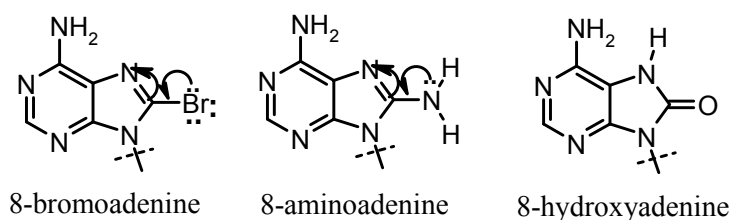


Figure 8: structures of 8-bromoadenine, 8-aminoadenine and 8-oxoadenine

The NMR study to calculate the binding stoichiometry and association constant between 8-amino-2'-deoxyadenosine and 2'-deoxythymidine, evidenced the existence of non-WC base pairing in 8-amino-dA:dT complex and favored Hoogsteen base pairing preferred in reverse mode, which would involve both amines present at *C*-6 and *C*-8 positions of adenine participate in base pairing (Figure 9).^{35c}

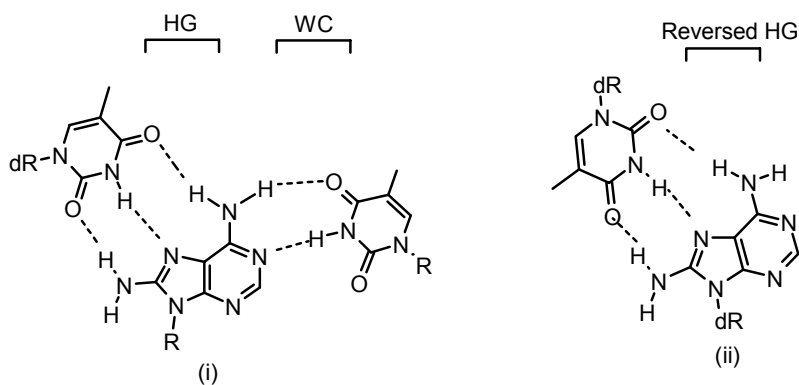


Figure 9: Structures of i) dT:8-NH₂-A:dT base triad and ii) dT:8-NH₂-A base pair

Binding of pyrimidine single strands by modified clamps containing 8-aminopurines has been shown to have high affinity for model homopyrimidine sequences, resulting in the formation of very stable antiparallel triplexes at room temperature.³⁶

2.2.4 Biological relevance of 8-aminoadenosine

Few reports on for 8-aminoadenosine have suggested it's interesting effects in biological systems: the cyclic ADP ribose antagonist 8-NH₂-cADP-ribose blocks cholecystokinin-evoked cytosolic Ca²⁺ spiking in pancreatic acinar cells³⁷ and C-8 modified ATP analogs inhibit the *Saccharomyces cerevisiae* Poly(A) polymerase.³⁸ 8-aminoadenosine is a potential therapeutic agent for multiple myeloma,^{39a} as it induces dephosphorylation of p38 nitrogen-activated protein kinase, extracellular signal-regulated kinase 1/2 and Akt kinase, that have role in induction of apoptosis in multiple myeloma.^{39b}

2.3 Objectives

The above resume on importance of cyanuric acid and 8-aminoadenine prompted us to synthesize the cyanuryl and 8-aminoadeninyl PNA oligomers and examine the stability of their duplexes and triplexes with corresponding complementary DNA.

Objectives of this chapter are

- 1) Synthesis of cyanuryl PNA monomer (**6**)
- 2) Synthesis 8-bromoadeninyl PNA monomer (**26**)
- 3) Synthesis of *aeg* PNA monomers (T/C/A/G) (**32, 34, 36, 38**)
- 4) Site specific incorporation of base modified PNA monomers into PNA oligomers

- 5) Conversion of the solid supported 8-bromoadeninyl PNA oligomers to 8-aminoadeninyl PNA oligomers
- 6) Cleavage of the oligomers from solid support and purification followed by the characterization.

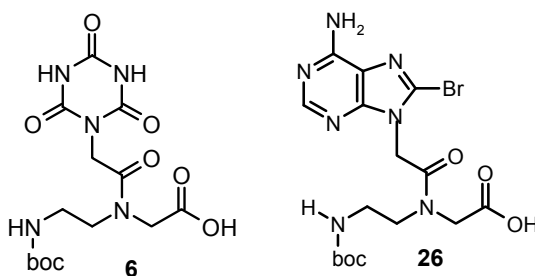
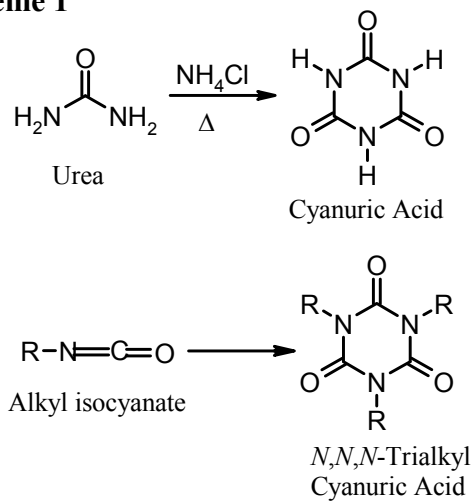


Figure 10: Structures of cyanuryl PNA and 8-bromoadeninyl PNA monomers

2.3.1 Synthesis of cyanuryl PNA monomer

The cyanuric acid can be prepared from urea and isocyanates. Urea was cyclized to cyanuric acid under solvent free conditions in the presence of ammonium chloride under vacuum at elevated temperatures.^{40a} Isocyanates under catalysts (calcium acetate, potassium acetate, oxalic acid, triethylamine and others) undergoes trimerization and forms different cyanuric acid derivatives (Scheme 1).^{40b}

Scheme 1



The synthesis of cyanuryl PNA monomer through cyanuric acid ring construction was attempted as per the earlier report (Scheme 2).^{41c} However poor yields in the scheme provoked us to search for new methods to synthesize cyanuryl PNA monomer.

For the synthesis of cyanuryl PNA monomer, different routes were attempted.

- a. Cyanuryl ring construction followed by monomer synthesis
- b. Alkylation of cyanuric acid with ethylbromoacetate
- c. Alkylation of cyanuric acid with PNA backbone [Ethyl *N*-(2-Boc-aminoethyl)-*N*-(1-haloacetyl) glycinate]

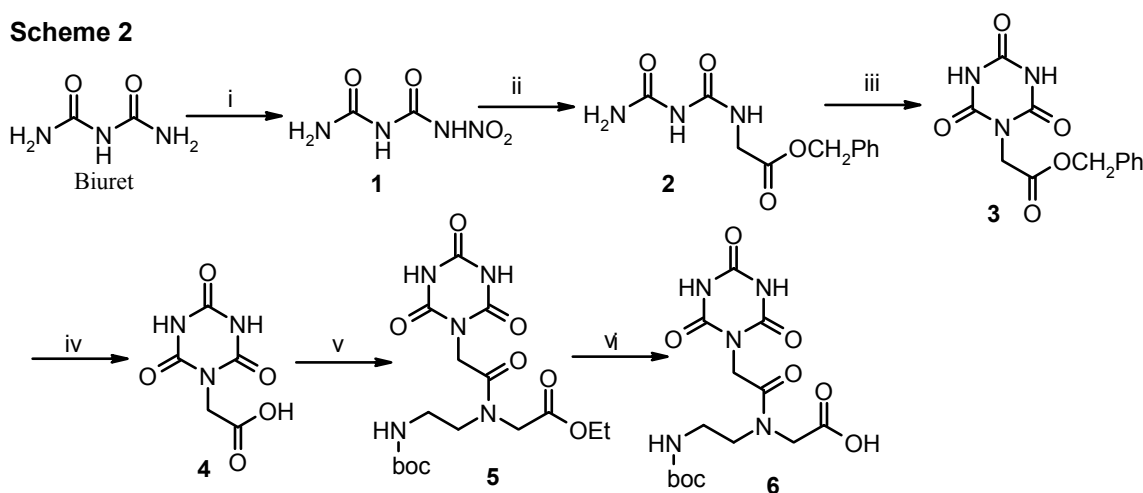
2.3.1a Cyanuryl ring construction followed by monomer synthesis

The reaction of biuret^{41a} with nitration mixture yielded nitrobiuret (1),^{41b} followed by treatment with *p*-toluene sulfonate (PTSA) salt of benzyl glycinate gave compound **2** (Scheme 2). Alkyl cyanuric acid **3** was formed by the carbonyl insertion-cyclization of alkyl biuret **2**.^{41c} Compound **3** was saponified to yield cyanuryl acetic acid **4** followed by HOBT mediated coupling with ethyl *N*-(2-Boc-aminoethyl)- glycinate to give the compound **5**. The hydrolysis of ester function in compound **5**, with aq LiOH followed by neutralization yielded the desired cyanuryl PNA monomer **6**.

The carbonyl insertion between two amides of compound **2** was tried with both carbonyl diimidazole (CDI) and triphosgene independently, but this reaction gave poor yields. Several conditions were employed using different bases, such as organic bases pyridine, triethylamine and inorganic bases NaHCO₃ and K₂CO₃ were used in both nonpolar solvents like DCM and polar solvents such as acetone to improve the yield. However nothing worked out to satisfaction with yields limited to range 8-15% only

(Table 1). The carbonyl insertion between two nucleophilic functions (alcohols, amines or amino alcohols) is well known in the literature.⁴² However the carbonyl insertion between two amides is difficult because of the poor nucleophilicity of amide nitrogens. The poor yields obtained in this scheme 2 motivated us to change the scheme for higher yielding route.

Scheme 2



Reagents: i) nitration mixture, 0 °C; ii) glycine benzyl ester toluene-4-sulfonate, Et₃N, DMF, 80°C, 6 h; iii) CDI, pyridine, reflux, 30 min; iv) KOH, aqueous MeOH, 60 min; iv) ethyl *N*-(2-Boc-aminoethyl)-glycinate, HOBT, 0 °C, DCC, DMF.

Table1: Experimental conditions employed to prepare benzyl (1-cyanuryl) acetate (4)

Entry	Condition	Yield (%)
1.	CDI, Pyridine	10
2.	Triphosgene, triethylamine/DCM	15
3.	Triphosgene, Pyridine	8
4.	Triphosgene, NaHCO ₃ , acetone	10
5.	Triphosgene, K ₂ CO ₃ , acetone	12

2.3.1b Alkylation of cyanuric acid with ethylbromoacetate/bromoacetic acid

An alternate method is the direct alkylation of the commercially available cyanuric acid to synthesize the target cyanuryl PNA monomer.

The problems involved with cyanuric acid alkylation are

- Poor solubility of cyanuric acid in organic solvents
- Possibility of multiple (mono, di and tri) alkylation
- Competition between *N*-alkylation and *O*-alkylation (Figure 11)

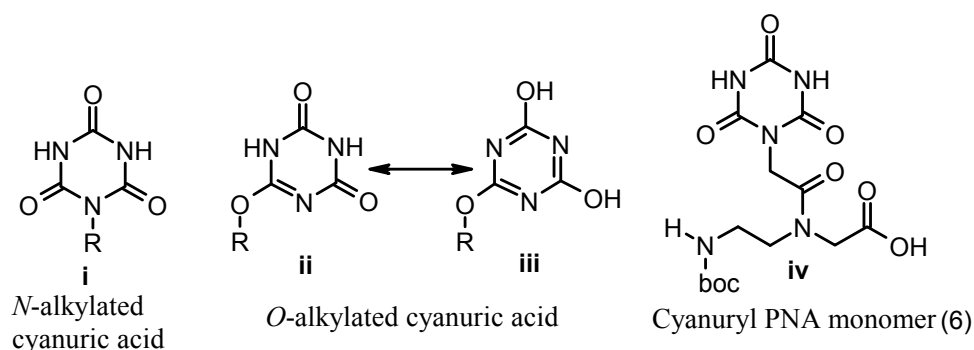
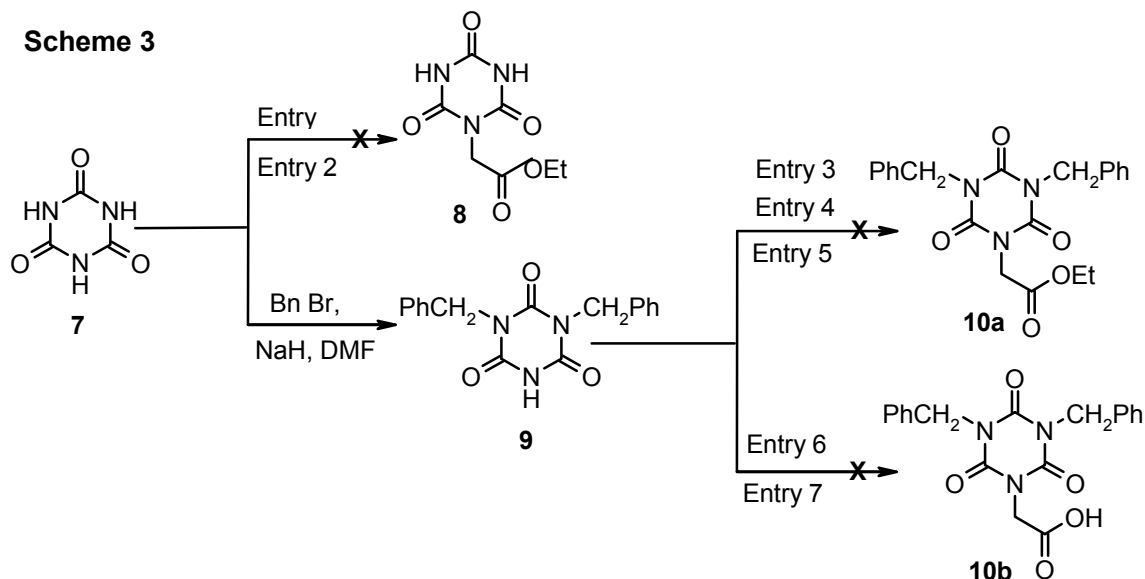


Figure 11: Structures of *N*-alkylated cyanuric acid (i) tautomers of *O*-alkylated cyanuric acid (ii & iii) and (iv) cyanuryl PNA monomer

Direct alkylation of cyanuric acid with ethylbromoacetate was attempted (Scheme 2). Under various conditions employed with different bases and solvents (Table 2, entry 1&2), no reaction was observed at ambient temperatures, but upon rising the temperature, formation of multiple products was observed on TLC.

Cyanuric acid's poor solubility in organic solvents seemed to be a major hurdle. To improve its solubility, it was intended to protect two imide nitrogens with benzyl groups to obtain the *N,N*-dibenzyl cyanuric acid derivative **9** and the remaining unprotected imide nitrogen could be then alkylated easily (Scheme 3). The alkylation of dibenzyl cyanuric acid **9** was attempted under different conditions, but all attempts were failed. Under room temperature conditions (Table 2, entry 3), no reaction was observed, but at higher temperature (Table 2, entry 4&5), multiple products were seen on TLC.

Alkylation with bromo acetic acid instead of ethylbromo acetate in polar solvents DMF or acetonitrile at high temperature like 80 °C or 100 °C also failed (Table 2, entry 6&7).



Scheme 3: Conditions employed to achieve ethyl (1-cyanuryl) acetate (**8**), ethyl (1-dibenzyl cyanuryl) acetate (**10a**) and (1-dibenzyl cyanuryl) acetic acid (**10b**)

Table 2: Experimental conditions employed to achieve ethyl (1-dibenzyl cyanuryl) acetate (**10**)

Entry no.	Reactant	Condition	Result
1	7	ethyl bromoacetate/ K_2CO_3 /DMF, 75 °C	No reaction
2	7	ethyl bromoacetate/NaH/DMF, 75 °C	Multiple products
3	9	ethyl bromoacetate, K_2CO_3 , acetonitrile	No reaction
4	9	ethyl bromoacetate and K_2CO_3 /DMF	Multiple products
5	9	ethyl bromoacetate, NaOH, DMF	Multiple products
6	9	bromo acetic acid, DMF at 100 °C	Multiple products
7	9	bromo acetic acid, acetonitrile, reflux	Multiple products

2.3.1c Alkylation of cyanuric acid with PNA backbone

While examining the cyanuric acid's solubility in organic solvents, DMSO was found to be the preferable solvent. Cyanuric acid dissolves well in DMSO above 50 °C. The direct alkylation of cyanuric acid with Ethyl N-(2-Boc-aminoethyl)-N-(1-halo acetyl) glycinate was attempted in DMSO and K₂CO₃. The PNA backbone (N-(2-Boc-aminoethyl)-N-(1-haloacetyl) glycinate) (**14,15**) was prepared from ethylene diamine according to the known procedure.^{43,44} Cyanuric acid is soluble in DMSO at high temperatures (>70 °C). The alkylation of cyanuric acid with compound **14** gave low yields and took longer hours for completion of reaction. But the alkylation of cyanuric acid with N-bromoacetyl compound **15** went to completion in 5 hours and compound **5** was obtained with good yield (Scheme 4). The hydrolysis of ester function in compound **5** followed by neutralization yielded the desired cyanuryl PNA monomer **6**, with good yield and all the compounds are characterized through ¹H/¹³C NMR. Compound **6** was used for coupling in solid phase peptide method to synthesize the cyanuryl PNA oligomers.

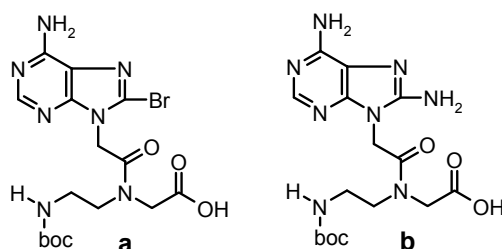
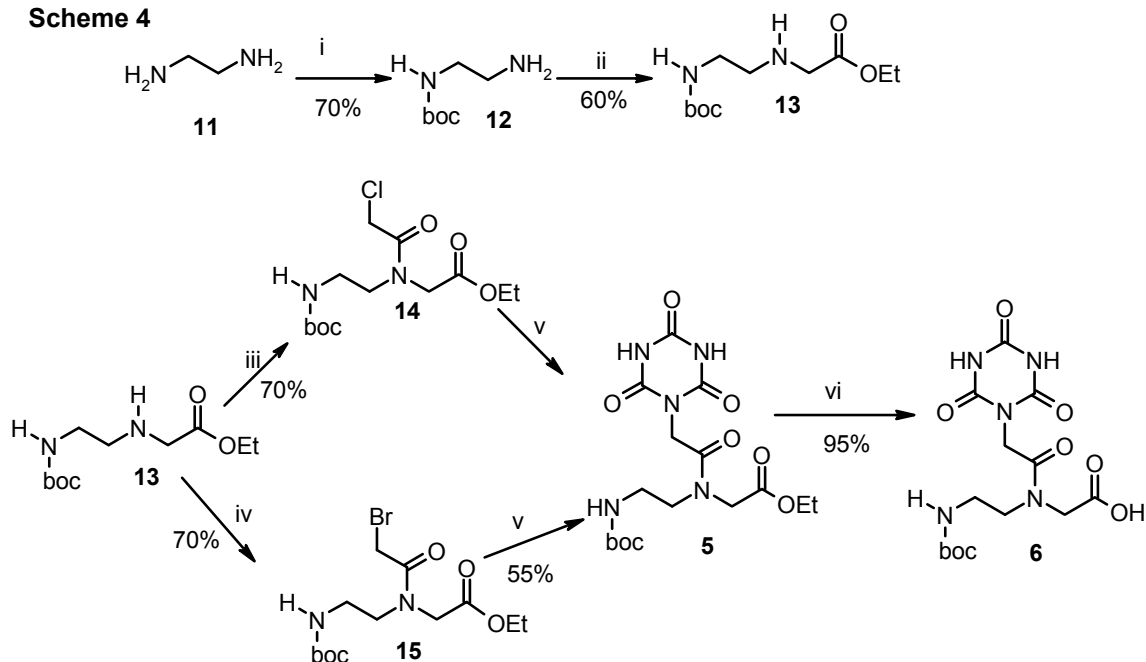


Figure 12: Structures of (a) 8-bromoadeninyl PNA monomer (b) 8-aminoadeninyl PNA monomer

Scheme 4

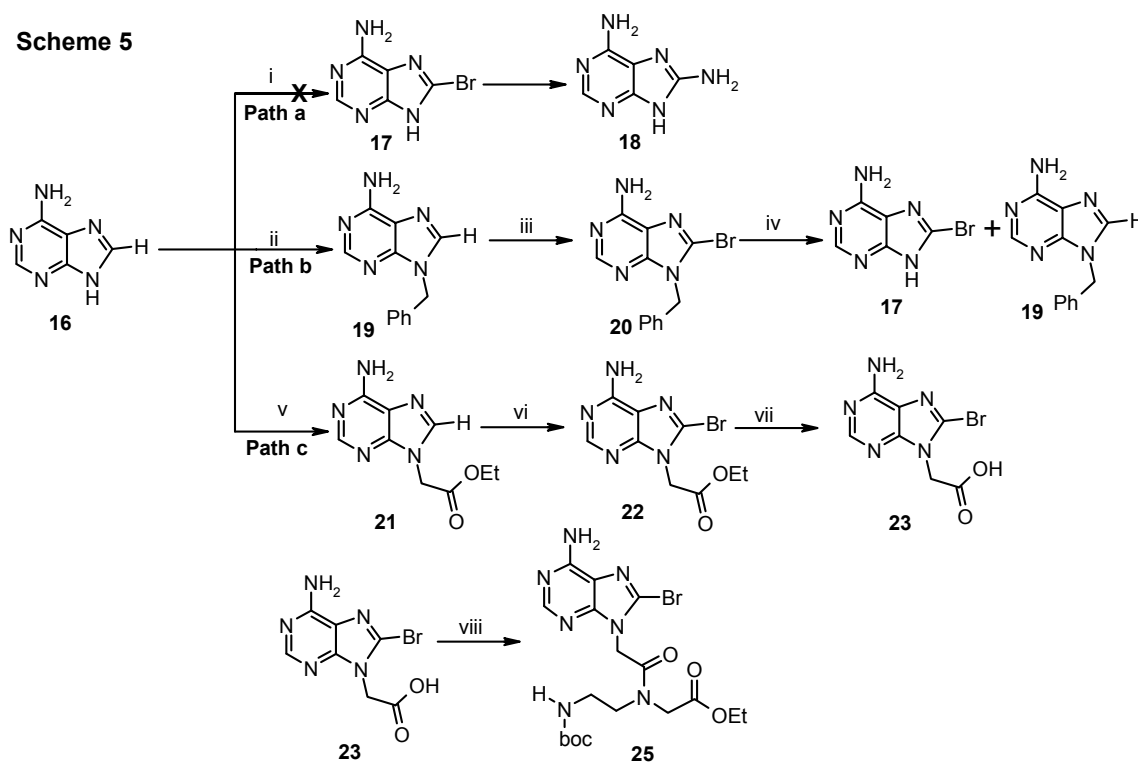


Reagents: i) $(\text{Boc})_2\text{O}$, THF; ii) Ethylbromoacetate, Et_3N , acetonitrile; iii) Chloroacetyl chloride, Et_3N , DCM; iv) Bromoacetyl chloride, Et_3N , DCM; v) Cyanuric acid, K_2CO_3 , DMSO; vi) 2N LiOH, methanol.

2.3.2 Synthesis of 8-bromoadeninyl PNA monomer

The objective of this part of work is the synthesis of 8-aminoadeninyl PNA. 8-bromoadeninyl PNA monomer acts as a synthetic precursor to achieve 8-aminoadeninyl PNA monomer (Figure 12).

8-Aminoadeninyl PNA monomer synthesis was proposed to be achieved via the bromination of adenine to get 8-bromoadenine (**17**), followed by amination to give 8-amino adenine (**18**) (Scheme 5, path a). However, the first step of bromination of adenine failed. The bromination at C-8 of *N*⁹-benzyl adenine⁴⁵ was reported in literature,⁴⁶ and was done accordingly. However, the hydrogenolysis for debenzilation yielded the debrominated product **19** as major product instead of the debenzylated product **17** (Scheme 5, path b).

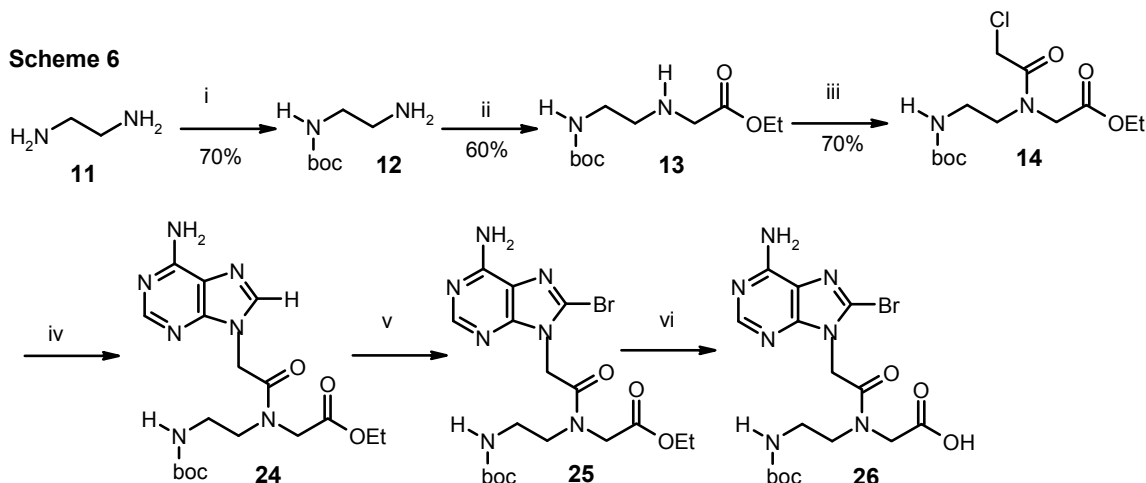


Reagents: i) Saturated bromine water, Sodium acetate; ii) benzyl chloride, TBAI, NaH, DMF; iii) Bromine in dioxane/10%aq. Na₂HPO₄; iv) H₂/Pd-C v) ethylbromoacetate, K₂CO₃, DMF; vi)

Bromine in dioxane/10%aq. Na_2HPO_4 ; vii) aq. LiOH in methanol; viii) Ethyl *N*-(2-Boc-aminoethyl)-glycinate, HOBt, HBTU, DMF

Adenine treated with ethylbromoacetate in presence of K_2CO_3 yielded compound **21**, which upon bromination afforded the corresponding 8-bromo compound **22** (Scheme 5, path c). The hydrolysis of ester function in compound **22** yielded the 8-bromoadeninylic acetic acid (**23**). The coupling of compound **23** and the amine (Ethyl *N*-(2-Boc-aminoethyl)-glycinate) (**13**) to yield 8-bromoadenine PNA monomer (**25**) gave poor yields. This motivated us to change the synthetic route.

The bromination was carried out on *N*⁹-benzyladenine (**19&21**) to yield the corresponding 8-brominated products (**20&22**), which were obtained in good yields. Since bromination on *N*⁹-alkyladenine worked out well, it was thought to brominate adeninylic PNA monomer (**24**) (Scheme 5). The reaction was fruitful and yielded 8-bromoadeninylic PNA monomer (**25**) with moderate yield of 55%. The hydrolysis of ester group in compound **25** with aq. LiOH, in methanol yielded the 8-bromoadeninylic PNA monomer acid (**26**) (Scheme 6), which was used for coupling in solid phase peptide synthesis to synthesize PNA oligomers.



Reagents: i) (Boc)₂O, THF; ii) Ethylbromoacetate, Et₃N, acetonitrile; iii) chloro acetyl chloride, NEt₃, DCM; iv) adenine, K₂CO₃, DMF; v) Br₂, dioxane; 10% aq. Na₂HPO₄; vi) LiOH, methanol

2.3.3 Synthesis of *aeg* PNA monomers (A^Z/G/C^Z/T)

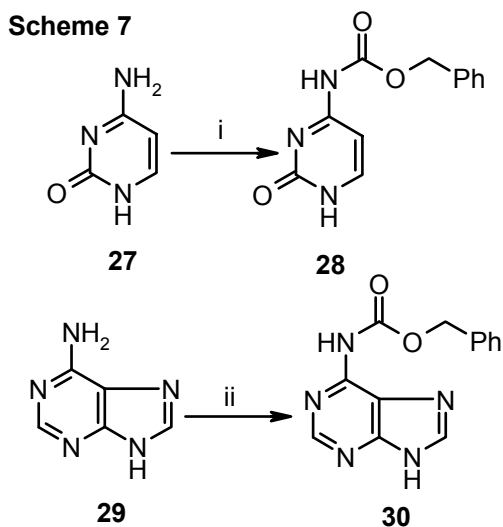
To study the influence of base modified *aeg* PNA monomers on hybridization properties of PNA oligomers, these were site specifically incorporated in *aeg* PNA oligomers along with the unmodified *aeg* PNA monomers, but the exocyclic amino group of cytosine (*N*⁴-H) and adenine (*N*⁶-H) need to be protected for its use in peptide synthesis. The *benzyloxycarbonyl* group is appropriate for this purpose.

*N*⁴-benzyloxycarbonylcytosine^{43, 47} (28)

Cytosine was treated with benzyloxycarbonyl chloride in dry pyridine at ice temperature yielded *N*⁴-benzyloxy carbonylcytosine 47 (Scheme 7).

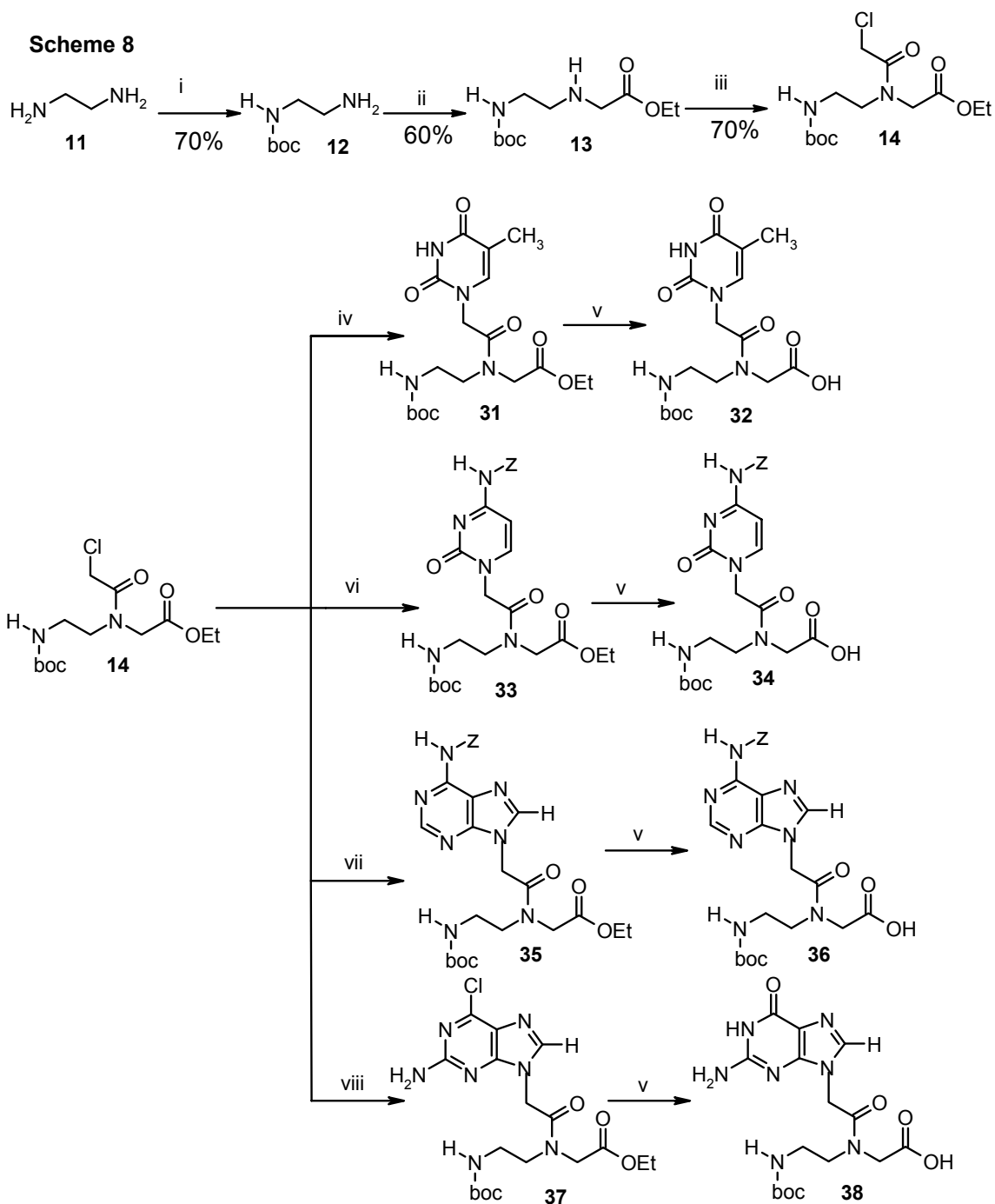
*N*⁶-benzyloxycarobnyladenine^{43, 47} (30)

Adenine, upon treatment with sodium hydride in dry DMF gave sodium adenylate, which was *in-situ* treated with benzyloxycarbonyl chloride to give the *N*⁶-benzyloxycarbonyladenine **30** (Scheme 7).



Reagents: i) Benzyloxy carbonyl chloride, dry pyridine; ii) Benzyloxy carbonyl chloride, NaH, DMF

The *aeg* PNA monomers, containing natural nucleobases (protected form in case of cytosine and adenine) were synthesized as described in Scheme 8.



The synthesis of **14** was carried out as reported in literature⁴³⁻⁴⁴ starting from the readily available 1,2-diaminoethane (Scheme 8). The monoprotected derivative **12** was

prepared by treating a large excess of 1,2-diaminoethane (10 equivalents) with di-*t*-butoxyanhydride in THF. High dilution and low temperature conditions minimize the formation of di-*boc* derivative. The di-*boc* compound being insoluble in water, it was removed by filtration through celite. The *N*¹-*t*-*boc*-1,2-diaminoethane was then subjected to *N*-alkylation using ethylbromoacetate and triethylamine as base in acetonitrile to give the ester **13**, which was not stable for a longer time at room temperature, it was treated with chloroacetyl chloride in DCM, in presence of triethylamine to yield the chloro compound **14**. The ethyl *N*-(*t*-*boc*-aminoethyl)-*N*-(chloroacetyl)-glycinate **14** was used as a common intermediate for the preparation of all the four PNA monomers.

Alkylation with the ethyl *N*-(*t*-*boc*-aminoethyl)-*N*-(chloroacetyl)-glycinate to thymine is regiospecific at *N*¹ of thymine. Thymine was reacted with ethyl *N*-(*t*-*boc*-aminoethyl)-*N*-(chloroacetyl)-glycinate using K₂CO₃ as a base to obtain *N*-(*t*-*boc*-aminoethylglycyl)-thymine ethyl ester **31** in high yield. In case of cytosine, the exocyclic amine *N*⁴ was protected as Cbz (Scheme 7) to obtain **28**,¹⁷ which was used for alkylation employing K₂CO₃ as the base to provide the *N*¹-substituted product **33**. The exocyclic amine of adenine *N*⁶ was protected with Cbz (Scheme 7) to obtain **30**, treated with K₂CO₃ in DMF, followed by its reaction with ethyl *N*-(*t*-*boc*-aminoethyl)-*N*-(chloroacetyl)-glycinate to obtain *N*-(*t*-*boc*-aminoethylglycyl) (benzyloxy carbonyl)adenine ethyl ester **35** in moderate yield. The alkylation of 2-amino-6-chloropurine with ethyl *N*-(*t*-*boc*-aminoethyl)-*N*-(chloroacetyl)-glycinate was facile with K₂CO₃ as the base and yielded the corresponding *N*-(*t*-*boc*-aminoethylglycyl)-(2-amino-6-chloropurine) ethyl ester **37** in excellent yield. All compounds exhibited ¹H and ¹³C NMR spectra consistent with the reported data.⁴³⁻⁴⁴

The ethyl esters except cytosine monomer were hydrolyzed in presence of 2N LiOH to give the corresponding acids **32**, **36**, **38** which were used for solid phase synthesis. In case of ester hydrolysis of the 2-amino-6-chloropurine monomer ester, the chloro group is also oxidized to *keto* group to give guanine monomer **33**. Cytosine monomer is more susceptible to Cbz deprotection in strong basic conditions, and in this case, mild base 1N aq. LiOH was used for hydrolysis to afford the monomer acid **34**. The need for the exocyclic amino group protection for adenine and guanine is eliminated, as they are found to be unreactive under the conditions used for peptide coupling.

2.3.4 Site specific incorporation of base modified PNA monomers into PNA oligomers

2.3.4a Solid Phase Peptide Synthesis

The solid phase peptide synthesis (SPPS) was devised by R. B. Merrifield in 1959.⁴⁹ In this method, the peptide is synthesized on an insoluble solid support. In contrast to solution synthesis, the solid phase method, offers great advantages. Here the C-terminal amino acid is linked to an insoluble matrix such as polystyrene beads (cross linked with divinyl benzene) having reactive functional groups, which also acts as a permanent protection for the carboxylic acid. The next *N*-protected amino acid is coupled to the resin bound amino acid either by using an active pentafluorophenyl (pfp) or 3-hydroxy-2,3-dihydro-4-oxo-benzotriazole (Dhbt) ester or by an *in situ* activation with carbodiimide reagent. The excess amino acid was washed out and the deprotection followed by coupling reactions was repeated until the desired peptide is achieved. The need to purify intermediates at every step is thus obviated. Finally, the resin bound

peptide and the side chain protecting groups are cleaved in one step. The advantages of the solid phase synthesis are (i) all reactions are performed in a single vessel, minimizing the loss due to material transfer, particularly in minimum synthesis scale (ii) large excess of monomer carboxylic acid component can be used to drive reaction to high coupling efficiency, (iii) excess reagents can be removed by simple filtration and washing with appropriate solvent and (iv) the method is amenable to automation and semi micro manipulation. The different resins used for SPPS showed in Figure 13.

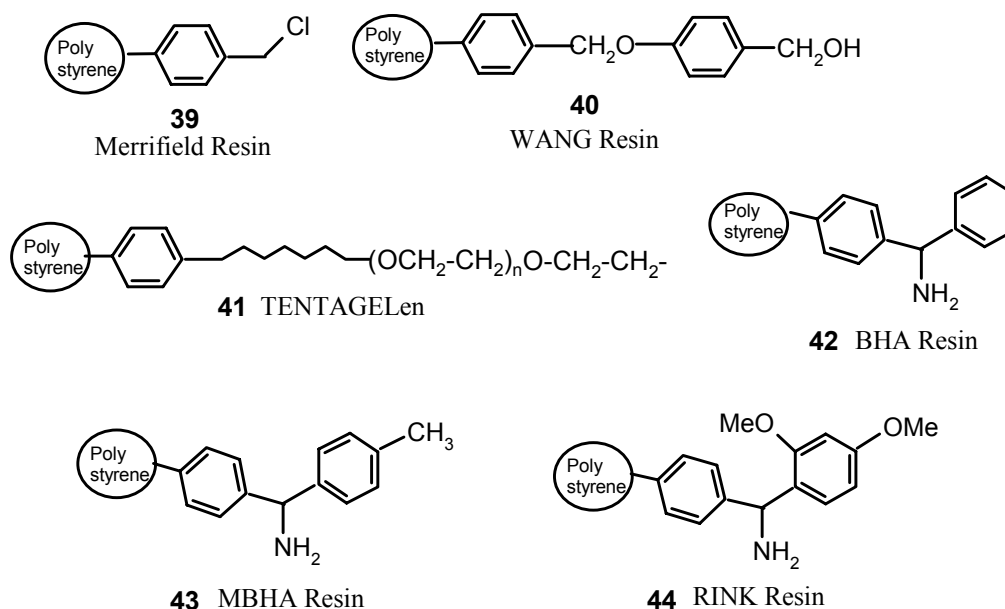


Figure 13: Examples of resins used in SPPS

2.3.4b Protocols

The *aeg*-PNA oligomers with modified bases (cyanuryl PNA monomer (**6**) and 8-bromo adeninyl PNA monomer (**26**)) were site specifically incorporated into PNA oligomers using the standard Solid Phase Peptide Synthesis (SPPS)⁵⁰ protocols, with ‘*boc*-chemistry’ strategies.

The synthesis can be conveniently carried out from C-terminus to N-terminus, using suitably protected amino functionalities with the free carboxylic groups. The readily available MBHA (methyl benzhydryl amine) resin was chosen as the polymer matrix for building the cyanuryl, adeninyl and 8-bromoadeninyl PNA oligomers.

Commercially available MBHA resin has a loading value of 2 meq/g, which is not suitable for oligomer synthesis. Since, at this level of loading, PNA oligomers aggregate there by decreasing the efficiency in successive coupling steps. Hence, it was necessary to lower the loading value to 0.25-0.35 meq/g to avoid the aggregation of growing oligomer. This was achieved by partial acetylation of the amine content with calculated amount of acetic anhydride (capping).^{51,52} The amount of free -NH₂ on the resin available for coupling was estimated by the picrate assay, before starting the PNA synthesis.

The first amino acid (linker) was attached *via* amide linkage to the resin which can be cleaved easily at the end of the synthesis either by acidolysis or aminolysis to get the free peptide with carboxamide at C-terminus. The *N*-protecting groups employed in this process are generally Boc or benzyloxycarbonyl (*Z*) groups which are also removed while performing the cleavage. Although Merrifield used benzyloxycarbonyl group for the protection of α -amino group, it has the disadvantage of unwanted side reactions and cleavage of the oligomers from the solid support using trifluoromethane- sulfonic acid (TFMSA) in the presence of trifluoroacetic acid (TFA) ("Low, High TFMSA-TFA method").⁵⁹ A milder and convenient protecting group *tert*butoxycarbonyl has become very useful and can be used in combination with other protecting groups in differential (Boc/Cbz) as well as orthogonal strategies (Boc/Fmoc).

The solid phase synthesis is an efficient method although some problems arise due to side reactions occurring in peptide synthesis during the neutralization, leading sometimes to self capping of the growing PNA chain. In both Fmoc and Boc chemistry HOBt/HBTU activation coupling strategy was employed.⁵³ Mainly, two types of self-capping occur during synthesis: (i) N-terminal detachment of the monomer during *N*-capping by uronium salt (Figure 14a) and (ii) transamidation derived from the primary amine i.e. acyl migration of the base linked acetyl segment (Figure 14b).

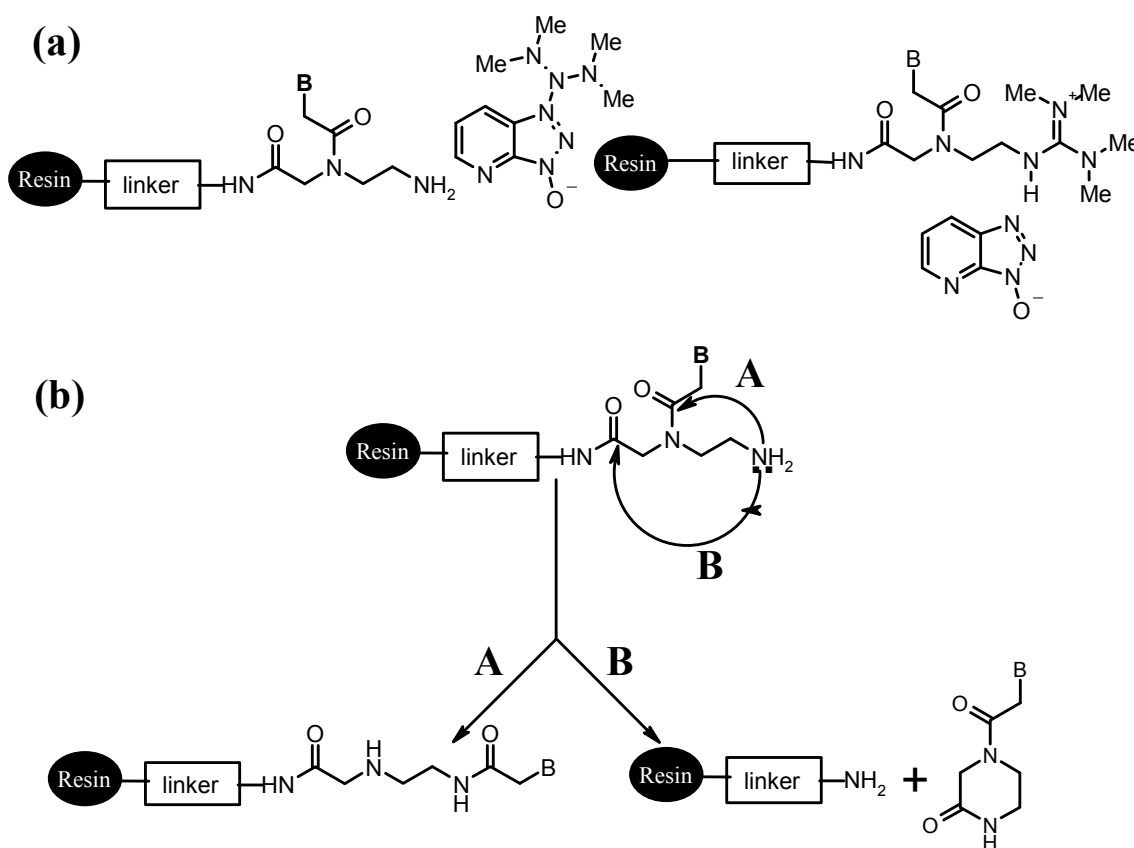


Figure 14: Possible side reactions in SPPS

In the present study, all the oligomers were built on MBHA resin using L-lysine as the *C*-terminal spacer amino acid linker employing *boc* chemistry. The PNA

oligomers were synthesized using repetitive cycles (Figure 15), each comprising of the following steps:

- Deprotection of the N^1 -*tert*-butoxycarbonyl (*boc*) group using 50% TFA in DCM followed by DCM/DMF washings
- Neutralization of the TFA salt to get the free amine using 5% DIPEA in DCM, followed by DCM/DMF washings
- Coupling of the amine with 3 to 4 equivalents of free carboxylic function of the incoming amino acid using HOBt/HBTU in DMF:NMP(1:1) as solvent.
- Capping of the unreacted amino groups using Ac_2O / Pyridine in CH_2Cl_2 in case coupling does not go to completion.

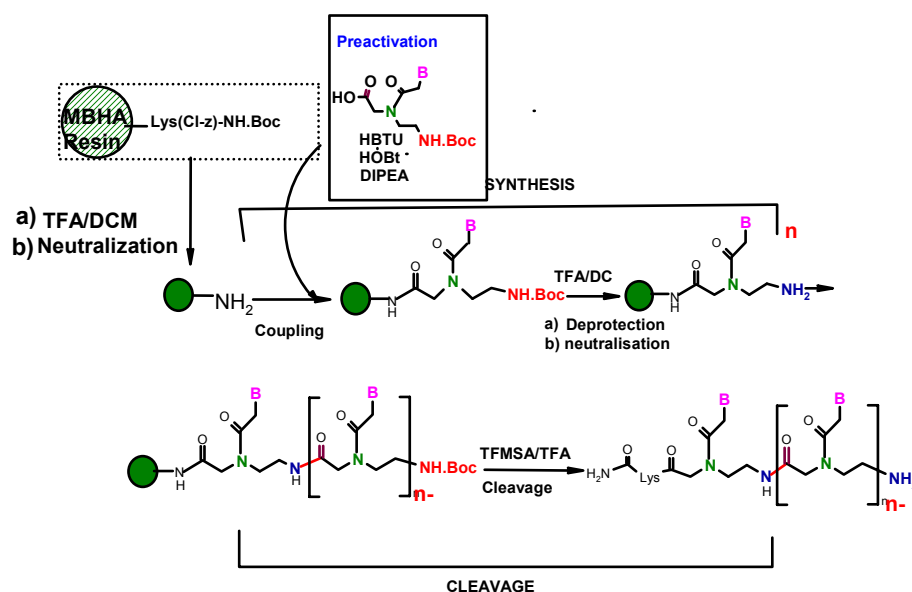


Figure 15: Schematic representation of Solid Phase Peptide Synthesis (SPPS)

Figure 15 represents a typical solid phase peptide synthesis cycle. The deprotection of the *N*-*t*-Boc protecting group and the coupling reactions were monitored by Kaiser's test.⁵⁵ Alternatively, chloranil assay⁵⁶ and De Clercq tests⁵⁷ are useful to

detect the secondary amine. The *t*-Boc-deprotection step leads to a positive Kaiser's test, wherein the resin beads as well as the solution are blue in color (Rheumann's purple). On the other hand, upon completion of the coupling reaction, the Kaiser's test is negative, the resin beads remain colorless.

2.3.4c Synthesis of cyanuryl/8-bromoadeninyl PNA oligomers

The synthesis of PNA oligomers (PNA 50-PNA 64) was achieved by incorporating the modified base containing PNA monomers at specific positions in the oligomers done on solid support using *boc* chemistry to extend the oligomers (Table 3). T_{8-aeg} PNA was used as the control sequence for comparison the properties of the cyanuryl PNAs (51-54), and Adeninyl PNAs (PNA 55-58) were used as control sequences for comparison of 8-bromoadeninyl PNA oligomers (PNA 59-62).

Table 3: The PNA sequences synthesized

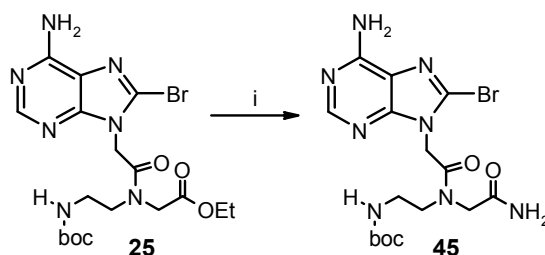
PNA No	Sequence	PNA No	Sequence
PNA 50	MBHA-Lys-TTTTTTTT-NHboc	PNA 59	MBHA-Lys-TTTTTTTT A -NHboc
PNA 51	MBHA-Lys-TTTTTTTT Cy -NHboc	PNA 60	MBHA-Lys-TTT A TTTT-NHboc
PNA 52	MBHA-Lys-TTT Cy TTTT-NHboc	PNA 61	MBHA-Lys- A TTTTTTT-NHboc
PNA 53	MBHA-Lys- Cy TTTTTTT-NHboc	PNA 62	MBHA-Lys-TTT A TTT A -NHboc
PNA 54	MBHA-Lys-TTT Cy TTT Cy -NHboc		
PNA 55	MBHA-Lys-TTTTTTTT A -NHboc		
PNA 56	MBHA-Lys-TTT A TTTT-NHboc		
PNA 57	MBHA-Lys- A TTTTTTT-NHboc		
PNA 58	MBHA-Lys-TTT A TTT A -NHboc		

T= thyminylnyl PNA; **Cy**= cyanuryl PNA; **A**= adeninylnyl PNA; **A**= 8-bromoadeninylnyl PNA

2.3.5 Conversion of 8-bromoadeninyl PNA oligomers to 8-aminoadeninyl PNA oligomers

One of the main objects of the present work is the synthesis of 8-aminoadeninyl PNA. For this 8-bromoadeninyl PNA monomer acts as synthetic precursor. It was planned to aminate the 8-bromoadeninyl PNA monomer. But under these reaction conditions, the ester which is susceptible for *trans* amidation was transformed to the corresponding 8-aminoadeninyl PNA monomer with carboxy amide functionality (Scheme 9). These are undesirable for the present application.

Scheme 9



Reagents: (i) *aq.* ammonia/methanol

As mentioned, the protecting group selection for the amino at 8th position of adenine is fairly difficult, because of its somewhat guanidinium character (Figure 16). According to earlier reports, amino function at C-8 position was protected as Schiff's base (Figure 16b),⁵⁸ but it is not stable under solid phase synthesis protocols of PNA, where 50% TFA in DCM is used for the deprotection of 'boc' group.

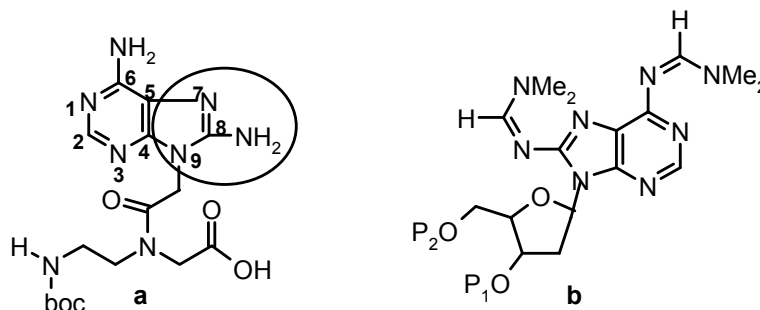
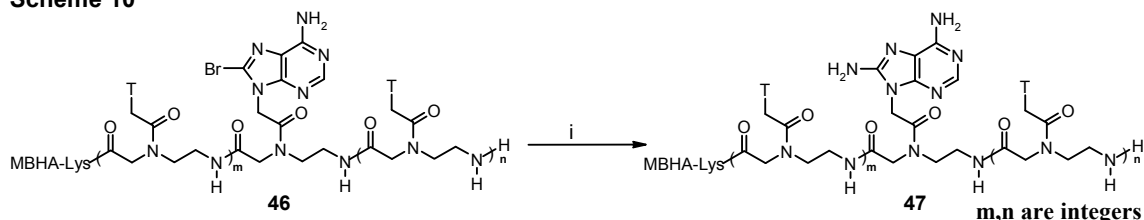


Figure 16 : Structures of a) 8-aminoadeninyl PNA monomer b) protected 8-aminodeoxy adenosine

Since problems were encountered in finding a suitable protecting group for amino function in 8-aminoadenine at monomeric level, the direct conversion of 8-bromo adeninyl PNA to 8-aminoadeninyl PNA was attempted on the oligomer level.

Scheme 10



Reagents: (i) $\text{NaNH}_2/\text{AgF}/\text{DMF}$, reflux, 10 hr.

8-Bromoadeninyl PNA oligomer (Table 4, entry 1-5) was reacted with sodamide/THF under reflux conditions to yield the corresponding 8-aminoadeninyl PNA oligomers. However, this reaction did not work satisfactorily with mixed PNA oligomers containing 8-bromoadenine. The reaction conditions were modified by addition of silver fluoride to facilitate removal of bromine by silver and make it more labile for amination (Scheme 10). The reactions were carried out on the 8-bromoadeninyl PNA oligomers bound to the resin and the completion of the reaction was monitored by HPLC (Figure 17) and MALDI-TOF spectroscopy (Figure 18). All results on the conversions of 8-bromoadenine containing PNA oligomer into 8-aminoadenine containing PNA showed in Table 4.

The oligomers were cleaved from the resin and initially purified with NAP column, followed by further purification done using HPLC. The retention time (Rt) value of 8-bromoadeninyl PNA was observed at ≈ 8.0 min, whereas the 8-aminoadeninyl PNA was observed between 9-9.35 min. The oligomers were characterized by MALDI-TOF mass spectrometry. The peaks indicate the mass of 8-bromoadeninyl PNA (2364.68,

2452.79) disappeared and the mass of 8-aminoadeninyl PNA were observed (2297.68, 2320.91) and shown in figure 18.

Table 4: Conversion of 8-bromoadeninyl PNA to 8-aminoadeninyl PNA

Sl. No.	8-bromoadeninyl PNA oligomer (Reactant)	HPLC retention time	8-aminoadeninyl PNA oligomer (Product)	HPLC retention time
1	PNA 78, H-ATTTTTTTT-Lys-NH ₂	7.94	PNA 82, H-aTTTTTTTT-Lys-NH ₂	9.2
2	PNA 79, H-TTTTTTTT A-Lys-NH ₂	7.71	PNA 83, H-TTTTTTTT a-Lys-NH ₂	8.93
3	PNA 80, H-TTTTATTT-Lys-NH ₂	7.82	PNA 84, H-TTTTaTTT-Lys-NH ₂	9.13
4	PNA 81, H-ATTT ATTT-Lys-NH ₂	7.85	PNA 85, H-aTTTaTTT-Lys-NH ₂	9.14
5	PNA 88, H-GTAGATCACT-Lys-NH ₂	9.2	PNA 89, H-GTaGaTCaCT-Lys-NH ₂	9.4

A= 8-bromoadeninyl PNA; a= 8-aminoadeninyl PNA

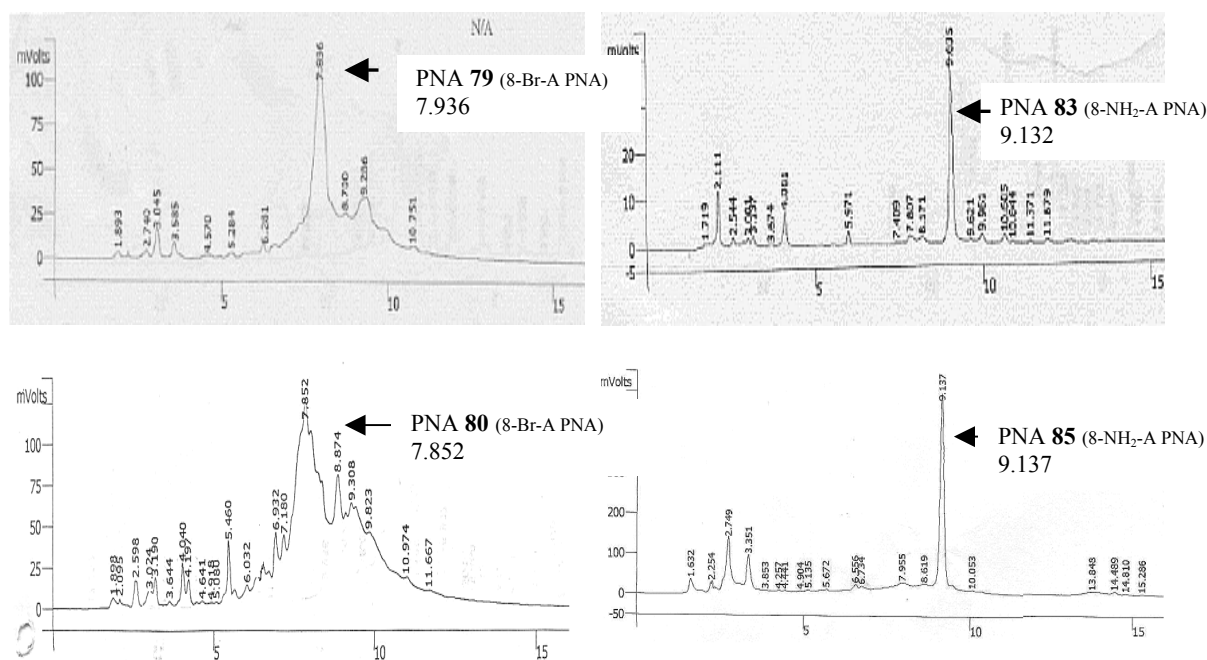


Figure 17: Crude HPLC profiles of (i) H-TTTTTTTT A-Lys NH₂ (PNA 79), (ii) H-TTTTTTTT a-LysNH₂ (PNA 83), (iii) H-ATTTATTT-LysNH₂, (iv) H-aTTTaTTT-LysNH₂ (PNA 85)

A= 8-bromoadeninyl PNA; a= 8-aminoadeninyl PNA

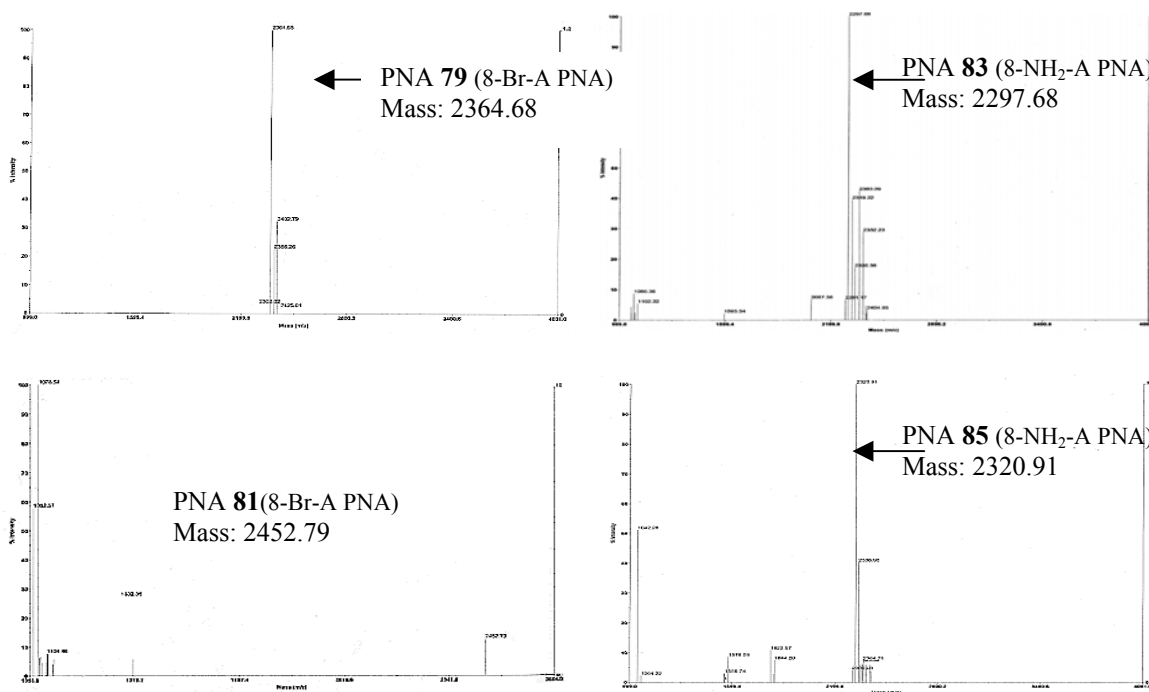


Figure 18: The MALDI-TOF spectra of PNA 77, PNA 81, PNA 83 and PNA 85

The diversity in the reaction of 8-bromoadeninyl PNA into different 8-aminosubstituted adeninyl PNA on solid supported oligomers was explored. The MBHA resin supported 8-bromoadeninyl PNA oligomer PNA **60**, was individually treated with 1,2-diaminoethane and 1,3-diamino propane under reflux conditions (Scheme 11).

The oligomers were cleaved from the resin and initially purified with NAP column, followed by further purification was done using HPLC to obtain 8-(2-aminoethyl)aminoadeninyl PNA and 8-(3-aminopropyl)aminoadeninyl PNA. The retention time (Rt) value of 8-bromoadeninyl PNA (PNA **80**) was observed between 7.59-8.0 min, whereas the 8-(2-aminoethyl)aminoadeninyl PNA (PNA **90**) and 8-(3-aminopropyl)aminoadeninyl PNA (PNA **91**) were observed between 9.2-9.3 min (Figure 19). The oligomers were characterized by MALDI-TOF mass spectrometry. The peaks

2.3.6 Purine-Pyrimidine Mix Sequences

In order to study the duplex formation potential of cyanuryl, 8-bromoadeninylyl, and 8-aminoadeninylyl PNAs, it was necessary to synthesize mixed sequences containing both purines and pyrimidines. The cyanuryl PNA monomer (**6**) was incorporated into PNA oligomer (PNA **65**) in place of the thyminylyl PNA monomer and 8-bromoadeninylyl PNA monomer (**26**) was used instead of the adeninylyl PNA monomer. The 8-bromoadeninylyl PNA oligomer (PNA **66**) converted into 8-aminoadeninylyl PNA oligomers (PNA **67**) using sodamide and silver fluoride on solid support as explained in section 2.3.5 (page 70). The list of oligomer sequences before their cleavage from the solid support (MBHA resin) showed in Table 5.

Table 5: The purine-pyrimidine PNA sequences synthesized

S. No.	PNA	Sequence
1	PNA 65	MBHA-Lys-TCACTAGATG-NHboc
2	PNA 66	MBHA-Lys-CyCACCCyAGACyG-NHboc
3	PNA 67	MBHA-Lys-TCACTAGATG-NHboc
4	PNA 68	MBHA-Lys-TCaCTaGaTG-NHboc

T= thyminylyl PNA; Cy= cyanurylyl PNA; A= adeninylyl PNA; A= 8-bromoadeninylyl PNA;
a= 8-aminoadeninylyl PNA

2.3.7 Cleavage of the PNA oligomers from solid support, purification and characterization

The PNA oligomers were cleaved from the solid support, using trifluoromethanesulfonic acid (TFMSA) in the presence of trifluoroacetic acid (TFA) ('Low, High TFMSA-TFA method')⁵⁹ which yields peptide oligomers blocked as amides at their C-terminus. The synthesized solid phase bound PNA oligomers were cleaved from the resin

using this procedure to obtain sequences bearing lysine-amide at their C-termini. A cleavage time of 60-90 min at room temperature was found to be optimum. The side chain protecting groups were also removed during this cleavage process, after which, the oligomer was precipitated from methanol with dry diethyl ether.

All the oligomers were cleaved from the resin subjected to initial gel filtration to remove small molecular weight impurities. These were subsequently purified by reverse phase HPLC (high pressure liquid chromatography) on a semi-preparative C8 RP column by gradient elution using acetonitrile in water or by isocratic elution in 10% acetonitrile-water on a semi- preparative HPLC RP C-4 column.

The purity of the oligomers was then checked by reverse phase HPLC on a C18 RP column and confirmed by MALDI-TOF mass spectroscopic analysis.⁶⁰ α -cyano-4-hydroxycinnamic acid (CHCA) was used as the matrix and dry droplet method was employed in MALDI-TOF mass spectroscopic analysis. Some representative HPLC profiles and mass spectra are shown in appendix of this chapter (Page 102-107 and 108). The purified PNA **69-91** sequences obtained are listed in Table 6.

Table 6: HPLC and MALDI-TOF mass spectral analysis of synthesized PNAs

Entry no.	Sequence	HPLC retention time (min)	Calculated mass (HRMS)	Observed mass
PNA 69	H-TTTTTTTT-Lys-NH ₂	7.95	2273.93	2275.24
PNA 70	H-CyTTTTTTT-Lys-NH ₂	8.995	2276.91	2300.64(M ⁺ +Na)
PNA 71	H-TTTTTTTTCy-Lys-NH ₂	9.014	2276.91	2276.62
PNA 72	H-TTTTCyTTT-Lys-NH ₂	9.007	2276.91	2280.34
PNA 73	H-CyTTTCyTTT-Lys-NH ₂	9.144	2279.88	2301.56(M ⁺ +Na)
PNA 74	H <u>A</u> TTTTTTTTLys-NH ₂	7.932	2282.95	2281.32
PNA 75	H-TTTTTTTT <u>A</u> Lys-NH ₂	7.936	2282.95	2284.84
PNA 76	H-TTTT <u>A</u> TTT-Lys-NH ₂	7.880	2282.95	2305.27(M ⁺ +Na)
PNA 77	H- <u>A</u> TTT <u>A</u> TTT-Lys-NH ₂	7.992	2291.96	2293.13
PNA 78	HATTTTTTTTLys-NH ₂	7.932	2360.85	2364.68
PNA 79	H-TTTTTTTT <i>A</i> Lys-NH ₂	7.936	2360.85	2364.68
PNA 80	H-TTTT <i>A</i> TTT-Lys-NH ₂	7.880	2360.85	2363.88
PNA 81	H- <i>A</i> TTT <i>A</i> TTT-Lys-NH ₂	7.992	2447.78	2452.79
PNA 82	H- a TTTTTTT -Lys-NH ₂	9.13	2297.96	2300.84
PNA 83	H-TTTTTTTT a -Lys-NH ₂	9.132	2297.96	2297.68
PNA 84	H-TTTT a TTT-Lys-NH ₂	9.139	2297.96	2300.11
PNA 85	H- a TTT a TTT-Lys-NH ₂	9.137	2321.98	2320.91
PNA 86	H-GT <u>A</u> G <u>A</u> TC <u>A</u> CT-Lys-NH ₂	9.16	2852.52	2856.08
PNA 87	H-GCy <u>A</u> G <u>A</u> CyC <u>A</u> CCy-Lys-NH ₂	9.11	2861.45	2863.28
PNA 88	H-GTAGATCACT-Lys-NH ₂	9.2	3089.85	3093.7
PNA 89	H-GT a G a T C aCT-Lys-NH ₂	9.4	2897.6	2899.64
PNA 90	H-TTTT <i>A</i> 'TTT-Lys-NH ₂	9.207	2339.96	2338.39
PNA 91	H-TTTT <i>A</i> " TTT-Lys-NH ₂	9.286	2354.96	2360.09

T= thyminy PNA; C_y= cyanuryl PNA; A= adeniny PNA; A= 8-bromoadeniny PNA; **a**= 8- aminoadeniny PNA; A'= 8-(aminoethyl)aminoadeniny PNA and A'' = 8-(3-amino ethyl) aminoadeniny PNA monomers

2.4 Synthesis of Complementary Oligonucleotides

The oligonucleotides **92-99** (Table 7) corresponding to complementary DNA sequences were synthesized on Applied Biosystems ABI 3900 DNA Synthesizer using standard β -cyanoethyl phosphoramidite chemistry.⁶¹ The oligonucleotides were synthesized in the 3' to 5' direction on polystyrene solid support, followed by ammonia treatment. These were desalted by gel filtration, and their purity as ascertained by RP HPLC on a C-18 column was found to be more than 98%. They were used without further purification for the biophysical studies of hybridization with PNAs.

Table 7: The oligonucleotides used

Sl. No.	DNA entry no.	Sequence (5'-3')	HPLC retention time
1	DNA 92	GCAAAAAAAAAACG	7.6
2	DNA 93	GCAAAAAAAAAATCG	7.1
3	DNA 94	GCAAATAAAAACG	7.6
4	DNA 95	GCAAATAAATCG	7.5
5	DNA 96	CGAAAACAAAAGC	7.6
6	DNA 97	CGAAAACAAATGC	7.9
7	DNA 98	AGTGATCTAC	8.1
8	DNA 99	CATCTAGTGA	8.0

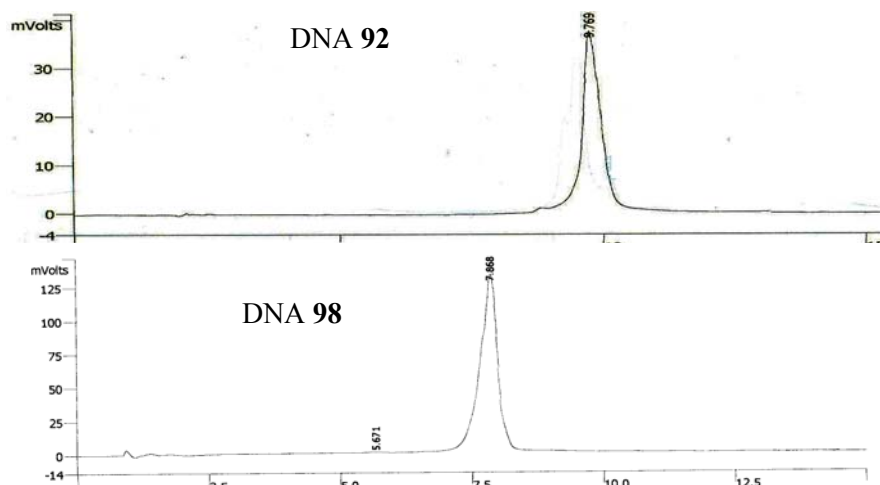


Figure 21: HPLC profiles of DNA 92 and DNA 98**2.5 Conclusions:**

This chapter has described the various attempts for synthesis of cyanuryl and 8-bromoadeninylyl PNA monomer and oligomers. The modified PNA monomers were introduced site specifically into the PNA oligomers by solid phase synthesis using “*boc*-chemistry”. To overcome the difficulty of finding suitable protecting group for the amino group present at 8th position of adenine in 8-aminoadenine, the novel conversion of 8-bromoadeninylyl PNA oligomers into 8-aminoadeninylyl PNA oligomers was carried out. This conversion further explored to prepare 8-(2-aminoethyl)aminoadeninylyl PNA and 8-(3-aminopropyl)aminoadeninylyl PNA. The PNA oligomers having cyanuryl, adeninylyl, 8-bromoadeninylyl and 8-aminoadeninylyl units were cleaved from the solid support resin. All the oligomers were purified through HPLC under standard conditions and characterized with MALDI-TOF mass spectrometry.

2.6 Experimental details:

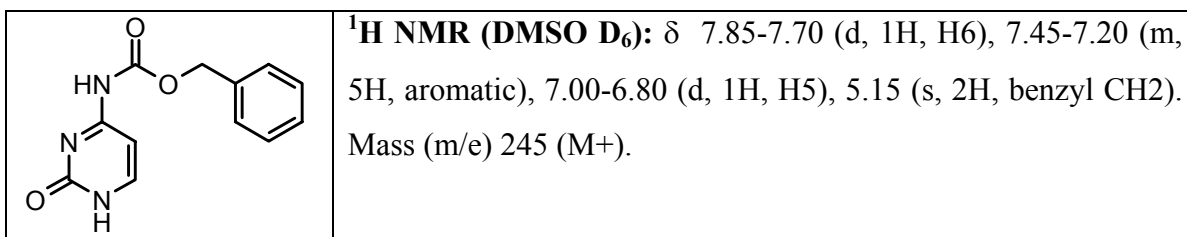
2.6.1 General

All reagents were obtained from commercial sources and used without further purification. NaH was obtained from Aldrich as 60% suspension in paraffin oil and the paraffin coating was washed off with pet-ether before use. All the solvents were dried according to literature procedures. IR spectra were recorded on a Perkin Elmer 599B instrument. ^1H NMR (200 MHz), ^{13}C NMR (50 MHz) spectra were recorded on Bruker ACF200 spectrometer fitted with an Aspect 3000 computer. All chemical shifts are with reference to TMS as an internal standard and are expressed in δ scale (ppm). The values given are directly from the computer printout and rounded to the decimal place. TLCs were carried out on (E.Merck 5554) precoated silicagel 60 F254 plates and the spots were visualized with UV light and/or ninhydrin spray, followed by heating after exposing the HCl for the deprotection of the tert-butoxycarbonyl group. All TLCs were run in pet-ether containing appropriate amount of ethyl acetate or dichloromethane containing appropriate amount of methanol to get the r_f value 0.5. All compounds were purified by column chromatography using 100-200 mesh silica gel obtained from Sisco Research Laboratory. NMR spectra of PNA monomers show doubling of peaks due to the presence of rotameric mixtures, arising from the tertiary amide linkage. The ratio of major: minor is 80:20 unless otherwise mentioned. In cases, where minor isomer is <10% only the

peaks of major rotamer are reported. Melting points of the compounds reported are uncorrected.

***N*⁴-Benzyloxycarbonyl cytosine (28)**

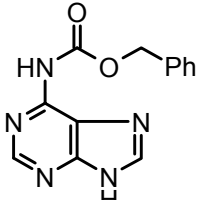
Cytosine **27** (1 g, 9 mmol) was suspended in dry pyridine (15 mL) and cooled to 0 °C and benzyloxycarbonyl chloroformate (3.0 mL, 18 mmol) was added drop wise over a period of 15 min. under nitrogen atmosphere. The reaction mixture was stirred for 10 hrs. The pyridine suspension was evaporated to dryness under vacuum. Water (10 mL) was added followed by the addition of 4N hydrochloric acid to bring the solution pH to 2. The resulting white precipitate was filtered off, washed with water and partially dried. The wet precipitate was boiled in absolute ethanol (25 mL) for 10 min. cooled to 0°C, filtered, washed thoroughly with ether, and dried, in vacuum to get **52** as a white solid.



***N*⁶-(Benzyloxycarbonyl) adenine (29).**

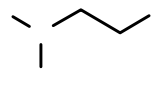
Sodium hydride (6.07 g, 152 mmol, 60% dispersion in oil) was washed with petroleum ether (3x10ml). After cooling in an ice bath, anhydrous DMF (150 mL) was added, followed by adenine (5.00 g, 37.0 mmol) in small portions. The suspension was stirred vigorously for 3 min and then benzyl chloroformate (11.6 mL, 81.5 mmol, 97%) was added dropwise. After stirring for 4 h, the reaction mixture was poured into ice water

(300 mL) and the pH adjusted to 6.0 with 1 N aqueous HCl. The light yellow precipitate was collected by filtration and washed with water and then with ether to afford the crude product (8.46 g). Recrystallization from methanol/chloroform afforded two crops of **10** (4.23 g, 44%) as a white solid

	¹ H NMR (d6-DMSO): 12.4 (br s, 1 H), 11.0 (br s, 1 H), 8.6 (s, 1 H), 8.4 (s, 1 H), 7.5-7.3 (m, 5 H), 5.3 (s, 2 H)
---	--

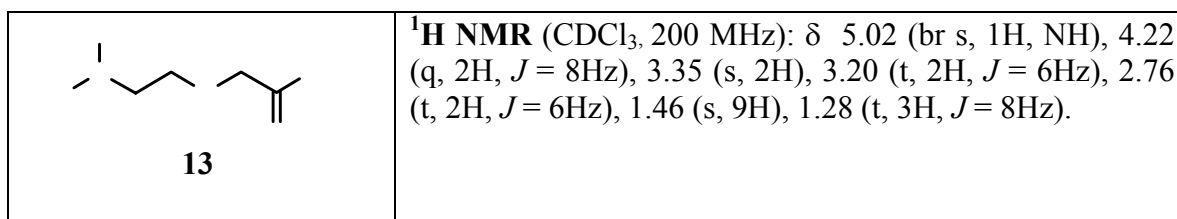
***N*₁-(*t*-Boc)-1,2-diaminoethane (12):**

1,2-diaminoethane (20 g, 0.33 mol) was taken in THF (500 ml) and cooled in an ice-bath. Boc-anhydride (5 g, 35 mmol) in THF (150 ml) was slowly added with stirring. The mixture was stirred at ambient temperature for 16 hr. and the resulting solution was concentrated to 100 ml. The *N*₁, *N*₂-di-Boc derivative precipitated after the addition of water 100 ml and it was removed by filtration through celite. The corresponding *N*₁-boc ethylene diamine was obtained by repeated extraction from the filtrate in DCM. The combined organic layers was kept on Na₂SO₄ and removal of solvent yielded the *N*₁-boc ethylene diamine **37** (3.45 g, 63%, R_f = 0.25, DCM: MeOH= 9:1).

	¹ H NMR (CDCl ₃ , 200 MHz): δ 5.21 (br s, 1H, NH), 3.32 (t, 2H, <i>J</i> =8 Hz), 2.54 (t, 2H, <i>J</i> =8 Hz), 1.42 (s, 9H).
---	--

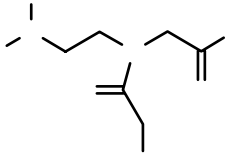
Ethyl *N*-(2-Boc-aminoethyl)-glycinate (13):

The N_1 -(*boc*)-1,2-diaminoethane **12** (3.2 g, 20 mmol) was treated with ethyl bromoacetate (2.25 ml, 20 mmol) in acetonitrile (100 ml) in the presence of NEt_3 (6.05 g, 60 mmol) at 0 °C, the mixture was stirred at ambient temperature for 12 h. The reaction mixture was concentrated to a gum and diluted with H_2O (20 ml) and extracted with ethyl acetate (5 x 20 mL). The combined organic phases were dried on anhydrous Na_2SO_4 and evaporation of the solvent afforded 4.3 gm (83%) of **13** as oily liquid.



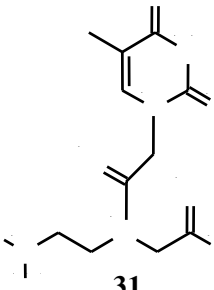
Ethyl *N*-(*boc*-aminoethyl)-*N*-(chloroacetyl)-glycinate (14**):**

The ethyl *N*-(2-*boc*-aminoethyl)-glycinate **14** (4.0 g, 14 mmol) was taken in 10% aqueous Na_2CO_3 (75 ml) and dioxane (60 ml). Chloroacetyl chloride (6.5 ml, 0.75 mmol) was added in two portions with vigorous stirring. The reaction was completed within 5 min and the reaction mixture was brought to pH 8.0 by addition of 10% aqueous Na_2CO_3 and concentrated to remove the dioxane. The product was extracted from the aqueous layer with dichloromethane and was purified by column chromatography to obtain the ethyl *N*-(*boc*-aminoethyl)-*N*-(chloroacetyl)-glycinate **14** as a colorless oil in good yield (4.2 g, Yield, 80%; $R_f = 0.3$, ethylacetate:petroleum ether; 2:8).

 <p style="text-align: center;">14</p>	¹ H NMR (CDCl ₃ , 200 MHz): δ 5.45 (br s, 1H), 4.1- 4.9 (S, 2H), 4.00 (s, 2H), 3.53 (t, 2H), 3.28 (q, 2H), 1.46 (s, 9H), 1.23 (t, 3H, <i>J</i> =8Hz).
--	---

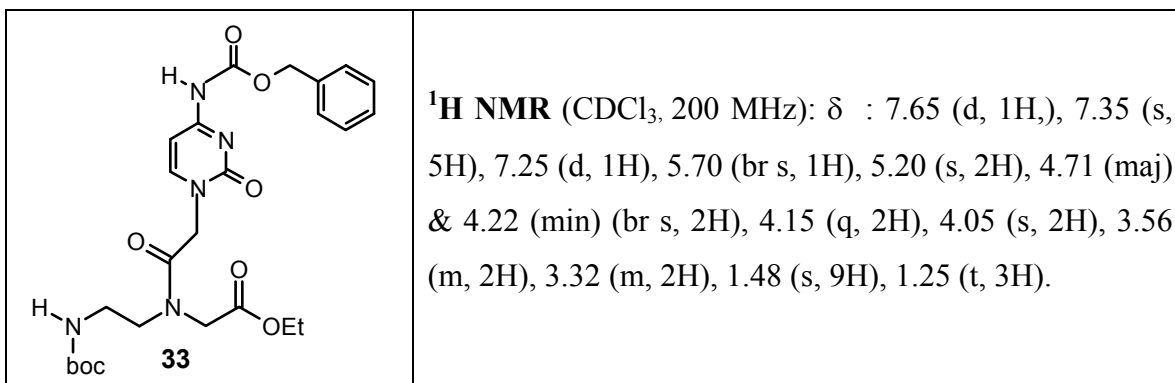
***N*-(Boc-aminoethylglycyl)-thymine ethyl ester (31):**

Thymine (0.41 g, 3.25 mmol) dissolved in DMF (15ml) containing anhydrous K₂CO₃ (0.47 g, 3.4 mmol) and heated at 60 °C for 60 min and slowly cooled to by 0 °C. Ethyl *N*-(boc-aminoethyl)-*N*-(chloroacetyl)-glycinate **14** (1.0 g, 3.1mmol, in 10 ml DMF) was added dropwise and the reaction mixture stirred for 6 hrs. After completion of the reaction, DMF was evaporated under reduced pressure and extracted with ethylacetate (3x25ml). The combined organic phases were dried over anhydrous Na₂SO₄ and concentrated, followed by column chromatography to obtain the desired compound **31** in good yield. (1 g, Yield 83%; R_f = 0.2, MeOH:DCM; 5:95).

 <p style="text-align: center;">31</p>	¹ H NMR (CDCl ₃ , 200 MHz): δ 9.00 (br s, 1H), 7.05 (min) & 6.98 (maj) (s, 1H), 5.65 (maj) & 5.05 (min) (br s, 1H), 4.58 (maj) & 4.44 (min) (s, 1H), 4.25 (m, 2H), 3.55 (m, 2H), 3.36 (m, 2H), 1.95 (s, 3H), 1.48 (s, 9H), 1.28 (m, 3H)
--	---

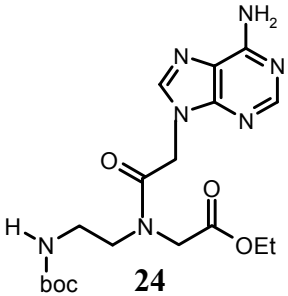
***N*-(Boc-aminoethylglycyl)-(*N*⁴-benzyloxycarbonyl cytosine)ethyl ester (33):**

A mixture of NaH (0.25 g, 6.2 mmol) and *N*⁴-benzyloxycarbonyl cytosine **17** (1.24 g, 6.2 mmol) was taken in DMF and stirred at 60 °C till the effervescence ceased. The mixture was cooled and ethyl *N*-(*boc*-aminoethyl)-*N*-(chloroacetyl)-glycinate **14** (2.0 g, 6.2 mmol) was added. Stirring was then continued to obtain the cytosine monomer, *N*-(*Boc*-aminoethylglycyl)-(*N*⁴-benzyloxycarbonyl cytosine) ethyl ester **33**, in moderate yield (1.75 g, 69%;).



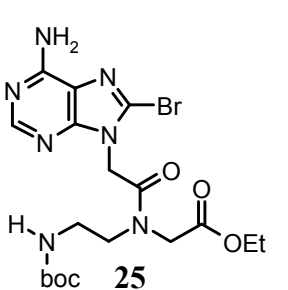
***N*-(*Boc*-aminoethylglycyl)-adenine ethyl ester (**24**):**

NaH (0.25 g, 6.1 mmol) was taken in DMF (15 ml) and adenine (0.8 g, 6.1 mmol) was added. The mixture was stirred at 60 °C, then slowly cooled to 0 °C and ethyl *N*-*Boc*-aminoethyl)-*N*-(chloroacetyl)-glycinate **14** (2.0 g, 6.1mmol) added dropwise. The reaction mixture was stirred at ambient temperature for 6 hrs. The DMF was removed under vacuum and the resulting thick oil was taken in water and the product, extracted with ethyl acetate (3x25ml). The organic layer was dried using anhydrous Na₂SO₄ and concentrated to obtain the crude product, which was purified by column chromatography to obtain the pure *N*- (*boc*-aminoethyl glycyl) - adenine ethyl ester **24** with good yield. (Yield 75%; R_f = 0.2, MeOH:DCM; 5:95).

 <p style="text-align: center;">24</p>	<p>¹H NMR (CDCl₃, 200 MHz): δ 8.32 (s, 1H), 7.95 (min) & 7.90 (maj) (s, 1H), 5.93 (maj) & 5.80 (min) (br, 2H), 5.13 (maj) & 4.95 (min), 4.22 (min) & 4.05 (maj) (s, 2H), 4.20 (m, 2H), 3.65 (maj) & 3.55 (min) (m, 2H), 3.40 (maj) & 3.50 (min) (m, 2H), 1.42 (s, 9H), 1.25 (m, 3H).</p>
--	---

***N*-(Boc-aminoethylglycyl)-(8-bromoadenine) ethyl ester (25):**

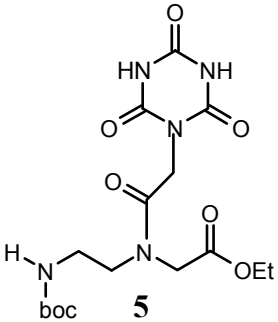
N-(Boc-aminoethylglycyl)-adenine ethyl ester (**24**) (1g, 2.38 mmol) was dissolved in dioxane (5ml) and Na₂HPO₄ (0.85 g, 5.95 mmol) dissolved in 5ml water was added dropwise. The reaction mixture was stirred at 0 °C and liquid bromine (0.24ml, 0.48 mmol) added dropwise and stirred at ambient temperature for 6h. Dioxane removed under vacuum, excess bromine was quenched with excess 1N Na₂S₂O₅, by stirring for 4 hrs and the reaction mixture extracted with ethyl acetate (3x50 ml), followed by drying over anhydrous Na₂SO₄. The organic layer was concentrated under vacuum, which was purified by column chromatography (hexane: Ethyl acetate) yielded *N*-(boc-aminoethylglycyl)-(8-bromoadenine) ethyl ester.

 <p style="text-align: center;">25</p>	<p>¹H NMR (CDCl₃, 200 MHz): δ 8.32 (s, 1H), 5.93 (maj) & 5.80 (min) (br, 2H), 5.13 (maj) & 4.95 (min), 4.22 (min) & 4.05 (maj) (s, 2H), 4.20 (m, 2H), 3.65 (maj) & 3.55 (min) (m, 2H), 3.40 (maj) & 3.50 (min) (m, 2H), 1.42 (s, 9H), 1.25 (m, 3H).</p> <p>¹³C NMR (CDCl₃): 169.30, 165.66, 155.99, 154.34, 152.61, 151.21, 127.95, 119.23, 61.46, 48.81, 44.36, 38.40, 28.19,</p>
--	--

	21.13. I. R: 757.97 (C-Br)
--	--------------------------------------

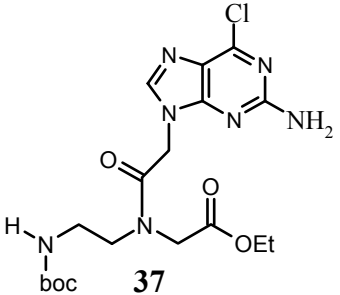
***N*-(Boc-aminoethylglycyl) cyanuryl ethyl ester (6):**

Cyanuric acid (1g) was dispersed in DMSO (50ml) and K₂CO₃ (1 g) added. The mixture heated at 55 °C for 1hr. and was slowly cooled to 0 °C and ethyl *N*-Boc-aminoethyl)-*N*-(bromoacetyl)-glycinate **15** (2.0 g, 6.1mmol) added dropwise. The reaction mixture was stirred at ambient temperature for 10 hrs. Water (20ml) was added to the reaction mixture and extracted with diethyl ether for several times (until compound **6** is not present in aqueous layer as confirmed by TLC). The combined ether layers were pooled and washed with water and brine solution several times to remove the DMSO dissolved in ether layer. The ether extracts were dried over anhydrous Na₂CO₃ and concentrated to obtain the crude product. This was purified by column chromatography to obtain the pure *N*-(boc-aminoethyl glycyl) cyanuryl ethyl ester **6** with good yield. (Yield 75%; R_f = 0.2, MeOH:DCM; 5:95).

 <p>5</p>	<p>¹H NMR (CDCl₃, 200 MHz): δ 9.00 (br s, 1H), 8.81(br s, 1H), 5.49 (maj) & 5.40 (min) (s, 1H), 4.63 (maj) & 4.48 (min) (s, 2H, Cy-CH₂), 4.11(maj) & 4.03 (min) (m, 2H, OCH₂), 3.95 (m, 2H), 3.25 (maj) & 3.2(min) (m, 2H), 1.95 (s, 3H), 1.36 (s, 9H), 1.20 (m, 3H).</p> <p>¹³C NMR (CDCl₃): δ: 167.35, 164.77, 154.06, 147.46,</p>
---	--

	146.61, 145.97, 77.71, 60.07, 59.44, 46.72, 40.50, 36.64, 26.21, 11.97, 12.2.
--	---

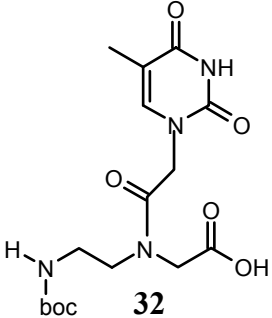
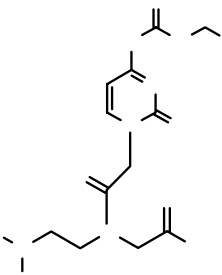
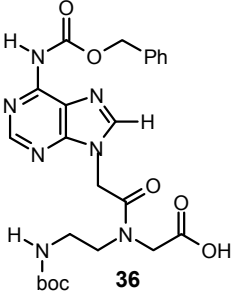
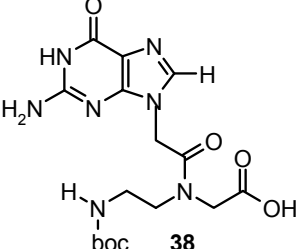
***N*-(Boc-aminoethylglycyl)-2-amino-6-chloropurine ethyl ester (43)**: A mixture of 2-amino-6-chloropurine (1.14 g, 6.8 mmol), K₂CO₃ (0.93 g, 7.0 mmol) and ethyl *N*-(Boc-aminoethyl)-*N*-(chloroacetyl)-glycinate **14** (2.4 g, 7.0 mmol) were taken in dry DMF (20 ml) and stirred at room temperature for 4 h. Solid K₂CO₃ was removed by filtration and the filtrate was concentrated under reduced pressure. The resulting residue was purified by column chromatography over silica gel to obtain the *N*-(boc-aminoethylglycyl)-2-amino-6-chloropurine ethyl ester (**37**) in excellent yield (2.55 g, 90%; R_f = 0.25, MeOH:DCM; 5:95).

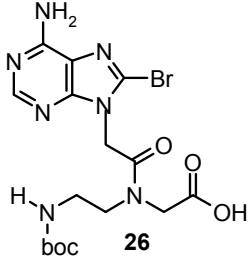
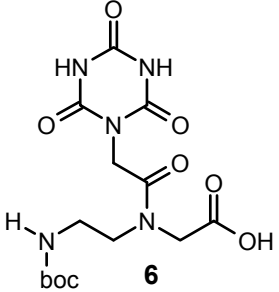
 <p style="text-align: center;">37</p>	¹ H NMR (CDCl ₃ , 200 MHz): δ 7.89 (min) & 7.85 (maj) (s, 1H), 7.30 (s, 1H), 5.80 (br s, 1H, NH), 5.18 (br, 2H), 5.02 (maj) & 4.85 (min) (s, 2H), 4.18 (min) & 4.05 (maj) (s, 2H), 3.65 (maj) & 3.16 (min) (m, 2H), 3.42 (maj) and 3.28 (min) (m, 2H), 1.50 (s, 9H), 1.26 (m, 3H).
--	--

Hydrolysis of the ethyl ester functions of PNA monomers (General method):

The PNA ester monomer was dissolved in methanol to which aq. LiOH (2N) added and stirred for 2 hrs, TLC indicated that the reactant was consumed. Methanol was evaporated under reduced pressure, residue dissolved in water and the aqueous layer washed 3 times with ethyl acetate (to remove organic impurities). The resulting product

was neutralized with activated Dowex-H⁺ till the pH of the solution was 6.0-7.0. The resin was removed by filtration and the filtrate was concentrated to obtain the resulting Boc-protected acids (**32/34/36/38**) in excellent yield (>85%). In case of cytosine and cbz-adenine, mild base 0.5 M LiOH was used to avoid deprotection of the exo cyclic amine-protecting group by strong bases.

 <p style="text-align: center;">32</p>	<p>¹H NMR (D₂O, 200 MHz): δ 7.39 (s, 1H), 4.72 (maj) & 4.63 (min) (s, 2H), 4.22 (maj) & 4.15 (s, 2H), 3.39 (m, 2H), 3.27 (m, 2H), 1.91 (s, 3H), 1.45 (s, 9H).</p>
	<p>¹H NMR (DMSO d₆, 200 MHz): δ : 7.65 (d, 1H), 7.35 (s, 5H), 7.22 (d, 1H), 5.70 (br s, 1H), 5.17 (s, 2H), 4.71 (maj) & 4.22 (min) (br s, 2H), 4.05 (s, 2H), 3.56 (m, 2H), 3.32 (maj) & 3.19 (min) (m, 2H), 1.43 (s, 9H).</p>
 <p style="text-align: center;">36</p>	<p>¹H NMR (DMSO d₆, 200 MHz): 10.65 (br, 1 H), 8.60 (s, 1 H), 8.32 (s, 1 H), 7.48-7.34 (m, 5 H), 5.23 (s, 2 H); 4.57 (maj) & 4.41 (min) (s, 2H,); 3.95 (maj) & 3.90 (min) (s, 2H); 3.40 (m, 2H), 3.15 (maj) & 3.05 (min) (m, 2H), 1.39 (s, 9 H)</p>
 <p style="text-align: center;">38</p>	<p>¹H NMR (D₂O, 200 MHz): 7.89 (min) & 7.85 (maj) (s, 1H), 7.30 (s, 1H), 5.35 (min) & 4.98 (maj)(s, 2H), 4.35 (min) & 3.87 (maj), (s, 2H), 3.65 (min), 3.45 (maj) (m, 2H), 3.25 (m, 2H), 1.38 (s, 9H)</p>

 <p style="text-align: center;">26</p>	¹ H NMR (D ₂ O, 200 MHz): 8.05 (min) & 8.00 (maj, 1H); 5.35 (min) & 4.98 (maj)(s, 2H), 4.35 (min) & 3.87 (maj), (s, 2H), 3.65 (min), 3.45 (maj) (m, 2H), 3.25 (m, 2H), 1.38 & 1.26 (s, 9H)
 <p style="text-align: center;">6</p>	¹ H NMR (D ₂ O, 200 MHz): 4.58 (s, 2H), 4.02 (min) & 3.95 (maj), (s, 2H), 3.50 (m, 2H), 3.29 (maj) (m, 2H), 3.19 (m, 2H), 1.38 (s, 9H).

2.6.2 Functionalization of MBHA resin

Commercially available MBHA resin (Jupiter Biosciences, West Marredpally, Hyderabad, India) has the loading value of (2meq/g) which is not suitable for oligomer synthesis and so it was required to minimize the loading value to 0.25-0.35 m eq/g to avoid the aggregation of the growing oligomer. The dry resin was taken in solid phase funnel and swelled in DCM for 1 h. The solvent was drained off and the resin was treated with calculated amount of acetic anhydride in 5% DIPEA/DCM solution for about 15 min, solvent was drained off, the resin was thoroughly washed with DCM and DMF to remove the traces of acetic anhydride and dried under vacuum. The dried resin was taken in solid phase funnel and swelled in DCM for about 1h and functionalized with *N*^α boc-*N*⁰ Z-Lysine.

2.6.3 Picric acid assay for the estimation of the amino acid loading

The functionalized dry resin (5 mg) was taken in a sintered funnel and swelled in CH₂Cl₂ for 1 h. The solvent was drained off and the resin was treated with 50% TFA/DCM for 15 min (1 mL x 2) each time (if the resin with *boc* functionalized amine only). The resin was thoroughly washed with CH₂Cl₂ and the TFA salt was neutralized with 5% diisopropyl ethylamine for 2 min (1 mL x 3). The free amine was treated with 0.1 M picric acid in DCM for 10 min (2 mL x 3) each time. The resin was thoroughly washed with CH₂Cl₂ to remove the unbound picric acid. The picrate bound to amino groups was eluted with 5% diisopropyl ethylamine in CH₂Cl₂, followed by washing with CH₂Cl₂. The elutant was collected into a 10 ml volumetric flask and made up to 10 ml using CH₂Cl₂. An aliquot (0.2 ml) of picrate eluant was diluted to 2 ml with ethanol and the optical density was measured at 358 nm (picric acid λ_{max}), and the loading value of the resin (0.35 meq/g) was calculated using the molar extinction coefficient of picric acid as $\epsilon_{358}=14,500 \text{ cm}^{-1} \text{ M}^{-1}$ at 358 nm.

2.6.4 Cleavage of the PNA oligomers from the solid support

The cleavage of peptides from the MBHA resin by using trifluoromethanesulphonic acid (TFMSA) in the presence of trifluoroacetic acid (TFA) (“Low, High TFMSA-TFA method”), yields peptides with free amine at *N*-terminus and amide at their 'C' termini.⁵⁹ The synthesized PNA oligomers (Table 3, 4&5 page no. 25, 28 and 29) were cleaved from the resin using TFA -TFMSA to obtain sequences bearing lysine free carboxylic amids at their 'C' termini (Table 6, page no. 30-31). After commencing the cleavage reaction, aliquots were removed after 60 min, the peptides isolated by gel filtration using Sephadex G 25 gel matrix (see in experimental section)

and then analyzed by HPLC. A cleavage time of ~ 2h at room temperature was found to be optimum for complete deprotection cleavage. The exocyclic amino groups of cytosine protected as benzyloxycarbonyl, was also cleaved during this process.

2.6.5 Purification of the PNA oligomers

All the cleaved oligomers were subjected to initial gel filtration to remove low molecular weight impurities. These were subsequently purified by reverse phase HPLC (high pressure liquid chromatography) on a semi-preparative C8 RP column by gradient elution using an acetonitrile in water or by isocratic elution in 10% acetonitrile-water on a semi- preparative HPLC RP C4 column. In some cases, HPLC did not produce a clean single peak profile. Hence, the sample was heated at ~80 °C for 4-5 min to destroy any secondary structure that might exist before injection.

The purity of the oligomers was then checked by reverse phase HPLC on a C18 RP column and confirmed by MALDI-TOF mass spectroscopic analysis.³¹ Some representative HPLC profiles and mass spectra are shown in appendix of this chapter. The purified PNA **66-86** sequences obtained are listed in Table **6** (page no. 30-31).

2.7 References:

1. Uhlmann, E.; Peyman, A. *Chem. Rev.* **1910**, *90*, 543-584.
2. *Antisense Research and Applications* (Eds.: Crooke, S. T.; Lebleu, B.), CRC Press, Boca Raton, FL, **1993**.
3. *Antisense Oligonucleotides- Chemical Modifications*. Uhlmann, E.; Peyman, A. in *Encyclopedia of Molecular Biology and Biotechnology* (Ed.: Meyer, E.), VCH, New York, 1995.
4. De Mesmaeker, A.; Haner, R.; Mertin, P.; Moser, H. E. *Acc. Chem. Res.* **1995**, *28*, 366.
5. *Methods in Molecular Biology, Vol, 20: Protocols for Oligonucleotides and analogs* (Ed.: Agarwal, S.), Humana Press, New Jersey, Totowa, Chapter 16, **1993**, *20*, 355-389.

6. Nielsen, P. E.: *Annu. Rev. Biophys. Biomol. Struct.* **1995**, *24*, 167.
7. De Mesmaeker, A.; Altmanna, K. H.; Wendeborn, S. *Curr. Opin Struct. Biol.* **1995**, *5*, 343.
8. Stirchak, E. P.; Summerton, J. E.; Weller, D. D.; *Nucleic Acids Res. Dev. Proc. Symp.* **1989**, *17*, 6129.
9. Nielsen, P. E.; Egholm, M.; Buchardt, O. *Science*, **1991**, *254*, 1497.
10. Nielsen, P. E.; Egholm, M.; Buchardt, O. *Bioconj. Chem.* **1994**, *5*, 3.
11. Hyrup, B.; Egholm, M.; Nielsen, P. E. *Bioorg. Med. Chem. Lett.* **1996**, *6*, 5.
12. Good, L.; Nielsen, P. E. *Antisense & Nucleic acids Drug Dev.* **1997**, *7*, 431.
13. Nielsen, P. E.; Haaima, G. *Chem. Soc. Rev.* **1997**, 73.
14. Uhlmann, E.; Peyman, A.; Breipohn, G.; Will, D. W. *Angew. Chem. Int. Ed. Engl.* **1998**, *37*, 2796.
15. Demidov, V. V.; Pataman, V. N.; Frank-Kamenetskii, M. D.; Egholm, M.; Buchardt, O.; Sonnichsen, S. H.; Nielsen, P. E. *Biochem, Pharmacol.* **1994**, *48*, 1310- 1313.
16. Hyrup, B.; Nielsen, P. E. *Bioorg. Med. Chem.* **1996**, *4*, 5.
17. Hanvey, J. C.; Peffer, N. J.; Bisi, J. E.; Thomson, S. A.; Cadilla, R.; Josey, J. A.; Ricca, D. J.; Hassman, F.; Bonham, M. A.; Au, K. G.; Carter, S. G.; Bruckenstein, D. A.; Boyd, A. L.; Noble, S. A.; Basiss, L. E. *Science* **1992**, *258*, 1481.
18. (a) Haaima, G.; Rasmussen, H.; Schmidt, G.; Jensen, D. K.; Kastrup, J. S.; Stafshede, P. W.; Norden, B.; Buchardt, O.; Nielsen, P. E. *New J. Chem.* **1999**, *23*, 833-840. (b) Brown, S. C.; Thomson, S. A.; Veal, J. M.; Davis, D. G. *Science*, **1994**, *265*, 777-780.

19. Koch, T.; Naesby, M.; Wittung, P.; Jorgensen, M.; Larsson, C.; Buchardt, O.; Stanley, C. J.; Norden, B.; Nielsen, P. E.; Orum, H. *Tetrahedron* **1995**, *36*, 6933.
20. Peterson, K. H.; Jensen, D. K.; Nielsen, P. E.; Egholm, M.; Buchardt, O. *Biorg. Med. Chem. Lett.* **1995**, *5*, 1119.
21. (a) Ganesh, K. N.; Nielsen, P. E. *Curr. Org. Chem.* **2000**, *4*, 931-943. (b) Kumar, V. A., *Eur. J. Org. Chem.* **2002**, 2021-2032.
22. Kumar, V. A.; Ganesh, K. N. *Acc. Chem. Res.* **2005**, *38*, 404-412.
23. (a) Soyfer, V. N.; Potaman, V. N. *Triple helical Nucleic Acids*; Springer: New York, 1996. (b) Ganesh, K. N.; Kumar, V. A.; Barawkar, D. A. *Supramolecular control of structure and reactivity* (chapter 6, Ed Hamilton, A. D) **1996**, 263-327.
24. Haaima, G.; Hansen, H. F.; Christensen, L.; Dahl, O.; Nielsen, P. E. *Nucleic Acids Res.* **1997**, *25*, 4639-4643.
25. Wojciechowski, F.; Hudson, R. H. E. *Curr. Top. Med. Chem.* **2007**, *7*, 667-679.
26. MacDonald, J. C.; Whitesides, G. M. *Chem. Rev.* **1994**, *94*, 2383-2420.
27. Ranganathan, A.; Pedireddi, V. R.; Rao, C. N. R. *J. Am. Chem. Soc.* **1999**, *120*, 1752-1753.
28. (a) Ranganathan, A.; Pedireddi, V. R.; Sanjayan, G.; Ganesh, K. N.; Rao, C. N. R. *J. Mol. Struct.* **2000**, *522*, 87-94. (b) Coppens, P.; Vos, A. *Acta Crystallogr.* **1971**, *B27*, 146. (c) Pedireddi, V. R.; Ranganathan, A.; Ganesh, K. N. *Org. Lett.* **2001**, *3*, 99-102.
29. Raoul, S.; Cadet, J. *J. Am. Chem. Soc.* **1996**, *118*, 1892-1898.
30. Gasparutto, D.; Da Cruz, S.; Bourdat, A. G.; Jaquinod, M.; Cadet, J. *Chem. Res. Toxicol.* **1999**, *12*, 630-638.

31. Guñimil Garcí'a, R.; Ferrer, E.; Macías, M. J.; Eritja, R.; Orozco, M. *Nucleic Acids Res.* **1999**, *27*, 1991.
32. Kawai, K.; Saito, I.; Sugiyama, H. *Tetrahedron Lett.* **1998**, *39*, 5221.
33. Soliva, R.; Guñimil-Garcí'a, R.; Blas, J. R.; Eritja, R.; Asensio, J. L.; González, C.; Luque, F. J.; Orozco, M. *Nucleic Acids Res.* **2000**, *28*, 4531.
34. Cubero, E.; Avino, A.; de la Torre, B. G.; Frieden, M.; Eritja, R.; Luque, F. J.; Gonzalez, C.; Orozco, M. *J. Am. Chem. Soc.* **2002**, *124*, 3133-3142.
- 35 (a) Guñimil Garcí'a, R.; Ferrer, E.; Macias, M.J.; Eritja, R.; Orozco, M. *Nucleic Acids Res.* **1999**, *27*, 1991–1998. (b) Chattopadhyaya, J. *Tetrahedron*, **1991**, *47*, 4693-4708. (c) Kumar R. K.; Gunjal A. D.; Ganesh K. N. *Biochem. Biophys. Res. Comm.* **1994**, *204* (2) 788.
36. Avino, A.; Cubero, E.; Gonzalez, C.; Eritja, R.; Orozco, M. *J. Am. Chem. Soc.* **2003**, *25*, 16127-16138.
37. Cancela, J. M. ; Petersen, O. H. *Eur J Physiol.* **1998**, *435*, 746–748.
38. Lisa. S.; Chen.; Terry, L.; Sheppard *J. Biol. Chem.* **2004**, *279*(39), 40405–40411.
39. (a) Krett, N. L.; Davies, K. M.; Ayres, M.; Ma, C.; Nabhan, C.; Gandhi, V.; Rosen, S. T. *Mol Cancer Ther.* **2004**, *3*(11), 1411-1419. (b) Ghias, K.; Ma, C.; Gandhi, V.; Plataniias, L. C.; Krett, N. L.; Rosen, S. T. *Mol Cancer Ther* **2005**; *4*(4), 569-577.
40. (a) Patil. S. P.; Padmanabhan, D. *J. Label Compd. Radiopharm.* **2002**, *45*, 539. (b) Saunders, J. H.; Slocombe, R. J. *Chem. Rev.* **1948**, *43*, 203. (c) Arnold, R. G.; Nelson, J. A.; Verbanc, J. J. *Chem. Rev.* **1957**, *57*, 47.
41. (a) Davis. T.; Blanchard, K. C. *J. Amer. Chem. Soc.*, **1929**, *51*, 1801.

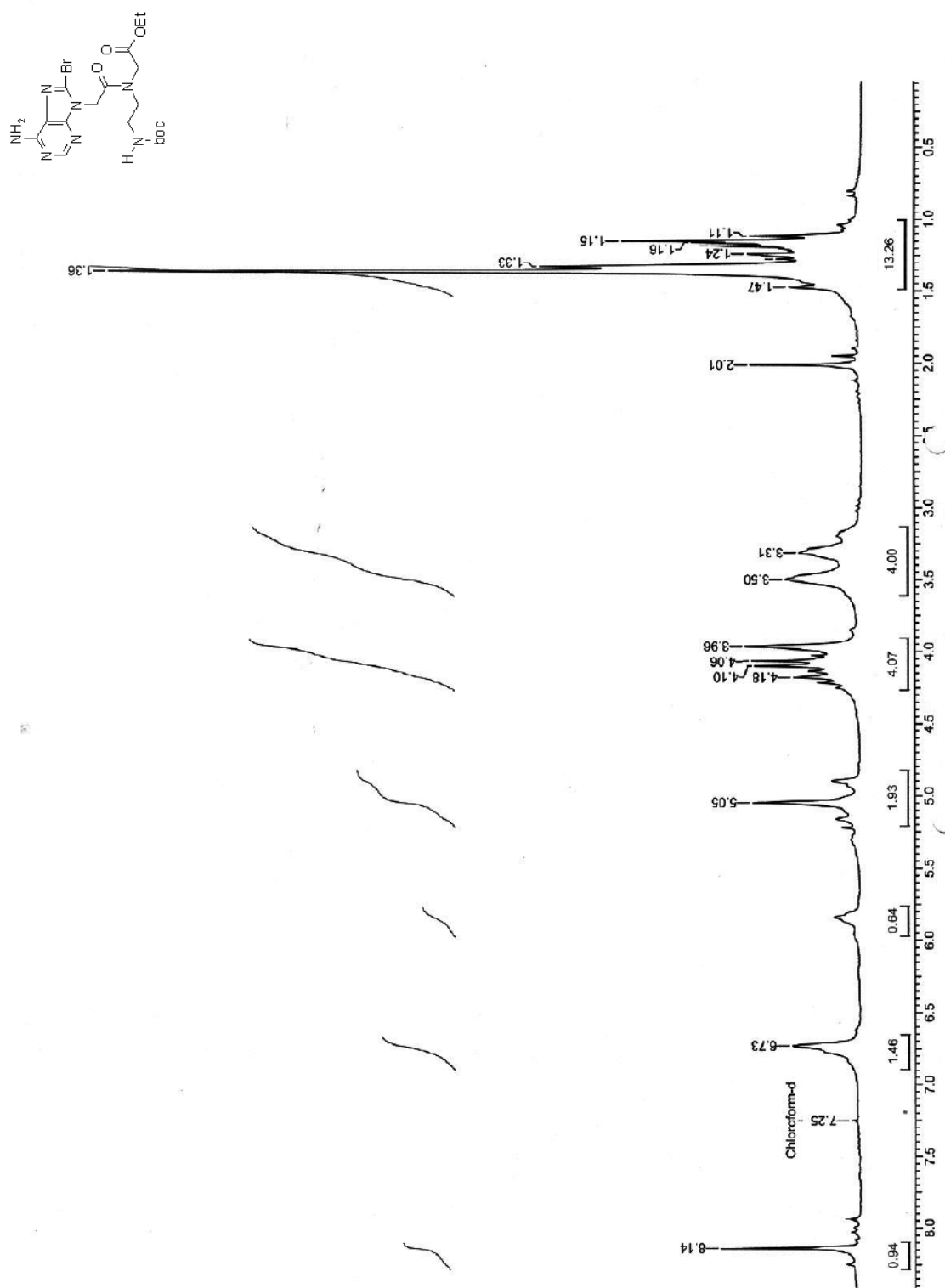
- (b) Dunnigan, D. A.; Close, W. J. *J. Am. Chem. Soc.* **1953**, *75*, 3615- 3616.
- (c) Sanjayan, G. J.; Pedireddi, V. R.; Ganesh, K. N. *Org. Lett.* **2000**, *2*, 2825.
42. Cotarca, L.; Delogu, P.; Nardelli, A.; Sunjic, V. *Synthesis*, **1996**, 553-576.
43. Dueholm, K. L.; Egholm, M.; Behrens, C.; Christensen, L.; Hansen, H. F.; Vulpius, T.; Petersen, K. H.; Berg, R. H.; Nielsen, P. E.; Buchardt, O. *J. Org. Chem.* **1994**, *59*, 5767-5773.
44. Meltzer, P. C.; Liang, A. Y.; Matsudaira, P. *J. Org. Chem.* **1995**, *60*, 4305-4308
45. Carraway, K. L.; Huang, P. C.; Scott, T. G. in *Synthetic Procedures in Nucleic Acid Chemistry* (Ed. Zorbach, W. W.; Tipson, R. S.) 3-5.
46. Isobe, Y.; Tobe, M.; Ogita, H.; Kurimoto, A.; Ogino, T.; Kawakami, H.; Takaku, H.; Sajiki, H.; Hirota, K.; Hayashia, H. *Bio org. Med. Chem.* **2003**, *11*, 3641–3647.
47. Egholm, M.; Buchardt, O.; Nielsen, P. E. *J. Am. Chem. Soc.* **1992**, *114*, 1895-1897.
48. Thomson, S. A.; Josey, J. A.; Cadilla, R.; Gaul, M. D.; Hassman, C. F.; Luzzio, M. J.; Pipe, A. J.; Reed, K. L.; Ricca, D. J.; Wiethe, R. W.; Noble, S. A. *Tetrahedron*, **1995**, *51*, 6179-6194.
49. Merrifield, B. *J. Am. Chem. Soc.* **1963**, *85*, 2149.
50. Koch, T. *Peptide Nucleic Acids: Protocols and Applications* (Section 2.1, *PNA oligomers synthesis by BOC chemistry*, Ed. Nielsen, P. E. & Egholm, M.) **1996**, 21-39.
51. Merrifield, R. B.; Stewart, J. M.; Jernberg, N. *Anal. Chem.* **1966**, *38*, 1905.

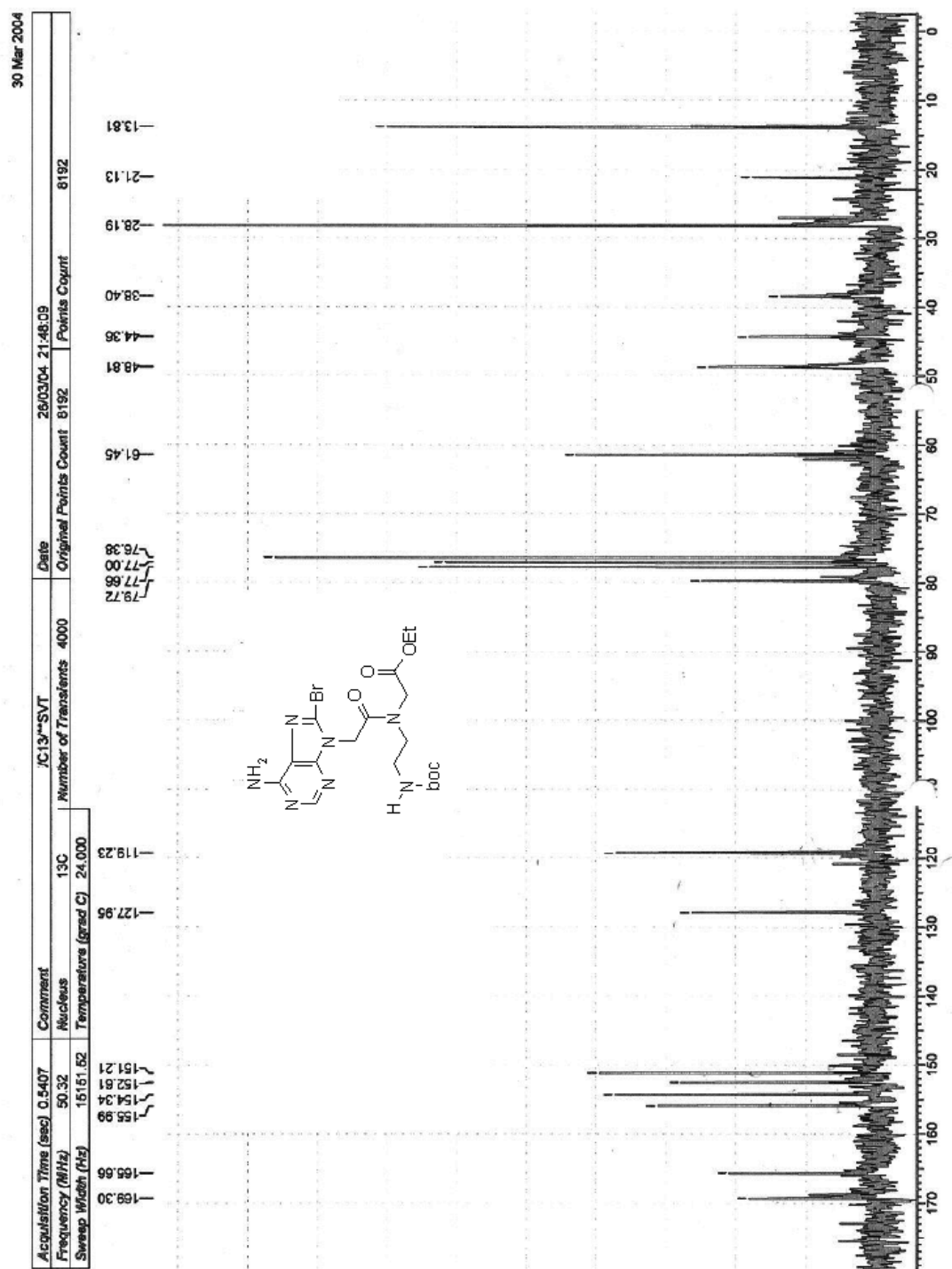
52. (a) Kaiser, E.; Colecott, R. L.; Bossinger, C. D.; Cook, P. I. *Anal. Biochem.* **1970**, *34*, 595. (b) Kaiser, E.; Bossinger, C. D.; Colecott, R. L.; Olsen, D. B. *Anal. Chim. Acta.* **1980**, *118*, 149. (c) Sarin, V. K.; Kent, S. B. H.; Tam, J. P.; Merrifield, R. B. *Anal. Biochem.* **1981**, *117*, 147.
53. Christensen, L.; Fitzpatrick, R.; Gildea, B.; Petersen, K.; Hansen, H. F.; Koch, C.; Egholm, M.; Buchardt, O.; Nielsen, P. E.; Coull, J.; Berg, R. H. *J. Peptide Sci.* **1995**, *3*, 175.
54. Erickson, B. W.; Merrifield, R. B. *Solid Phase Peptide Synthesis In The Proteins* Vol. II, 3rd Ed. H. Neurath and R. L. Hill, eds. Academic Press, New York, **1976**, pp 255.
55. (a) Kaiser, E.; Colecott, R. L.; Bossinger, C. D.; Cook, P. I. *Anal. Biochem.* **1970**, *34*, 595. (b) Kaiser, E.; Bossinger, C. D.; Colecott, R. L.; Olsen, D. B. *Anal. Chim. Acta.* **1980**, *118*, 149. (c) Sarin, V. K.; Kent, S. B. H.; Tam, J. P.; Merrifield, R. B. *Anal. Biochem.* **1981**, *117*, 147.
56. Christensen, T. *Acta, chem. Scand.* **1979**, *34*, 594.
57. Madder, A.; Farcy, N.; Hosten, N. G. C.; De Muynck, H.; De Clereq, P.; Barry, J.; Davis, A. P. *Eur. J. Org. Chem.* **1999**, *11*, 2787.
58. Garcia, R. G.; Ferrer, E.; Macias, M. J.; Eritja, R.; Orozco, M. *Nucleic Acids Res.* **1999**, *27*, 1991–1998.
59. Christensen, L.; Fitzpatrick, R.; Gildea, B.; Petersen, K. H.; Hansen, H. F.; Koch, T.; Egholm, M.; Buchardt, O.; Nielsen, P. E.; Coull, J.; Berg, R. H. *J. Peptide Sci.* **1995**, *3*, 175.

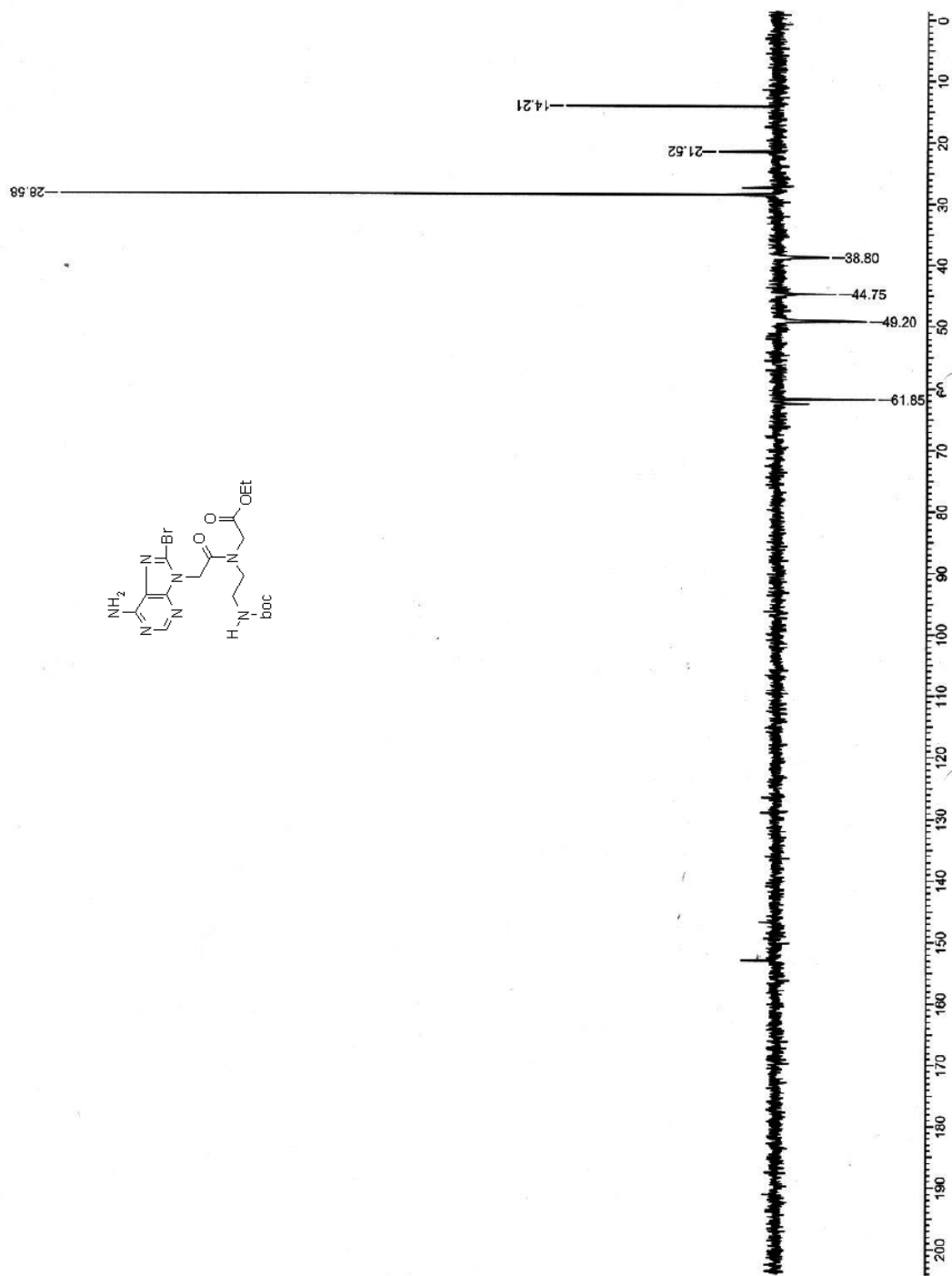
60. (a) Butler, J. M.; Jiang-Baucom, P.; Huang, M.; Belgrader, P.; Girard, J. *Anal. Chem* **1996**, *68*: 3283. (b) Ross, P. L.; Lee, K.; Belgrader, P., *Anal. Chem* **1997**, *69*, 4197. (c) Jiang-Baucom P, Girard, J. E. *Anal. Chem* **1997**, *69*: 4894.
61. (a) Gait, J. M. "Oligonucleotide synthesis: A practical approach". IRL Press Oxford, Uk, 217, 1984. (b) Agrawal, S. in "Protocols for oligonucleotides and analogs: Synthesis and properties" *Methods in Molecular Biology*. Agrawal, S. (ed): vol 20: Totowa, NJ. Humana Press, Inc., **1993**.

2.8 Appendix

Entry	Details	Page Number
1	Compound 25 ; ^1H NMR and Mass spectra	100
2	Compound 25 ; ^{13}C spectra	101
3	Compound 25 ; DEPT spectra	102
4	Compound 24 ; IR spectra	103
5	Compound 25 ; IR spectra	104
6	Compound 6 ; ^1H NMR and Mass spectra	105
7	Compound 6 ; ^{13}C spectra	106
8	Compound 6 ; DEPT spectra	107
9	Compound 7 ; ^1H NMR and Mass spectra	108
10	Compound 7 ; ^{13}C spectra	109
11	Compound 7 ; DEPT spectra	110
12	HPLC-Profiles of PNA oligomers	111-112
13	MALDI-TOF spectra of PNA oligomers	113-117
14	HPLC-Profiles of DNA oligomers	118

Figure 22: Compound 25 ^1H NMR

Figure 23: Compound 25 ¹³C NMR

Figure 24: Compound 25 ^{13}C DEPT

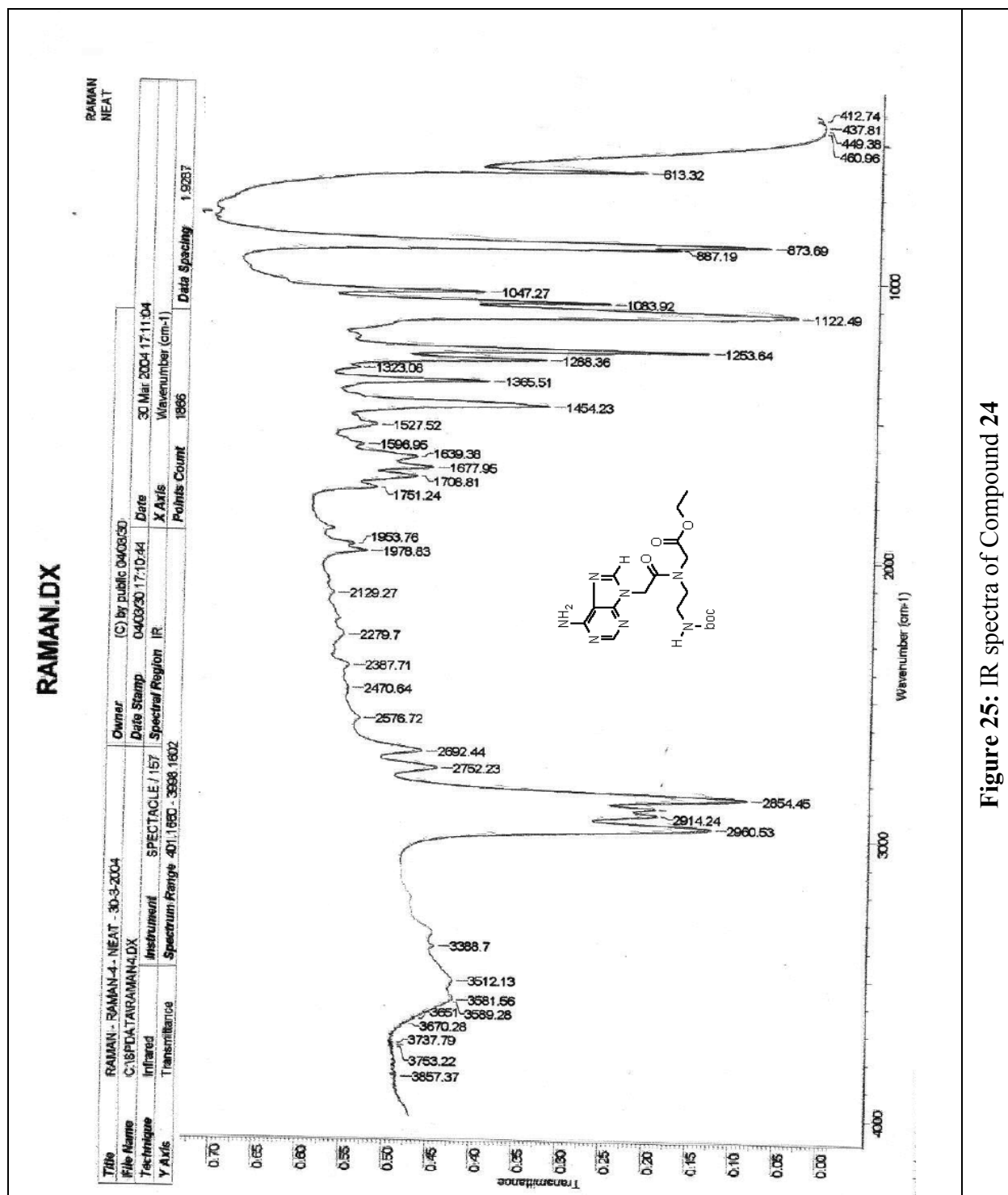


Figure 25: IR spectra of Compound 24

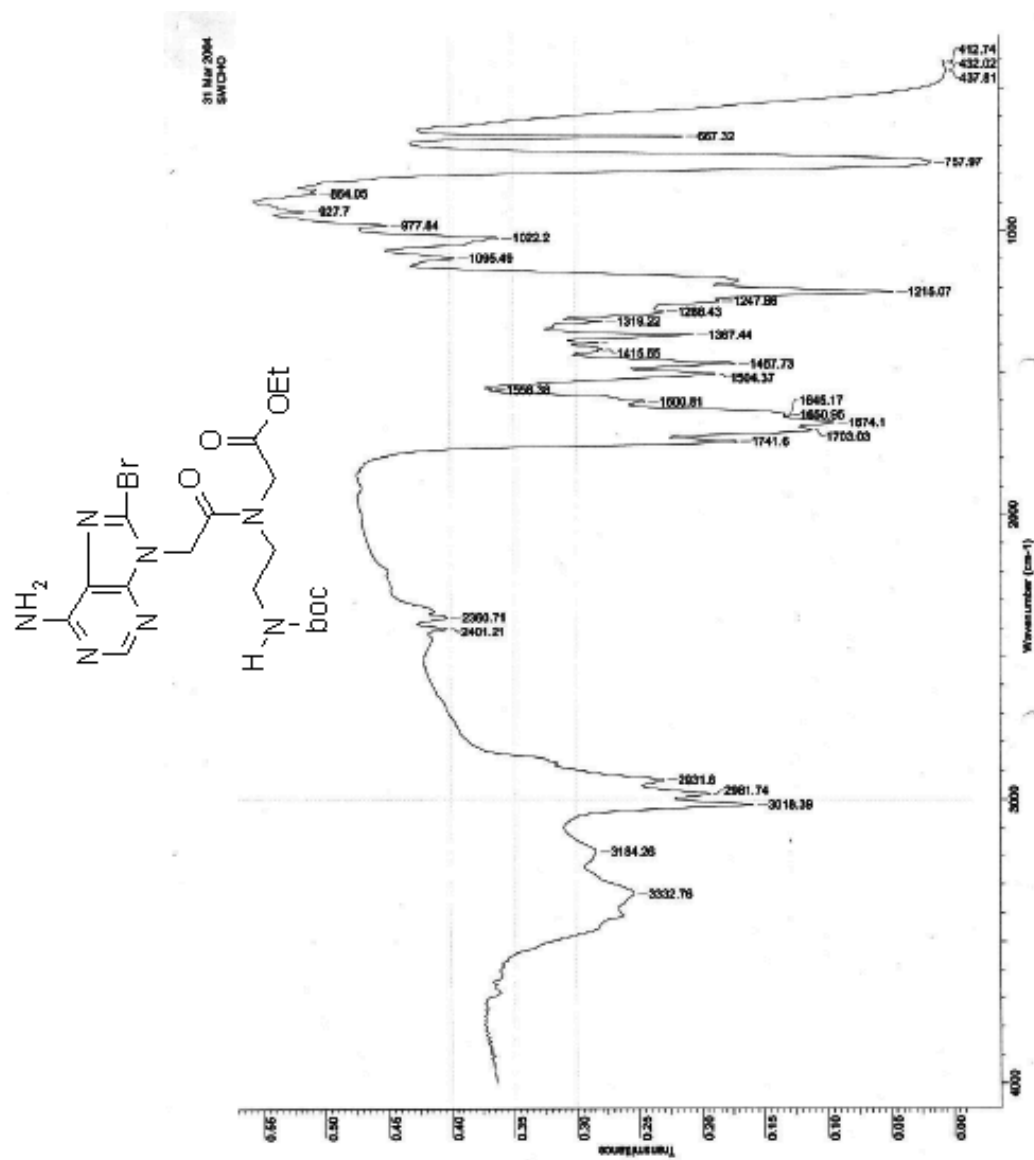
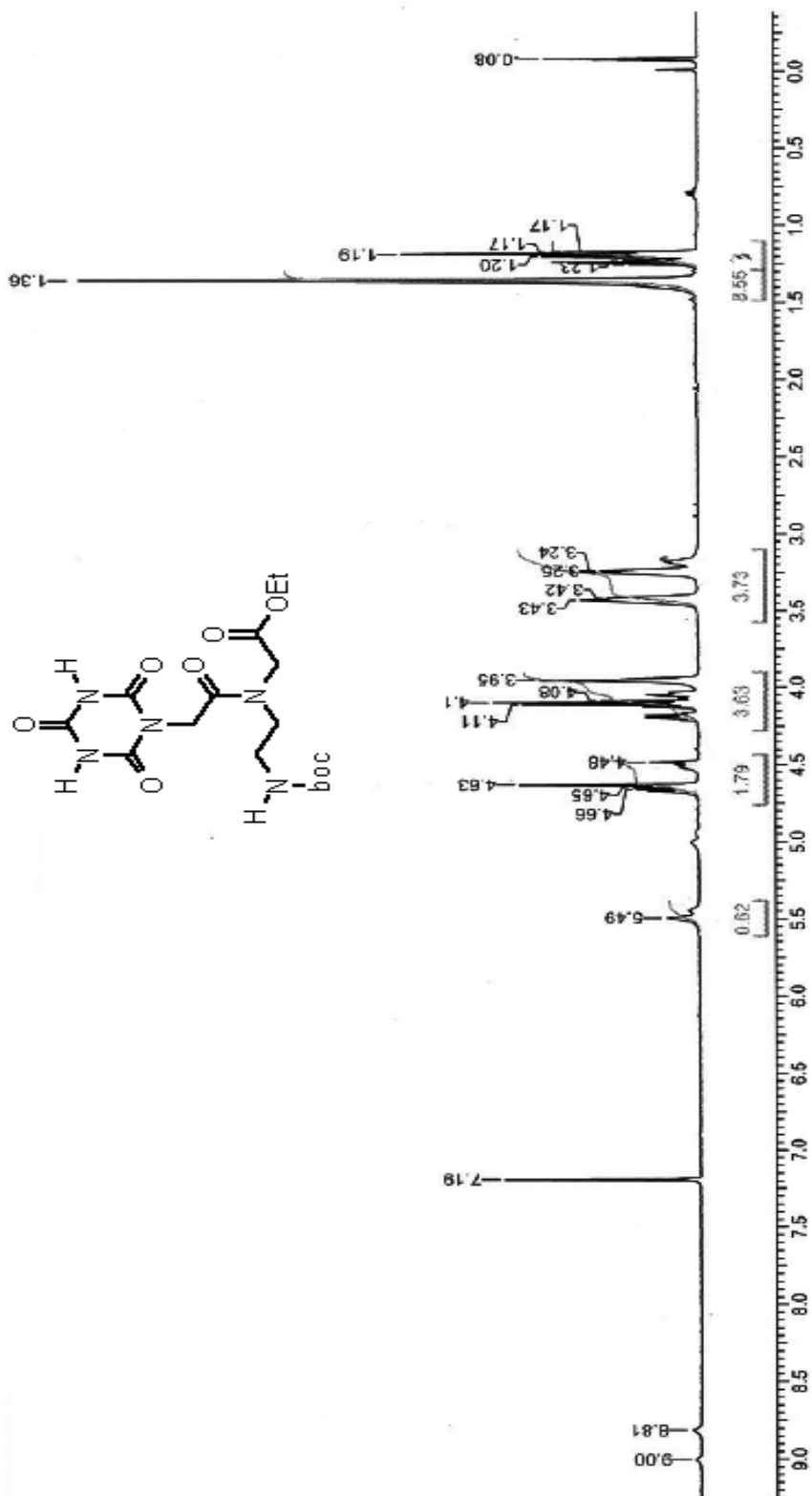
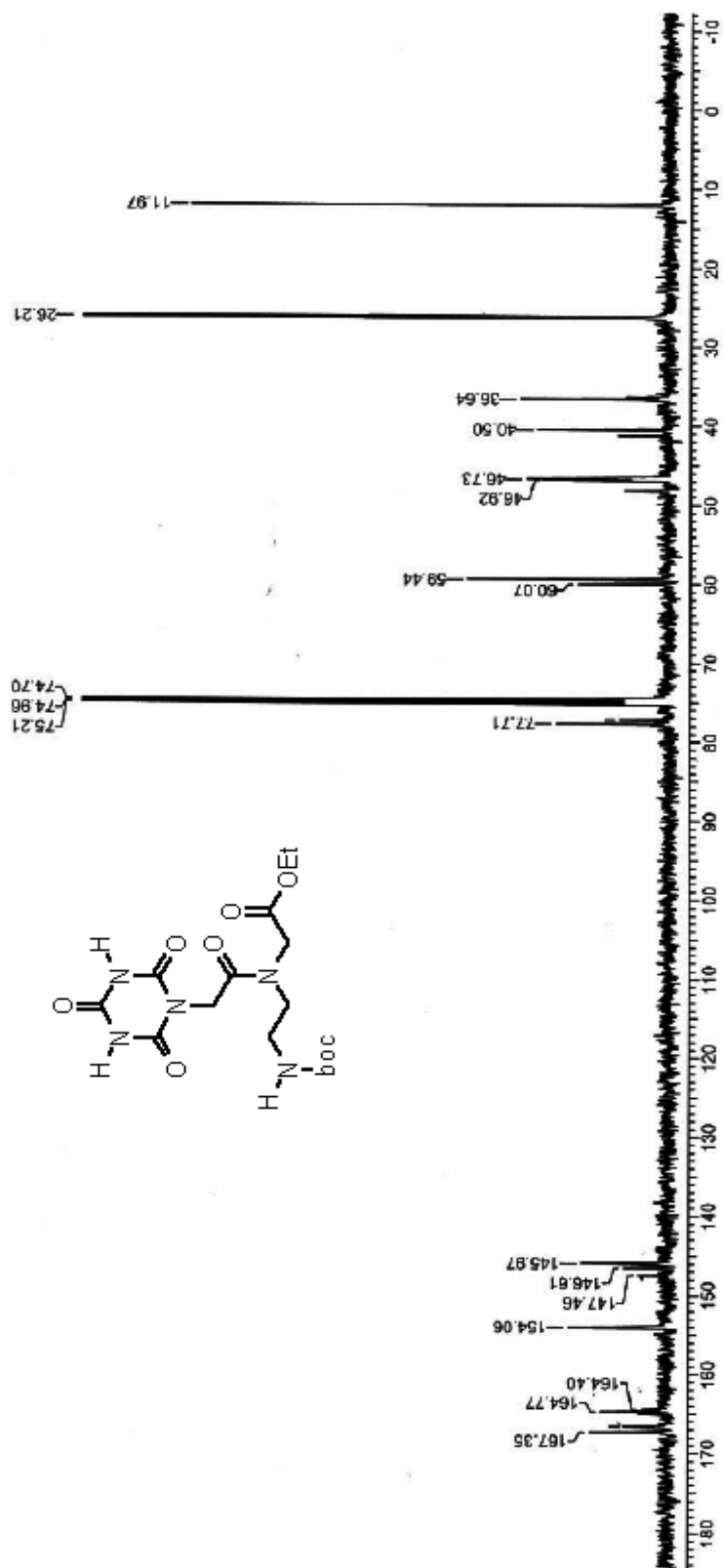


Figure 26: IR spectra of Compound 25

Figure 27: ¹H NMR of Compound 5

Figure 28: ^{13}C NMR of Compound 5

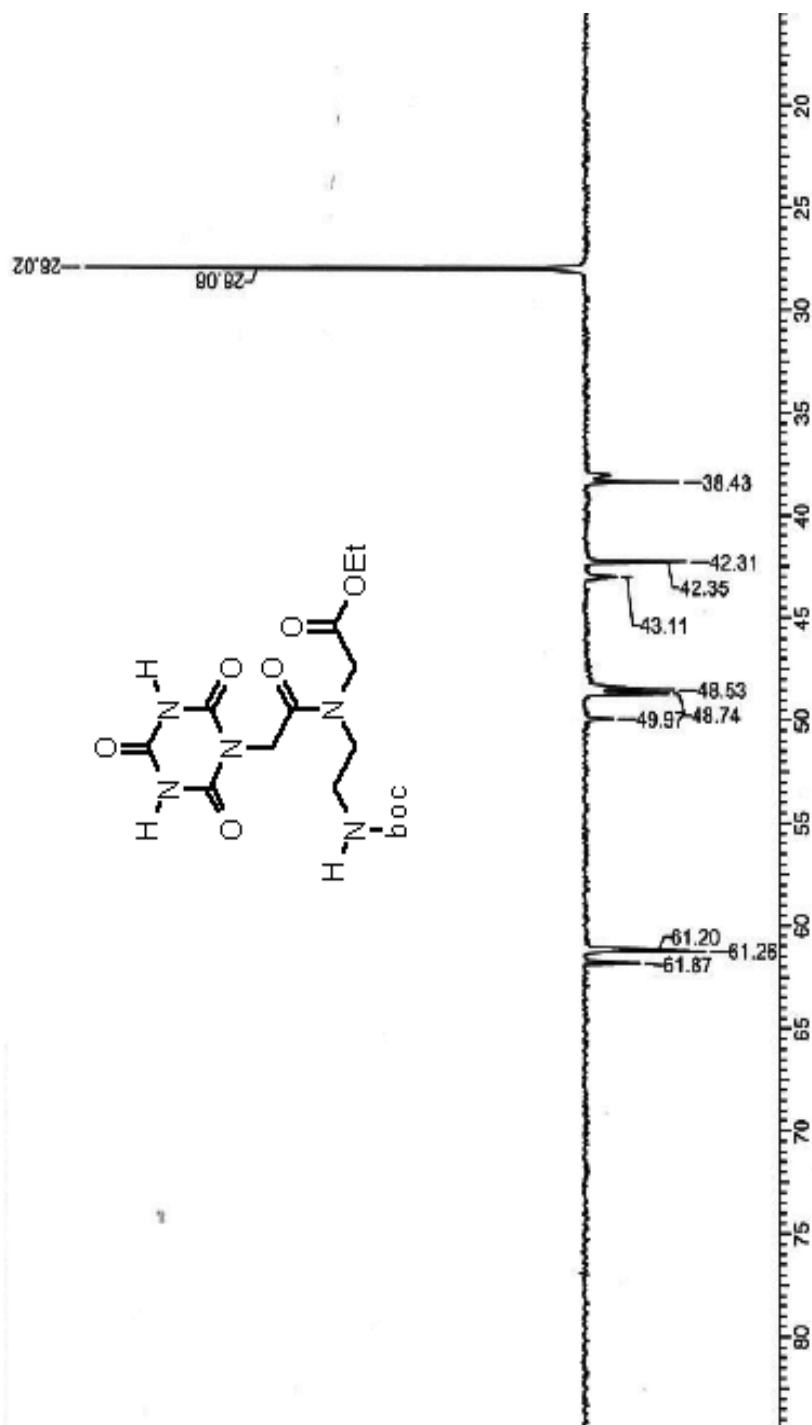


Figure 29: ^{13}C NMR (DEPT) spectra of Compound 5

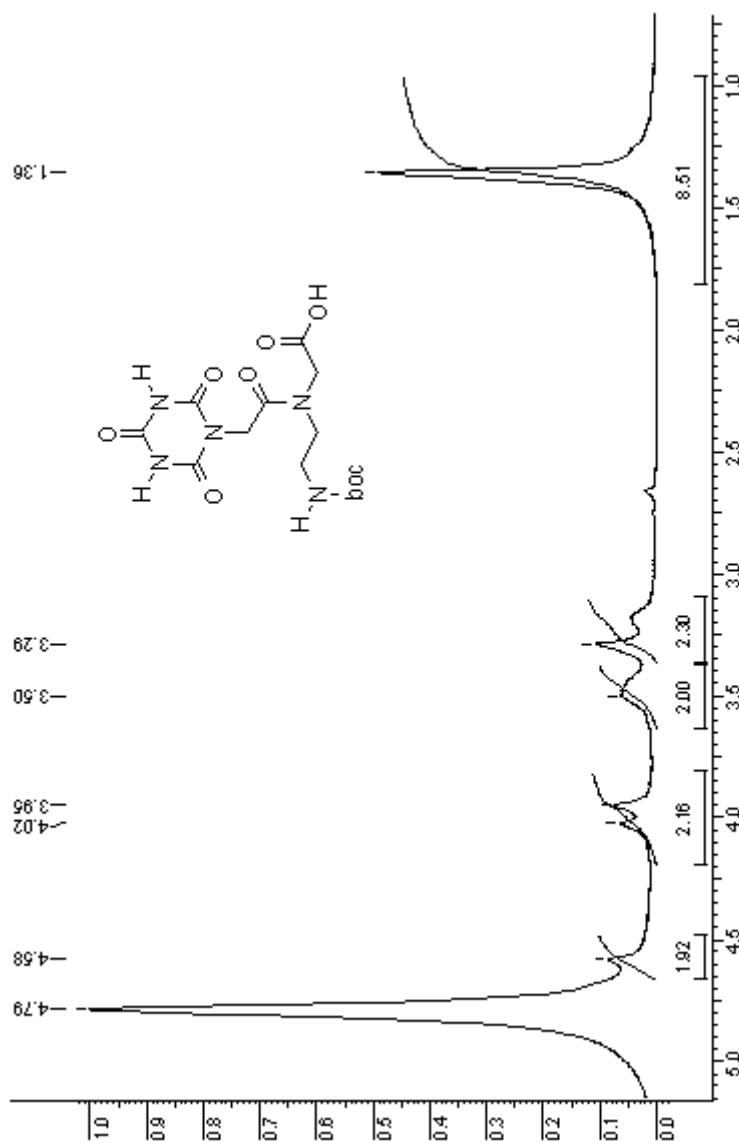
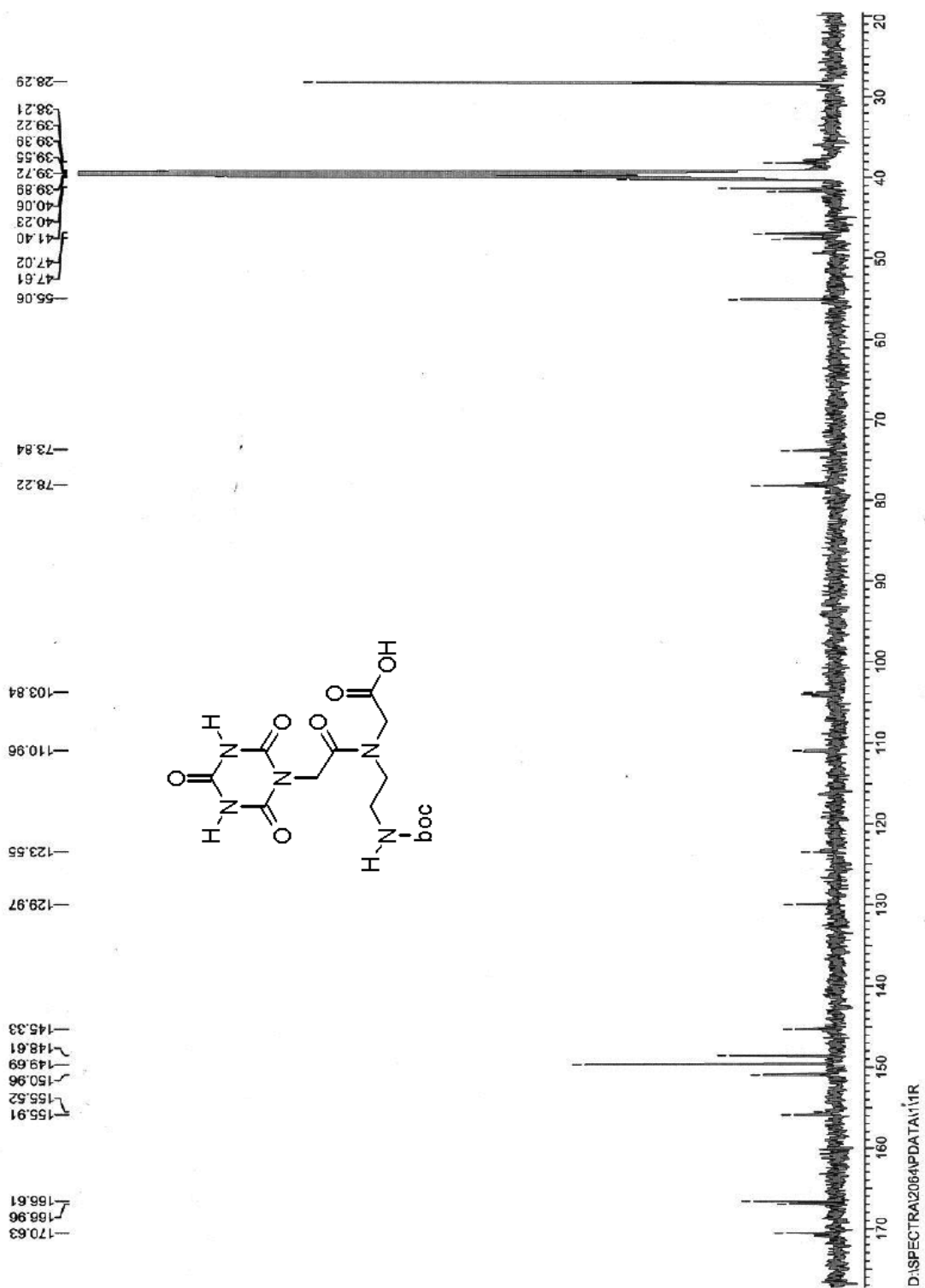


Figure 30: ¹H NMR spectra of Compound 6

Figure 31: ^{13}C NMR spectra of Compound 6

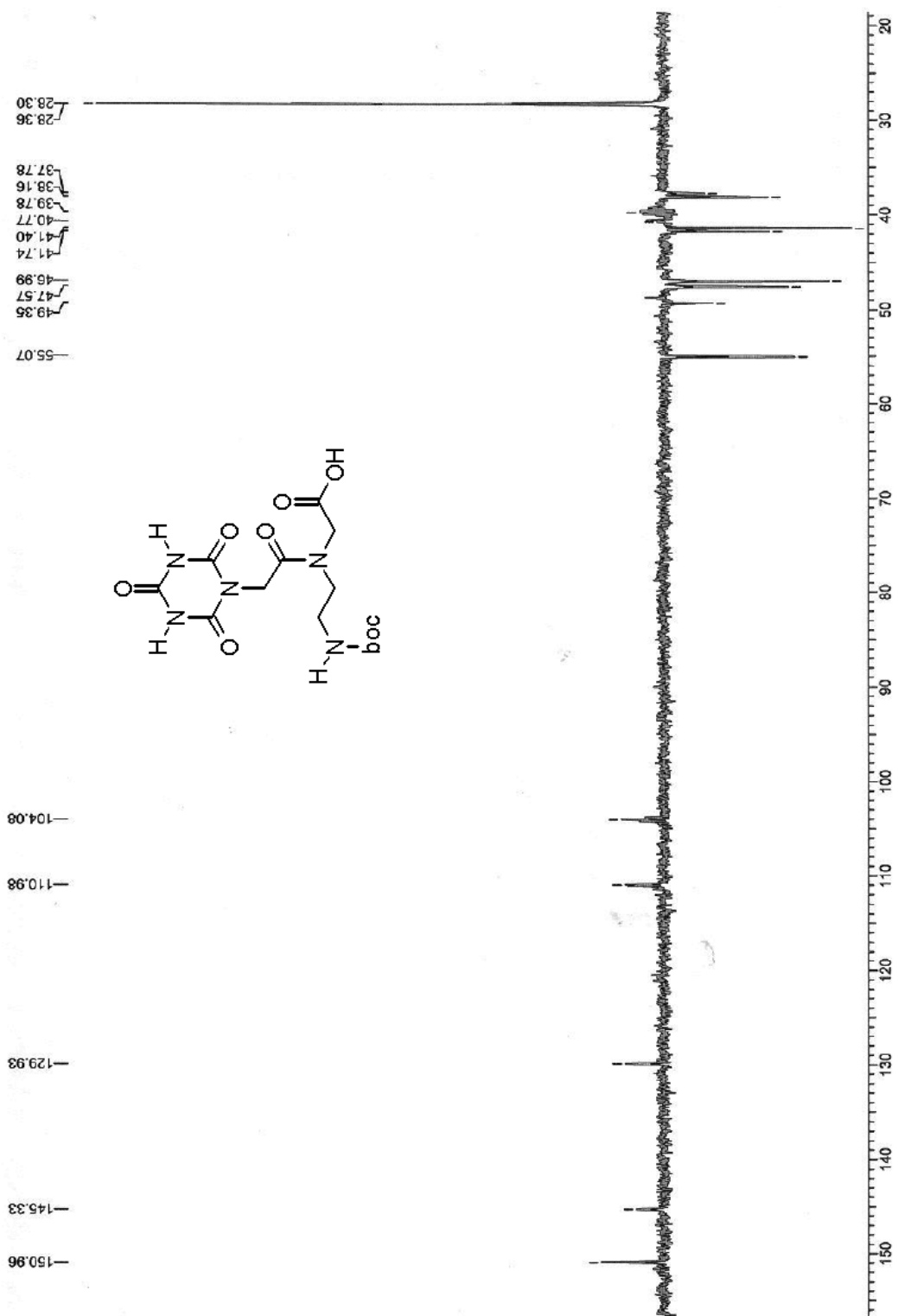
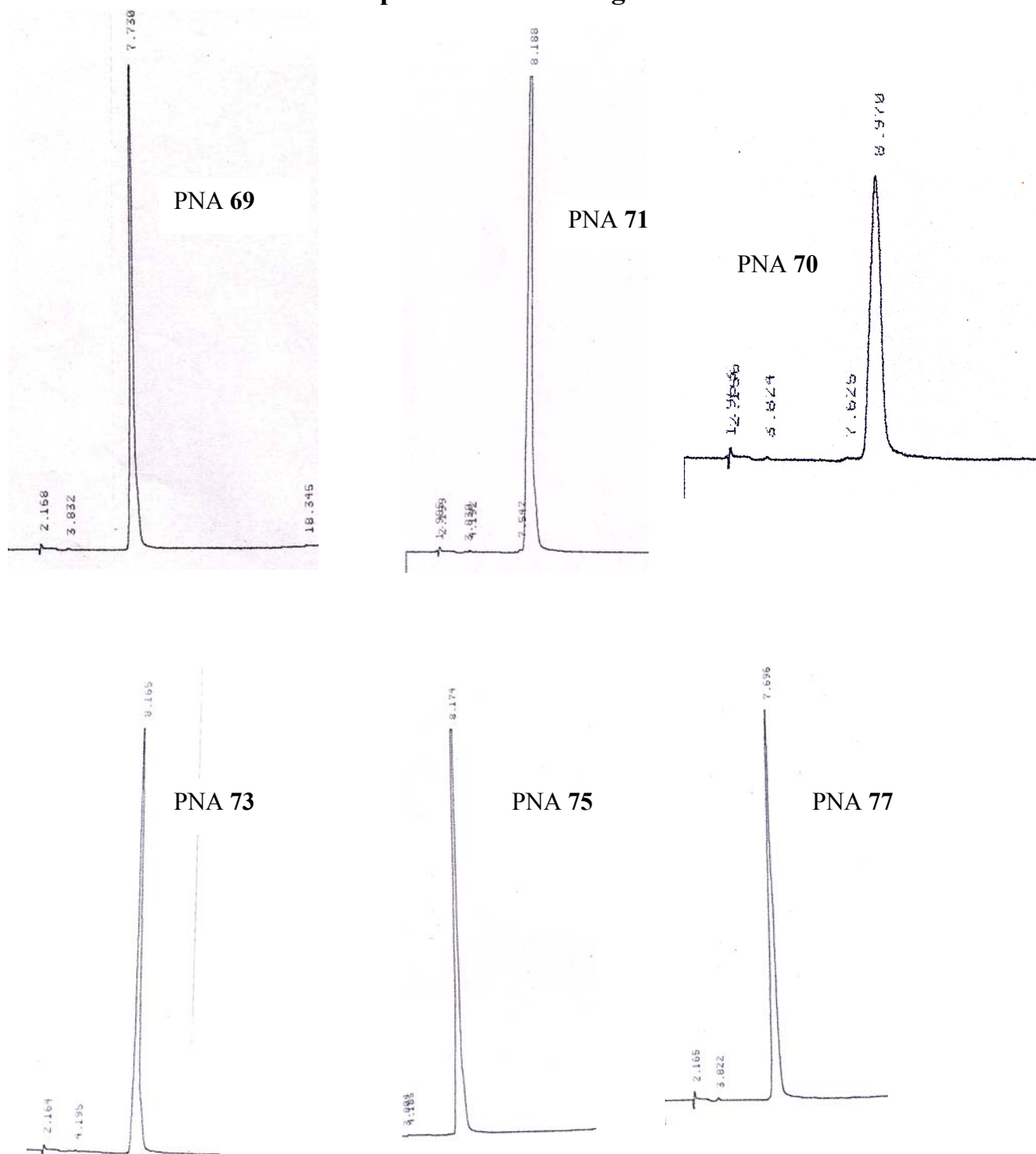


Figure 32: ^{13}C NMR (DEPT) spectra of Compound 6

HPLC profiles of PNA oligomers

**Figure 38:** HPLC profiles of PNA 69, 70, 71, 73, 75 and 77

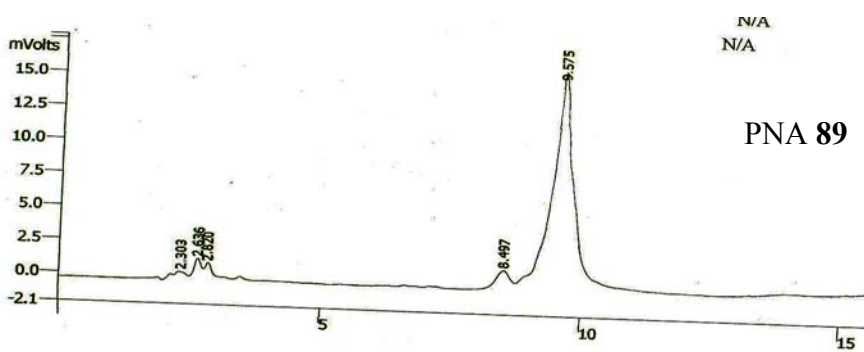
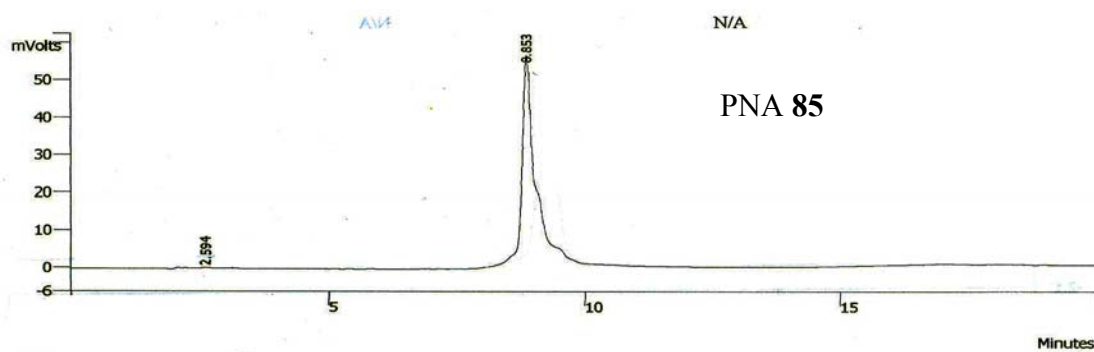
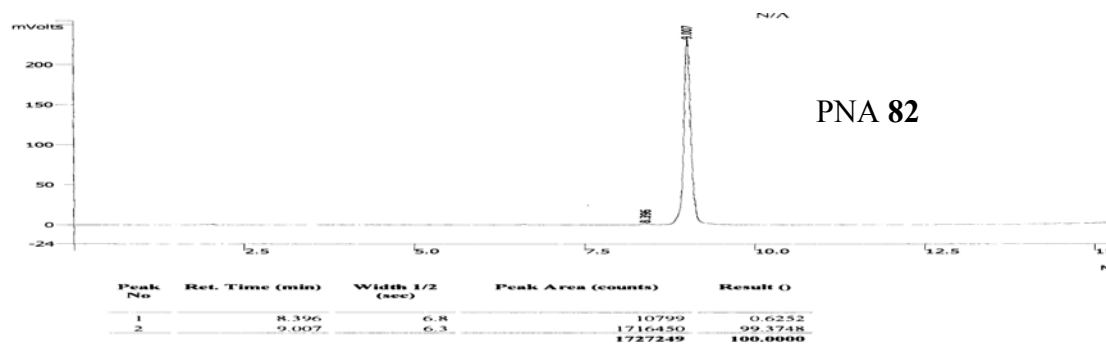
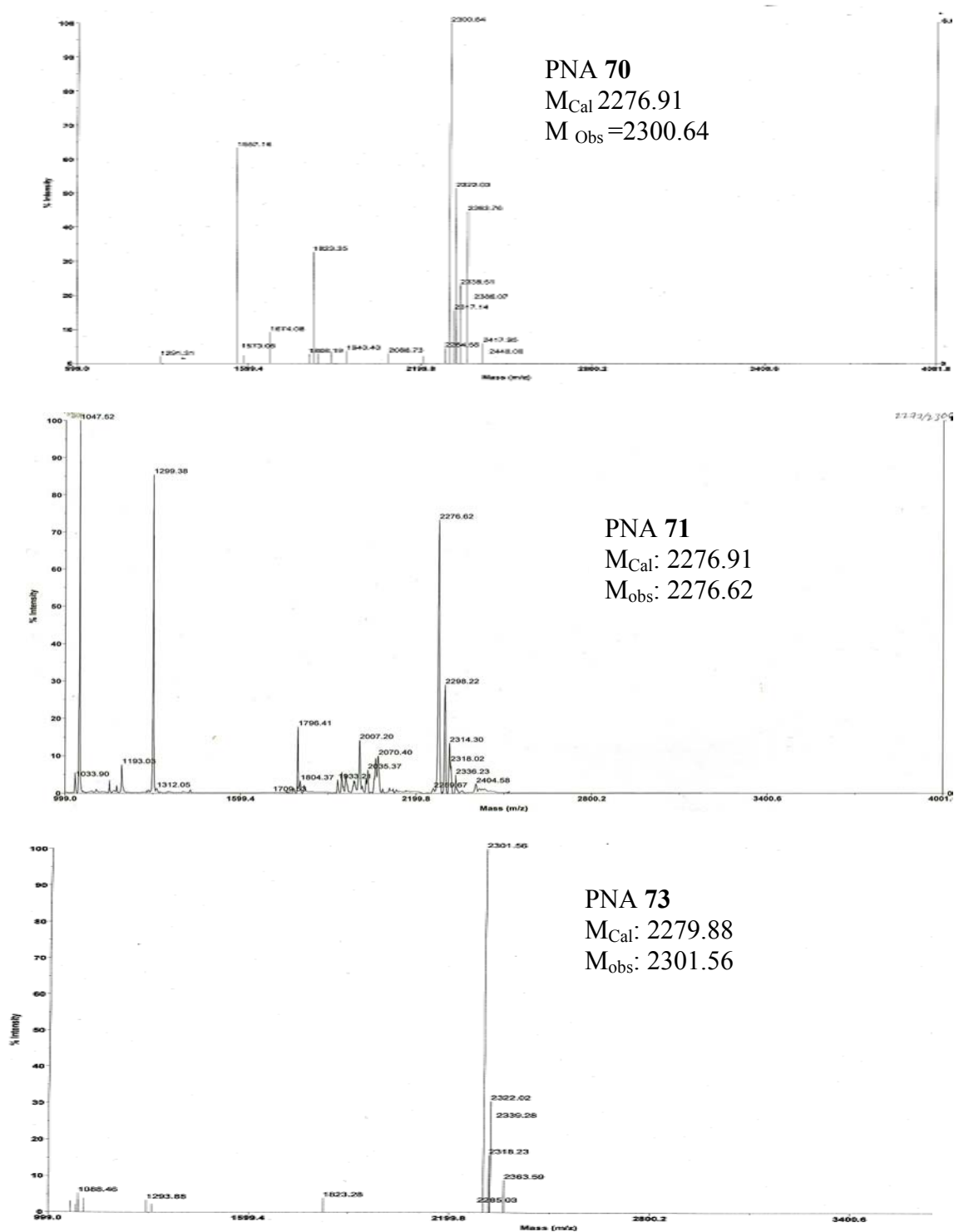


Figure 38: HPLC-Profiles of PNAs 82, 85 and 89

MALDI-TOF mass spectra of synthesized PNA oligomers**Figure 33: MALDI-TOF spectra of PNA 70, 71 and 73**

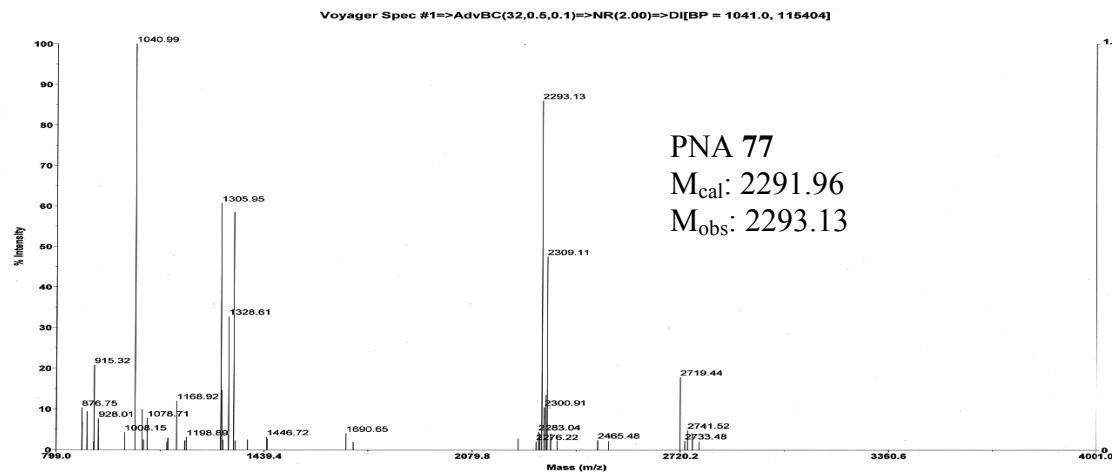
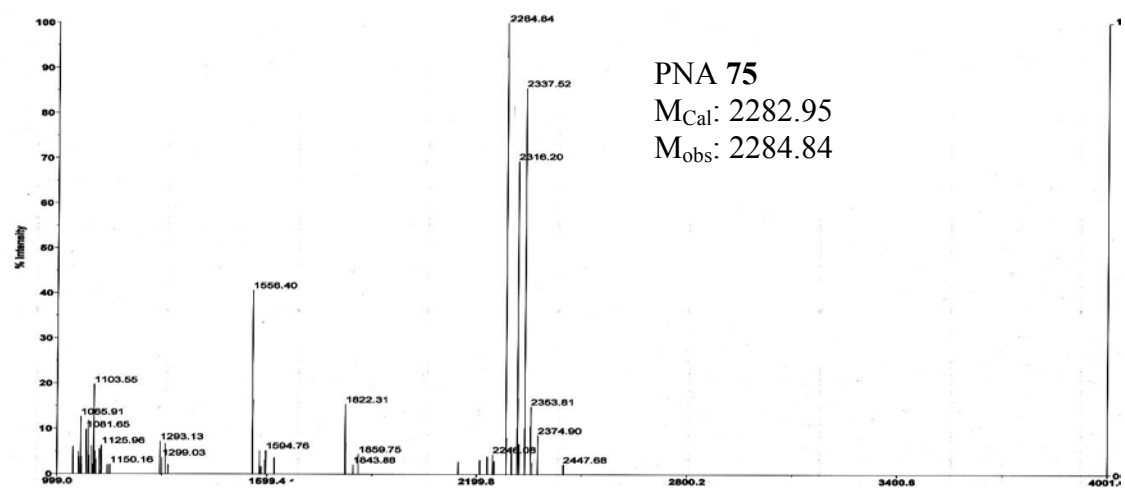
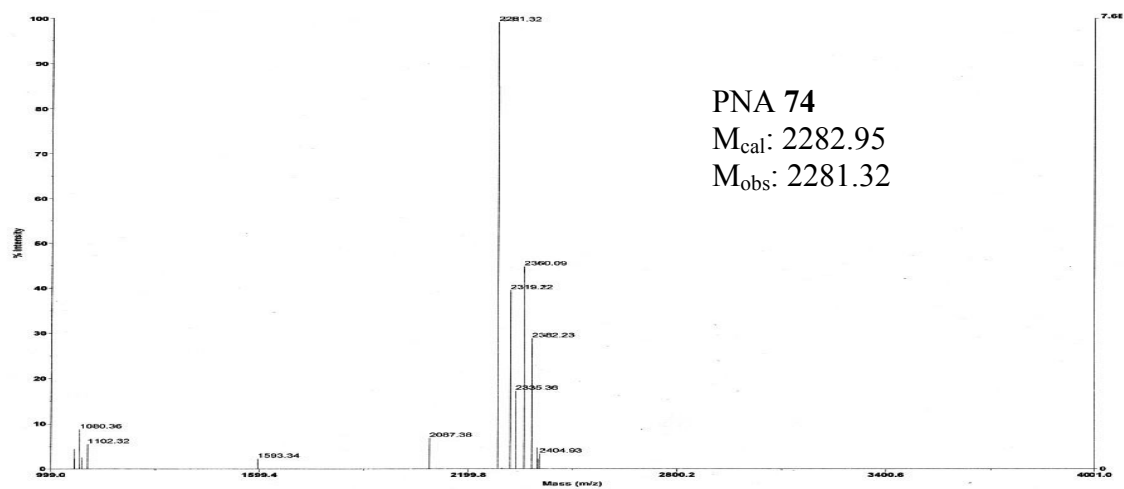


Figure 34: MALDI-TOF spectra of PNA 74, 76 and 77

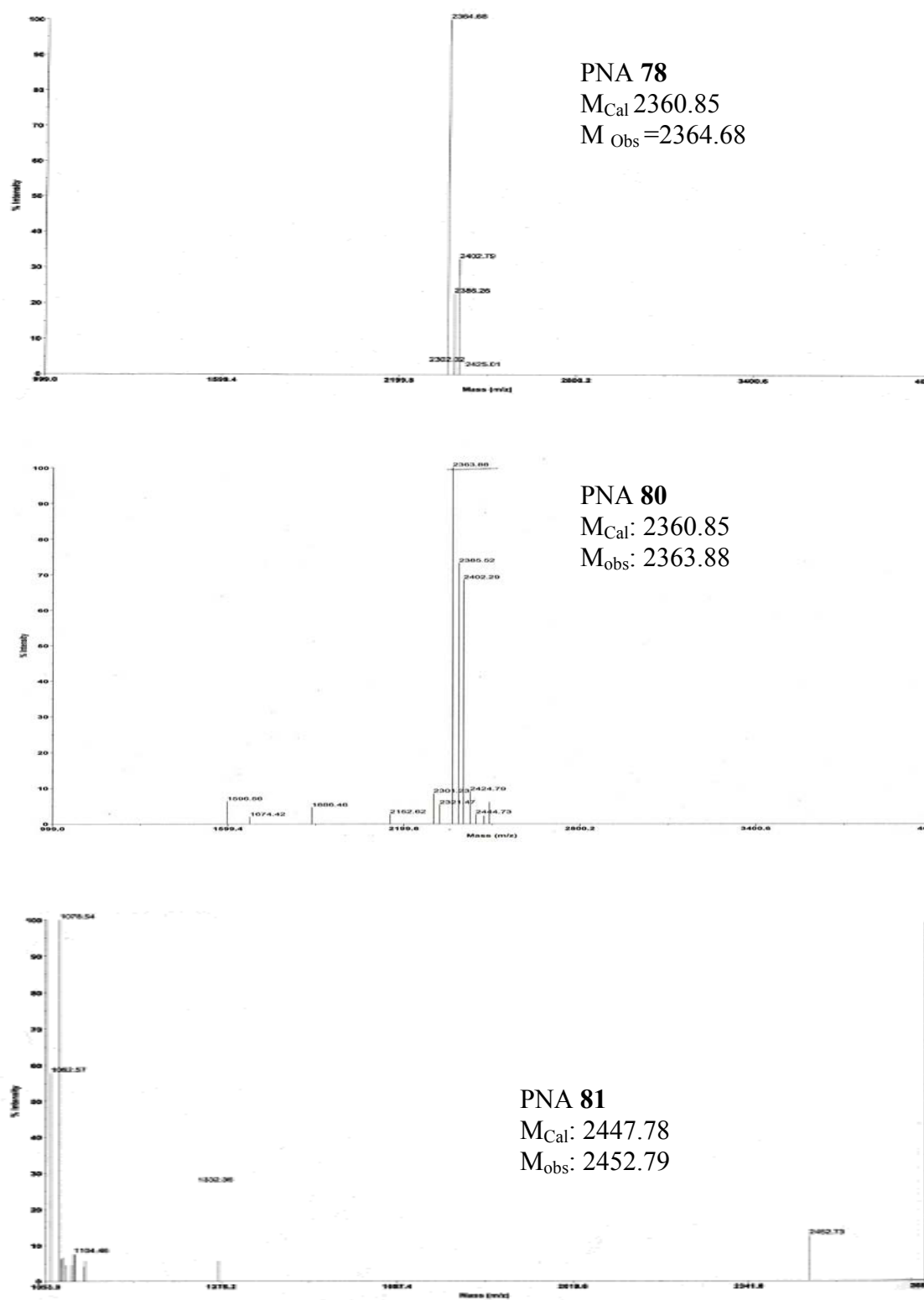


Figure 35: MALDI-TOF spectra of PNA 78, 80 and 81

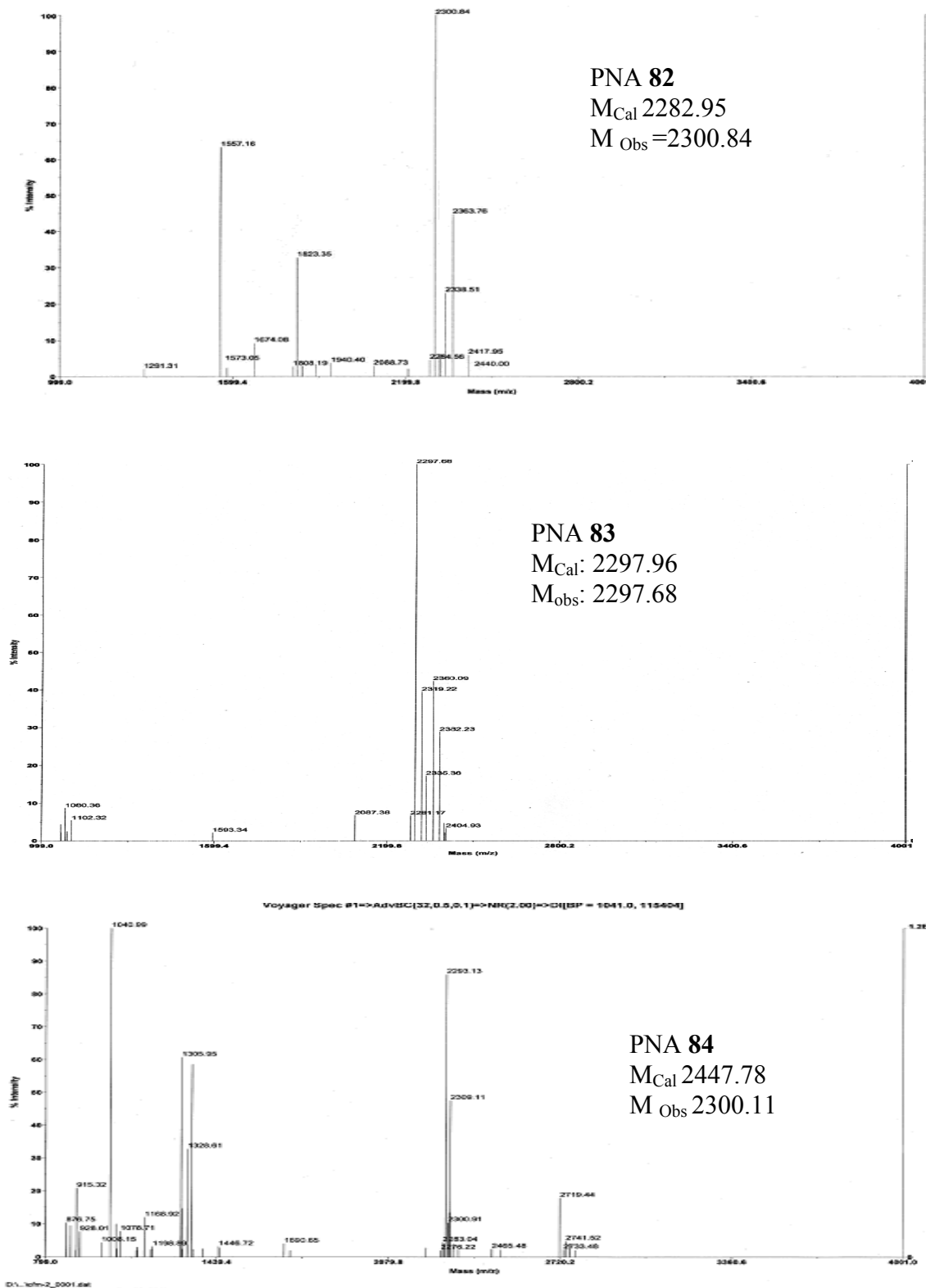


Figure 36: MALDI-TOF spectra of PNA 82, 83 and 84

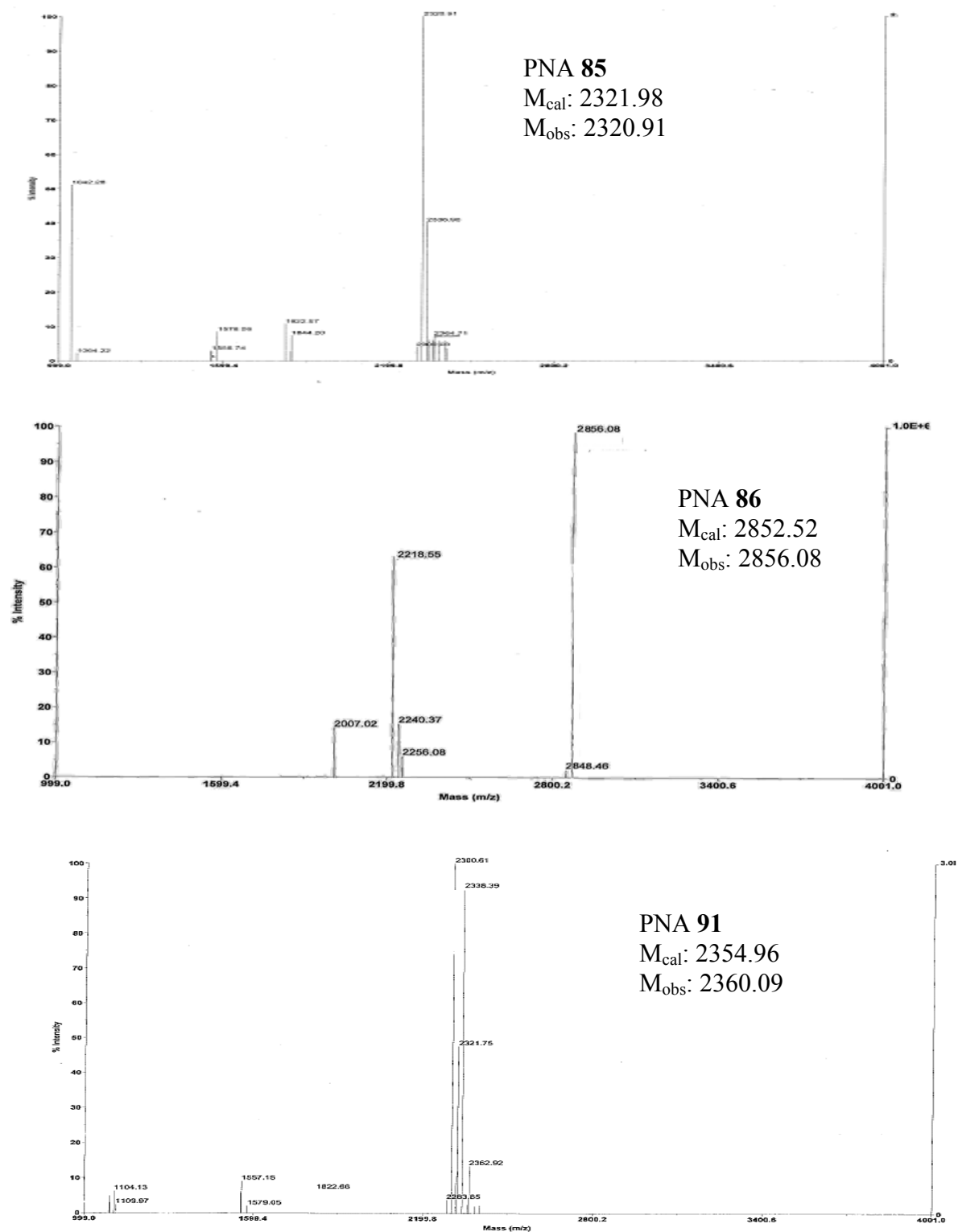
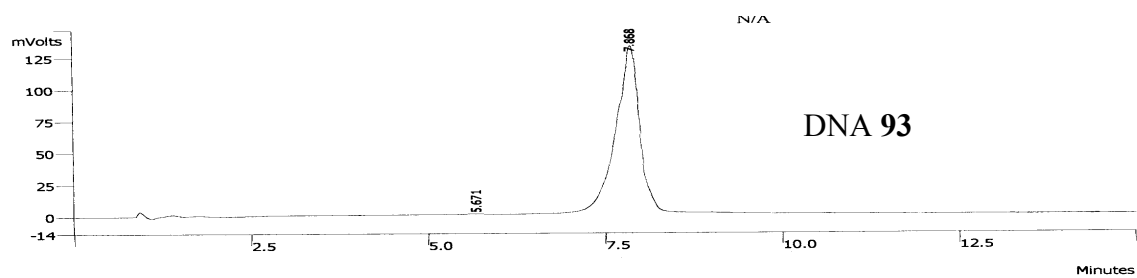
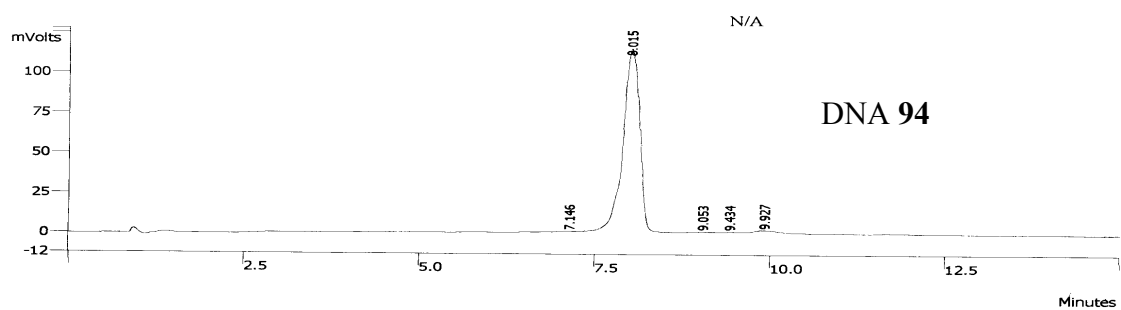


Figure 37: MALDI-TOF spectra of PNA 85, 86 and 91

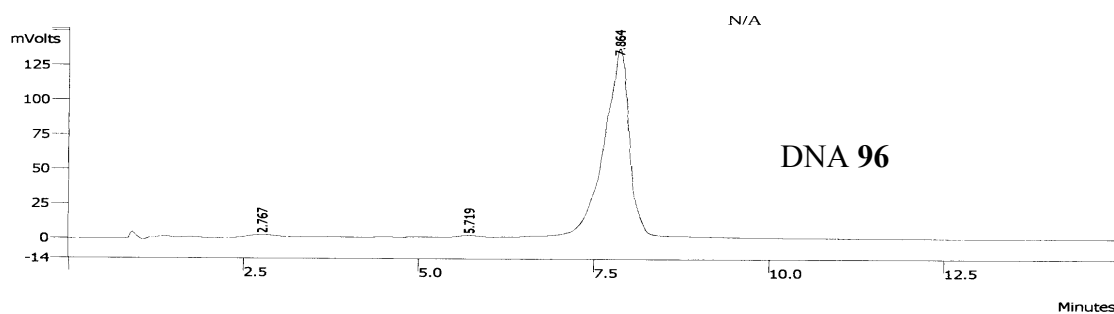
HPLC profiles of DNA oligomers



Peak No	Ret. Time (min)	Width 1/2 (sec)	Peak Area (counts)	Result (%)
1	5.671	20.3	12422	0.3752
2	7.868	20.9	3298753	99.6248
			3311175	100.0000



Peak No	Ret. Time (min)	Width 1/2 (sec)	Peak Area (counts)	Result (%)
1	7.146	23.0	17097	0.8312
2	8.015	15.1	1975341	96.0302
3	9.053	0.0	7996	0.3887
4	9.434	0.0	8946	0.4349
5	9.927	0.0	47619	2.3150
			2056999	100.0000



Peak No	Ret. Time (min)	Width 1/2 (sec)	Peak Area (counts)	Result (%)
1	2.767	10.6	11359	0.3238
2	5.719	19.0	22085	0.6295
3	7.864	21.9	3475116	99.0468
			3508560	100.0001

Figure 39: HPLC profiles of DNA 93, 94 and 96

CHAPTER 3

Biophysical Studies of Cyanuryl PNA and 8-Substituted Adeninyl PNA

3.1 Introduction to Biophysical techniques

Biophysics is an interdisciplinary field in which the techniques from the physical sciences are applied to understand the biological structure and function. The biophysical techniques are useful in studying structure and properties of nucleic acids, proteins, peptides and their analogues.

In this chapter, the binding selectivity and specificity of modified nucleobase containing PNAs towards complementary DNA has been investigated using the biophysical techniques CD and temperature dependent UV-spectroscopy. The stoichiometry of the PNA:DNA complexes was determined using Job's method. The UV-melting studies were carried out with all modified PNA:DNA complexes and analyzed with respect to that of control PNA:DNA complexes. These give information on the stability of the complexes of modified PNAs with DNA.

The following sections review the applications of biophysical techniques.

3.1.1 Circular Dichroism Spectroscopy (CD spectroscopy):

CD spectroscopy belongs to a class of absorption spectroscopy that can provide information on the structures of many types of chiral biological macromolecules that possess UV-Vis absorbing chromophores. Circular dichroism is the difference between the absorption of left and right handed circularly-polarized light and is measured as a function of wavelength. The absence of chirality in a regular structure results in zero CD intensity, while an ordered chiral structure results in a spectrum which contains either positive or negative signals.

Although detailed structural information at atomic level as obtained from, X-ray crystallography or NMR spectroscopy is not available from CD spectra, it can provide a reliable determination of the overall conformational state of biopolymers and structural changes induced by modification when compared with the CD spectra of reference samples. In case of nucleic acids, the sugar units of the backbone possess chirality and the bases attached to sugars are the chromophores. CD spectroscopy has utility in recognizing DNA/RNA/PNA triplexes and duplexes, and complexes formed between protein-DNA¹.

3. 1.2 CD spectroscopy of PNA:DNA triplexes

CD spectroscopy is a useful technique to monitor the structural changes of nucleic acids in solutions and for diagnosing whether new or unusual structures are formed by particular polynucleotide sequences. PNA is non-chiral and shows weak CD signature. CD is predominantly an effect of coupling between the transition moments of the nucleobases as a result of their helical stacking. The reliance on CD spectroscopy to study nucleic acid conformations has stemmed from the sensitivity and the ease of CD measurements, the non-destructive nature and the fact that conformations can be studied in solution.

In the CD spectrum of DNA, deep intensive negative band is observed between 200-210nm, a high intensive positive band in the region 210nm-240nm, a low intensity negative band between 240-260nm and a moderately intensive positive band in the region 260-300nm (Figure 1A).

PNA being achiral, shows insignificant CD signature. However being a polyamide, it can form left or right handed coil structures with equal facility. Due to these type of structures, very low intense negative signature band between 205-240nm is seen due to amide bonds present in PNA oligomer and no absorptions of consequence were seen in between 240-300nm range (Figure 1A).

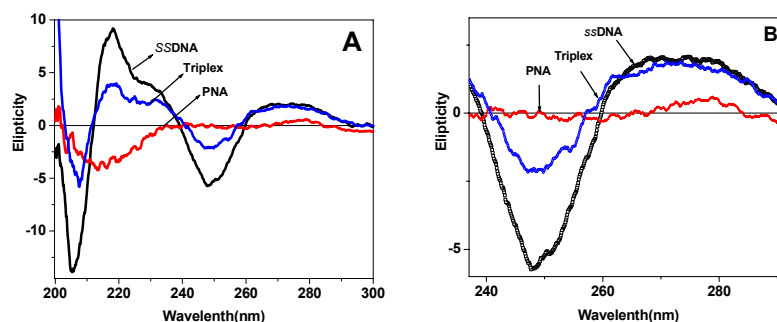


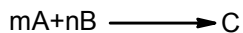
Figure 1: The graph A) CD signatures of ssDNA, PNA and triplex B) the characteristic CD signature of triplex

Even though PNA shows low profile CD signals in spite of its achiral nature, PNA:DNA complexes exhibit characteristic CD signature since, PNA adopts helicity when it binds to DNA and forms the chiral PNA-DNA complex (Figure 1A). In case of PNA₂:DNA triplex, the CD pattern is observed with a negative band between 205-210nm, followed by high intensity positive band in the region 210nm-240nm, low intense negative band between 240-255nm and a positive band in 260-300nm range. The PNA₂:DNA triplex shows characteristic band between 260nm-285nm (Figure 1B). The ellipticity of triplex in PNA₂:DNA triplex in the region of 255-265 nm was more than both single stranded DNA and PNA.

3.1. Binding Stoichiometry of PNA:DNA complexes:

Binding stoichiometry is a quantitative relationship between the numbers of reactant molecules to form products complex in an association reaction (Scheme 1).

Scheme 1



The stoichiometry of A and B in C is m:n

Binding stoichiometry can be determined by the method of “Continuous Variation” also called Job's Method. To implement this method experimentally, a series of solutions (reaction mixtures) were prepared with gradual change in the mole fractions of each component, keeping the total volume and concentration of each solution constant. The amount of complex obtained in each solution is calculated experimentally from the observable spectral parameters. The break in the plot between amounts of product formed in each solution (reaction) versus mole fraction of the variable component gives the binding stoichiometry.

The complementary strands of PNA/DNA are mixed to form duplexes/triplexes. These in principle give rise to PNA:DNA (1:1) or PNA:DNA (1:2) complexes depending on the sequence, conditions in the medium and the binding ability of the two interacting oligomers.

The stoichiometry of PNA:DNA complexes may be determined either by CD-JOB's plot² and UV-mixing curves. Keeping the total concentration constant, a series of mixtures having different relative molar equivalent amounts of PNA and DNA were generated (0:100, 10:90, 20:80, 30:70, 40:60, 50:50, 60:40, 70:30, 80:20, 90:10 and 100:0) and CD is recorded individually for all these mixtures, the CD plots of different molar ratios show an isodichroic point around 255 nm. The ellipticity values of all the

mixtures at 258 or 260nm are plotted against mole fraction of PNA (Figure 2A).^{3,4} The ellipticity of PNA readily increases, reaches a maximum and then decreases. The maxima at the intersection give the binding stoichiometry (Figure 2A).

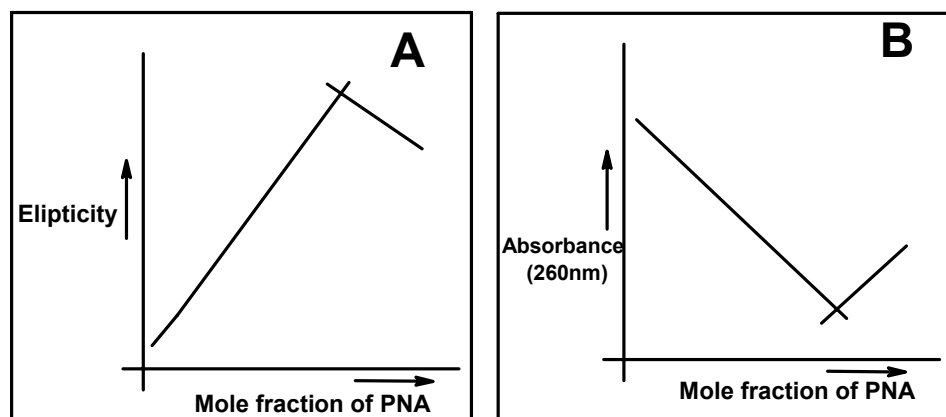


Figure 2: Schematic representation of A) CD job's plot, B)UV-mixing curves (UV job's plot)

3.1.4 Binding stoichiometry through UV-mixing curves (Job's plot)

The UV mixing experiments are carried out similarly by mixing the appropriate oligomers in different molar ratios keeping the total concentration constant. The stoichiometry of paired strands may be obtained from the mixing curves, in which the absorbance at a given wavelength is plotted against the mole fraction of each strand, to yield Job's plot (Figure 2B).⁴

In a UV-mixing curve experiment, the net absorbance at 260nm steadily decreases as PNA concentration increased until all the strands present are in complex formation due to the hypochromic effect. The absorbance then risen upon addition of excess *ss*PNA. The stoichiometry of complexation corresponds to minima in the plot of absorbance Vs to mole fraction (Figure 2B).

3. 1.5 UV-Spectroscopic study of PNA:DNA complexes

Monitoring the UV absorption at 260 nm as a function of temperature has been extensively used to study the thermal stability of nucleic acid complexes and consequently, PNA:DNA/RNA hybrids was investigated by this technique. Increasing the temperature dissociates the complexes, inducing dissociation into individual components by disruption of hydrogen bonds between the base pairs. This results in decrease of stacking between adjacent nucleobases leading to a loss of secondary and tertiary structure. This is evidenced by an increase in the UV absorption at 260 nm with temperature rise, termed as hyperchromicity. A plot of absorbance *versus* temperature gives a sigmoidal curve in case of duplexes/triplexes and mid point of transition gives the T_m (Figure 3A). In case of DNA triplexes, double transition sigmoidal curve is seen, the first transition corresponding to triplex melting to the duplex (Watson–Crick duplex), whereas the second transition is due to duplex dissociation into two single strands.⁵ In case of PNA:DNA complexes, the PNA₂:DNA triplexes show single sigmoidal curve since the temperature difference between two transition states is too low to distinguish them independently.⁶ The melting temperature T_m can be obtained from the maxima of the first derivative plots (Figure 3B). This technique has provided valuable information regarding complementary interactions in nucleic acid hybrids involving DNA, RNA and PNA.

The fidelity of base-pairing in PNA:DNA complexes can be examined by challenging the PNA oligomer with a DNA strand bearing mismatches. Even a single the base mismatch leads to incorrect hydrogen bonding between the bases causing a drop in the melting temperature. A modification of the PNA structure is considered good if it

gives a much lower T_m with DNA sequences containing mismatches as compared to complexes of unmodified PNA.

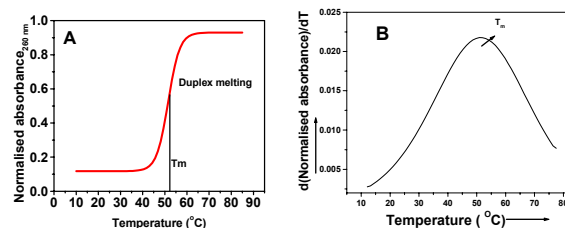


Figure 3: Schematic representation of UV melting, A) Sigmoidal curve, B) Its corresponding first derivative curve.

RESULTS AND DISCUSSION

3.2 Biophysical studies of cyanuril PNA

3.2.1 Establishment of binding stoichiometry of cyanuril PNA with cDNA

The CD signature of 2:1 complex of cyanuril PNA **71** with DNA **92** showed characteristic band with region 255-285nm expected for triplex. Various stoichiometric mixtures of *cya*-PNA **71** and DNA **92** were made by changing the relative molar ratios of *cya*-PNA **71**:DNA **92** as follows: 0:100, 20:80, 40:60, 50:50, 60:40, 70:30, 80:20, 90:10, 100:0, keeping the same total strand concentration 2 μ M in each case. The solutions were made in sodium phosphate buffer (10 mM, pH 7.3), NaCl (100 mM). The ellipticity values at wavelength corresponds to 250-260nm used to compute the isodichoric point confirmed stoichiometry of PNA:DNA complex as 2:1 triplex (Figure 4B).

The UV absorbance was recorded for all the samples individually at room temperature. The absorbance at 260nm decreased from 0.15 to 0.07 then raised and reached to 0.12. The mole ratio at the minima of the curve confirmed the binding stoichiometry of PNA:DNA complex be 2:1 as necessary for triplex formation (Figure 4C).

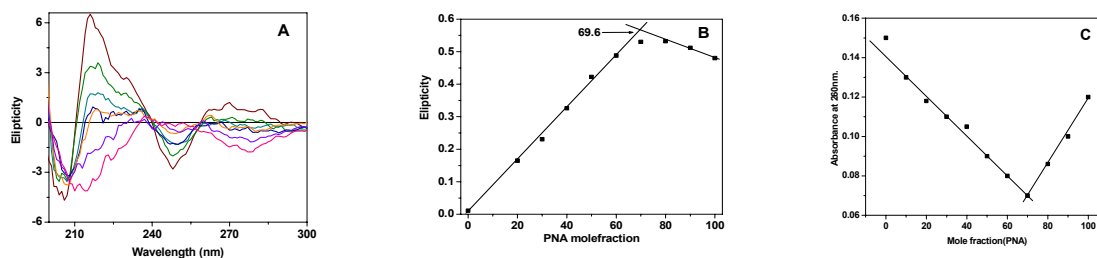


Figure 4: A) CD-curves for PNA **71**, H-TTTTTTTCya-Lys-NH₂ and DNA **92** d(CGCA₁₀CGC) mixtures in the molar ratios of 0:100, 20:80, 30:70, 40:60, 50:50, 60:40, 70:30, 80:20, 90:10, 100:0 (Buffer, 10 mM Sodium phosphate pH 7.2, 100 mM NaCl, 0.1 mM EDTA), B) CD-Job's plot corresponding to 255 nm, C) UV-Job's plot corresponding to above mixtures of different molar ratios, absorbance recorded at 260 nm.

3.2.2 UV-Melting studies of cyanuryl PNA₂:DNA complexes

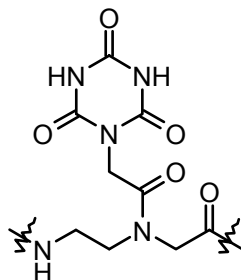


Figure 5: Structure of cyanuryl PNA

Hybridization studies of modified PNAs with complementary DNA sequences were done by temperature dependent UV-absorbance experiments. The stoichiometry for *cyanuryl* PNA:DNA complexation was established by UV absorbance mixing data at 260 nm (Job' plot) as 2:1 ratio (Figure 4). The thermal stabilities (T_m) of PNA₂:DNA triplexes were obtained for different PNA modifications with both complementary DNA (DNA **92**) (Figure 6, Table 1) and DNA having a single mismatch (DNA **96**) (Figure 7, Table 2).

3.2.3 UV-Melting studies of cyanuryl PNA complexes with complementary DNA

Table 1 shows the T_m values for PNA₂:DNA complexes derived from various *cyanuryl* PNA (*cya* PNA) sequences of different degree or position of modifications. The first derivative plots of normalized absorbance with respect to change in temperature

(dA/dT), for PNA₂:DNA triplexes indicated a single transition (Figure 6), characteristic of both PNA strands dissociating simultaneously from DNA in a single step.

The control PNA₂:DNA triplex derived from unmodified *aeg*PNA-T₈ (PNA **69**) had a T_m of 44.6 °C (entry 1, Table 1), which was increased by 23.3 °C when *cya*PNA unit was incorporated at C-terminus PNA **71** (entry 3, Table 1). However, when the *cya*PNA unit was substituted at N-terminus (PNA **70**), the PNA₂:DNA triplex was destabilized by 10.4 °C (entry 2, Table 1). Interestingly, the substitution of *cya*PNA unit in the middle of the sequence (PNA **72**) stabilized the triplex by 12.1 °C (entry 4, Table 1). PNA **73** (entry 5, Table 1) with two simultaneous modifications at N-terminus and middle, formed a triplex with stability as good as that from unmodified PNA **69**, without much further stabilization. The stabilization by the center modification seems to negate the destabilization effects of N-terminus modification. All the above experiments were conducted with complementary DNA (DNA **92**).

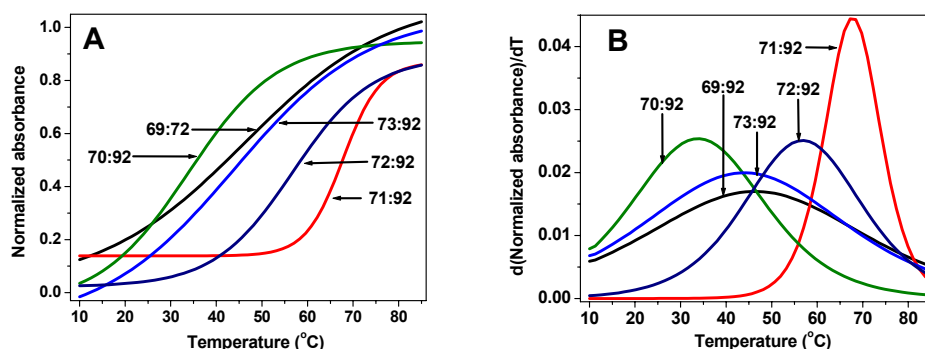


Figure 6. A) UV-Melting profiles of *cy*PNA₂:DNA complexes. B) UV-Melting First derivative curves of PNA₂:DNA complexes (*aeg* PNA **69**, *cya*PNA **70**, **71**, **72** and **73** with DNA **92**), (Buffer, 10 mM Sodium phosphate pH = 7.3, 100 mM NaCl).

Table 1: UV-Melting temperatures (T_m values in °C)^a of *cy*PNA₂:DNA triplexes

Entry No	Triplex (PNA ₂ :DNA)	T_m (°C) PNA ₂ :c DNA triplex	ΔT_m (°C)	ΔT_m (°C)/ modification
1	PNA 69 , H ₂ N-Lys-TTTTTTTT- H DNA 92 5'CG-AAAAAAAAA-GC3' PNA 69 H-TTTTTTTT-Lys-NH ₂	44.6	--	--
2	PNA 70 , H ₂ N-Lys-TTTTTTTT Cya - H DNA 92 5'CG-AAAAAAAAA-GC3' PNA 70 , H- Cya TTTTTTT-Lys-NH ₂	34.2	-10.4	-5.2
3	PNA 71 , H ₂ N-Lys- Cya TTTTTTT- H DNA 92 5'CG-AAAAAAAAA-GC3' PNA 71 , H-TTTTTTTT Cya -Lys-NH ₂	67.8	+23.2	+11.6
4	PNA 72 , H ₂ N-Lys-TTT Cya TTTT- H DNA 92 5'CG-AAAAAAAAA-GC3' PNA 72 , H-TTTT Cya TTT-Lys-NH ₂	56.7	+12.1	+6.0
5	PNA 73 , H ₂ N-Lys-TTT Cya TTT Cya - H DNA 92 5'CG-AAAAAAAAA-GC3' PNA 73 , H- Cya TTT Cya TTT-Lys-NH ₂	44.2	-0.4	-0.2

T_m = melting temperature (measured in the buffer 10 mM sodium phosphate, 100 mM NaCl, pH = 7.3), PNA₂-DNA complexes. Values in the ΔT_m indicate the difference in T_m with the control experiment PNA 66. The values reported here are the average of 3 independent experiments and are accurate to $\pm 0.5^\circ\text{C}$

3.2.4 UV-Melting studies of cyanuryl PNA complexes with mismatch DNA

The sequence specificity of PNA hybridization was examined through studying hybridization properties of PNA with DNA having single mismatch at middle, DNA **89** (Figure 7). The PNA₂:DNA complexes comprising control sequence (PNA **69**: DNA **96**) and the C- terminus modified cyanuryl PNA (PNA **71**: DNA **96**) were individually subjected for UV-melting (Figure 8). The control sequence PNA **69** formed triplex with single mismatch sequence (DNA **96**) with T_m lower by 9.6°C (entry 2, Table 2), while C-terminus modified cyanuryl PNA **71** exhibited destabilization by 13.2°C . Cyanuryl PNA thus showed a better sequence discrimination (entry 4, Table 2). The melting profiles were exhibited in figure 8.



Figure 7: Mismatched PNA₂:DNA complex

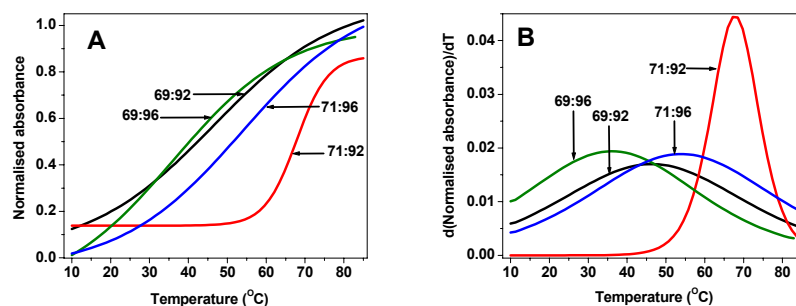


Figure 8: A) UV-Melting profiles of *cy*PNA₂:DNA complexes. B) UV-Melting First derivative curves of PNA₂:DNA complexes, PNA **66**, *cy*PNA **68** with single mismatch DNA, DNA **91**.

Table 2: UV-Melting temperatures (T_m values in °C)^a of *cy*PNA₂:DNA triplexes

Entry No.	Triplex (PNA ₂ :DNA)	T_m (°C) PNA ₂ :c DNA triplex	ΔT_m (°C)	ΔT_m (°C)/ modification
1	PNA 69 , H ₂ N-Lys-TTTTTTTT- H DNA 92 5'CG-AAAAAAAAA-GC3' PNA 69 H-TTTTTTTT-Lys-NH ₂	44.6		
2	PNA 69 , H ₂ N-Lys-TTTT T TTT- H DNA 96 5'CG-AAAACAAA-GC3' PNA 69 H-TTTTTTTT-Lys-NH ₂	34.4	-10.2	-5.1
3	PNA 71 , H ₂ N-Lys- Cya TTTTTTT- H DNA 92 5'CG-AAAAAAAAA-GC3' PNA 71 , H-TTTTTTTT Cya -Lys-NH ₂	67.8		
4	PNA 71 , H ₂ N-Lys- Cya TTTTTTT- H DNA 96 5'CG-AAAACAAA-GC3' PNA 71 , H-TTTTTTTT Cya -Lys-NH ₂	54.5	-13.3	-6.6

^a T_m = melting temperature PNA₂:DNA complexes (measured in the buffer 10 mM sodium phosphate, 100 mM NaCl, pH = 7.3). Values in the parenthesis (ΔT_m) indicate the difference in T_m with the control experiment PNA **69**.

3.3 Biophysical studies of adenine containing-PNAT₈ (H-T_nAT_m-LysNH₂)

3.3.1 UV-Melting studies of adenine containing PNA₂:DNA complexes

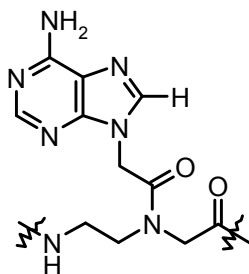


Figure 9: Structure of adeninyl PNA

The PNAs (Figure 9) having adenine at different positions, were synthesized as control sequences for studies of modified PNAs consisting of 8-bromoadenine and 8-aminoadenine. Thermal stability of the different adeninyl PNAs with complementary DNAs was studied to understand the effect of degree and position of modifications on thermal stability of the corresponding triplexes. The results of 8-bromo/amino adeninyl PNAs were compared with the results of corresponding adeninyl PNAs.

Table 3 shows T_m values for PNA₂:DNA complexes derived from various adenine containing PNA sequences. The melting profiles (Figure 10A) and the first derivative plots of normalized absorbance with respect to change in temperature (dA/dT) (Figure 10B) for PNA₂:DNA triplexes indicated a single transition, characteristic of both PNA strands dissociating simultaneously from DNA in a single step. The T_m data obtained from UV melting experiments of various adeninyl PNAs with their complementary DNA are summarized in the Table 3.

The PNA **74** (*N-terminus modified*) (entry 1 of Table 3) showed melting temperature 60.0 °C, while PNA **75** (*C-terminus modified*) exhibited T_m of 65.5 °C (entry 2 of Table 3), with complementary DNA **93**. PNA **76** (*middle modified*) showed 44.4 °C

with complementary DNA **94** (entry 3 of Table 3), and PNA **77** (*both N-terminus and middle modified*) showed 56.0 °C of melting temperature of triplexes with complementary DNA **95** (entry 4 of Table 3). The melting transitions of adenine containing PNAs with corresponding complementary DNA are shown in Figure 10.

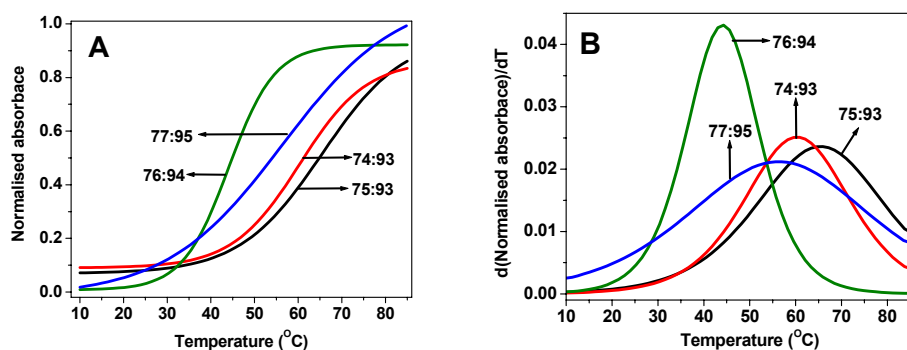


Figure 10: A) UV-melting profiles of (adeninylPNA)₂:DNA complexes, B) UV-melting first derivative curves of PNA₂:DNA complexes (Buffer, 10 mM Sodium phosphate pH = 7.3, 100 mM NaCl).

Table 3: UV-Melting temperatures (T_m values in °C)^a of adeninylPNA₂:DNA triplexes

Entry No.	Triplex (PNA ₂ :DNA)	T_m (°C) PNA ₂ :cDNA triplex
1	PNA 74 H ₂ N-Lys-TTTTTTT A -H DNA 93 5'GCAAAAAAATCG3' PNA 74 H A TTTTTTTTLys-NH ₂	60.0
2	PNA 75 H ₂ N-Lys- A TTTTTTTT-H DNA 93 5'GCAAAAAAATCG3' PNA 75 H-TTTTTTT A Lys- NH ₂	65.5
3	PNA 76 H ₂ N-Lys-TTT A TTTT-H DNA 94 5'GCAAATAAAACG3' PNA 76 H-TTTT A TTT-Lys-NH ₂	44.4
4	PNA 77 H ₂ N-Lys-TTT A TTT A -Lys-H DNA 95 5'GCAAATAAATCG3' PNA 77 H- A TTT A TTT-Lys-NH ₂	56.0

^a T_m = melting temperature PNA₂:DNA complexes (measured in the buffer 10 mM sodium phosphate, 100 mM NaCl, pH = 7.3).

3.4 Biophysical studies of 8-bromo/aminoadeninyl PNA

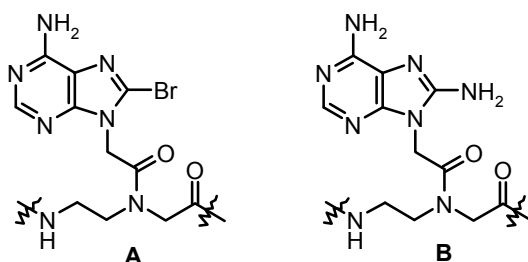


Figure 11: Structures of A) 8-bromoadeninyl PNA and B) 8-aminoadeninyl PNA

3.4.1 Establishment of binding stoichiometry of 8-bromo/aminoadeninyl PNA with cDNA

Various stoichiometric mixtures of 8-bromo/aminoadeninyl PNA (PNA **79/83**) and DNA **93** were made with relative molar ratios of PNA **79/83**:DNA **93** strands of 0:100, 20:80, 40:60, 50:50, 60:40, 80:20, 90:10, 100:0, keeping the same total strand concentration 2 μ M in sodium phosphate buffer (10 mM, pH 7.3), 100 mM NaCl. The elliptic values at isodichoric point confirmed the stoichiometry of PNA:DNA complex to be triplex (Figure 12B and 13B).

Keeping the total concentration constant, a series of mixtures of PNA and DNA in different relative molar equivalents of PNA and DNA were constituted and the UV absorbance of each composition was recorded at 260nm. The net UV absorbance steadily decreased due to hypochromic effect upon complexation (as PNA concentration increased), until all the strands present were fully involved in complex formation. The absorbance then rose upon addition of excess PNA. The stoichiometry of 8-bromo/aminoadeninyl PNA:DNA complexation was derived from the minimum in the plot of absorbance with respect to mole fraction (Figure 12C and 13C) and was found to be 2:1.

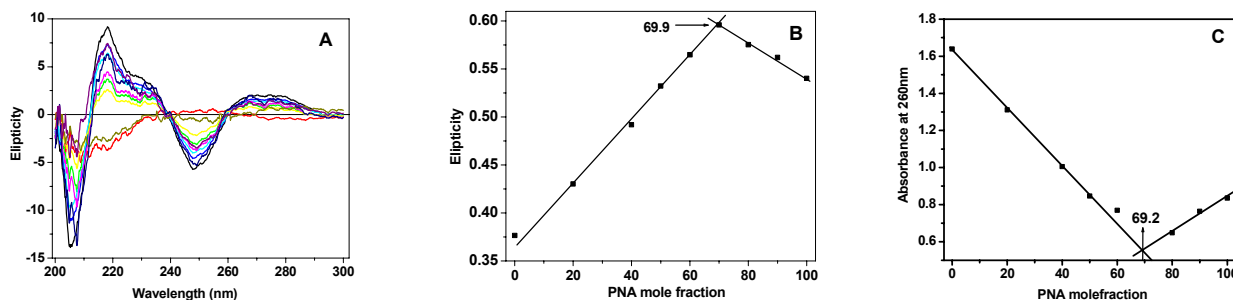


Figure 12: A) CD-curves for PNA **79**, H-TTTTTT**A**-Lys-NH₂ and the complementary DNA **93** d(GCTA₇CG) mixtures in the molar ratios of 0:100, 20:80, 40:60, 50:50, 60:40, 70:30, 80:20, 90:10, 100:0 (Buffer, 10 mM Sodium phosphate pH 7.0, 100 mM NaCl, 0.1 mM EDTA), B) CD-Job plot corresponding to 255 nm, C) UV-job plot corresponding to above mixtures of different molar ratios, absorbance recorded at 260 nm.

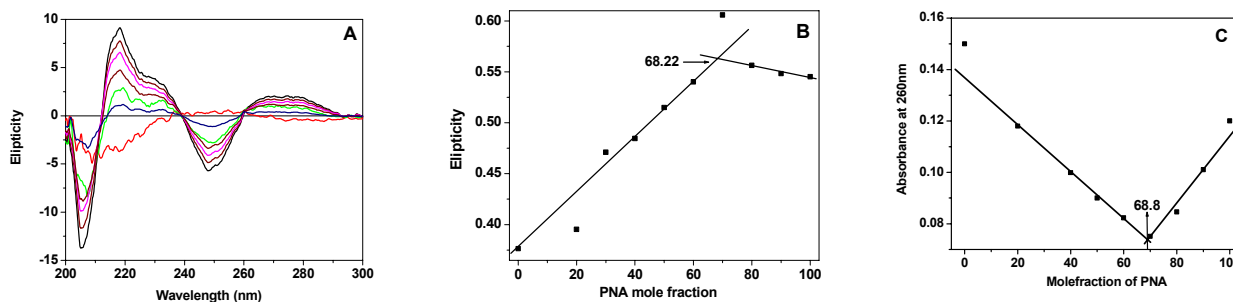


Figure 13: G) CD-curves for PNA **83**, H-TTTTTT**a**-Lys-NH₂ and the complementary DNA **93** d(GCTA₇CG) mixtures in the molar ratios of 0:100, 10:90, 20:80, 30:70, 40:60, 50:50, 60:40, 70:30, 80:20, 90:10, 100:0 (Buffer, 10 mM Sodium phosphate pH 7.0, 100 mM NaCl, 0.1 mM EDTA), H) CD-Job plot corresponding to 255 nm, I) UV-job plot corresponding to above mixtures of different molar ratios, absorbance recorded at 260 nm.

3.4.2 UV-Melting studies of 8-bromo/aminoadeninyl PNA₂:DNA complexes

The UV- T_m studies of 8-bromo/aminoadeninyl PNA₂:DNA triplexes was done to understand the effect on thermal stability in terms of the modified base and degree of modifications. The triplex formation of 8-bromoadeninyl PNA (Figure 21) and 8-aminoadeninyl PNA (Figure 21) with complementary DNA were confirmed through Job's plot (Figure 12 & 13). The triplex stability of various 8-bromo/amino adeninyl PNAs was compared with the melting temperatures of the corresponding adeninyl PNA

complementary DNA complexes. Summary of the T_m data obtained for UV melting experiments of various PNA₂:DNA hybrids are tabulated in Table 5.

Modification by position

The stability of triplexes of different adenine containing PNAs with complementary DNA was monitored and the T_m of triplexes of 8-bromoadeninyI PNA and 8-aminoadeninyI PNA were compared according to site of modification (Figure 14,15 and Table 4).

The triplexes from *N*-terminus modified PNA [H-AT₇-Lys] (PNA 74) with DNA 93 showed a melting temperature of 60.0 °C (entry 1 of Table 4). *N*-terminus modified 8-bromoadeninyI PNA [H-(8-BrA)₇-Lys], PNA 78 exhibited stabilization with T_m 68.2 °C (entry 1 of Table 4), while the triplex from the corresponding 8-amino adeninyI PNA [H-(8-NH₂A)₇-Lys], PNA 82 showed T_m of 35.0 °C with complementary DNA 93 (entry 3 of Table 4).

The triplexes of *C*-terminus modified adeninyI PNA [H-T₇A-Lys] PNA 75 with complementary DNA 93 showed T_m of 65.5 °C (entry 4 of Table 4), whereas the triplex from 8-bromoadeninyI PNA [H-T₇(8-BrA)-Lys] PNA 79 showed T_m of 70.2 °C (entry 5 of Table 4). The 8-aminoadeninyI PNA [H-T₇(8-NH₂A)-Lys] PNA 83 triplex with the complementary DNA 93 showed T_m of 74.8 °C of melting temperature (entry 6 of Table 4).

The triplexes from middle modified adeninyI PNA [H-T₄AT₃-Lys] (PNA 76) exhibited a T_m of 44.4 °C (entry 7 of Table 4), triplexes of its corresponding 8-bromoadeninyI PNA [H-T₄(8-BrA)₃-Lys] PNA 80 showed 34.4 °C (entry 8 of Table 4)

and that from 8-aminoadeninyl PNA [H-T₄(8-NH₂)AT₃-Lys] PNA **83** showed 75.2 °C (entry 9 of Table 4), all with the complementary DNA **94**.

The triplexes of double modified adeninyl PNA[H-AT₃AT₃-Lys] (*both N-terminus and middle modified*), PNA **77** showed T_m of 56.4 °C (entry 10 of Table 4), whereas triplex T_m of triplex from 8-bromoadeninyl PNA [H-(8-BrA)T₃(8-BrA)T₃-Lys], PNA **81** was 63.7 °C (entry 11 of Table 4). The triplex derived from *bis* modified 8-aminoadeninyl PNA [H-(8-NH₂A)T₃(8-NH₂A)T₃-Lys], PNA **85** showed the T_m of 49.5 °C (entry 12 of Table 4) with the complementary DNA **95**.

Modification by type

The stability of triplexes of PNAs having adenine and complementary DNA was monitored and the results of PNAs having different derived adenine analogues (8-bromoadeninyl PNA and 8-aminoadeninyl PNA) were compared according to site of modification (Figure 14,15 and Table 4).

Among the unmodified adenine containing PNA:DNA triplexes, *N-terminus modified*, PNA **74** (Entry 1 of Table 4) showed triplex melting temperature of 60.0 °C, while *C-terminus modified*, PNA **75** exhibited T_m of 65.5 °C (entry 2 of Table 4), with DNA **93**. The triplexes with *middle modified* PNA **76** showed T_m of 44.4 °C (complementary DNA **94**, entry 3 of Table 4), and the *bis* modified PNA **77** (*both N-terminus and middle modified*) showed T_m of 56.0 °C (complementary DNA **95**, entry 4 of Table 4).

Among the triplexes derived from modified oligomers of 8-bromoadeninyl PNA (PNA **78-81**), the *N-terminus modification* (PNA **78**) stabilizes the corresponding triplex with 8.2 °C. Triplexes from PNA **79** (*C-terminus modification*) and PNA **81** (*N-terminus*

and middle modification) are stabilized by 4.7 °C and 7.7 °C respectively compared to unmodified triplexes. However triplexes from PNA **80** with middle modification destabilized the hybrid by 10.0 °C. The melting profiles showed in Figure 14.

Among the triplexes of modified oligomers of 8-aminoadeninyl PNA (PNA **82-85**), those from PNA **83** (*C-terminus modification*) and PNA **84** (*middle modification*) stabilized the derived triplexes with corresponding complementary DNA **93/94** by 9.3 °C and 30.8 °C, respectively. The triplexes of PNA **82** (*N-terminus modification*) and *Bis* modified PNA **85** (*N-terminus and middle modification*) destabilized the triplex compared to unmodified triplexes by 25.0 °C and 6.5 °C respectively (complementary DNA **93/95**). The melting profiles are shown in Figure 15.

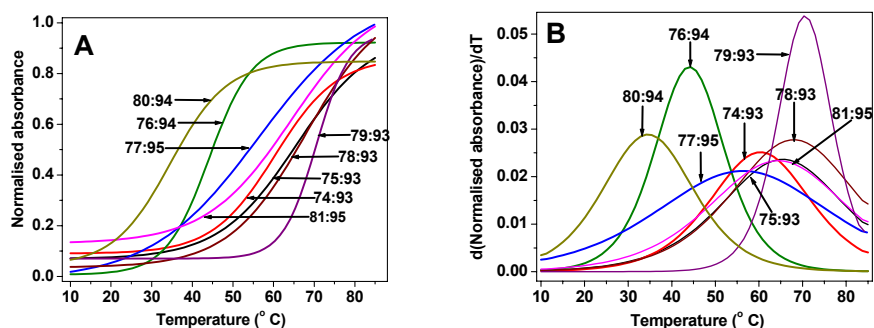


Figure 14: A) UV-melting profiles of (8-bromoadeninylPNA)₂:DNA complexes, B) UV-melting first derivative curves of (8-bromoadeninylPNA)₂:DNA complexes (Buffer, 10 mM Sodium phosphate pH = 7.3, 100 mM NaCl).

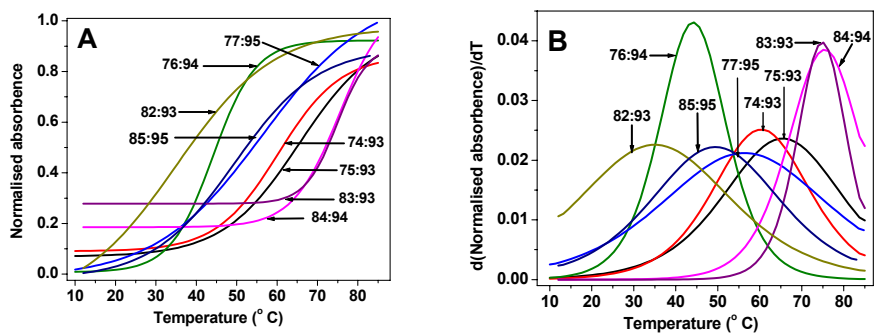


Figure 15: A) UV-melting profiles of (8-aminoadeninylPNA)₂:DNA complexes, B) UV-melting first derivative curves of (8-aminoadeninylPNA)₂:DNA complexes Buffer, 10 mM Sodium phosphate pH = 7.3, 100 mM NaCl).

Table 4: UV- T_m s of adeninyl, 8-bromoadeninyl, 8-aminoadeninyl PNA oligomers with complementary DNA (according to modification position)

Entry No.	Triplex (PNA ₂ :DNA)	T_m (°C) PNA ₂ :c DNA triplex	ΔT_m (°C)	ΔT_m (°C)/ modification
N-Terminus modifications				
1	PNA 74 H ₂ N-Lys-TTTTTTT <u>A</u> -H	60.0	--	
	DNA 93 5'GCAAAAAAATCG3'			
	PNA 74 H <u>A</u> TTTTTTTTLys-NH ₂			
2	PNA 78 H ₂ N-Lys-TTTTTTT <u>A</u> -H	68.2	+8.2	+4.1
	DNA 93 5'GCAAAAAAATCG3'			
	PNA 74 H <u>A</u> TTTTTTTTLys-NH ₂			
3	PNA 82 H ₂ N-Lys-TTTTTTT <u>a</u> -H	35.0	-25.0	-12.5
	DNA 93 5'GCAAAAAAATCG3'			
	PNA 82 H <u>a</u> TTTTTTTTLys-NH ₂			
C-Terminus modifications				
4	PNA 75 H-TTTTTTT <u>A</u> Lys- NH ₂	65.5	--	
	DNA 93 5'GCAAAAAAATCG3'			
	PNA 75 H ₂ N-Lys- <u>A</u> TTTTTTTT-H			
5	PNA 79 H-TTTTTTT <u>A</u> Lys- NH ₂	70.2	+4.7	+2.4
	DNA 93 5'GCAAAAAAATCG3'			
	PNA 79 H ₂ N-Lys- <u>A</u> TTTTTTTT-H			
6	PNA 83 H-TTTTTTT <u>a</u> Lys- NH ₂	74.8	+9.3	+4.7
	DNA 93 5'GCAAAAAAATCG3'			
	PNA 83 H ₂ N-Lys- <u>a</u> TTTTTTTT-H			
Middle modifications				
7	PNA 76 H ₂ N-Lys-TTT <u>A</u> TTTT-H	44.4	--	
	DNA 94 5'GCAAATAAAACG3'			
	PNA 76 H-TTTT <u>A</u> TTT-Lys-NH ₂			
8	PNA 80 H ₂ N-Lys-TTT <u>A</u> TTTT-H	34.4	-10.0	-5.0
	DNA 94 5'GCAAATAAAACG3'			
	PNA 80 H-TTTT <u>A</u> TTT-Lys-NH ₂			
9	PNA 84 H ₂ N-Lys-TTT <u>a</u> TTTT-H	75.2	+30.8	+15.4
	DNA 94 5'GCAAATAAAACG3'			
	PNA 84 H-TTTT <u>a</u> TTT-Lys-NH ₂			
Bi modifications				
10	PNA 77 H ₂ N-Lys-TTT <u>A</u> TTT <u>A</u> -Lys-H	56.0	--	
	DNA 95 5'GCAAATAAAATCG3'			
	PNA 77 H- <u>A</u> TTT <u>A</u> TTT-Lys-NH ₂			
11	PNA 81 H ₂ N-Lys-TTT <u>A</u> TTT <u>A</u> -Lys-H	63.7	+7.7	+1.9
	DNA 95 5'GCAAATAAAATCG3'			
	PNA 81 H- <u>A</u> TTT <u>A</u> TTT-Lys-NH ₂			
12	PNA 85 H ₂ N-Lys-TTT <u>a</u> TTT <u>a</u> -Lys-H	49.5	-6.5	-1.6
	DNA 95 5'GCAAATAAAATCG3'			
	PNA 85 H- <u>a</u> TTT <u>a</u> TTT-Lys-NH ₂			

A= adenine, A=8-bromoadenine and a=8-aminoadenine; All values are an average of at least 3 experiments and accurate within $\pm 0.5^\circ\text{C}$, Buffer: Sodium phosphate (10 mM), and 100 mM NaCl, pH 7.2.

3.5 UV-Melting studies of adeninyl/8-bromoadeninyl/8-aminoadeninyl PNA complexes with mismatch DNA

The sequence specificity of PNA hybridization was examined through studying the hybridization properties of PNA with single mismatch containing DNA.

The triplex from *C*-terminus modified adenine containing PNA **75**, exhibited a melting temperature of 60.0 °C (entry 1, Table 5) with complementary DNA **93**, whereas a melting temperature of 57.4 °C (entry 2, Table 5) was seen for triplex with single mismatch containing DNA **97**. The triplex of *C*-terminus modified 8-bromoadeninyl PNA **79** (entry 3, Table 5), showed a triplex melting temperature of 70.2 °C (entry 4, Table 5) with complementary DNA **93**, while the T_m of triplex with single mismatch sequence DNA **97** was 61.7 °C (entry 5, Table 5). The triplex from corresponding sequence of 8-aminoadeninyl PNA (*C*-terminus modified, PNA **80**), showed a melting temperature of 74.8 °C (entry 5, Table 5) with complementary DNA **93**, whereas its melting temperature was observed as 66.4 °C with single mismatch sequence DNA **97** (entry 6, Table 5). All the melting profiles and corresponding first derivatives plots are shown in figure **16**.

The complex of control sequence PNA **75** formed triplex with single mismatch sequence (DNA **97**) with T_m lower by 8.1 °C (entry 1&2, Table 5), while the *C*-terminus modified 8-bromoadeninyl PNA **79** (entry 3&4, Table 5) exhibited destabilization by 8.5 °C and *C*-terminus modified 8-aminoadeninyl PNA **83** (entry 5&6, Table 5) showed 8.4 °C respectively. Thus 8-bromo/aminoadeninyl PNA thus showed sequence discrimination as good as the control sequence PNA **75**. The 8-bromo or 8-amino

substitution of adenine thus show a lower influence on the sequence specificity compared to unmodified adeninyl PNA.

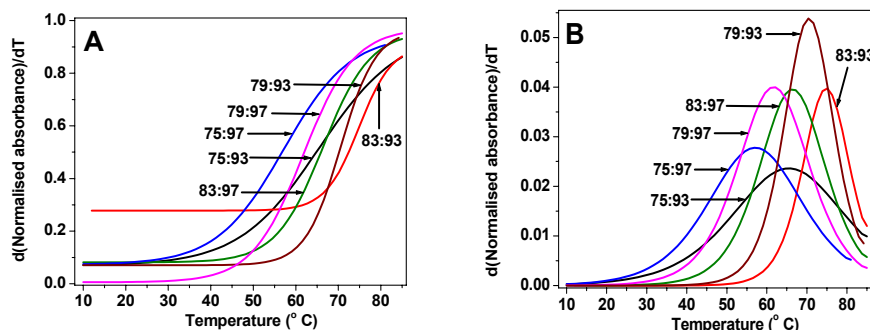


Figure 16: A) UV-melting profiles of (8-aminoadeninylPNA)₂:DNA complexes, B) UV-melting first derivative curves of (8-aminoadeninylPNA)₂:DNA complexes Buffer, 10 mM Sodium phosphate pH = 7.3, 100 mM NaCl).

Table 5: UV-Melting temperatures (T_m values in °C)^a of adeninyl/8-bromoadeninyl/8-amino adeninyl PNA₂:DNA triplexes

Entry No.	Triplex (PNA ₂ :DNA)	T_m (°C) PNA ₂ :c DNA triplex	ΔT_m (°C) (match-mismatch)
1	PNA 75 H-TTTTTTTT <u>A</u> Lys- NH ₂ DNA 93 5'GCAAAAAAATCG3' PNA 75 H ₂ N-Lys- <u>A</u> TTTTTTTT-H	65.5	8.1
2	PNA 75 H-TTTTTTTT <u>A</u> Lys- NH ₂ DNA 97 5'GCAAACAAATCG3' PNA 75 H ₂ N-Lys- <u>A</u> TTTTTTTT-H	57.4	
3	PNA 79 H-TTTTTTTT <u>A</u> Lys- NH ₂ DNA 93 5'GCAAAAAAATCG3' PNA 79 H ₂ N-Lys- <u>A</u> TTTTTTTT-H	70.2	8.5
4	PNA 79 H-TTTTTTTT <u>A</u> Lys- NH ₂ DNA 97 5'GCAAACAAATCG3' PNA 79 H ₂ N-Lys- <u>A</u> TTTTTTTT-H	61.7	
5	PNA 83 H-TTTTTTTT <u>a</u> Lys- NH ₂ DNA 93 5'GCAAAAAAATCG3' PNA 83 H ₂ N-Lys- <u>a</u> TTTTTTTT-H	74.8	8.4
6	PNA 83 H-TTTTTTTT <u>a</u> Lys- NH ₂ DNA 97 5'GCAAACAAATCG3' PNA 83 H ₂ N-Lys- <u>a</u> TTTTTTTT-H	66.4	

^a T_m = melting temperature (measured in the buffer 10 mM sodium phosphate, 100 mM NaCl, pH = 7.3), PNA₂-DNA complexes. Values in the parenthesis (ΔT_m) indicate the difference in T_m of PNA with complementary sequence (DNA 93) and single mismatch sequence (DNA 97). The values reported here are the average of 3 independent experiments and are accurate to $\pm 0.5^\circ\text{C}$

3.6 UV- T_m studies of *cyanuranyl/8-bromoadeniny/8-aminoadeniny* PNA:DNA Duplexes (*parallel/antiparallel*)

The mixed purine -pyrimidine sequence, PNA **86** was synthesized to examine the stability of derived PNA:DNA duplexes. The *cyanuranyl* PNA **87**, was synthesized by replacing the thyminy/ PNA units of PNA **86** with cyanuranyl PNA unit, whereas *8-bromoadeniny* PNA **88** was synthesized by replacing the adeniny/ PNA with 8-bromoadeniny/ PNA and 8-aminoadeiny/ PNA **89** was synthesized by direct amination of solid supported 8-bromoadeniny/ PNA oligomer as mentioned in Chapter 2 (2.35.2).

Entry **1** of table **6** indicates that PNA **86**: DNA **98** antiparallel duplex showed T_m of 51.2 °C compared to T_m of duplex with DNA **99** (entry 1, Table 6) as 48.6 °C. Cyanuranyl PNA **87** showed triplex of melting temperature (entry 2, Table 6), 48.2 °C with DNA **98** (*antiparallel*) and the melting temperature with corresponding parallel DNA sequence (DNA **99**) was 45.7 °C (entry 2, Table 6).

The T_m of triplex of 8-bromoadeniny/ PNA **88** with *antiparallel* DNA **98** was 53.3 °C (Entry 3, of Table 6), while the corresponding triplex with *parallel* DNA **99** was seen to be 49.7 °C (Entry 4, Table 7). In contrast, 8-aminoadeniny/ PNA **89** showed 52.8 °C of melting temperature of its triplex with DNA **98** (*antiparallel*) and corresponding triplex with parallel oriented DNA **99** was 46.1 °C.

The control sequence PNA **86**, showed 2.7 °C of sequence discrimination between parallel and antiparallel complementary DNA sequences, whereas corresponding *cyanuranyl* PNA **87** showed 2.5 °C of discrimination in sequence orientation (*antiparallel or parallel*). The 8-bromoadeniny/ PNA (PNA **88**) and 8-aminoadeniny/ PNA (PNA **89**)

showed better discrimination of 3.6 °C and 6.7 °C in sequence orientation respectively. Eventhough the modifications 8-bromo/aminoadeninyl PNAs may not enhance the binding strength with complementary DNA in duplexes, they discriminate the *parallel* and *antiparallel* sequences better than the control sequence PNA **86**.

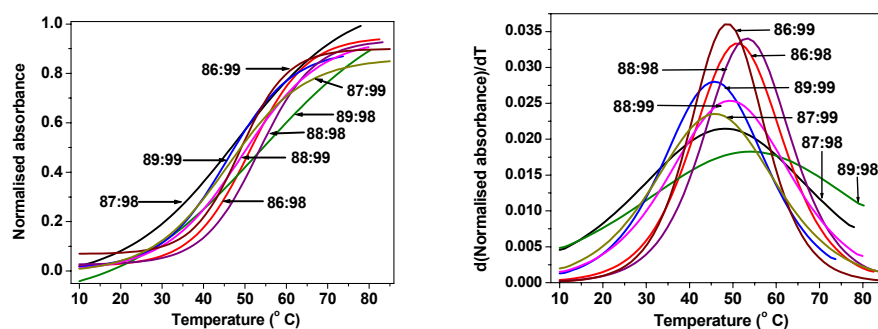


Figure 17: A) UV-melting profiles of PNA:DNA duplexes, B) UV-melting first derivative curves of PNA:DNA duplexes (Buffer, 10 mM Sodium phosphate pH = 7.3, 100 mM NaCl).

Table 6: UV-Melting temperatures (T_m values in °C)^a of PNA:DNA duplexes

Entry No	Duplex (PNA:DNA)	T_m (°C)	
		PNA:DNA duplex	ΔT_m (°C) (<i>ap-p</i>)
1	PNA 86 H-GT <u>A</u> GATC <u>A</u> CT-Lys-NH ₂ DNA 98 5' AGTGATCTAC 3'	51.3	2.7
2	PNA 86 H-GT <u>A</u> GATC <u>A</u> CT-Lys-NH ₂ DNA 99 5' CATCTAGTGA 3'	48.6	
3	PNA 87 H-G <u>Cy</u> <u>A</u> G <u>A</u> <u>Cy</u> C <u>ACC</u> <u>Cy</u> -Lys-NH ₂ DNA 98 5' AGTGATCTAC 3'	48.2	2.5
4	PNA 87 H-G <u>Cy</u> <u>A</u> G <u>A</u> <u>Cy</u> C <u>ACC</u> <u>Cy</u> -Lys-NH ₂ DNA 99 5'CATCTAGTGA3'	45.7	
5	PNA 88 H-GT <u>A</u> GATC <u>A</u> CT-Lys-NH ₂ DNA 98 5' AGTGATCTAC 3'	53.3	3.6
6	PNA 88 H-GT <u>A</u> GATC <u>A</u> CT-Lys-NH ₂ DNA 99 5'CATCTAGTGA3'	49.7	
7	PNA 89 H-GT <u>a</u> G <u>a</u> T <u>Ca</u> CT-Lys-NH ₂ DNA 99 5'CATCTAGTGA3'	52.8	6.7
8	PNA 89 H-GT <u>a</u> G <u>a</u> T <u>Ca</u> CT-Lys-NH ₂ DNA 98 5' AGTGATCTAC 3'	46.1	

Cy= cyanuryl, A= adenine, A=8-bromoadenine and a=8-aminoadenine a T_m is measured in the buffer 10 mM sodium phosphate, 100 mM NaCl, pH = 7.3. Values in the ΔT_m indicate the difference in the melting temperatures of the PNA:DNA **99** and DNA **98**. The values reported here are the average of 3 independent experiments and are accurate to $\pm 0.5^\circ\text{C}$

3.7 Discussion:

In case of cyanuric PNA, *C*-terminus, middle and *bis* modifications (*N*-terminus and middle modification) stabilized the corresponding triplex, whereas the *N*-terminus modified PNA destabilized the triplex.

Among the PNA oligomers containing 8-bromo-adenine at *C*-terminus modified (PNA **78**), middle modified (PNA **80**) and *bis* modified (PNA **81**) stabilized the triplexes with corresponding complementary DNA, whereas *N*-terminus modified PNA (PNA **79**) destabilized the corresponding triplex.

Among the PNA oligomers containing 8-amino-adenine, *C*-terminus (PNA **83**), middle (PNA **84**) modified PNAs are stabilized the triplexes with the corresponding complementary DNA, whereas *N*-terminus (PNA **82**) and *bis* modified (PNA **85**) PNAs are destabilized the corresponding the triplexes.

In comparison, the oligomers containing 8-bromo/amino-adenine at *C*-terminus (PNA **79** and PNA **83**) stabilized the triplexes. In contrast to 8-bromo-adenine PNA, the 8-amino-adenine PNA (PNA **82**) containing *N*-terminus modification destabilizes the triplex by 25°C and consequently PNA **85** with *bis* modifications at *N*-terminus and middle also destabilized the triplex by 8.6 °C. Interestingly the middle modified 8-amino-adeninyl PNA (PNA **84**) stabilized the triplex with 30.8 °C. This may well support the hypothesis that 8-amino-adenine stabilized the triplex through simultaneous formation of both Watson-Crick and Hoogsteen hydrogen bonding.

3.8 Binding stoichiometry of 8-bromoadeninyI PNA and 3',5'-O-disilyl thymidine/ thymidinyl PNA monomers through NMR titrimetry

In view of the variable results on PNA:DNA triplex/duplex stabilization in oligomers, it was thought worthwhile to understand difference in their base pairing properties at the monomer level.

The specific association of purine and pyrimidine bases is fundamental to the function of nucleic acids. Forces that contribute to the stability of double stranded nucleic acids can be conceptually expressed as sum of base-base hydrogen bonding and stacking interactions. The hydrogen bonding between the base pairs adenine:thymine and guanine:cytosine was proposed by Watson-Crick in 1953.⁷ However complete understanding of physical basis for this observed complementarity has proved difficult.

There have been several approaches to model the nucleic acid interactions. The properties of nucleic acid monomers have provided considerable insight into those of polymeric nucleic acids. The hydrogen bonding interaction in the low dielectric environment of the **interior** of polymeric nucleic acids can be modeled by soluble nucleic acid monomers in non-aqueous solvent such as chloroform and DMSO. Spectroscopic techniques such as NMR (¹H and ¹³C) and IR are particularly useful to identify the hydrogen bonds in these complementary base pairs and characterization of important structural motifs such as Watson-Crick (WC) and Hoogsteen (HG) base pairing.^{8,9} While WC base pair domains were also observed between monomers G and C in low dielectric

medium, higher order structures such as C:G₂ dimers and (C:G)₂ tetramers have also been seen to co-exist.⁸

The effect of substituents on purine and pyrimidine bases, in particular, on their ability to form complementary hydrogen bonding pairs is not only important but also has practical relevance in designing new antisense agents. The substitution directly affects the delicate balance of electronic and geometric complementarity existing in the natural base pairing. It has been demonstrated from IR studies of model substituted bases that base substitution also determines the strength and extent of self association relative to the complementary base pairing.¹⁰

3.8.2 Rationale design behind the work

Peptide Nucleic Acids (PNAs) are an established field of nucleic acid mimics and are known to form duplex and triplex with complementary nucleic acids.¹¹ PNA suffers from drawbacks such as self aggregation, poor cellular uptake and discrimination between DNA and RNA, which resists its application as an antisense agent. To overcome these, a number of chemically modified PNAs have been synthesized.^{11b,12} These chemical modifications include that of both the backbone and the bases. Several modified base containing peptide nucleic acids have been synthesized and examined for their hybridization properties with complementary DNA/RNA.¹² Substitution at 8-position of a purine ring is known to affect its base pairing properties through effecting the electron density changes on the 5 membered ring.^{5,6} The PNA oligomers are known to form duplexes and triplexes with corresponding complementary nucleic acids, whereas the binding stoichiometry between PNA monomers and complementary nucleosides (protected) needs to be examined.

3.8.3 Complexation titrimetry for evaluation of binding constants through NMR studies:

The modified nucleobase containing PNA oligomers form triplex with complementary oligonucleotides, as confirmed through Circular Dichroism (CD) and UV Job's plot. It was needed to investigate the binding stoichiometry of the modified nucleobase PNA monomer with the complementary nucleobases.

The binding stoichiometry between the complementary nucleobase pair was determined through two sets of NMR experiments,

- i) The titration between 3',5'-di-O-silyldeoxyribothymidine (**100**) and adeninyl (**24**)/8-bromoadeninyl PNA (**25**) monomer
- ii) The titration between thymidinyl PNA (**31**) and adeninyl(**24**)/8-bromoadeninyl PNA (**25**) monomer

The silyl derivative of nucleoside was used to make them soluble in CHCl_3 in which the NMR titration experiments were done.

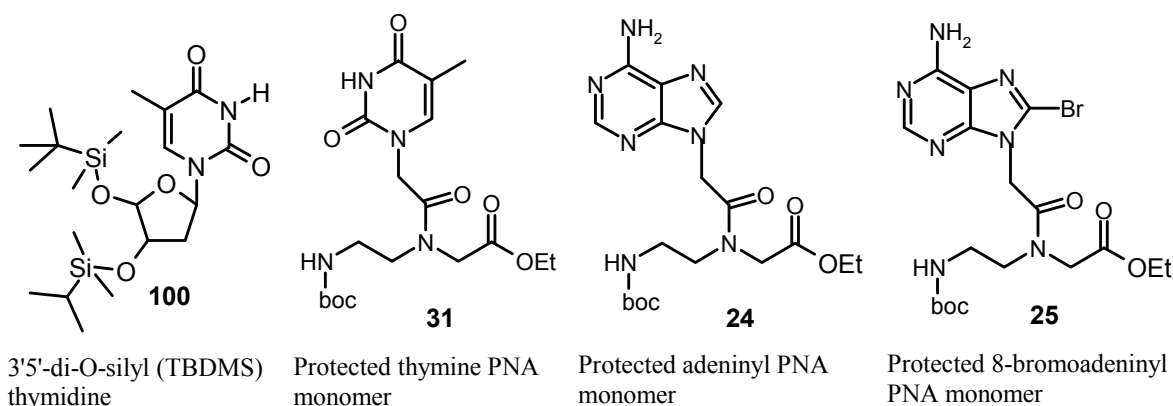


Figure 18: The monomers used for NMR titration study

3.8.4 Experimental method of NMR titrimetry

The DNA-thymine component (**100** or **31**, 30 mM) in dry CDCl_3 (600 μl) was titrated with the PNA-adenine component (**24** or **25**) (30 mM in 120 μl in dry CDCl_3). The titration was followed by NMR for each addition of 5 mM (100 μl) of prepared adenine component (**24** or **25**). The chemical shift of N^3 -H of thymine moves downfield progressively as it forms hydrogen bonding with adenine component. After the complete binding, the downfield shift of N -H δ reaches saturation.

The N^3 -H of 3',5'-di-O-silyldeoxyribothymidine (**100**), showed δ value 8.33, and the addition of equimolar adeninyl PNA **24** in CDCl_3 , shifted it downfield to δ 9.5, ($\Delta\delta \approx +1.2$ ppm) and further addition of adeninyl PNA showed negligible increment of δ value of N^3 -H (Figure 19A & 22).

The extent of base pairing in DNA:PNA complexes of monomers was also examined.

The N^3 -H of 3',5'-di-O-silyldeoxyribothymidine (**100**), upon addition of equimolar 8-bromoadeninyl PNA **25** in CDCl_3 , showed δ value to increase to 9.16 ($\Delta\delta = +0.8$ ppm) and further addition of 8-bromoadeninyl PNA insignificantly changed δ value of N^3 -H (Figure 19B & 23).

The N^3 -H of thymidinyl PNA **31**, showed δ value 8.58, which increased to 9.7 ($\Delta\delta = +1.12$ ppm) upon addition of equimolar adeninyl PNA **24** in CDCl_3 . Further addition of adeninyl PNA showed only a small effect on the increment of δ value of N^3 -H (Figure 20A & 24).

The N^3 -H of thymidinyl PNA **31**, upon addition of equimolar 8-bromoadeninyl PNA **25** in CDCl_3 , showed a downfield shift to $\delta 9.7$ ($\Delta\delta = +1.12$ ppm) (Figure 20B & 25).

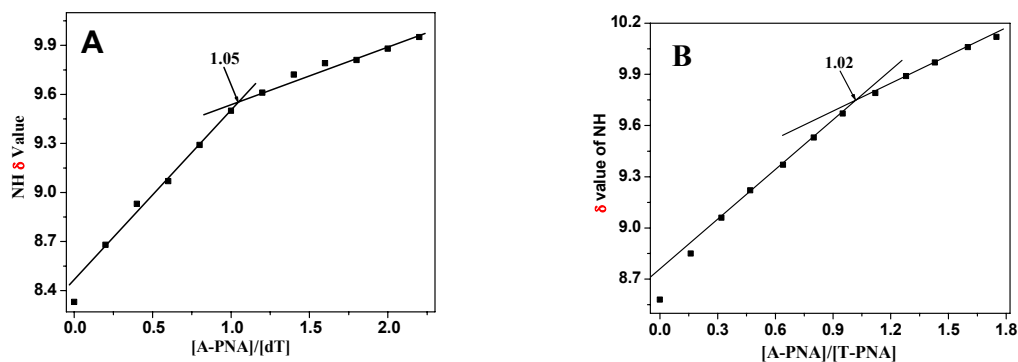


Figure 19: The NMR titration experiment curves of A) adeninyl PNA: dT, B) adeninyl PNA: thymidinyl PNA

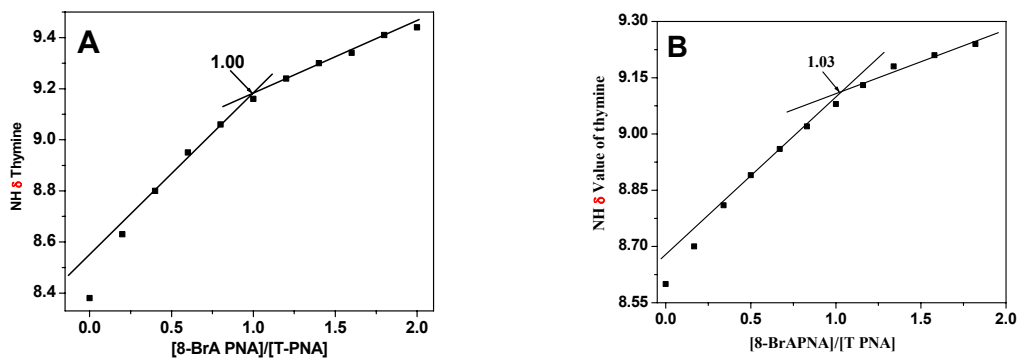


Figure 20: The NMR titration experiment curves of A) 8-bromoadeninyl PNA: thymidinyl PNA and B) 8-bromoadeninyl PNA: thymidinyl PNA

The incremental downfield shift of N^3 -H of thymine in various DNA:PNA complexes was plotted against the concentration ratios and in all plots, a breakpoint was observed at 1:1 ratio. This suggested that the binding stoichiometry between 8-bromoadeninyl PNA with complementary disilyl thymidine to be 1:1. The binding stoichiometry between 8-bromoadeninyl PNA with thymidinyl PNA monomer also established as 1:1, corresponds to a dimer. The corresponding studies could not be done

on 8-aminoadeninyl PNA monomer due to the synthetic difficulties in preparing the same (See chapter 2, section 2.3.5)

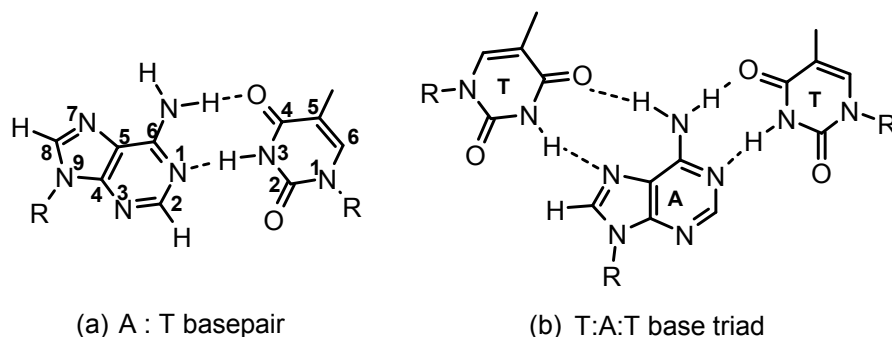


Figure 21: Hydrogen bonding in (a) Adenine-Thymine base pair and (b) Thymine-Adenine-Thymine base triad

The binding stoichiometry of unmodified adeninyl PNA and 3',5'-O-disilyldeoxy thymidine was studied through a titration of 3',5'-di-O-silyldeoxyribothymidine with adeninyl PNA. Besides of the expected downfield shift of N^3 -H of thymidine due to hydrogen bonding, slight upfield shift of the protons corresponding to adenine were observed. At lower concentration of adeninyl PNA, the signals corresponds to C^8 -H and C^2 -H were merged and appeared single peak at δ 8.15. As the concentration of adeninyl component increased both show different chemical shifts at 8.1 ppm and 8.2 ppm respectively corresponding to C^8 -H and C^2 -H of adenine. The exocyclic NH_2 signal of adenine, which was downfielded at 8.5 ppm shifted to 7.7 ppm gradually as the concentration of adenine increases.

This kind of pattern was even observed in the titration experiment between thymidinyl PNA Vs adeninyl PNA (Figure 24). The down field shift of N^3 -H of thymidinyl PNA, slight upfield shift of the protons corresponding to adenine were observed. At lower concentration of adeninyl PNA, the signals corresponds to C^8 -H and C^2 -H were merged and appeared as single peak at 8.25 ppm. As the concentration of

adeninyl component increased both show different chemical shifts at 8.2 ppm and 8.3 ppm respectively corresponding to C^8 -H and C^2 -H of adenine. The exocyclic NH_2 signal of adenine, which was upfielded from 8.7 ppm to 7.7 ppm gradually as the concentration of adenine increases.

This can be possibly explained as, at initial stages of titration experiment, adeninyl component in lower concentration, exists as T:A:T triad with both the protons of amine (H_2N^6) bounded to two thymine components (Figure 21b). As the concentration of adeninyl component increased, the equilibrium is shifted towards A:T dimer as seen by the binding stoichiometry as 1:1 (Figure 21a). Relaxation of hydrogen bonding NH_2 from triad to diad will bring overall upfield shift of NH proton.

But this pattern was not observed in the titration experiment between 3',5'-disilyldeoxyribothymidine/thymidinyl PNA Vs 8-bromo adeninyl PNA. C^2 -H proton consistently appeared at δ 8.2 throughout the titration experiment and the chemical shift of the exocyclic amine of 8-bromoadeninyl PNA did not change much from 6.2 ppm. This can be probably explained as, due to the bulkier bromo atom in 8-bromoadeninyl PNA resists formation of T: A^{Br}:T triad at lower concentration of 8-bromoadeninyl PNA and only A^{Br}:T diad is formed even at lower concentrations.

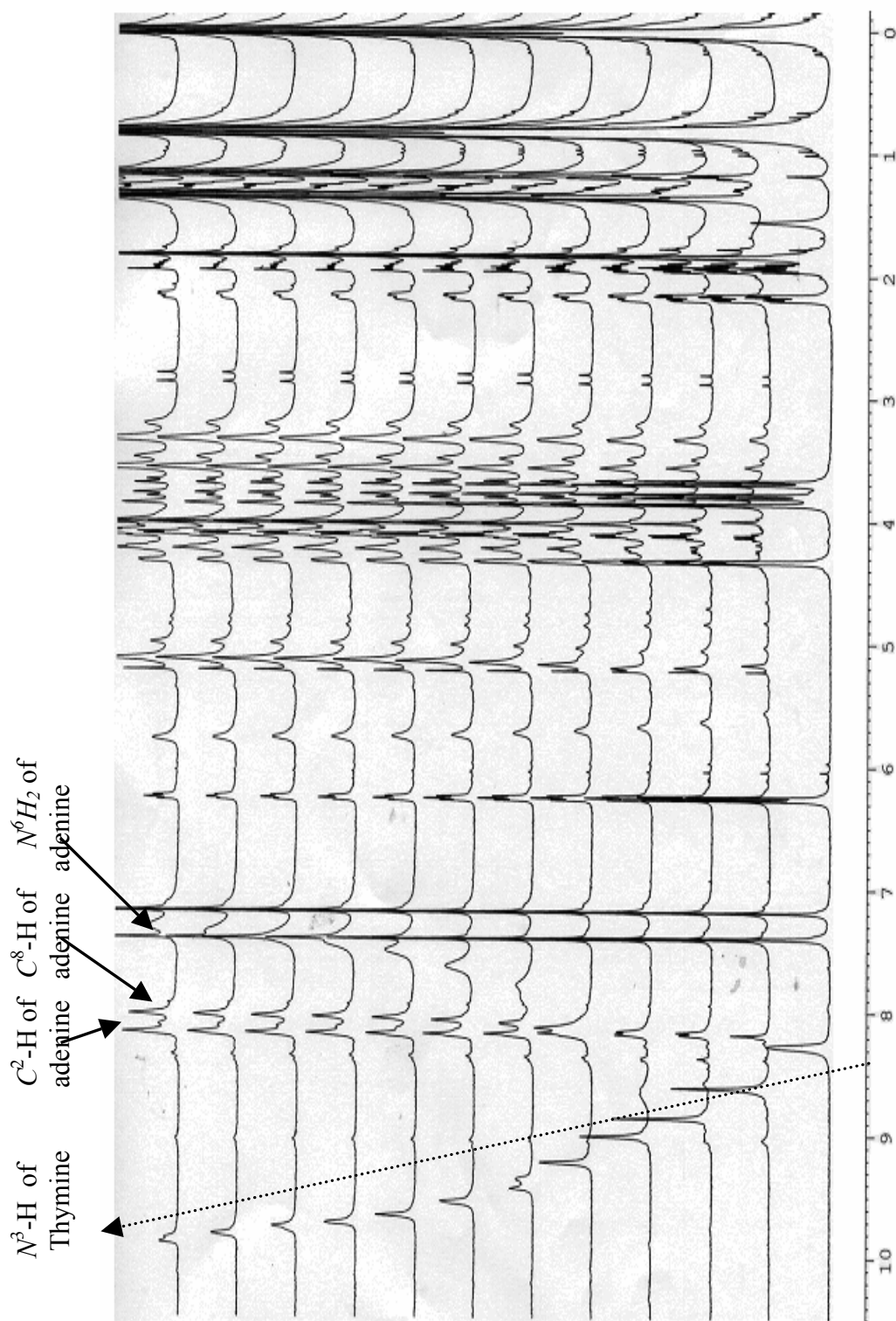


Figure 22: The stacked plots of titration experiment between 3',5'-disilyldeoxyribothymidine Vs adenine| PNA

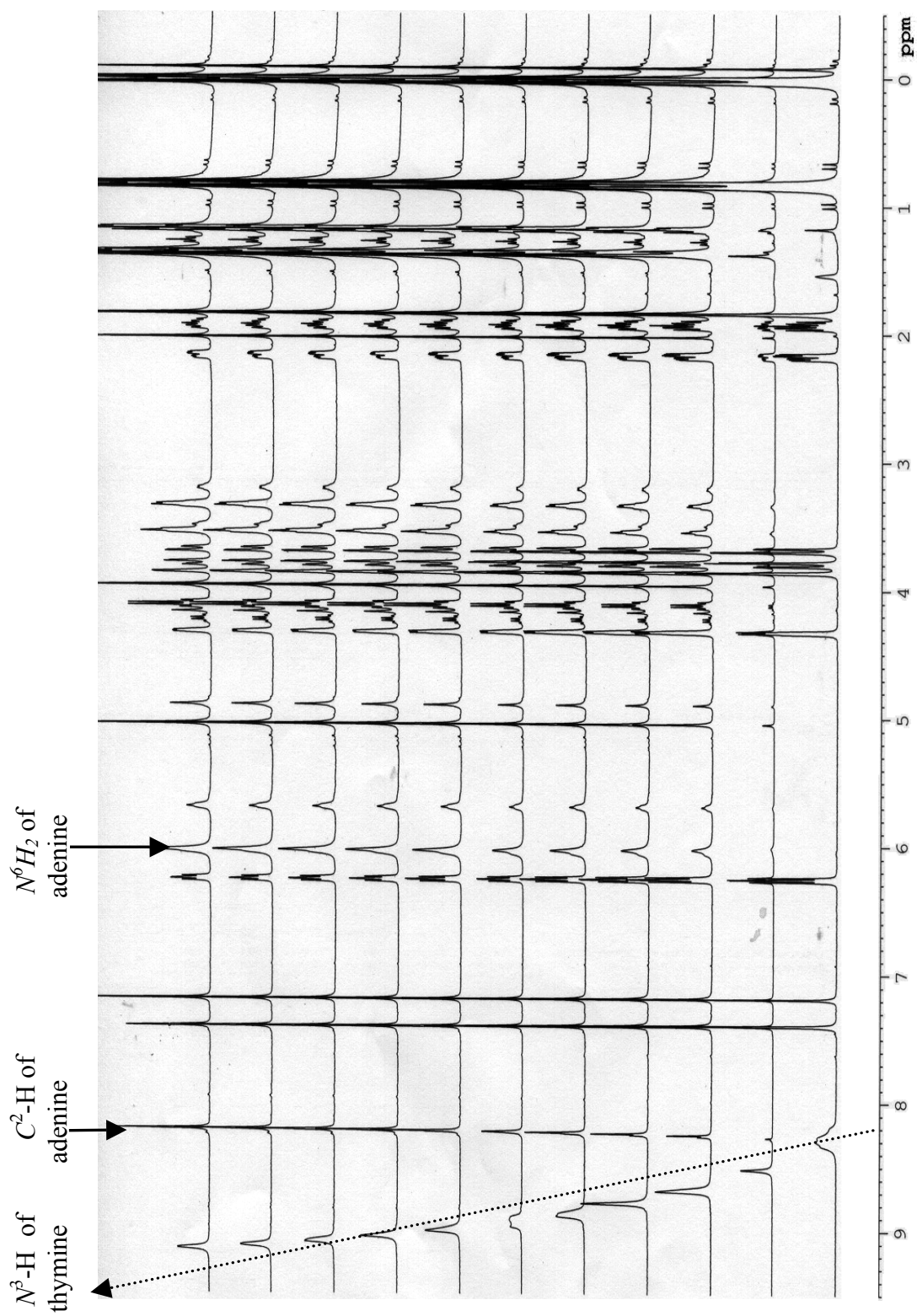


Figure 23: The stacked plots of titration experiment between 3',5'-disilyldeoxyribothymidine V vs 8-bromo adeninyl PNA

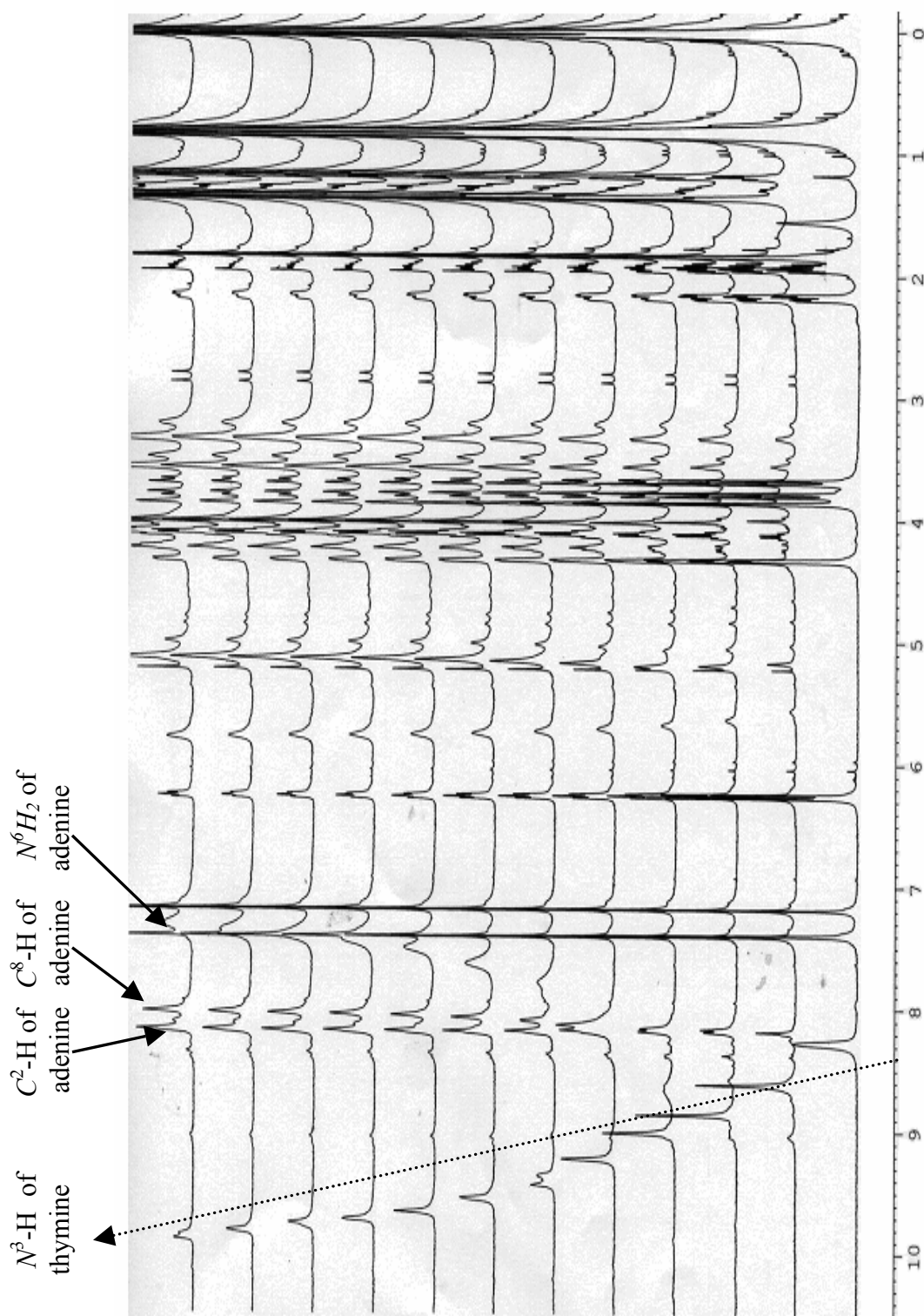


Figure 24: The stacked plots of titration experiment between thymidyl PNA Vs adeninyl PNA

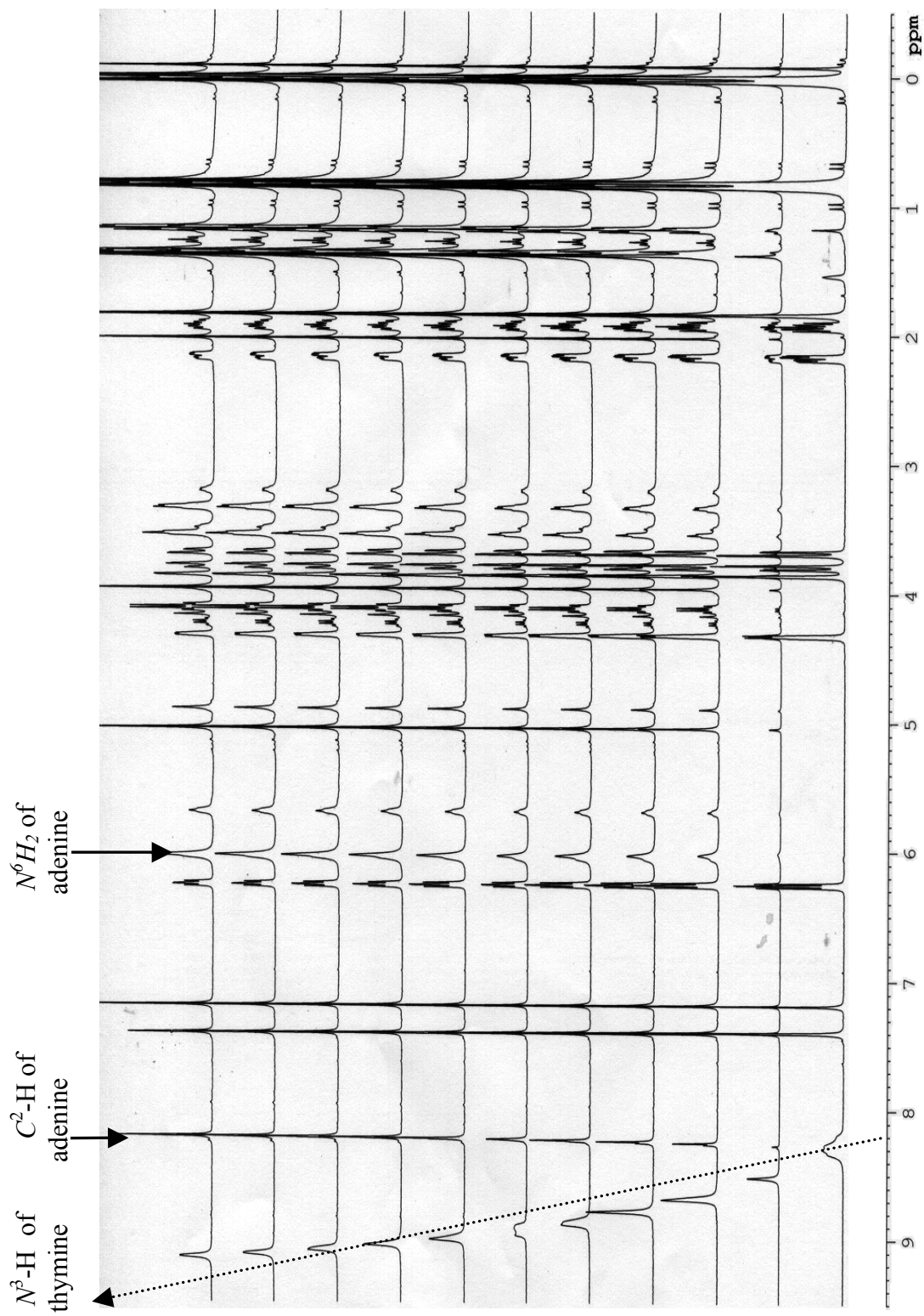
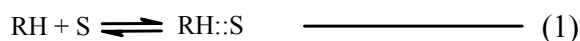


Figure 25: The stacked plots of titration experiment between thymidinyl PNA Vs 8-bromoadeninyl PNA

3.8. 5 Calculation of Binding Constant Through NMR Titration Method¹³

The association constant between two substrates can be calculated through NMR titrimetry. The titration between the components receptor (RH) and a substrate (S) lead to formation of complex (RH::S) with equilibrium (equation 1) and the association constant of complex is defined as in equation 2.



$$K_a = \frac{[\text{RH}::\text{S}]}{[\text{RH}] [\text{S}]} \quad \text{—————} \quad (2)$$

The observed chemical shift of the corresponding proton (RH::S) is the average of the chemical shifts in two possible environments, one is unbound state (δ_s) and another is complex state ($\delta_{\text{RH}::\text{S}}$). The observed chemical shift corresponds to the molefraction of the substrate in unbound and complex states. If the initial substrate concentration is S_o , then the equation 3 applies to calculate the δ_{obs} .

$$\delta_{\text{obs}} = \frac{S_o - [\text{RH}::\text{S}]}{S_o} \delta_s + \frac{[\text{RH}::\text{S}]}{S_o} \delta_{[\text{RH}::\text{S}]} \quad \text{—————} \quad (3)$$

The equation 3 can be rearranged as equation 4, as the difference in chemical shifts in two environments defined as $\Delta\delta$ ($\Delta\delta = \delta_{\text{RH}::\text{S}} - \delta_s$).

$$\delta_{\text{obs}} = \delta_s + \frac{[\text{RH}::\text{S}]}{S_o} \Delta\delta \quad \text{—————} \quad (4)$$

The association constant can be calculated through the equation 5, provided initial concentration of receptors (S_o , R_o), δ_s and $\Delta\delta$ are known.

$$\delta_{\text{obs}} = \delta_s + \frac{1}{2 S_o} \left[\frac{1}{K_a} + R_o + S_o - \sqrt{\left(\frac{1}{K_a} + R_o + S_o \right)^2 - 4 R_o S_o} \right] \quad \text{—————} \quad (5)$$

The $\Delta\delta$ can be calculated if the chemical shift of saturated complex (100%) is known. Since, the saturation is not observed in the titration curves of either 3',5'-di-O-silyldeoxy thymidine Vs adeninyl/8-bromoadeninyl PNA (Figure 19A and 20A) or thymidinyl PNA Vs adeninyl/8-bromoadeninyl PNA (Figure 19B and 20B), it is difficult to calculate the binding constant in this case. However, through computer programs, by assumption and iteration, it is possible to solve such equation (5), with two unknowns. However due to non availability of such program, we have been unable to compute the association constant (K_a) at present.

3.9 General Experimental Procedure of Biophysical studies

3.9.1 UV studies

All the UV spectrophotometric studies were performed either on a Perkin Elmer $\lambda 15$ UV-VIS spectrophotometer equipped with a Julabo temperature programmer and a Julabo water circulator or a Perkin Elmer $\lambda 35$ UV-VIS spectrophotometer with peltier to maintain the temperature. The samples were degassed by purging nitrogen or argon gas through the solution for 2-3min prior to the start of the experiments. Nitrogen gas was purged through the cuvette chamber below 15°C to prevent the condensation of moisture on the cuvette walls.

3.9.1 UV- T_m studies

The PNA oligomers and the appropriate DNA oligomers were mixed together in stoichiometric amounts (2:1, PNA:DNA for oligothymine- T_8 PNAs or 1:1 for the duplex forming PNAs, *viz.*, the mixed base sequences) in 0.01M sodium phosphate buffer, pH 7.3 to achieve a final strand concentration of either 0.5 or 1 μ M each strand. For the AT-rich PNAs, *antiparallel* and *parallel* complexes were constituted by employing DNA.

The samples were heated at 85°C for 5 min. followed by slow cooling to room temperature for 7 hrs. They were allowed to remain at room temperature for at least half an hour and refrigerated overnight prior to running the melting experiments. Each melting experiment was repeated at least twice. The normalized absorbance at 260 nm was plotted as a function of the temperature. The T_m was determined from the first derivative plots of normalized absorbance with respect to temperature and is accurate to $\pm 0.5^\circ\text{C}$. The concentration of DNA, RNA and PNA were calculated with the help of extinction coefficients, A= 15.4, T= 8.8, C= 7.3 and G= 11.7.

3.9.2 Circular Dichroism

CD spectra were recorded on a Jasco J-715 spectropolarimeter. The CD spectra of the PNA:DNA complexes and the relevant single strands were recorded in 0.01M sodium phosphate buffer, pH 7.4. The temperature of the circulating water was kept below the melting temperature of the PNA:DNA complexes, at 10°C.

The CD spectra of the single strands (PNA/DNA) and triplexes were recorded as an accumulation of 10 scans response of 1sec. from 320 to 200nm using a 1cm cell and a scan speed of 200nm/min.

3.9.3 Job's plot through Circular Dichroism

Various stoichiometric mixtures of PNA and its complementary DNA were prepared with relative molar ratios of (PNA:DNA) strands of 0:100, 10:90, 20:80, 30:70, 40:60, 50:50, 60:40, 70:30, 80:20, 90:10, 100:0 individually. The total strand concentration in all the samples is 2 μM in 2ml sodium phosphate buffer (10 mM, pH 7.2 and contains 100 mM NaCl, 0.1 mM EDTA). The samples with the individual strands were annealed and the CD spectra of each sample were recorded.

The ellipticity values of all the mixtures at 258 or 260nm were plotted against mole fraction of PNA. The ellipticity values of the sample at this wavelength readily increased and reaches to maximum followed by gradually decreased. These values were plotted against molefraction of PNA. The maxima of intersect found to be the binding stoichiometric molar ratio.

3.9.4 Job's plot through UV-mixing curves

Absorbance spectra at 260 nm was also recorded for the mixtures of PNA:DNA in different proportions as mentioned above. A mixing curve was plotted, absorbance at fixed wavelength (λ_{max} 260 nm) against molefractions of PNA. There is a drastic shift in the absorbance value readily decreased, when the molefraction of PNA in the mixtures increased 60 to 70, which further increases behind that proportions. The minima of intersect found to be the binding stoichiometric molar ratio.

3.9.5 NMR titration experiment

The 30 mM of thymine component (**100** or **31**) in 600 μ l of dry $CDCl_3$ was taken in NMR tube and titrated with the adenine component (30 mM in 1200 μ l of dry $CDCl_3$). The titration was followed by recording NMR spectra for each addition of 100 μ l or 5 mM of prepared adenine component. The chemical shift of N^3 -H of thymine moves downfield progressively as it involves hydrogen bonding. After saturation, negligible increment of δ value of N^3 -H was observed with further addition of adenine component. The δ value of N^3 -H was plotted against the conc. adeninyl component/ con. thyminyl component provides an intersecting point express about the binding stoichiometry.

3.10 Conclusions:

- i) The modified PNA oligomers (cyanuryl PNA, 8-bromoadeninylyl PNA and 8-amino adeninylyl PNAs) formed stable triplex complexes with corresponding DNA strands confirmed by CD and Job's plot.
- ii) In case of cyanuryl PNA, *C*-terminus, middle and bi modifications (*N*-terminus and middle modification) stabilized the corresponding triplex, whereas the *N*-terminus modified PNA destabilized the triplex.
- iii) 8-bromoadeninylyl PNA oligomers with middle modification destabilized the triplex, whereas the *C*-terminus and bi modifications (*N*-terminus and middle modified) stabilized the corresponding triplexes.
- iv) 8-aminoadeninylyl PNA oligomers with *N*-terminus modification destabilized the triplex and *C*-terminus, middle modified and double modified (*N*-terminus and middle modified) stabilized the triplexes.
- v) The sequence discrimination through studying the hybridization properties of the modified PNA oligomer with single mismatch sequence, established the better sequence selectivity of modified PNA oligomers over the control PNAs.
- vi) The duplex stability of the cyanuryl PNA, 8-bromoadeninylyl PNA and 8-aminoadeninylyl PNA were studied.
- vii) Mix sequence of cyanuryl PNA (PNA **87**) showed less stable duplex in comparison with control sequence PNA (PNA **86**) and PNA **87** discriminates the *parallel* and *antiparallel* sequences as good as the control sequence PNA **86**

- viii) Eventhough the modifications, 8-bromo/aminoadeninyl PNAs (PNA **88&89**) may not enhance the binding strength with *c*DNA, they discriminate the *parallel* and *antiparallel* sequences better than the control sequence PNA **86**.
- ix) The binding stoichiometry at monomer level between adeninyl PNA:thymidine, adeninyl PNA: thymidinyl PNA, 8-bromoadeninyl PNA:thymidine, 8-bromoadeninyl PNA: thymidinyl PNA established as 1:1 through NMR complexation titrimetry at monomer level.

References:

- 1) Cantor, C. R.; Warshaw, M. W.; Shapiro, H. *Biopolymers*, **1970**, *9*, 1059-1070.
- 2) (a) Job, P. *Ann. Chim.* **1928**, *9*, 113.
(b) Cantor, C. R.; Schimmel, P. R. *Biophys. Chem. Part III* **1980**, 624.
- 3) Kim, S. K.; Nielsen, P. E.; Egholm, M.; Buchardt, O.; Berg, R. H.; Nord, B. *J. Am. Chem. Soc.* **1993**, *115*, 6477.
- 4) Peptide Nucleic Acids Protocols and Applications, Edited by Nielsen, P. E.; Egholm, M. Horizon scientific Press, 1999.
- 5) Soyfer, V. N.; Potaman, V. N. *Triple helical Nucleic Acids*; Springer: New York, 1996.
- 6) Ganesh, K. N.; Kumar, V. A.; Barawkar, K. A. *Supramolecular control of structure and reactivity* (Chapter 6, Ed Hamilton, A. D) **1996**, 263-327.
- 7) Watson, J. D.; Crick, F. H. C. *Nature*, **1953**, *171*, 737-738.
- 8) Williams, N. G.; Williams, L. D.; Shaw, B. R. *J. Am. Chem. Soc.* **1989**, *111*, 7205-7209.
- 9) Kyogoku, Y.; Lord, R. C.; Rich, A. *Biochem. Biophys. Acta.* **1969**, *179*, 10
- 10) Kyogoku, Y.; Lord, R. C.; Rich, A. *Pro. Natl. Acad. Sci, USA.* **1967**, *57*, 250-257.
- 11)(a) Nielsen, P. E.; Egholm, M.; Buchardt, O. *Science*, **1991**, *254*, 1497.
(b) Ganesh, K. N.; Nielsen, P. E. *Curr. Org. Chem.* **2000**, *4*, 916-928.
- 12) Wojciechowski, F.; Hudson, R. H. E. *Curr. Topic. Med. Chem.* **2007**, *7*, 667-679.
- 13) Wilcox, C. S. *Frontiers in Supramolecular Chemistry and Photochemistry*, (Ed Schneider, H. J.) **1990**, 123-143.